UNIVERSITY OF LIVERPOOL

An evaluation of hepatitis B virus in England and the host-virus interplay as a key determinant of disease outcomes

This thesis is submitted in accordance with the requirements of the University of Liverpool for the degree of Doctor of Philosophy by:

Mr Harrison Butler Austin

Supervised by

Dr Daniel Neill *antea* Professor Anna Maria Geretti

Department of Clinical Infection, Microbiology and Immunology

This work is dedicated to all people living with hepatitis B whose voices are not yet heard.

And to my Dad, Mom and step-father.

1 Declaration of Authorship

I hereby certify that this thesis constitutes my own product, that where the language of others is set forth, quotation marks so indicate, and that appropriate credit is given where I have used the language, ideas, expressions or writings of another.

I declare that the thesis describes original work that has not previously been presented for the award of any other degree of any institution.

Harrison Austin

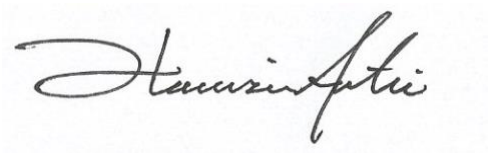

July 2022

2 Acknowledgements

For all of the PhD students who experience mental health difficulties during the process…keep going.

Along the way there were several dark days when I wanted to give this work up. There were also several incredibly joyous days. Ryan, my amazing husband, you kept me going when nothing else would and were there to celebrate with me like there was no tomorrow. I love you to the moon and back and back again.

The work presented in this thesis would not be possible without an extraordinary group of people that mean so much to me.

To all the patients participating in all of the studies within this thesis – thank you for your time and your thoughts. Sitting with you and hearing your stories during the consultation prior to joining my study lite a fire in me that made me want to fight for your equal representation and care.

I have been beyond fortunate to be guided by my supervisory team. None of this work would have been possible without Anna Maria. Thank you for taking a chance on me all those years ago. You have always gone above and beyond to mould me into a better thinker, researcher and writer. I will be forever grateful! Dan, thank you so much for taking me under your wing and guiding me from the beginning (sorry about the commas). Collette, your patience, and perspective have been incredible – thank you for giving me real confidence in statistics. Kris, a large part of this thesis would never have happened without you and for that I will be forever grateful – also our talks kept me going on some very down days.

Thank you to my supportive family: Mom, Dad, Don, Helen and Paul for your never-ending support!

My RLUH family, thank you for taking me in and always looking after me; Jill, Eimear, Shirley, Gaynor, Carl, Melissa, John. I will never forget the laughs, tears and seemingly endless supply of cake, candy and tea. You all are a part of my family now.

Libby, there are several patients that would not have been part of this study if it were not for your motivation to come out of my shell during Wednesday and Thursday clinics and approach them with the patient information sheet. Thank you! Also, thank you for your support during the NUC-B Study.

To my dear friends at UoL Yasmin, John, Jordan, Charlotte, Angharad, Eleri, Daan, Libby, Alessandra I hope we remain friends for a very long time.

The Geretti Crew were some of the most hardworking and intelligent individuals I've met. It was a pleasure working alongside and befriending Giovanni, Adam, Alessandra and Alex.

3 Abstract

An evaluation of hepatitis B virus in England and the host-virus interplay as a key determinant of disease outcomes

Harrison Butler Austin

The scale of the HBV epidemic and the burden of HBV-related disease is substantial, yet our current understanding of the epidemiology, disease pathogenesis and immunological control is incomplete. Strategies for the elimination of hepatitis B as a public health threat will require an integrated approach; strengthened by potential new curative therapeutics and supported by diagnosing most individuals who are currently unaware of their HBV status. The work presented in this thesis utilises a large database of primary care records to explore patterns of HBsAg screening and seropositivity across England, and a diverse cohort of people living with chronic HBV infection to characterise new biomarkers and to identify elements of immune control and pathogenesis.

In England, targeted HBsAg screening is recommended for patients with a background or risk-practices that may increase infection risk. Current English guidelines include people from endemic countries, men who have sex with men and individuals with: a history of injecting drugs, in close HBV contact, a history of imprisonment, or a record of another blood borne virus or sexually transmitted infection. We used the Oxford Royal College of General Practitioners Research Surveillance Network, a large scale quasi-representative database of 6,975,119 GP healthcare records to explore HBsAg screening and seropositivity across England. We found that the offer of screening was increased in patients with risk-factors, however screening practices were less than optimal. HBsAg seropositivity was localised to urban locations and highly associated with socioeconomic deprivation. Additionally, we found that a record of syphilis was independently associated with a record of HBsAg seropositivity. Worryingly, these data indicated that although England has a relatively low rate of HBsAg seropositivity, opportunities to diagnose individuals unaware of their status may be missed.

Not unlike the need to improve screening and diagnostic practices, the utility of current clinical markers will likely only be partially adequate for identifying and monitoring patients that may benefit from future anti-HBV curative therapies. Soluble PD-L1 has been evaluated diagnostically and prognostically in cancer and anti-cancer therapy. In a heterogenous, well-

described cohort of people living with HBV infection, we measured levels of soluble PD-L1 (sPD-L1) by two analytically distinct platforms (Ella and SIMOA). The measurement of sPD-L1 was highly discordant between the two platforms. This was reflected in the associations found; levels of sPD-L1 by Ella were associated with females, younger age and HBeAg positivity while sPD-L1 by SIMOA was solely associated with levels of ALT. Importantly, this study revealed that if sPD-L1 levels are to be used to guide future therapies, they will need to be extensively evaluated and standardised.

sPD-L1 may influence the PD-1/PD-L1 axis that is thought to be partially responsible for the ineffective adaptive T-cell responses that support the establishment of chronic HBV infection. We conducted a hypothesis-generating study by characterising PD-1, the natural receptor for PD-L1, in the global T-cell compartment of patients with paired sPD-L1 quantification to elucidate potential mechanistic patterns. We found that levels of sPD-L1 correlated positively with the proportion of PD-1^+ $CD4^+$ T-cells. Additionally, we found that platelet count was also inversely correlated with the proportion of PD-1^+CD4^+ T-cells.

Recent advances in cytometry have allowed for greater resolution of the complex immune interplay in chronic HBV infection not easily obtained with traditional methods. We paired CyTOF deep immunophenotyping with machine learning techniques to elucidate potential lymphocyte signatures predictive of patients with increased sPD-L1 levels and HBsAg. We describe a novel $CD8^+$ T-cell phenotype ($CD45_{RA}$CCR7-$CCR6^+CXCR3^+CD127^-CD28^-CD57^+CD20^+$) with increased PD-1 expression that is raised in people living with chronic HBV infection compared to healthy volunteers and is predictive of patients with both increased levels of sPD-L1 and levels of HBsAg. The relationships identified between the T-cell phenotype described and levels of HBsAg and sPD-L1 suggest a possible antigen driven mechanism identifiable in peripheral PBMCs.

The work presented in this thesis provides a greater understanding of the multifaceted barriers that need to be overcome to increase levels of diagnosis in a high-income country. Additionally, we describe a nuanced pattern between sPD-L1 levels, global lymphocyte PD-1 expression and novel T-cell phenotypes identified via machine learning. Collectively these data highlight the complexities involved in the inter-play between host and virus that may need to be overcome to achieve future curative therapies.

4 Table of Contents

Table of Contents

5 List of Tables

6 List of Figures

7 List of Abbreviations

3TC	Lamivudine
ADAMs	A Disintegrin and Metalloproteinases
ADF	Adefovir
AHB	Acute hepatitis B
AIDS	Acquired immunodeficiency syndrome
ALT	Alanine aminotransferase
AOPI	Acridine orange and propidium iodide
BB/STI	Blood borne virus or sexually transmitted infection
BCP	Basal core promoter
cccDNA	covalently closed circular DNA
CD	cluster of differentiation
CITRUS	cluster identification, characterization, and regression
CMV	cytomegalovirus
CV	cross validation
DAAs	Direct acting antivirals
DMSO	di-methyl sulfoxide
dsLDNA	double-stranded linear DNA
ELLA®	Ella Protein Simple platform
EM	Effector memory
ETV	Entecavir
FBS	Foetal bovine serum
FDR	False discovery rate
FMO	Fluorescence minus one
GC	Gonococcal
GH	Genital herpes
GP	General practice
HBc	Hepatitis B core protein
HBeAg	Hepatitis B e antigen
HBpol	Hepatitis b polymerase
HBsAg	Hepatitis B surface antigen
HBV	Hepatitis B virus
HBx	Hepatitis B x protein
HCV	Hepatitis C virus
HIV	human immunodeficiency virus
HLA	human leukocyte antigen
HPV	human papilloma virus
IDU	Injecting drug user
IFN	Interferon
IMD	Indices of multiple deprivation
IR	intercalator

LAD	local authority district
LCMV	lymphocytic choriomeningitis virus
LHBs	large hepatitis B surface antigen
LSOA	lower super output area
MHBs	medium hepatitis B surface antigen
MHC	major histocompatibility complex
MMPs	matrix metalloproteinases
mRNA	messenger RNA
MSM	men who have sex with men
MTCT	mother to child transmission
NHS	National Health Service
NICE	National Institute for Health and Care Excellence
NK	Natural Killer
NTCP	Sodium taurocholate co-transporting polypeptide
NUC	nucleos(t)ide analogue therapy
ORF	open reading frame
PAMPS	pathogen associated molecular patterns
PBMC	peripheral blood mononuclear cells
PD-L1	Programmed death-ligand 1
PD1	Programmed cell death protein 1
Peg-IFN	pegylated interferon
PEI	Paul Ehrlich Institute
pgRNA	pregenomic RNA
rcDNA	relaxed circular DNA
RPMI	Roswell Park Memorial Institute Media
RT	Reverse Transcription
sHBs	small hepatitis B surface antigen
SIMOA®	Single molecule array
sPD-L1	soluble programmed death-ligand 1
SVP	sub-viral particles
TAF	tenofovir alafenamide
TCF1	T-cell factor 1
TDF	Tenofovir disoproxil fumarate
Temra	T effector memory cells re-expressing RA
TLR	Toll-like receptor
TM	terminal memory
TNF	tissue necrosis factor
TOX	thymocyte selection-associated BOX
TV	trichomoniasis vaginalis
WHO	World Health Organization

1 General Introduction

Hepatitis B virus (HBV) is a member of the family of *Hepadnaviridae*, genus *Orthohepadnavirus*[1]. HBV is transmitted primarily through contact with infected blood, semen and other bodily fluids. A majority of adults clear the infection. Conversely, those infected perinatally, or in childhood through adolescence, typically develop a chronic infection. In 2019, it was estimated that almost 300 million people were living with chronic HBV infection. Despite a vaccine being available since 1981 and antiviral therapy being capable of suppressing virus replication, nearly 1 million die each year of HBV-attributable disease, primarily cirrhosis and liver cancer. Worryingly, the true figures are likely much higher, as only 10% of those with HBV are aware of their infection[2] (WHO 2021). With the current interventions, over half a million people are expected to die annually due to HBV associated mortality until at least 2070[3].

1.1 Discovery of HBV, origin and genetic diversity

HBV is ancient. Phylogenetic analysis has shown that Hepadnaviridae may have spilt over from avian into mammalian hosts as early as 12.1 million years ago[4] (Suh, 2013). Remarkably, reconstructed HBV genomes sourced from Neolithic and Bronze age mummy dental calculus have molecular signatures similar to current genotypes[5,6]. The Sumerians first noted epidemic icteric hepatitis in 4000BC, later described in a clinical context by Hippocrates in *De Morbus Internis* in 460BC[7]. It was not until 1963 that the first viral protein was identified. While studying circulating lipoprotein polymorphisms, Professor Baruch Blumberg and his team precipitated a novel antigen with a double diffusion gel. The gel band had an unusually high protein content. The serum from a patient that had received multiple blood transfusions reacted with serum derived from an Australian Aboriginal[8]. The antigen discovered would be described as the Australian Antigen (AuAg) and then become known as hepatitis B surface antigen (HBsAg)[9]. In 1976, Professor Baruch received the Nobel Prize for discovering HBV[10,11].

HBsAg was classified based on antigenic determinants, the common *a* determinant and the mutually exclusive *d* or *y* and *w* or *r* determinants[12]. Together, these define the main four serotypes *adr*, *adw*, *ayr* and *ayw*. However, these serological subtypes do not mirror the genetic diversity of HBV[13]; in fact, the genomes of HBV are much more diverse.

During virus replication, 10^{-4} to 10^{-6} substitutions/site/year are introduced into the HBV genome by the HBV encoded polymerase, which lacks proofreading ability[14]. The mutation rate in HBV is lower than in other viruses that similarly rely on reverse transcription such as HIV. Genetic evolution is constrained by the partially overlapping structure of the genome. Due to the unique structure, not all regions mutate at the same rate as a mutation in one region will be mirrored in the adjoining genomic region coding for another amino acid. For example, mutations in the S-ORF would be constrained by potential mutations in the overlapping P-ORF[15]. Nonetheless, HBV is characterised by high genetic diversity at both the population level and within each host. Distinct genotypic lineages of HBV circulate. Currently, there are ten recognised major genotypes (A-J) based on a sequence intergroup divergence of >8%[16–18]. Major genotypes can be further classified by subgenotype, if divergence is >4%. Genotypes are highly associated with geographic regions (Figure 1.1). For example, genotype A is predominant in east sub-Saharan Africa and genotype E is highly prevalent in west sub-Saharan Africa. In contrast, genotype F can be found in South America and genotype D in the Middle East and Indian subcontinent[19]. The geographic distribution of HBV genotypes has been used to track human migration and provide timelines for the emergence of HBV genotypes. For example, subgenotype A1 is predominantly found in eastern Africa, and subgenotype A5 is found in Benin. Today A1 and A5 subgenotypes are found at high rates in Haiti, likely arriving during the slave trade[20]. There is a noticeable absence of genotype E in Haiti that is now predominant in West Africa, indicating this genotype may have emerged after the slave trade[20,21].

Figure 1.1: Global distribution of HBV genotypes

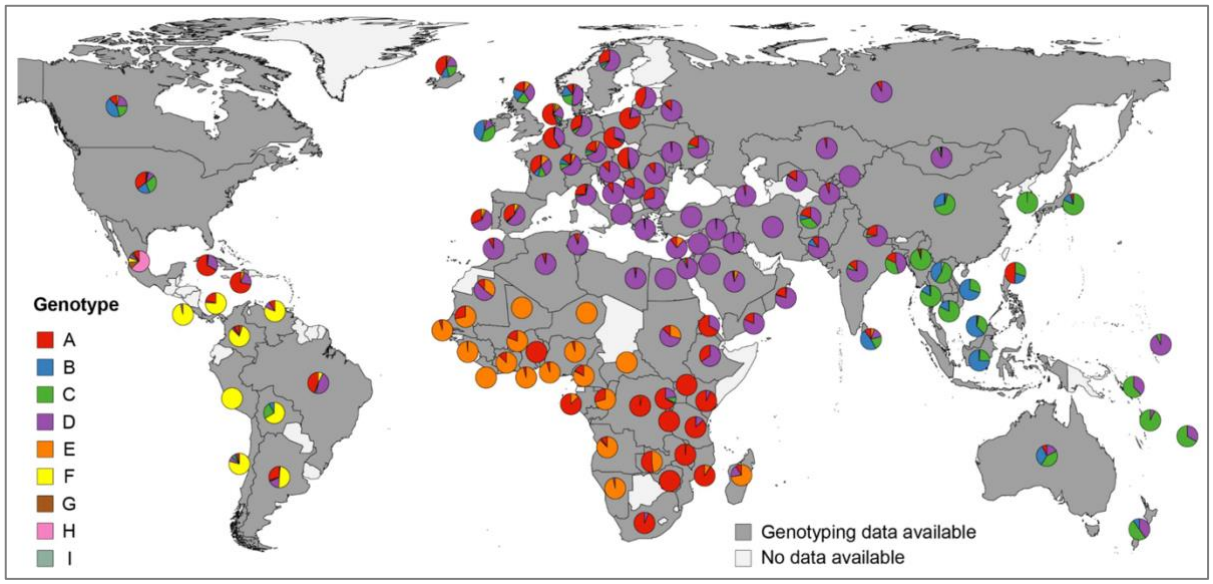

Distribution of HBV genotypes based on geographical location. Adapted from Velkov,S et al. 2018[22] *Genes*.

1.2 Epidemiology, the burden of disease of HBV and case finding

The scale of the HBV pandemic is often overlooked. Almost 300 million people are chronically living with HBV, a population that grows by almost 2 million per year[23,24]. The prevalence of HBsAg positivity is highest among the Western Pacific and African WHO regions with 6.2% (95% CI 2.7-5.0) and 6.1% (95% CI 4.6-8.5%) positivity, respectively[24]. Despite an effective vaccine, which offers >95% protective efficacy, and suppressive therapy, over a million people living with HBV die each year due to associated complications, including liver cancer[24]. It is estimated that globally $\leq$ 8% of those diagnosed with HBV are receiving treatment[23]. Treatment eligibility is challenging to determine. In low- and middle-income countries, healthcare facilities may lack the specialist diagnostic equipment needed to evaluate all relevant parameters for treatment eligibility screening[25,26]. Additionally, international treatment eligibility guidelines may have a low sensitivity in different populations and many who would benefit may be misclassified as inactive carriers[27,28].

HBV related mortality is expected to continually surpass half a million annually until at least 2070[3] and will likely rise in parallel with global increases in non-alcoholic fatty liver disease and metabolic syndrome and increased alcohol consumption[29]. In the 2016 global burden of disease study, HBV was associated with 51.6 age-adjusted disability-adjusted life years lost per 100,000 people, yet the global investment in HBV elimination strategies remains inadequate[30,31]. People living with HBV also experience significant stigma and discrimination that is potentially under-reported[32–34].

The first commercially available HBV vaccine was introduced in 1981 and consisted of an inactivated form of HBV virions derived from pooled HBsAg positive plasma[35,36]. Today, HBV vaccination is either given as a monovalent or combination formulation with either Hepatitis A or diptheria, tetanus, acellular pertussis, polio and *Haemophilus influenzae* B. The HBV vaccine offers substantial protection by inducing the production of anti-HBs in over 95% of those vaccinated[37,38]. HBV vaccination has been part of the UK childhood immunisation programme since 2017 and is also routinely offered to those at high risk of infection or as post-exposure prophylaxis, including infants born to HBsAg-positive mothers[37]. Increased vaccination rates and birth-dose programmes have successfully decreased the prevalence of HBsAg, particularly among children <5 years old. However, it will likely be decades before the impact of this decrease is noticed in morbidity and mortality figures[23].

The basis of the continuum of services for HBV is testing. Globally, only ~9% of those living with HBV are aware of their status, likely a reflection of the long asymptomatic period and inaccessibility of testing in areas of high prevalence and limited resources[39,23]. Screening programmes have been suggested in HBV endemic countries, yet many still struggle to increase uptake and integration of testing within standard services[40]. However, large-scale studies have found that screening and linkage to care are feasible in community settings with high prevalence rates and limited resources[41.]

In the UK, the estimated prevalence of HBV varies by community but overall is estimated at <1%[42]. Screening for HBsAg in the UK is indicated in high-risk populations and is freely available and accessible through primary care services. Despite this, there is likely a substantial underdiagnosis and many people living with HBV are not offered screening, despite it being recommended[43,44]. This is discussed in detail in Chapter 2.

1.3 Natural history and the immune response against HBV

HBV is highly infectious – the infectious dose required to establish infection is estimated to be as low as 16 copies/ml of blood ~ 3 IU of HBV DNA[45]. Viral particles are highly stable and remain infectious for up to 7 days on surfaces outside the body[44]. HBV DNA can be detected in the blood approximately 30 to 180 days after transmission and infection results in either self-limiting acute hepatitis or persistence as a chronic infection. Without intervention, chronic infection progresses through dynamic stages categorised by HBsAg-positivity, HBeAg status, HBV DNA load and level of liver inflammation, indicated by increased alanine aminotransferase (ALT) levels[46]. As previously mentioned, HBV replication is non-cytopathic. Instead, the natural history of infection and the resulting pathogenesis is due to an intricate interplay between the virus and innate and adaptive immune responses.

1.3.1 Transmission and Determinants of chronicity

Hepatitis B is a blood borne virus. In childhood, transmission is typically from mother to child (MTC) via exposure to infected maternal blood during delivery or perinatally[2]; horizontal transmission is also observed in children. MTC transmission is the route for a large proportion of total chronic infections. MTC transmission is dependent on the HBeAg status and HBV DNA load of the mother, with HBeAg positivity and maternal viral loads $\geq 10^6$ associated with

greater transmission risk[47]. *In-utero* transmission of HBV is debated[48,49]. In adulthood, intravenous drug use and sexual transmission are common infection routes alongside blood products and the re-use of needles[2,37,46]. Importantly, transmission before the age of five results in established chronic infection in 90% of cases, whilst only 5% of transmissions in adulthood result in chronic infection.

1.3.2 Acute HBV Infection

Acute hepatitis B (AHB) is characterised by a lengthy asymptomatic period. HBV is often termed a "stealth virus" as there is little evidence of immune activation during this period[50]. Once a threshold of replication is reached, there is an exponential rise in viremia; however, there is a noticeable absence of pro-inflammatory signals, including type 1 and type 2 interferons (IFN)[51]. Instead, there is enhanced production of the immunosuppressive cytokine IL-10 and lack of adaptive effector function[51]. Viral proteins, specifically pol, may actively block the production of IFNs and IFN-stimulating genes by inhibiting TLR3, RIG-I and STAT1[52,53]. Early responses are directed by natural killer (NK) cells, specifically through secretion of IFN-y, which coincides with a decrease in HBV DNA load[50]. Eventually, sustained recognition of HBV pathogen-associated molecular patterns (PAMPs) via Toll-like receptors (TLRs)[54] results in vigorous innate and adaptive responses. Only after partial decrease in viremia do effector CD4 and CD8 regain function and support infection resolution[51]. Helper $CD4^+$ responses support both cytotoxic $CD8^+$ T-cell and B-cell responses, which are required to clear infected hepatocytes and develop lasting protective humoral immunity, respectively. In self-limiting HBV infection, T-lymphocyte responses are typically polyclonal and directed against HBpol and HBx early in infection, while a higher proportion are directed toward HBe, HBs and HBcore following resolution[51,55–57].

A majority of viremia is contained prior to peak liver damage[57] . The resulting hepatic damage manifests clinically with disturbance of synthetic liver function e.g., bilirubinaemia and elevations in alanine aminotransferase (ALT) and aspartate transferase (AST)[58]. Associated jaundice is evident in approximately 20% of acute infections[59]. An exaggerated immune response during acute infection can result in acute liver failure or fulminant hepatitis, which is associated with a 28-day mortality rate of approximately 80% without intervention or transplantation[60]. In most AHB cases, the cellular and humoral responses are sufficient and develop neutralising antibodies against HBsAg that are characteristically absent in chronic

infection. Importantly, cccDNA can persist in the liver of patients with resolved AHBs for decades and serves as a source of viral rebound and reactivation following treatment discontinuation or periods of immunosuppression[61]. Enduring immunity is responsible for lifelong control of HBV. Suppression of the immune system, for example during cancer therapy, is associated with a risk of HBV reactivation[62,63].

1.3.3 Chronic HBV Infection

Chronic infection is defined by HBsAg positivity for more than 6-months after the first HBsAg test and is rarely symptomatic prior to the onset of advanced liver disease. Spontaneous clearance of HBsAg and seroconversion to anti-HBsAg+ is rare, occurring in only ~ 1% of cases annually and predominantly among those who have previous partial immune control, as evident by anti-HBeAg positivity[64]. In patients who sustain lifelong HBsAg seropositivity, there are five main clinical phases that are not necessarily sequential: HBeAg+ infection (previously termed "immunotolerant"), HBeAg+ hepatitis, HBeAg- infection (previously "low-level carriers"), HBeAg- hepatitis, and reactivation.

The early phase of chronic infection was previously termed the immunotolerant phase but is now referred to as HBeAg+ infection and is characterised by extremely high levels of replication, with high HBV DNA load and HBeAg positivity, but with minimal clinical evidence of liver inflammation in the form of ALT elevations[46]. There is suboptimal virological response to antiviral treatment, which is not generally recommended [46]. This phase is the most common outcome for children infected at birth, in whom it typically lasts for two or three decades. During this phase, specific HBV immune responses, mostly with Th1 profiles, can be detected but are geared toward a less inflammatory profile and have signs of functional exhaustion, including PD-1 expression. This phenotype has been hypothesised to be a legacy response to preserve homeostasis *in utero*[65,66]. One important study that redefined the immunological view of EPI was conducted by Kennedy et al., where *ex vivo* PBMCs were sourced from children and adults with ENI and immune active chronic HBV. They found that children and young adults with ENI harboured global T-cell populations with a greater ability to produce TNF-a but reduced CCL-3 responses, the latter an important chemokine for recruiting innate immune cells. Additionally, they found that PD-1 expression on global populations did not differ from immune active phases, and that younger people with HBeAg+ infection had a greater proportion of HBV-specific responses compared to older patients with

immune active chronic HBV[65]. This may partially explain why the use of Peg-IFN-a therapy is partially efficacious in patients with the HBeAg+ infection disease profile[67]. Although HBV-specific responses are found in this phase, they have a reduced propensity to trigger inflammatory events[68]. Elevations in serum ALT are not necessarily reflective of the underlying immune-directed pathogenesis or the quantity of specific HBV T-cells [69]. In a study among people with HBeAg+ infection profiles, it was found that hepatocytes were highly expanded in this phase, and there was evidence of increased HBV DNA integration in the absence of ALT elevations. This suggests that there is low-level immune directed hepatocyte killing occurring among those living with HBeAg+ infection and that mechanisms associated with the development of hepatocellular carcinoma (HCC) may already be underway[70]. Although the "switch" that allows for greater control of chronic HBV infection and the end of the HBeAg- infection phase is not yet fully understood, increased age is associated with a tendency of the immune response to shift toward a more inflammatory profile and a transition of patients to subsequent disease profiles and lymphocytes with a greater propensity to activation[71–73].

The HBeAg+ hepatitis phase, also called the immune clearance phase, is characterised by high levels of viral replication and HBV DNA (though generally lower than the HBeAg+ infection profile), HBeAg positivity and elevated ALT levels. It can take decades before this profile emerges for those infected during early childhood[46]. In a prospective study of 133 children with HBeAg+ infection disease profile, 28% entered the HBeAg+ hepatitis phase at the age of 12-18 years old. As previously mentioned, HBV-specific cytotoxic lymphocytes are already present in the liver during this phase, and the necro-inflammatory events associated with ALT elevation are amplified instead by non-HBV specific immune responses[69] . *In vitro* studies have revealed that cytotoxic lymphocytes are likely not the main drivers of hepatocyte damage during HBV clearance; instead $CD8^+$ cells were found to efficiently inhibit HBV replication without cytolysis via IFN-y and TNF-a dependent mechanisms[74,75]. Changes to the extracellular matrix of hepatocytes by matrix-metalloproteases, induced by cytotoxic T-lymphocytes, may lead to the recruitment of non-antigen specific innate immune cells including NK cells, macrophages, monocytes and dendritic cells. Raised ALT levels are likely a reflection of the activation of these innate immune cells as their absence, even with continued cytotoxic lymphocyte activation, was associated with minimal liver damage in animal models, as described by Sitia et al[75]. Regulation of hepatocyte damage by negative regulatory pathways such as PD-1/PD-L1 is key, as overamplification of inflammatory processes can, in rare cases,

lead to hepatic decompensation and liver failure[76]. Importantly, this active immune environment favours B-cell activation and humoral responses, resulting in the development of anti-HBeAg antibodies and peripheral loss of HBeAg[77]. HBeAg seroconversion with development of anti-HBeAg antibodies prior to the age of 30 is beneficial. In contrast, the extension of the HBeAg+ hepatitis phase beyond the age of 40 is associated with the development of liver cirrhosis and HCC[78]. Following partial control of HBV infection, most patients have a reduction in HBV DNA load and subsidence of hepatic necroinflammation. Antiviral therapy is recommended for patients with HBeAg+ hepatitis, to be continued in those with HBeAg seroconversion through a consolidation phase prior to attempting discontinuation; in a select group of patients, with favourable biomarker levels (including HBsAg) antiviral therapy discontinuation may be attempted [46].

The low-level carrier stage or HBeAg- infection phase is a common status among those living with chronic HBV infection. HBeAg- infection is characterised by minimally elevated levels of HBV DNA, normalised ALT values, HBeAg negativity and minimal necroinflammation or fibrosis[46]. There is a substantial reduction in both cccDNA activity and pgRNA production when compared to HBeAg+ disease[79]. The life-long prognosis of those with ENI is generally uncomplicated, with few showing signs of progressive liver damage and antiviral treatment is not indicated [80]. However, some evidence suggests that there may be sub-populations within this category that may progress to HCC, thus increased monitoring is warranted[81]. Immunologically, patients within the HBeAg- infection phase may have the highest proportion of T-lymphocytes with signs of exhaustion when compared to phases with active disease. A study by Boni et al. found that in a prospective study of 27 HBeAg- patients, with varying levels of viraemia, global T-lymphocyte populations had sustained high levels of PD-1 expression that were inversely correlated with levels of DNA. Despite this, Boni et al found that directly *ex-vivo* HBV-specific T-lymphocytes were only found in patients with comparatively low levels of HBV DNA and were less likely to produce antiviral cytokines[82]. It is possible that the detectability of lymphocytes with antigen-specific receptors in the ENI phase, but not others, is due to their deletion in a majority of other clinical phases[83]. However, an enduring propensity toward immune exhaustion within this phase is also supported by the finding that HBeAg- infection is associated with stably raised intrahepatic expression of PD-L1[84]. It is estimated that up to 1.9% of HBeAg- infection patients per year resolve their infection, with the development of anti-HBs antibodies and loss of HBsAg[85]. The potential for HBsAg loss increases with age (up to ~18% per year after 15 years) and is associated with

lower antigenic burden and lower DNA levels early in infection[86]. Spontaneous loss of HBsAg may be predicted by phenotypic analysis of T-lymphocytes. In a study by Xiong et al, the phenotypic characteristics of T-lymphocytes obtained from 141 HBV carriers were analysed prospectively. They found that T-lymphocytes from 3 patients who lost HBsAg over the 60-week study period had a distinct immunoprofile, including upregulation of CTLA-4 and CD107a[87]. Identifying true HBeAg- infection status is complex, as it can partially overlap with the clinical presentation of HBeAg- hepatitis, with largely different outcomes. Additional markers such as HBV RNA and HBsAg quantification have been suggested as tools to guide differentiation between HBeAg- infection and hepatitis, where HBV DNA and ALT levels do not provide a clear picture[88,89].

In patients with HBeAg- infection, reactivation of cccDNA expression within the nucleus of the hepatocyte may occur spontaneously, through a process yet to be understood, or due to drug mediated immunosuppression with agents such as Rituximab[90,91].

In a subset of patients who seroconvert to HBeAg-, there is evidence of ongoing transaminitis and HBV replication, though to a lesser extent than patients who are HBeAg+; this is referred to as HBeAg- hepatitis[46]. The infecting HBV of a large proportion of patients in this group harbour mutations in the precore region of the C-ORF, specifically G1896A, resulting in a premature stop codon and loss of HBeAg secretion[92]. Additionally, mutations in the basal core promoter sequence, frequently A1762T and G1764A, reduce, but do not eliminate HBeAg production[93]. The precore/core region mutations that result in reduced or eliminated HBeAg secretion are likely selected in the HBeAg+ hepatitis phase by immune pressures and may result in stabilisation of pgRNA structure [94,95]. Those with HBeAg- hepatitis are at heightened risk of HCC and progressive fibrosis; thus, antiviral treatment and ongoing surveillance in this population is recommended[46,96].

Chronic hepatitis B is a dynamic disease and not all patients can be neatly described within the categorisation above, based on clinical or immunological parameters. In a retrospective study of 4,759 patients with confirmed chronic HBV infection over four years, almost 30% (1,322/4,759) of patients did not fulfil the traditional criteria and were classed as being in a 'Grey Zone" [46,97]. Little is known of the outcomes of those within the group, but it has been suggested that they are at increased risk of fibrosis and HCC, while other studies have shown that they may not require therapeutic intervention[97,98].

Figure 1.2: Phases of chronic HBV infection

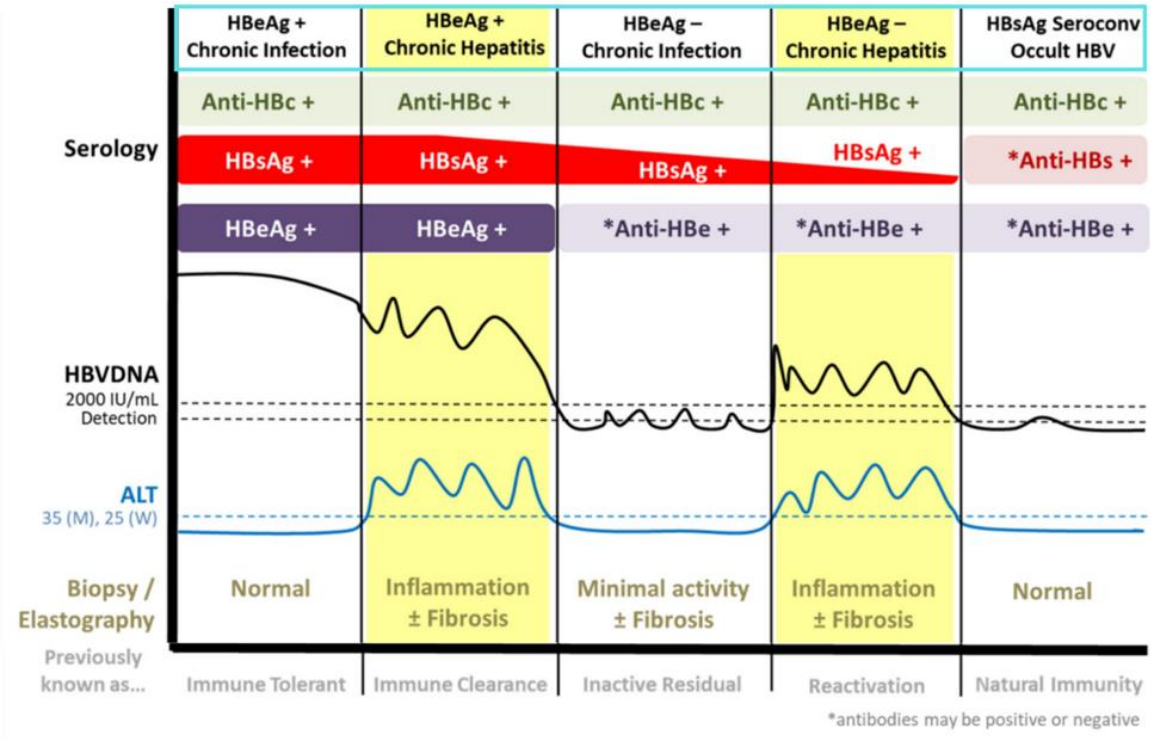

Phases of chronic hepatitis B infection. Adapted from: Lau, K. et al. 2020[99] *Impact of hepatitis B virus genetic variation, integration, and lymphotropism in antiviral treatment and oncogenesis. Microorganisms. 8(10), 1470. DOI: 10.3390/microorganisms8101470.*

1.4 Prophylaxis against HBV and treatments for chronic HBV infection

The formation of the stable episomal cccDNA within the nuclei of hepatocytes prevents a total cure for HBV. Due to the unique reverse transcription step during replication, targeted therapies are available that reduce HBV DNA load to undetectable levels and partially reduce antigenic load with minimal side effects. However, as cccDNA remains detectable for decades, therapy is often needed for life.

1.4.1 Nucleoside or nucleotide analogue (NUC) therapy

NUCs are natural deoxy-nucleo(s/t)ide (NT) analogues that are incorporated by the viral polymerase enzyme into nascent DNA, during reverse transcription of pgRNA. However, NUCs lack a 3' hydroxyl group needed to bind the next NT, thus NUC incorporation into a growing DNA strand leads to early chain termination. There are currently five NUCs approved for the treatment of chronic HBV infection; lamivudine (3TC), entecavir (ETV), adefovir dipivoxil (ADF), tenofovir alafenamide (TAF), and tenofovir disoproxil fumarate (TDF)[100]. Of

these, ETV, TAF and TDF are preferred due to high potency and high barrier to the emergence of drug resistance[46].

The introduction of NUC therapy for people living with chronic HBV infection often leads to the reversal of fibrosis and cirrhosis and reduces (although it does not abolish) the risk of developing HCC[46,101,102]. Therapy is only indicated for those with active signs of disease, typically those with HBeAg+ and negative hepatitis[46]. Expanding of therapy eligibility is debated, as high HBV DNA loads are directly associated with the development of HCC[102,103 104]. NUC therapy is not curative; in most patients, if therapy is halted, replication will promptly resume. A proportion of patients who seroconvert to HBeAg- during therapy may discontinue without virological rebound[105]. Inhibition of viral replication via RT blockade does not interfere with the production of sub-viral particles containing HBV RNA[106]. As a result, the ratio of HBV RNA to HBV DNA is modified with the administration of NUC therapy which blocks the production of HBV DNA. Excess production of HBV RNA due to highly transcriptionally active cccDNA can continue to occur in patients with suppressed HBV DNA. This can lead to an overestimation of HBV DNA levels when measured by HBV DNA load assays that use enzymes with reverse transcription activity for template amplification (e.g.. TMA-based)[107]. There is interest in exploring the direct quantification of HBV RNA in blood as a proxy for cccDNA transcriptional activity. For example, in patients who are virologically suppressed on NUCs, absence of detectable HBV RNA in the serum signals a reduced risk of viral rebound upon NUC discontinuation[108]. Additionally, viral genomic sequences integrated into the host genome are still transcribed, regardless of NUC therapy, although these transcripts mainly consist of HBsAg[109]. Despite a reduced cccDNA burden in those with HBeAg- infection, there is still a high turnover suggesting there may be long lived sanctuary sites where cccDNA persists[110]. In a small proportion (~10-12% after 7-8 years of NUCs), immunological control improves to lead to a typically durable loss of HBsAg[46,111].

1.4.2 Immunomodulators

Therapeutic injection of interferon alpha can suppress HBV replication and stimulate immune responses. While the exact mechanism of action of therapeutic interferon remains elusive, it is thought to inhibit several steps of the replication cycle and may stimulate the breakdown of cccDNA[112]. The overall advantage of IFN alpha based therapies is a sustained virological response with a finite treatment duration of one year. However, efficacy is only moderate (in

selected patients) and tolerability is poor, with several important contraindications. It is estimated that up to 13-30% of patients achieve a sustained response in optimal conditions[113]. Generally, those with low DNA and antigen burden achieve higher response rates with IFN alpha therapy alone, but a combination NUC + IFN alpha approach may also be effective[114].

1.5 The life-cycle of HBV

1.5.1 Form and Function: the viral structure

The Dane particle measures approximately 42nm in diameter and is the complete and infectious particle[115](Figure 1.2). Dane particles are composed of a membranous phospholipid bi-layer envelope that is host-derived and embedded with small, medium and large HBsAg proteins[11]. The inner icosahedral core is composed of HBV core protein (HBcAg) that surrounds a partially double-stranded, relaxed-circular (rc)DNA genome that is approximately 3,200 base-pairs in length and is covalently bound to the viral DNA polymerase. HBeAg exists as an unbound protein in the space between the inner core and outer envelope [116].

In addition to the Dane particle, several distinct sub-viral particles (SVPs) have been identified[115]. SVPs are classed as either containing HBV nucleic acids or particles that do not. Particles that do not contain nucleic acids are either small spherical and filamentous particles solely composed of HBsAg (the Australian antigen) or empty enveloped capsids. SVPs are produced in up to 10^5 fold greater abundance for the former and 10^2 fold greater for the latter, compared to mature Dane particles[11,117]. SVPs that contain HBV nucleic acids are replicative deficient and either contain double-stranded, linear DNA (dslDNA) or contain a single-stranded pre-genomic RNA (Figure 1.3)[108,118,119].

Figure 1.3: Structure of the Dame particle and subviral particles

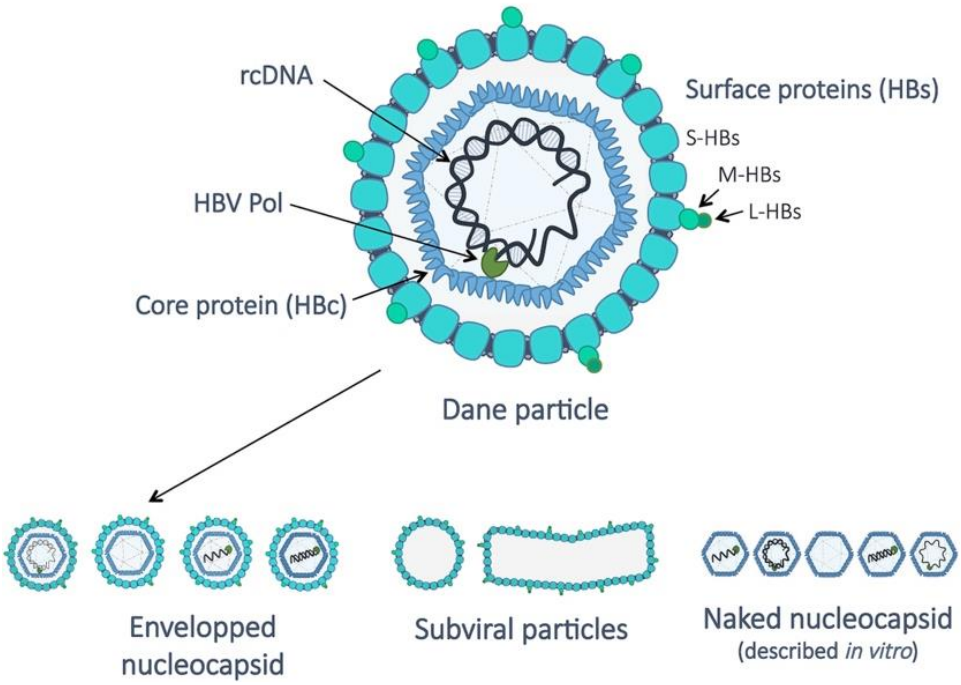

Representation of a mature Dame particle (central) and the associated proteins. HBeAg is not represented but is located between the inner nucleocapsid and the envelope. Enveloped virus-like particles include empty nucleocapsids, those containing pgRNA and double stranded-linear DNA. Also represented are the filamentous and spherical subviral particles composed of HBsAg. Adapted from: Tsukuda, S et al [120]. (2020) Hepatitis B virus biology and life cycle. Antiviral Research. 182,104925.

1.5.2 Genome and proteins

HBV has one of the smallest genomes amongst pathogens, consisting of approximately 3,200 base pairs, organised in a partially double-stranded, relaxed circular DNA genome. Though small, the genome is transcribed efficiently with multiple AUG initiation sites in the four overlapping open reading frames (ORFs), S, C, Pol and X, that encode seven functionally distinct proteins: small (SHBs), medium (MHBs) and large (LHBs) HBsAg components, the X protein, HBeAg, HBcAg, and polymerase[118]. At the 5' end of the negative strand, the terminal protein domain of the viral polymerase is covalently attached with a tyrosyl-DNA phosphodiester bond, and the 3' end of the positive strand is capped with an RNA primer[121].

The components of HBsAg (SHBs, MHBs and LHBs) are all transcribed from the S-ORF but are under different in-frame promotor control[122]. The preS1 promoter controls LHBs expression, while MHBs and LHBs are controlled by the downstream preS2/S promoter, suggesting there may be separate regulatory mechanisms[123]. All S-ORF products have the same carboxy terminus but differ in the length of their amino-terminus, approximately 226 amino

acid residues (aa) for SHBs, 281aa for MHBs and 400aa for LHBs[122]. Common to all HBsAg proteins is the immunodominant α-determinant (aa 124-147), against which most anti-HBsAg responses are targeted[124]. Functionally, SHBs is the dominant protein produced and constitutes a large proportion of the HBsAg molecules in the viral envelope[125]. The LHBs protein, while produced in significantly lower quantities, when compared to SHBs, is the only protein that carries the PreS1 domain that is key for viral entry into hepatocytes[125,126]. MHBs is highly conserved within Hepadnaviridae, but its role remains speculative, as it is not essential for assembly or infectivity[127]. Structurally, the SHBs, MHBs and LHBs are bound together in varying proportions, resulting in distinct regions in the Dame particle envelope as shown in figure 1.3.

Two functionally distinct proteins, hepatitis B core (HBcAg) and hepatitis B e (HBeAg), are produced from the C-ORF under the control of the core and pre-core promoters, respectively[128]. The HBcAg is composed of 183aa and self-assembles to form the icosahedral nucleocapsid. The carboxy-terminal region of HBcAg is found on the inner nucleocapsid surface and binds nucleic acid to aid reverse transcription of pgRNA and particle maturation[129,130]. The localisation of newly endocytosed virions to the nuclear pore complex is aided by HBc-protein domains on the outer surface of the nucleocapsid[131]. Both internal and external HBc domain processes are carefully controlled with post-translation modifications by host kinases and phosphatases, where lack of phosphorylation is associated with a decrease in pgRNA packaging. At the same time, dephosphorylation favours reverse transcription[132,133]. The protein product of the precore promoter is the p22 protein which undergoes proteolytic cleavage to form the mature HBeAg and the carboxy-terminal by-product[134,135].

The hepatitis B x protein (HBxAg) is a 154 aa *transactivating element* required for replication and produced from the X-ORF under regulation by the X-promoter and enhancer I [135].

The polymerase protein (pol) is a DNA polymerase with reverse transcription activity and is encoded by the bulk of available base-pairing space resulting in an 832aa protein. Pol is composed of four distinctly functional domains; the reverse transcriptase (RT), terminal protein (TP) that covalently links to the complete relaxed circular genome, the spacer protein[136] and ribonuclease H (RNaseH). Notably, the HBV polymerase lacks a proofreading exonuclease domain found in most DNA polymerases[137].

Figure 1.4: Annotated HBV genome

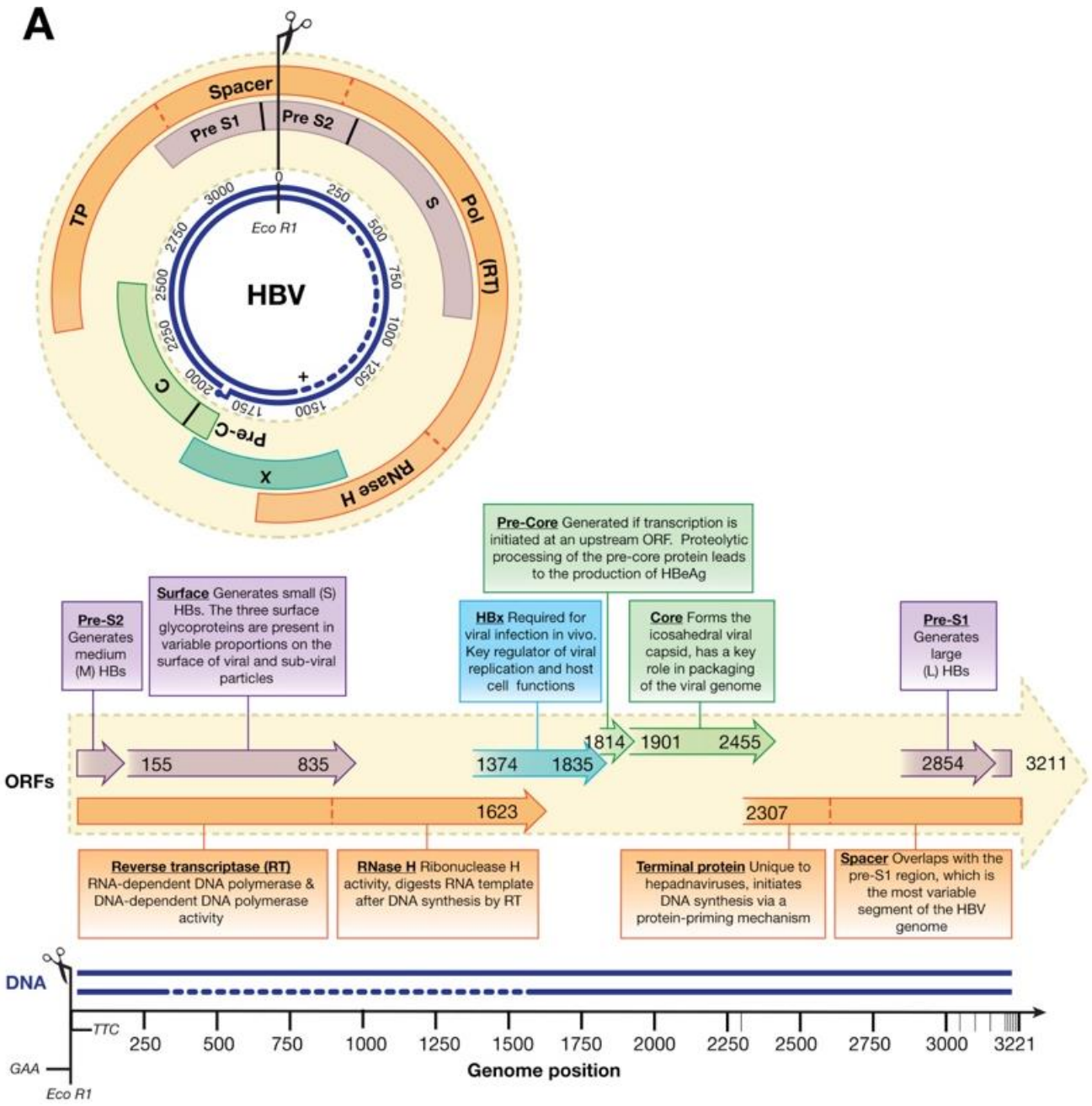

The annotated partially double-stranded genome of HBV with open reading frames and their products. Adapted from: *McNaughton, A et al. 2019. Insights from deep sequencing of the HBV genome – Unique, Tiny and Misunderstood. Gastroenterology; 156:384-399.*

1.5.3 Replication

The replication cycle of HBV is complex and involves a series of steps outlined below that are unique to the Hepadnavirus family (Figure 1.5).

1.5.3.1 Binding and fusion with host cells

HBV begins its replication cycle when the preS1 domain of LHBs non-covalently attaches to heparin sulphate proteoglycans on the cell surface. The initial binding is not stable and easily removed. Subsequently, the amino-terminus of the preS1 domain is myristoylated and binds the sodium taurocholate co-transporting polypeptide (NTCP) that is primarily expressed in the liver. There are several features of HBV binding that remain unclear, such as how the amino-terminus becomes myristoylated and presented for binding and the role of co-receptors in promoting internalisation[126,138,139].

The NTCP-bound viral particle is internalised via clathrin-mediated endocytosis. A pit is formed in the phospholipid bilayer membrane, and the viral particle is gradually enclosed in a cytosolic endosome[140,141]. A drop in endosomal pH is thought to trigger conformational changes in the hydrophobic domain of the LHBs envelop protein, allowing interaction with the endosomal membrane and fusion of the two membranes[142].

The nucleocapsid transits across a network of microtubules, via active translocation mechanisms, through the cytosol to the nucleus, which takes approximately 30-60 minutes[143,144]. The nucleocapsid then localises and docks to the nuclear pore complex via core protein interaction with Importin-alpha and beta. The genome is then released into the nucleoplasm[145] via mechanisms yet to be elucidated. It is worth noting that this process is selective; only nucleocapsids containing mature rcDNA genomes are released into the nucleus[131].

A critical step in HBV replication is the conversion of the rcDNA genome to stable episome-like cccDNA. Nuclease and protease dependant mechanisms initiate cccDNA formation by removing the covalently attached pol enzyme from the 5' end of the negative DNA strand. Removal of the pol leaves a residual sequence of redundant DNA that is also removed, the resulting nick in the negative strand that is subsequently repaired by host ligases. The 3’ position of the positive single-stranded DNA acts as a primer for host-derived polymerase

gamma, which synthesises the remaining positive strand. The 3' primer on the positive strand is removed and completed by host ligase before chromitinization[146].

1.5.3.2 Integration of dsLDNA

There are several alternative forms of viral particles, including those containing double-stranded linear DNA (dslDNA). The release of dslDNA into the nucleus results in replication-incompetent cccDNA formation[147]. However, this form of the genome can integrate within the host chromosome, likely through the host repair mechanism of alternative non-homologous end joining[148]. Though integrated HBV genomes cannot produce viral particles, they are a primary source of HBsAg and HBX, as this is the only ORF with an intact promoter sequence[149]. Additionally, the random integration of the HBV genome may drive the development of HCC as integration promotes chromosomal instability[109].

1.5.3.3 Expression of dsDNA and translation of viral transcripts

Fully repaired cccDNA is the functional template for transcription of the five main mRNA species. Transcription is regulated by epigenetic, transcriptional and restriction factors, and under the control of the four previously mentioned promoters (core, preS1, preS2 and X), in addition to enhancer regions I and II [150,151]. One crucial regulator is the HBx-protein, which has been implicated in epigenetic transcript activation via histone acetylation and CREB-p300 interactions[152]. The HBx-protein also activates replication by suppressing restriction factors, including SMC/5[92,153]. The core promoter, which contains the basal core promoter region, is responsible for transcription of both the 3.5kb longer than genome length (pgRNA) and the pre-core mRNA. Incorporating point mutations within this region can result in early termination and variants lacking HBe-protein production[92]. The core mRNA directs the synthesis of both the HBc subunits and pol once translocated to the cytoplasm, while pre-core transcripts result in the pre-core protein that is post-translationally modified in the endoplasmic reticulum (ER) and processed for secretion. Additionally, activation of the preS1, S2 and S promoters leads to the production of the L, M and SHBs mRNAs, which are subsequently transported to ribosomes on the surface of the rough ER and translated, followed by glycosylation. The resulting proteins are then transported to the cell membrane via the secretory pathway[122,123].

1.5.3.4 Viral particle assembly, budding, maturation

Assembly of replication-competent viral particles initiates with the pol-protein complexing with the RNA-binding motif at the 5' ε-region[154–157]. The structure of pgRNA contains two bulging self-paired ε-regions at both the 5' and 3' ends. Additionally, pgRNA has a 5' cap and 3' poly-A tail. The formation of the pol-pgRNA complex signals the polymerisation of HBc-proteins, resulting in the packaging of the complex.

Reverse transcription (RT) of the pgRNA into rcDNA occurs in the nucleocapsid containing the ribonucleoprotein complex. DNA synthesis is initiated by a unique protein priming method. An empty hydroxyl group on a tyrosine motif within pol binds with a dGTP nucleotide, followed by polymerisation of an additional four nucleotides complementary to residues within the 5' ε-region of pgRNA[158,159]. Pol then folds onto the 3' end of direct repeat 1 (DR1) and synthesises the entire minus-strand, while the RNaseH domain within pol degrades the remaining RNA template. A residual RNA sequence containing the DR1 remains after elongating the minus strand and base pairs with an additional direct-repeat region (DR2). This reaction initiates DNA polymerisation and elongation of the plus strand and the formation of the characteristic circular genome. The pol protein remains covalently attached to the rcDNA in the mature viral particle. Capsids with completed HBV rcDNA are then either trafficked to the cell membrane and egress via the multivesicular body secretory pathway into the circulatory system, or are recycled back to the nuclear pore complex to amplify the concentration of cccDNA in the nucleus[160–162].

1.5.3.5 Sub viral particles and HBV RNA

The population of viral particles in peripheral blood is heterogeneous. Viral particles containing pgRNA that is either partially reverse transcribed, partially degraded by RNaseH, or in its native form, can be found in the periphery either as naked capsids or enveloped, suggesting these particles egress via a similar pathway to mature Dane particles[108,163,164]. Virus-like pgRNA particles still contain the ε-region, so it has been suggested this species may be a result of viral polymerase failure[165]. Virus-like particles containing HBV RNA are not able to initiate

new infection. However, levels of circulating HBV RNA may reflect the transcriptional activity of cccDNA; potential clinical applications are under investigation[166].

Figure 1.5: Replication cycle of HBV

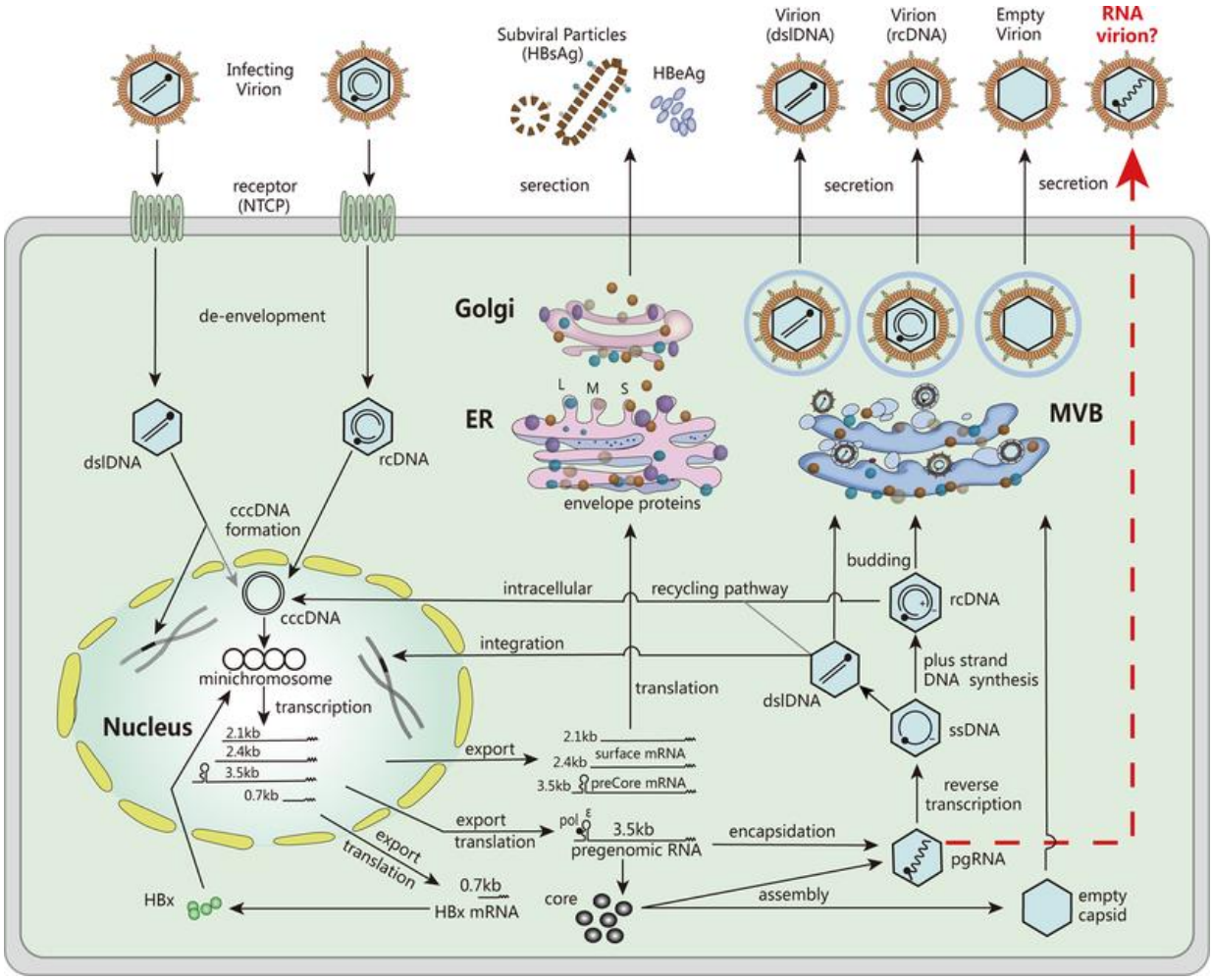

Replication cycle of hepatitis B with a proposed mechanism for producing virus-like virions containing pgRNA. Adapted from: Liu, S et al. 2019[166]. Serum HBV RNA: a new potential biomarker for chronic hepatitis B virus infection. Hepatology 69(4):1816-1827.

1.5.4 The immune response to HBV, T-cell exhaustion, and chronic HBV infection

The central dogma of cellular immunity begins when an antigen is proteolytically processed, covalently bound to major histocompatibility complexes (MHC) I or II, and subsequently presented to $CD8^+$ and $CD4^+$ T-lymphocytes, respectively to bind to the T-cell receptor (TCR) and initiate the adaptive immune response[167].

Major histocompatibility complexes are divided into two classes, MHC-I and MHC-II – both provide similar functions, but operate in different cellular compartments and are loaded with peptide by different pathways. The expression of MHC-II molecules is restricted to antigen

presenting cells including dendritic cells, macrophages and B-cells[168.] An MHC-II molecule generally presents self, bacterial and viral peptide sequences more than nine-mers in length and acquired via exogenous macroautophagy. This process occurs within late endosomes; following the loading of the MHC-II molecule with peptide fragments, the endosome is then trafficked to the plasma membrane[169.] The peptide cargo presented by MHC-II molecules is recognized by the TCR expressed on the surface of $CD4^{+}$T-cells. The TCR/MHC stimulation pathways is detailed below in figure 1.6.

In contrast to MHC-II, MHC-I molecules are expressed by all nucleated cells and acquire their peptide sequences via 26Sproteosome degradation of proteins from cytosolic and nuclear origin[168,170.] Following the loading of peptide sequences approximately eight to nin-mers in length within the peptide groove, the MHC molecule is then trafficked from the endoplasmic reticulum to the plasma membrane for recognition by the cognate TCR expressed on the cell surface of $CD8^{+}$ T-cells[168]. The TCR/MHC-I stimulation pathway is detailed below in figure 1.6.

The interaction between the TCR and MHC with bound antigenic peptide is a carefully orchestrated event that initiates a signalling cascade, ending in T-cell activation. While the TCR/MHC binding event is key, co-stimulatory pathways such as CD28, expressed on the T-cell surface, binds with CD80[171]. The interaction of TCR with MHC and subsequent co-stimulation is a continuous process. It is estimated that a minimum of 1,000 TCRs need to be engaged to overcome the activation barrier and may take up to 6 hours[171].The T-cell activation pathway is further characterised in figure 1.6. Unchecked T-cell activation can be pathogenic, thus there is biological need to curtail T-cell activation following successful activation. Negative regulatory signals are provided by checkpoint molecules PD-1, expressed on the surface of T-cells, NK-cells and some B-cells, binding with PD-L1, constitutively expressed by all nucleated cells non-hematopeoetic cells[172]. The role of PD-1 and PD-L1 interaction will be discussed in detail in section1.5.7.1. Additional checkpoint molecules include cytotoxic T-lymphocyte antigen 4 (CTLA-4), OX-40 and 4-1BB[173]

Activation or inhibition of NK cell activity may also be directed via interaction with MHC-I molecules. Specifically, the binding of the NK-cell receptor NKG2D to MHC-1 molecules can stimulate the cytotoxicity in response to viral infection[174,175].

Figure 1.6: MHC presentation and T-cell activation: Key players

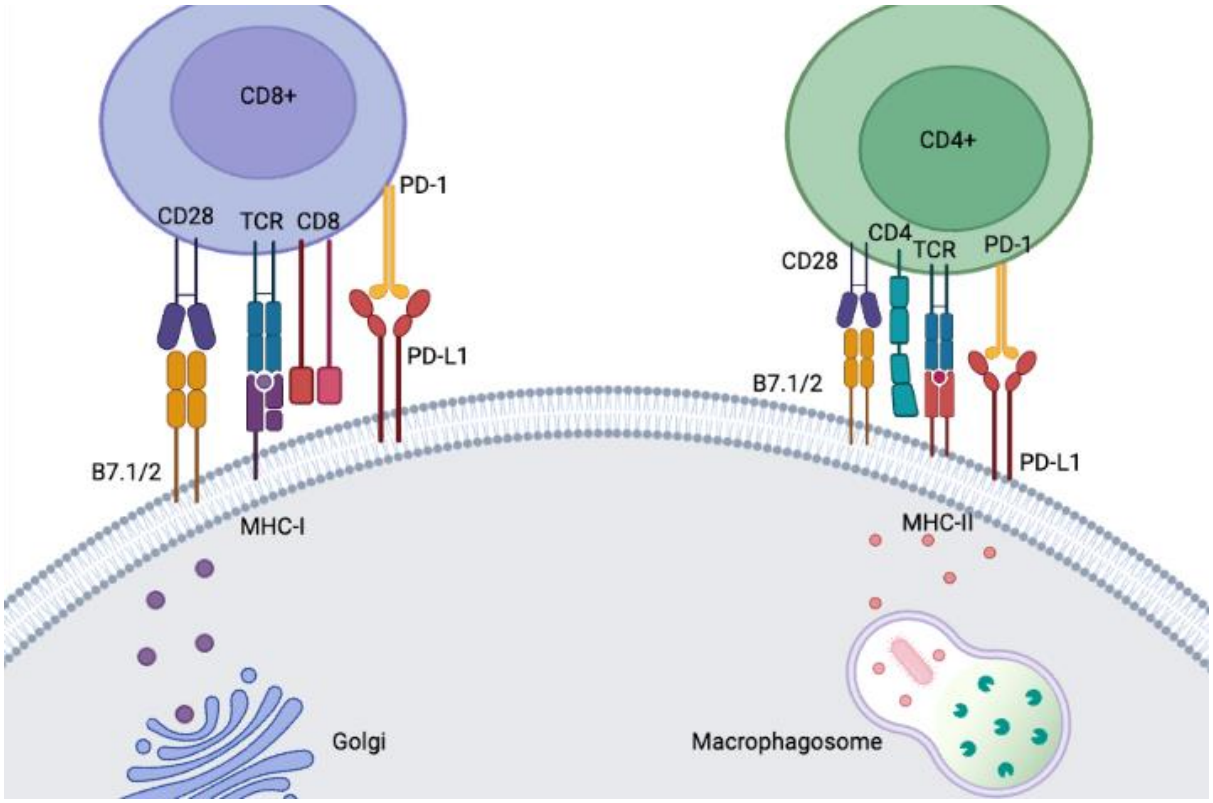

The key players involved in MHC presentation and T-cell activation. Activation of the adaptive immune responses is initiated by the interaction of the TCR and either MHC-I and MHC-II. The binding is stabilised by flanking CD8 and CD4 molecules, dependant on the cell type. Co-stimulatory molecules including CD28 provide a positive signal to overcome activation barriers that are intrinsic to activation, including the need for multiple TCR/MHC interactions. This figure was created in Biorender and adapted from Kaufmann SHE, Parida SK 200. Cell Host and Microbe. 4 (3):219-228.[176]

1.5.5 The liver microenvironment

The liver itself is a tolerogenic environment[177,178]. The liver is supplied directly with blood from the portal vein, which is supplied from the gastrointestinal tract, primarily the stomach and intestines. As such, immune cells in the liver are constantly subjected to a high antigenic load. Additionally, due to the intricate network of capillaries with a small diameter, the velocity at which blood travels through the liver is low, resulting in extended antigen exposure. As a result of these factors, the liver has evolved to restrict hyperresponsiveness and contains a high proportion of T-regulatory cells to maintain homeostasis[178], limiting the potential for runaway and pathological inflammation. However, this anatomical feature creates an optimal environment for hepatotropic pathogens such as HBV to persist in the presence of a less robust immune response, as compared to other organs.

1.5.6 T-lymphocyte exhaustion profile

Anergy and functional exhaustion have been described in many chronic viral infections, including LCMV, HCV and HIV and are characterised by an upregulation of inhibitory markers and a lack of effector function by antigen-activated T-cells, NK cells and other mononuclear cells. This process is driven by continuous rounds of *de novo* T-cell activation in an environment with a high antigenic burden[179]. HBV produces viral proteins in excessive quantities, which may directly contribute to the characteristic T-cell exhaustion observed in people living with chronic HBV infection. The limiting of effector function and development of inhibitory markers is progressive; involving the loss of homeostatic cytokine recognition and production, increases in inhibitory markers, alterations in the metabolic profile and changes in the epigenetic landscape. These profound changes are outlined below.

Functionally exhausted lymphocytes have a marked decrease in their cytokine mediated responsiveness. The loss of IL-2 is followed by loss of both TNF-a and eventually IFN-y and decreased expression of the IL-7 receptor CD127[180–182]. Development of antigen-specific TCRs requires a continued supply of IL-7 and IL-15 to maintain the resulting T-memory cells[183,184]. However, a hallmark of exhausted lymphocytes is the loss of IL-7 and IL-15 receptors, thus limiting antigen-independent self-renewal and limiting proliferation[184]. Additionally, exhausted lymphocytes have an altered metabolic programme. In a study of *ex vivo* PBMCs derived from people living with chronic HBV infection, it was found that HBV-specific $CD8^+$T-cells with exaggerated expression of PD-1 were not able to use the more efficient mitochondrial oxidative phosphorylation pathway and their energy requirements were instead being met solely with glycolytic pathways. This was in contrast with $CD8^+$T-cells specific for LCMV, derived from the same patient, which could use both oxidative phosphorylation and glycolysis[185]. Changes at the transcriptional level also have a profound impact on the development of exhaustion. Factors such as T-bet, EOMES and TCF-1 are required for the induction of genes for antiviral cytokines, homeostasis and proliferation, all of which can be found at decreased levels in chronic HBV infection[186–189]. Recently, the thymocyte selection-associated high mobility group box (TOX) was found to be a key transcriptional regulator of T-lymphocyte exhaustion, specifically in chronic HBV infection[189] . Collectively, these factors result in either the reversible non-terminally exhausted T-cell incapable of exerting anti-HBV activity or an irreversibly terminally exhausted state. Terminally exhausted cells are also eventually marked for deletion. T-lymphocyte deletion via Fas-FasL, Bim and TRAIL mediated mechanisms have been proposed[190–192]. Interestingly, the

HBx-protein is implicated in increasing the expression of Fas, thus providing a mechanism of immune evasion[193]. Identification of exhausted lymphocyte populations is an intensely researched subject as technologies evolve and allow for expansive marker identification at a single-cell level[189,194]. However, there is consensus that sustained upregulation of the PD-1 marker partially indicates T-cell exhaustion. Novel assays which may identify unique phenotypic signatures of potentially exhausted T-lymphocytes will be discussed further in Chapter 6.

1.5.7 The PD-1/PD-L1 pathway

When T-cells are presented with peptide sequences bound by MHC molecules, an activation cascade is initiated, and the interaction is strengthened by co-stimulatory mechanisms such as CD28 expressed on T-cells and CD80/CD86[195,196] on the presenting cell. However, balance is key during this interaction, and the absence of immune checkpoints and negative feedback can be pathological[196]. The PD-1 pathway is one of the most well-described immune checkpoint pathways. It provides a robust negative feedback signal that may prevent runaway amplification of T-cell activation. The natural ligands for PD-1 are PD-L1 and PD-L2. For this thesis, we will solely focus on PD-L1. The pathway is initiated when a lymphocyte expressing PD-1 binds to a cell expressing PD-L1, which in the context of chronic HBV infection include hepatocytes and non-parenchimal liver cells, as well as intra-hepatic and circulating antigen-presenting cells and NK cells[197]. The situation in which the PD-1/PD-L1 pathway activation occurs is critical. In non-chronic infections, PD-1/PD-L1 engagement is transient, allowing activated T-cells to exert effector function. Antigen clearance is followed by decreased expression of PD-1. However, in chronic infections such as chronic HBV infection, with continuous *de novo* activation events due to a large antigen burden, PD-1 and PD-L1 become hyper expressed and the pathway itself may become a key player in pathogenesis.

1.5.7.1 Discovery, expression and mode of action

The gene encoding the PD-1 receptor was discovered in 1992 by the Honjo Group at Kyoto University and was first thought to induce T-cell apoptosis during the negative selection of lymphocytes in the thymus[198]. Later, the same group elucidated the properties of the PD-1 molecule as a negative regulator of immune activation[199].

The PD-1 molecule is encoded by the *pdcd1 gene* and belongs to the B7 superfamily. PD-1 is a transmembrane protein with an extracellular immunoglobulin-like binding region for interacting with the PD-L1 molecules on the surface of antigen-presenting cells[200,201]. The ligation of PD-1 with PD-L1, within proximity of the T-cell receptor (TCR) complex, results in the cessation of downstream TCR signalling processes via sequestration of SHP2 and degradation of the TCR[201]. This engagement can be overcome in acute infection; however, in chronic HBV infection, the balance is tipped, and PD-1 expression and TCR inhibition are sustained . Downstream consequences of continued PD-1 expression are diverse and include limited expansion capacity, altered metabolism and inability to produce antiviral cytokines such as IFN-y and TNF-a and the cytolytic molecules perforin and granzyme-B.

Figure 1.7: The PD-1/PD-L1 signalling pathway

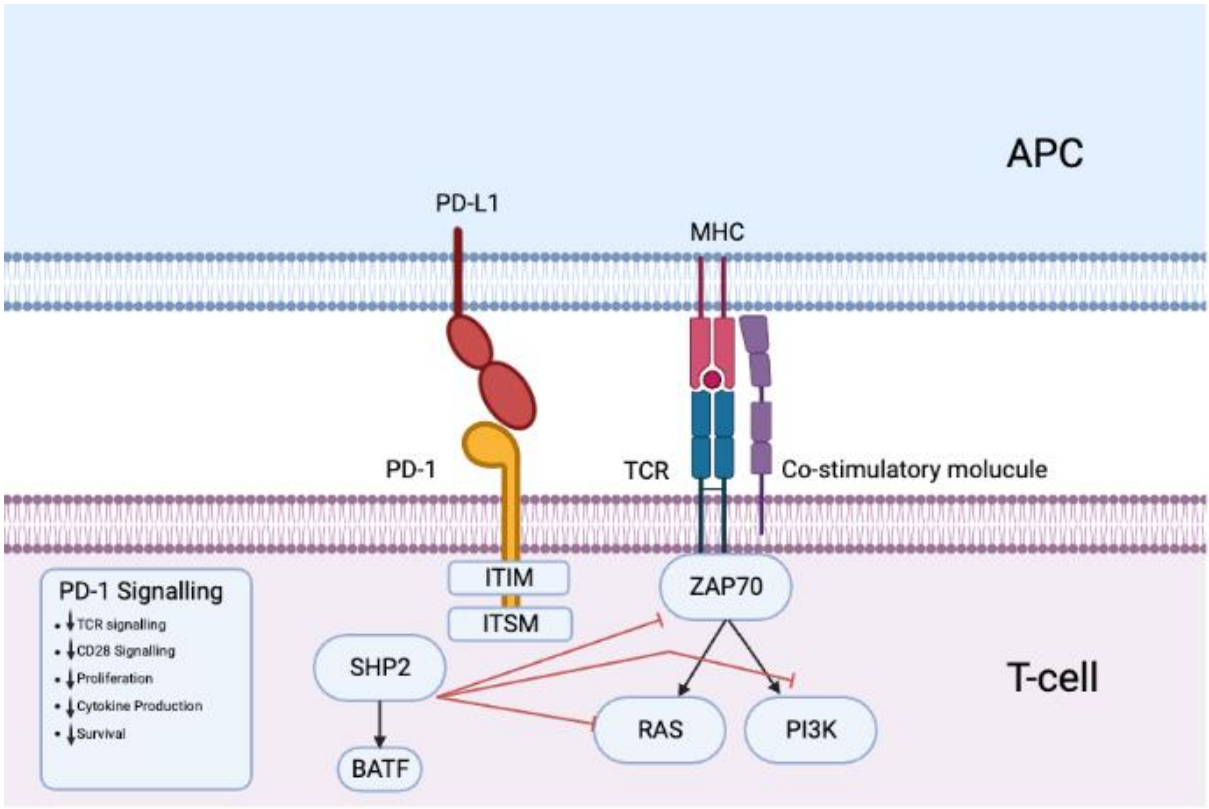

The mechanisms of PD-1 signalling in lymphocytes. The negative regulation of PD-L1 is constrained to cells that also express the MHC molecule that is bound to fragmented peptides. The PD-1 tail contains a motif, the immunoreceptor tyrosine-based switch motif (ITSM) that has the ability to sequester the SHP2 phosphatase which blocks positive signals propagated from the TCR inclusing ZAP70, and the RAS and PI3K pathways. This figure was created in Biorender and adapted from Sharpe AH, Pauken KE 2018. Nat Revs Immunology. The diverse function of the PD1 inhibitory pathway. 18 (153-167)[202].

1.5.7.2 PD-1 and PD-L1 Expression

Broad expression of PD-1 is well defined within the T-cell compartment, but the receptor is also expressed by B-cells, monocytes, neutrophils and NK-cells[203,204]. Regulation of expression

is primarily via T-cell receptor engagement with cognate antigenic peptides. Secondary disease-specific mechanisms have been proposed. In HBV, the HBc protein may induce PD-1 on T-cells through JNK signalling, thereby aiding immune evasion[205]. This is further supported in mouse modelling studies, where blockade of PD-1 induces IFN-y production from HBcAg specific T-cells[206].

PD-L1 is expressed on a range of nucleated, such as haematopoietic cells (including T-cells and B-cells and NK cells), non-haematopoietic cells such as hepatocytes and non-nucleated cells including platelets. The HBx and HBpol proteins may directly induce over-expression of PD-L1 on hepatocytes via the beta-catenin/c-Myc signalling pathway, limiting the possibility of cytotoxic T-cell mediated apoptosis[207]. The role of PD-L1 in chronic HBV infection outside of the traditional T-cell-hepatocyte interaction has recently been evaluated. In a study by Diniz et al. Chronic HBV infection, modelled in mice, not only resulted in upregulation of PD-1 on T-lymphocytes but also led to an increase in PD-L1 on NK-cells. NK cells expressing PD-L1 and suppressing $CD8^+$T-cell function could be overcome with PD-L1 blockade, subsequently assisting in boosting $CD8^+$ responses to therapeutic vaccination[197].

1.5.7.3 Soluble forms of PD-1 and PD-L1

Soluble isoforms of both PD-1 and PD-L1 (sPD-L1) molecules can be found circulating in peripheral blood. For this thesis, we will focus on soluble PD-L1 (sPD-L1) only. It is thought that sPD-L1 can be generated in many ways. This can include proteolytic cleavage of membrane-bound PD-L1 by MMPs, or sPD-L1 may be secreted via cellular mechanisms as a truncated protein lacking the transmembrane domain generated by posttranscriptional alternative splicing. Circulating extracellular vesicles harbouring membrane bound PD-L1 may also mimic soluble forms[208–210]. Secretion of sPD-L1 may be limited to only mature dendritic cells[210]. sPD-L1 adds to the complexity of the PD-1/PD-L1 pathway by removing the spatial element that is required during the physical engagement of lymphocyte associated PD-1 and hepatocyte PD-L1 during T-cell activation. This potentially allows for systemic and non-specific promotion of T-lymphocyte tolerance and exhaustion.

Given the importance of the PD-1/PD-L1 pathway, it is possible that quantification of sPD-L1 may provide a valuable measure of immune regulatory processes in people living with chronic HBV infection, without the need for invasive liver biopsies. Indeed, sPD-L1 has been used

previously to indicate treatment efficacy and predictors of long-term prognosis in people with cancer[211,212]. Few studies have evaluated sPD-L1 in the context of chronic HBV infection, which will be discussed further in chapter 4.

1.5.8 Detecting exhausted T-cells in peripheral blood

The emerging dogma of T-cell exhaustion describes the fate of antigen-specific T-cells as highly dysfunctional and marked for deletion via Fas dependant processes, resulting in a severely diminished pool of measurable cells that also exhibit signs of tissue residence. Many researchers advocate for the use of liver biopsies, despite the potentially serious adverse effects, the need for multiple needle passes to recover a sufficient quantity of tissue and the potential need to sample multiple spatial areas of the liver, as there are distinct antigenic differences in different areas of the liver[213,214]. HBV-specific T-cells with an exhausted profile can be detected in peripheral blood, but only after enrichment with HLA-specific multimers for various HBV epitopes[187,215]. Previous studies of HBV-specific responses almost exclusively use HLA-A*0201 for T-cell selection. This may limit the broad use of HBV specific studies; for example, a large burden of HBV is within sub-Saharan Africa, where HLA classes are highly diverse[216,217]. Additionally, there is a lack of consistency in selecting HBV protein epitopes used in multimer selection[218]. Collectively, there is a need for peripheral, non-HBV specific methodologies, accessible for clinical laboratories, that may be useful in monitoring.

1.5.8.1 Anti-PD-1/PD-L1 therapies

Given the potency of the PD-1/PD-L1 pathway in curtailing the immune response, it is a popular choice for therapeutic targeting. Anti-PD-1 and anti-PD-L1 therapies have been proven effective in reinvigorating T-cell responses in many cancer types[219]. The overexpression of PD-1 during chronic HBV infection pathogenesis has driven interest in adopting a similar immunotherapeutic approach. In a phase 1 randomised clinical trial, nivolumab, an anti-PD-1 monoclonal antibody, was administered to virologically suppressed patients with HBeAg-infection with and without a novel therapeutic vaccine. Nivolumab monotherapy and in combination with therapeutic vaccination was associated with a partial restoration of HBsAg specific T-cells. However, the level of response was variable, and only one patient had a sustained response[220]. Several novel therapeutics that target the PD-1/PD-L1 pathway are in early-stage clinical trials, with either competitive inhibition using monoclonal antibodies, or inhibition of the expression of PD-L1[221] mRNA. It is important to highlight that the end goal

for most immunotherapies for chronic HBV infection is loss of HBsAg, the “functional cure”, which is more likely to be achieved than the loss of cccDNA, often called the “sterilising cure”.

1.6 Aims of this thesis

HBV is worryingly underdiagnosed, despite significant associated mortality and the requirement of lifelong therapeutic interventions in a subset of patients. The development of a therapeutic agent that results in sustained viral control with a finite dosing schedule is of great interest. Chronic infection with HBV detrimentally alters the immune response and characteristically induces lymphocyte dysfunction through the PD-1/PD-L1 checkpoint pathway. Biomarkers for therapeutic monitoring have been suggested but have yet to be put in the context of HBV.

In relation to these questions, I believed there was a need to first understand the programmatic infrastructure in place in the UK to identify the hidden population of those living with HBV that may benefit from the immense push for the development of curative therapeutics. To attempt to understand the landscape of HBV screening and seropositivity in England, I used a nationally representative framework of GP practices to assess factors associated with the offer of HBsAg screening and seropositivity and explore recorded linkage to specialist care.

I then set up and recruited a cohort of patients living with chronic HBV infection, with a diverse background of disease profiles. In this cohort, I measure plasma levels of sPD-L1 and assessed associations with a range of standard and novel biomarkers and parameters. I then explored PD-1 expression on PBMCs and potential associations with sPD-L1 expression and clinical characteristics.

Finally, I utilised a novel, deep immunophenotyping platform and machine learning algorithms to elucidate potential phenotypes associated with sPD-L1 levels or antigen load in patients living with chronic HBV infection.

Overall, this thesis aims to highlight the epidemiological disparities of the HBV pandemic that will need to be addressed prior to or in concordance with future curative strategies

2 Materials and Methods

2.1 Patient-centred language

The stigma associated with hepatitis B infection is strong and often overlooked[33]. In 2011, UNAIDS published terminology guidelines of the preferred terminology when addressing HIV related communication to normalise and strengthen the global response to the HIV epidemic[222]. These guidelines have been subsequently adopted by several leading research journals as submission guidelines. To our knowledge, no such guidelines have been published related to HBV despite the need for a global and multifaceted approach needed to tackle the ongoing HBV epidemic. Although it is likely that the effect of person-centred language will take time to adopt, attempts must be made to afford the same benefit and respect to patients living with hepatitis B as is given to those living with other chronic viral infections[222].

2.2 Study populations and sampling

2.2.1 Oxford Royal College of General Practitioners (RCGP) Research Surveillance Network (RSC)

Data from 419 primary care practices comprising all patients who had a general practitioner (GP) record between January 2008 and July 2019 were extracted using READ2 or CTV3 codes. READ2 and CTV3 act as reference codes that identify patient demographics, clinical interactions, tests, and diagnoses in electronic healthcare records[223]. The READ2 and CTV3 codes used for data extraction are available in appendix 9.3. The data extraction included demographics, country of birth, ethnicity, National Health System (NHS) region (i.e., London, Midlands and East, North, South), and time registered with the current GP practice. Country of birth was categorised as high (≥8%), intermediate (2-7%), or low (<2%) HBsAg seroprevalence. Referrals to specialist follow-up were also extracted.

The case definition for HBsAg screening was a record of i) recognition of the need for HBsAg testing, or ii) offer of HBsAg testing.

The case definition for HBsAg seropositivity was a record of i) history of HBsAg seropositivity or ii) positive HBsAg test result.

2.2.1.1 Socioeconomic and geographical data

Location data, including Indices of Multiple Deprivation (IMD), local super output area (LSOA) and urban-rural classification, were derived from the practice postcode. IMD is a measure of relative deprivation which considers seven domains: income, employment, education, health, local crime, barriers to housing and services, and living environment[224]. LSOAs are small geographical areas containing approximately 1,500 people, which are used to describe national statistics. The local settlement classification was presented in two broad categories: urban and rural. The maps of the prevalence of HBsAg screening and HBsAg seropositivity were generated by matching LSOAs to their corresponding local authority district (LAD) using data available from the office of national statistics[225]. The prevalence of HBsAg screening per LAD was calculated using the total number of individuals per LAD in the cohort and mapped using the 2017 LAD boundaries available from the office of national statistics[226]. LSOAs that did not match to a LAD in England were removed from the analysis. All maps were created in ArcGIS Pro (Version 2.6 API).

2.2.1.2 HBsAg screening indicators

Screening indicators included in the analyses were adapted from those in the NICE recommendations[227], according to the availability of suitable codes within the GP records. They comprised country of birth, MSM, current or past IDU, close HBV contact, history of imprisonment, and a recorded diagnosis of a blood-borne or sexually transmitted infection (BB/STI), including hepatitis C virus (HCV), HIV, syphilis, gonorrhoea (GC), scabies, *trichomonas vaginalis* (TV), genital herpes (GH) and human papillomavirus (HPV). Chlamydia was not included as screening results were not recorded. Potential screening indicators of interest that did not have suitable codes within GP records (e.g., having multiple sexual partners and people living in care homes) were not included. Screening indicators were considered if they were identified prior to or at the same time as HBsAg screening; if there was no record of HBsAg screening, we considered indicators at any time they were recorded. Pregnancy status during the study period was captured based on published ontologies[228].

2.2.2 The INTERFACE study

INTERFACE was an observation study, cross-sectional in design. Patients were recruited at the Royal Liverpool University Hospital Liverpool, UK while attending routine clinic visits. All patients provided written and informed consent prior to sampling. The trial received ethical

approval from the Yorkshire and Humber Research ethics committee (REF: 18/YH/0286). The favourable ethical approval letter can be found in appendix 9.1 and 9.2. Patients were recruited with the aim of sampling all HBV disease phases as described in Table 2.1. Patients with histologically or documented cancers, presence of AIDS defining illnesses, pregnant or breastfeeding women, history of chronic or systemic inflammatory diseases were excluded from recruitment. Whole venous blood was collected via venepuncture in either K_2EDTA or serum separator tubes SST™ II advanced tubes, processed and stored. Pseudoanonymised data were collected from the participants' medical records. Clinical data collected were from routine blood tests either on the day of study sampling or the previous two weeks. Following recruitment patients were then grouped into HBV infection phases as described in table 2.1 with routine biomarkers measured as part of routine care at recruitment.

Table 2.2.1: Clinical characterisation of people with chronic HBV

HBV Disease Category	HBsAg	HBeAg	HBcAb	HBV DNA[a]	ALT[b]	NUC
HBeAg+ Infection	+	+	+	+++	↔	-
HBeAg+ Hepatitis	+	+	+	+++	↑↑	+/-
HBeAg- Hepatitis	+	-	+	++	↑↑	+/-
HBeAg- Infection	+	-	+	+/-	↔	-

[a] (+) = <2,000 IU/ml (++) = ≥2,000- <19,999 IU/ml (+++) = ≥ 20,000 [b] (↔) = <40 IU/ml (↑↑) = ≥40IU/ml

2.3 Sample Preparation

All reagents with suppliers and reference numbers are available below in section 2.8.1.

2.3.1 Serum and plasma

Whole blood was allowed to clot in the serum separator tube (SST) or EDTA tube for up to 60 minutes in a vertical position. Tubes were then centrifuged at 1,500 x g for 10 minutes in a swinging bucket rotor. The break was disengaged for plasma tubes. The resulting serum or plasma was aspirated an aliquoted into sterile cryovials and stored at -80°C

2.3.2 PBMCs

Whole blood was collected in EDTA tubes from venepuncture and processed within 2 hours of collection. 30ml of whole blood was split equally into two 50ml Falcon tubes containing 13ml of pre-warmed RPMI-1640. The EDTA tubes were then washed with 2ml of RPMI-1640 to remove any remaining blood. The whole blood + RPMI mixture was then carefully layered on top of 15ml of Lymphoprep in a fresh 50ml Falcon tube. The layered diluted blood and

Lymphoprep tube was then centrifuged at 800xg 20°C for 15 minutes with full acceleration and no brake. PBMCs were carefully harvested by aspiration from the resulting interface between the diluted plasma and underlying Lymphoprep with Pasteur pipettes into a clean Falcon tube. The PBMCs were then washed twice by resuspending in 50ml of R-10 media and centrifuged at 400xg for 10 minutes (full acceleration and deceleration). The PBMCs were then resuspended in 10ml of R-10 media and counted as described in section 2.2.4. A total of $1.2x10^7$ cells were removed for use in fresh flow cytometry, the remaining cells were then cryopreserved as follows. PBMCs were centrifuged at 400xg for 10 minutes and supernatant aspirated. The PBMC pellet was then resuspended in a mixture of 90% heat-inactivated FBS and 10% DMSO (SIGMA) at a concentration of $5x10^6$cells/ml and divided evenly among cryovials. The outer chamber of a room temperature Nalgene® Mr. Frosty™ was filled with 2-propanol; all cryotubes were then transferred to the Mr. Frosty™ which was subsequently transferred to a -80°C freezer for 24-48 hours to cool slowly at 1°C min^{-1}. The cryovials containing PBMCs were then transferred to liquid nitrogen for long-term storage.

2.3.3 Cell counting

The PBMCs were counted by removing 20µl of stock PBMCs and diluted 1:1 with ViaStain™ AOPI staining solution and mixed well. A disposable Cellometer counting slide was loaded with 20µl of stained PBMCs and loaded into the Cellometer Auto 1000. Brightfield microscopy was used for focusing, before live/dead discrimination and automatic counting under fluorescence. The resulting cell count recorded alongside the calculated viability. All samples had viability of $\geq$90%.

2.4 Immunology

2.4.1 Flow cytometry

The flow-cytometry panel used was designed to include broad detection of immune cell subsets and to determine the expression of PD-1. The antibodies used at their working concentration are detailed in table 2.2. All antibodies were sourced from Biolegend and mouse IgG1, k isotype. Optimal antibody concentration was determined by titration on archived cryopreserved PBMCs.

Table 2.2: Antibodies used for lymphocyte phenotyping

Antibody	Flurophore	Product Code	Clone	Concentration	Panel A	Panel B
CD56	PE	362508	5.1H11	1:300	✓	

CD3	BV421	344834	SK7	1:300	✓	✓
CD8	APC/Fire 750	344746	SK1	1:300	✓	✓
CD279 (PD-1)	APC	329908	EH12.2H7	1:100	✓	✓
CD45	FITC	304006	HI30	1:300	✓	✓
CD4	PerCP/Cy5.5	300530	RPA-T4	1:300	✓	
CD39	BV 510	328219	A1	1:300		✓
CD127	PE/Cy7	351319	A019D5	1:300		✓
TCF1[a]	PE	655207	7F11A10	1:100		✓
FcX (anti-CD16/32)	N/A	422302	N/A	1:50	✓	✓

[a] Intracellular antibody. Conjugated antibody-flurophores used in flow cytometry phenotyping.FcX=Fc receptor Ig blocking agent. PE=phycoerythrin, PE/Cy7=phycoerythrin-cyanine 7, APC/Fire 750=allophycocyanin-cyanine 750, APC=allophycocyanin, FITC=fluorescein, PerCP/Cy5.5=peridinin chlorophyll cyanine 5.5.

2.4.1.1 Flow cytometry spectral compensation

Compensation was performed at each sample acquisition day with BD anti-mouse IgG-k compensation beads according to manufacturer instructions as follows. A separate 5ml round-bottom tube was labelled for each antibody. To each tube, 100µl of staining buffer, 60µl of negative control compensation beads and 60µl of anti-mouse IgG-k compensation beads was added and vortexed. To each tube, 20µl of individual antibody prediluted to working concentration was added; no antibodies were added to the unstained tube. Tubes were vortexed and incubated at room temperature for 30 minutes. Following incubation, 2ml of staining buffer was added to each tube and centrifuged at 200xg for 10 minutes, to pellet the beads, and supernatant aspirated. Each pellet was resuspended in 500µl of cold staining buffer prior to acquisition. Each tube was acquired separately on medium flow rate. The compensation was applied at acquisition with the BD FACS DIVA software.

2.4.1.2 Flow cytometry controls

Fluorescence minus one (FMO) controls were used to determine and gate positive populations. FMO controls contained an antibody mixture of all panel markers minus the one being controlled for. FMO controls were used for PD-1 (APC), CD14 (PE/Cy7), CD56 (PE), CD127 (PE/Cy7) and CD39 (BV510). FMO controls were not used for populations with clear and discrete separations e.g. CD4, CD8, CD45 populations.

2.4.1.3 Extracellular staining

The PBMCs were seeded onto a 96-well round-bottom plate at a density of $1x10^6$ cells per well for the two experimental tubes and $5x10^5$ cells per well for each FMO control well. All cells

were used fresh. The 96-well plate was kept on a bed of wet ice. The plate was then spun at 300xg for 5 minutes at 4°C. The supernatant was removed by inverting the plate and flicking briefly. The cells were resuspended with cell staining buffer supplemented with a 1:50 dilution of Fc-block (unconjugated anti-CD16/32), to prevent non-specific binding and incubated on ice for 20 minutes. The plate was then centrifuged at 300xg for 5 minutes at 4°C and the supernatant removed by inversion. The cells were then resuspended in 200ul of the respective panel A antibody cocktail as detailed in table 2.2 and incubated on ice protected from light for 30 minutes. Following incubation, each well was washed with 300µl of staining buffer and centrifuged at 300xg for 5 minutes; the wash step was repeated twice.

2.4.1.4 Intracellular staining

All extracellular markers for panel A or B were stained as described above prior to intracellular staining. The 96-well plate containing extracellularly stained PBMCs was gently pulse vortexed to resuspend the cell pellet in residual volume of staining buffer remaining from the extracellular staining procedure. To each well, 200µl pre-diluted Foxp3 Fixation/permeabilization buffer was added and incubated in the dark for 30 minutes on ice. The cells were then washed with 200µl of permeabilization buffer in each well and then centrifuged at 600xg for 5 minutes at room temperature. The supernatant was discarded, and the wash step repeated for a total of two washes. After the final wash, the cells were resuspended in 100µl of permeabilization buffer supplemented with 1:50 dilution of Fc-block and incubated for 20 minutes on ice, protected from light. Without washing, the cells were stained with intracellular antibodies in panel B at their respective working concentration were added to each well and incubated for 30 minutes on ice, protected from light. Following staining, the cells were washed with 200µl of 1x permeabilization buffer per well and centrifuged at 600xg for 5 minutes at room temperature. The wash step was repeated for a total of two washes and transferred to 5ml round-bottom polystyrene test tubes. The remaining cell pellet was then resuspended in 500µl of staining buffer and kept on ice or at 4°C until acquisition.

2.4.1.5 Acquisition of stained PBMCs

All tubes were acquired on BD Canto II flow cytometer (Becton Dickinson, San Jose, CA) utilizing BD FACS DIVA software (Becton Dickinson, San Jose, CA). Prior to experimental tube acquisition, the compensation matrix was calculated by acquiring the compensation control tubes. Tubes were acquired at medium flow rate until dry.

2.4.1.6 Analysis of FCS files

All flow cytometry data collected were then analysed in FlowJo version 9 (Becton Dickinson Life Sciences). FMO controls were used to determine positive gates. A representative gating diagram is available in Figure 2.1. As tubes were acquired until dry, the number of cells varied therefore cell counts used in this analysis were normalised to the total number of leukocytes ($CD45^+$ cells) and presented as a percentage of the $CD45^+$ population unless otherwise stated.

Figure 2.1: Representative gating diagram for the identification of T-lymphocyte populations

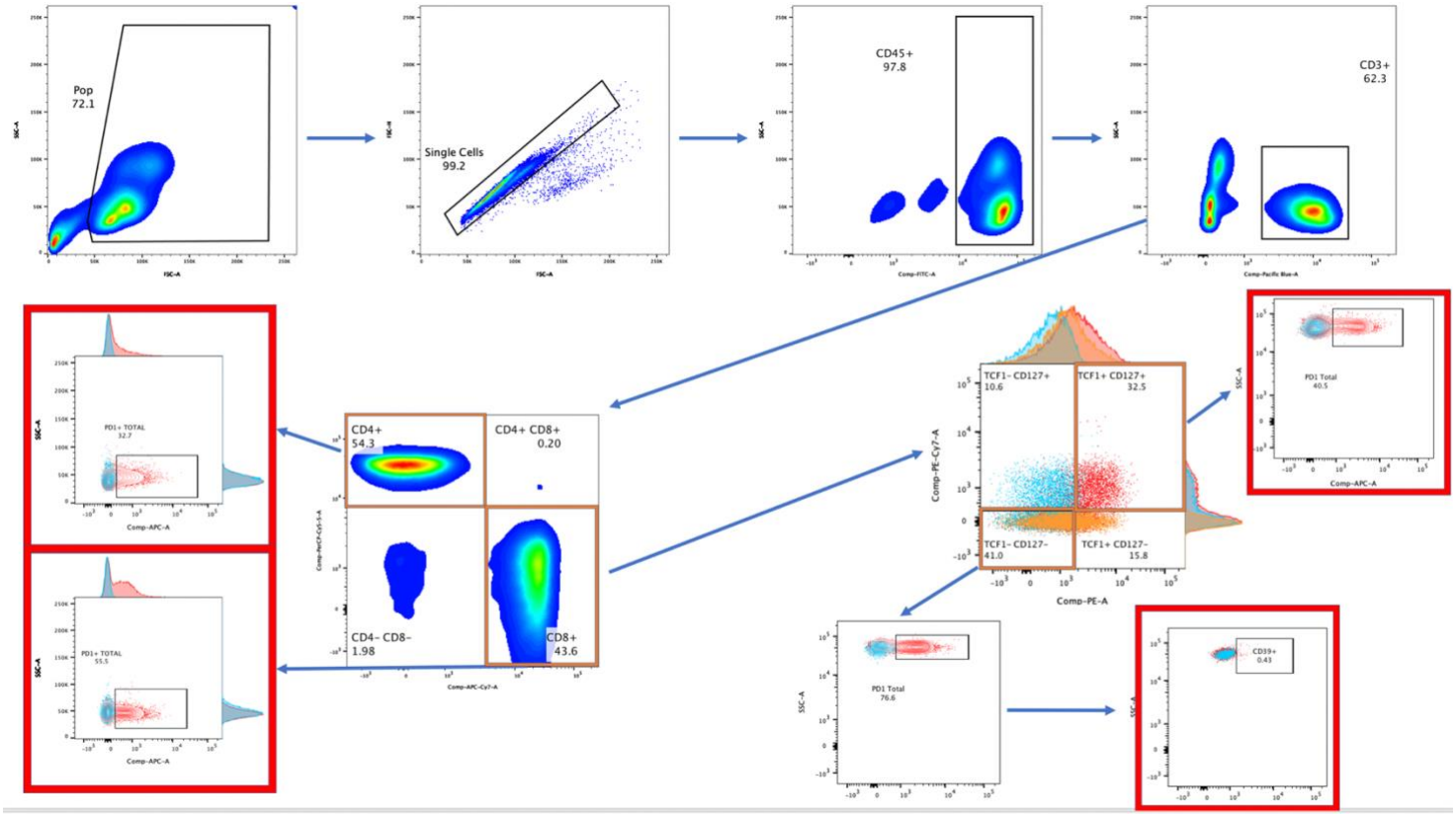

Representative gating diagram for the identification of T-lymphocytes. Orange outline boxes represent terminal parent populations and red outline boxes identify terminal populations. Overlaid blue and orange populations represent the FMO controls.

2.4.2 Mass Cytometry

2.4.2.1 PBMC Preparation and cadmium barcoding

PBMCs isolated from patients described in section 2.3.2 were retrieved from liquid nitrogen and quickly thawed by swirling in a 37°C water-bath. When a small ice pellet remained, 1ml of R-10 media pre-warmed to 37°C was added to the cryovial. The cell suspension was then transferred to a 15ml conical tube containing 9ml of R-10 at 37°C and centrifuged at 300xg for 10 minutes. The supernatant was removed and resuspended in 1ml of R-10 supplemented with 500 units of Benzonase and transferred to a 12 well plate. The cells were allowed to rest for one hour at 37°C and 5% CO_2. Following a rest, the cells were then removed by aspirating the suspension with a Pasteur pipette and transferred to a 15ml conical tube. The well was then washed twice with RPMI-1640 and checked under a light microscope to ensure there was no adherent cells. The cell suspension was centrifuged for 10 minutes at 300xg. The supernatant was aspirated, and the cells resuspended in 1ml of RPMI-1640 for counting. The cells were counted as described in section 2.2.4. The cells from individual patients were then barcoded with a single cadmium isotope anti-CD45 antibody (Fluidigm).

2.4.2.2 Anti-CD45 Cadmium isotope barcoding

A cell viability of $\geq$80% was required for the MAXPAR staining procedure. The PBMCs were resuspended at a concentration of $1x10^6$/ml if three samples were barcoded and $1.5x10^6$ if two samples were barcoded, in MAXPAR cell staining buffer (MCSB). The PBMCs were then briefly pelleted by centrifugation at 300xg and resuspended in 50µl of cold MCSB. Fc-block was added at a volume of 5ul and incubated for 5 minutes at room temperature. MCSB supplemented with 1 test (1µl) of anti-human anti-CD45 bound to cadmium isotope 106, 110 or 111 was then added to the cell-Fc-block suspension and incubated for 30 minutes at room temperature. The PBMCs were then washed with 1ml of cold MCSB and centrifuged at 500xg for 10 mins. The wash was repeated for three cycles to ensure removal of excess anti-CD45 barcoding antibody. All patient samples were then combined into a single tube and resuspended in 50µl of cold MCSB.

2.4.2.3 Maxpar Direct Immune Profiling assay

The Maxpar Direct Immune Profiling Assay (MDIPA) was selected to minimise intersample and interrun variability[229]. All reagents unless otherwise stated were provided by the manufacturer with the MDIPA assay to minimise metal contamination. The cadmium isotope labelled anti-CD45 PBMCs were supplemented with 5ul of Fc-block and incubated for 10

minutes at room temperature. MCSB supplemented with anti-PD-L1 and anti-PD-1 at a concentration of 1:50 and 1:100, was then added followed by the entire cell suspension then added to the MAXPAR staining tube that contained the lyophilized antibody mixture as described in Table 2.3 and incubated at room temperature for 30 minutes. The stained cells were then washed with 3ml of MCSB and centrifuged at 500g for 5 minutes. The cell was procedure was repeated for three cycles. The supernatant was discarded on the final wash and cell pellet resuspended in 1ml of freshly prepared and filtered 1.6% formaldehyde (SIGMA) prepared in PBS. The fixed-stained cells were then centrifuged at 800xg for 10mins and resuspended in 1ml of fix/perm buffer supplemented with 125nM intercalator-IR and incubated 4°C overnight or until acquisition.

Table 2.3: Metal isotope tagged antibodies

Antibody (clone)	Isotope
CD45 (HI30)	^{89}Y
CD196 /CCR6 (G034E3)	^{141}Pr
CD123 (6H6)	^{143}Nd
CD19 (HIB19)	^{144}Nd
CD4 (RPA-T4)	^{145}Nd
CD8a (RPA-T8)	^{146}Nd
CD11c (Bu15)	^{147}Sm
CD16 (3G8)	^{148}Nd
CD45RO (UCHL1)	^{149}Sm
CD45RA (HI100)	^{150}Nd
CD161 (HP-3G10)	^{151}Eu
CD194/CCR4 (L291H4)	^{152}Sm
CD25 (BC96)	^{153}Eu
CD27 (O323)	^{154}Sm
CD57 (HCD57)	^{155}Gd
CD183/CXCR3 (G025H7)	^{156}Gd

Antibody (clone)	Isotope
CD185/CXCR5 (J252D4)	^{158}Gd
CD28 (CD28.2)	^{160}Gd
CD38 (HB-7)	^{161}Dy
CD56/NCAM (NCAM16.2)	^{163}Dy
TCRgd (B1)	^{164}Dy
CD294 (BM16)	^{166}Er
CD197/CCR7 (G043H7)	^{167}Er
CD14 (63D3)	^{168}Er
CD3 (UCHT1)	^{170}Er
CD20 (2H7)	^{171}Yb
CD66b (G10F5)	^{172}Yb
HLA-DR (LN3)	^{173}Yb
IgD (IA6-2)	^{174}Yb
CD127 (A019D5)	^{176}Yb
Cell-ID Intercalator-103Rh	^{103}Rh

Antibodies were provided in lyophilised form in a single tube to which cadmium isotope barcoded PBMCs were added.

Acquisition of stained MDIPA cells

On the day of acquisition cells were centrifuged at 800xg for 5 minutes and the supernatant aspirated. The cells were washed by adding 2ml of MCSB, centrifuging at 800xg for 5 minutes and aspirating the supernatant and repeated for a total of 2 washes. The cell pellet from the final wash was resuspended in 2ml of Maxpar acquisition buffer (Fluidigm). The cells were then counted as described in 2.3.3. The cells were resuspended at a concentration of $5x10^5$ in acquisition buffer supplemented with 0.1X equalizer beads (Fluidigm). The cells were then strained with a 35µm cell strainer and acquired with the WB injector at a rate of 300 events per second until 300,000 events were recorded.

2.4.2.4 Bivariate gating of MDIPA

The quality of the mass cytometry events and presence of metal contamination signals was assessed automatically normalised with Fluidigm® Maxpar Pathsetter® software. Bivariate gating was conducted in FlowJo® and guided by the Fluidigm technical note *Approach to Bivariate Analysis of Data Acquired Using the Maxpar Direct Immune Profiling Assay*[230] where most positive signals are considered for cells $>x10^1$.

2.4.2.5 CITRUS machine learning

CITRUS supervised machine learning pipeline employed in chapter six was adapted from[231]. The CITRUS analysis is described in detail chapter 6. Dr. Zaida Vergara, a field specialist from Cytobank, Inc, provided guidance for the interpretation and execution of CITRUS analysis.

2.5 ELISA

2.5.1 sPD-L1

Soluble PD-L1 was measured in paired plasma samples at Microcoat Biotechnologie GmbH, Germany by Dr. Patricia Wolf.

2.5.1.1 Ella

sPD-L1 levels were measured with the biotechne® protein simple Simple Plex™ Ella platform as directed by the manufacturer's instructions.

2.5.1.2 SIMOA

sPD-L1 levels were measured with the PD-L1 assay (ref: 102648) on the quanterix HD-X Analyzer™ as directed by the manufacturer's instructions.

2.5.2 HBsAg

The concentration of HBsAg was measured in serum with the Roche Elecsys® HBsAg II quant II immunoassay as directed by the manufacturer's instructions. The assay was run on the cobas e 602 module at the Royal Liverpool University Hospital, Liverpool Clinical Laboratory with the assistance of Dr. Anu Chawla.

2.5.3 HBeAg

The concentration of HBeAg was measured in serum of patients with confirmed HBeAg positivity by utilising the Roche Elecsys® HBeAg assay as directed by the manufacturer's instructions. Briefly, serial dilutions of the 1st WHO International Standard for hepatitis B virus e antigen (Paul-Ehrlich-Institute, Langen Germany), reconstituted in sterile ultrapure water, and run in parallel with patients samples to produce a standard curve. The concentration of HBeAg was then calculated based on the standard curve and expressed as PEI U/ml. The samples were run on the cobas e 602 module at Roche pRED, Basel, Switzerland by Dr. Priscila Teixeira.

2.6 Virological Parameters

2.6.1 HBV DNA

Plasma concentrations of HBV DNA was determined by either the Hologic® Aptima™ HBV Quant assay as part of routine care at the Royal Liverpool, Liverpool Clinical Laboratories by local staff, or by Cepheid® Xpert® HBV Viral load assay performed in the Ronald Ross building as per manufacturers instructions. Where HBV DNA loads were detectable below the respective lower limit of quantification (LLOQ), HBV DNA values were assigned an arbitrary value of 5 IU/ml. If HBV DNA was not detected, they were assigned a value of 1.5 IU/ml.

2.6.2 HBV RNA

Plasma concentrations of HBV RNA were determined with real-time PCR methods adapted from van Brömmel et al 2015[232]. Measurement was conducted at DDL Diagnostic Laboratories, Rijswijk, Netherlands under the supervision of Dr. Sanne Hulpas.

2.7 Statistical Analysis

A variety of statistical techniques and approaches were used throughout this thesis and specifics will be described in each chapter. In general, the data were summarised with dichotomous variables represented as counts and continuous variables as medians with interquartile ranges (IQR). Non-parametric Kruskal-Wallis was used to compare grouped categorical variables

with significant finding (<0.05) evaluated with Dunn's post-hoc test. Differences between two groups were detected with Fisher's exact test. Continuous variables were either assessed with non-parametric Spearman's rank correlation or parametric linear regression analysis depending on requirements of statistical test. Due to the exploratory nature of many of these studies, no p-value corrections were performed, thus should only be considered indicative of possible associations unless indicated. All statistical analysis was done in STATA version 14 (College Station, TX, USA) and GraphPad Prism 9 for Mac (La Jolla, California, USA) under the supervision of Dr. Colette Smith at the Institute for Global Health, University College London.

2.8 Reagents and Recipes

2.8.1 Reagents and source

Table 2.4: Reagents and suppliers

Reagent/Kit	Supplier	Reference Number
RPMI 1640 -/-	Gibco	21870092
Lymphoprep	Stemcell Technologies	07851
Fetal Bovine Serum heat inactivated	Gibco	16140070
DMSO	Sigma	D2650
2-propanol	Merck	278475-1L
Penicillin/Streptomycin	Gibco	15140-122
GlutaMAX	Gibco	35050-061
ViaStain® AOPI Staining solution	Nexcelom	CS2-0105-5ml
Cellometer counting slides	Nexcelom	SD100
Anti-mouse Ig, k/Negative control compensation particles set	BD Biosciences	552843
Staining Buffer	Biolegend	420201
Foxp3/ Transcription factor staining buffer set	Invitrogen	00-5523-00
Benzoase 2500Units	Merck	E1014-25KU
MDIPA Profiling assay	Fluidigm	201325
Pierce 16% formaldehyde	Fisher	10751395
Elecsys® HBsAg II quant II	Roche®	N/A
Elecsys® HBeAg	Roche®	N/A
WHO 1st international standard HBeAg	Paul-Ehrlich-Institute	129097/12
Anti-human CD45 (HI30)-106Cd	Fluidigm	3106001C
Anti-human CD45 (HI30)-110Cd	Fluidigm	3110001C
Anti-human CD45 (HI30)-111Cd	Fluidigm	3111001C
Anti-human PD-1(EH12.2H7)-175Lu	Fluidigm	3175008B
Anti-human PD-L1(29E.2A3)-159Tb	Fluidigm	3159029B

2.8.2 Recipes

2.8.2.1 R-10 media

The following ingredients were added to a 50ml falcon tube and mixed by swirling. 44.5ml of RPMI + 0.5ml of penicillin/streptomycin + 0.5ml of GlutaMAX. The media was stored at 4°C until use.

2.8.2.2 Freezing media

The following ingredients were added to a sterile 50ml falcon tube and mixed by swirling. 20ml of FBS + 5ml of DMSO. The media was stored at 4°C until use.

3 Hepatitis B virus infection in primary care across England: Data from the Royal College of General Practitioners Research Surveillance Network

3.1 Introduction

The World Health Organisation (WHO) estimates that in 2019 there were 296 million people living with chronic hepatitis B virus (HBV) infection, defined as seropositivity for the hepatitis B surface antigen (HBsAg)[233]. Modelling studies estimate that the global prevalence of HBsAg was 3.9% (3.4-4.6%)[234] in 2016, with substantial variations by location and population; only approximately 10% of those living with chronic HBV infection have been diagnosed, and 22% of those with a diagnosis receive antiviral treatment[233]. In 2019, 820,000 people died of HBV-related complications, primarily liver cirrhosis and hepatocellular carcinoma (HCC) [233]. Although vaccination programmes are reducing HBsAg seroprevalence in children <5 years of age, HBV-related mortality is predicted to continue to exceed 500,000 annually until at least 2070[235]. WHO has called for enhanced efforts to increase awareness of chronic hepatitis B, improve the use of prevention strategies, and expand access to testing and care [236].

The United Kingdom (UK) introduced hepatitis B into the routine infant immunisation programme in 2017[37]. In 2018, the annual incidence of acute or probable acute HBV infection was 0.68 per 100,000 individuals in England, reaching 1.52 per 100,000 among men aged 45-54 years[237]. The estimated prevalence of chronic HBV infection is <1%,[238] although it is acknowledged that prevalence may vary regionally and between communities, and that estimates may not account for substantial underdiagnosis[237]. Notably, the incidence of HCC in England has increased nearly three-fold in the past two decades [239]. Universal HBsAg screening of pregnant women has been part of antenatal care for two decades and uptake is high[240]. Other forms of screening are targeted to specific screening indicators: in 2013, the National Institute for Health and Care Excellence (NICE) recommended HBsAg testing for several groups, including people born or brought up in countries with HBsAg prevalence ≥2%, those with a history of current or past injecting drug use (IDU), close contacts of people with HBV infection, prisoners, people in residential care, men who have sex with men (MSM), and other people at risk via unprotected sexual exposure such as those with multiple sexual partners or diagnosed with sexually transmitted infections (STIs)[227]. Sentinel surveillance indicates that in 2018 HBsAg seroprevalence was 0.3% among 133,236 women attending for antenatal care and 0.9%

among 417,617 people undergoing testing within other front-line primary and secondary care services, with the largest non-antenatal dataset (~23%) coming from general practice[241]. Given the role of primary care in driving HBsAg testing, we analysed data from the Royal College of General Practitioners (RCGP) Research and Surveillance Centre (RSC) to define HBsAg testing patterns and HBsAg seroprevalence in general practice across England[242]. In collaboration with the University of Oxford and the UK Health Security Agency, the RCGP-RSC collects and monitors pseudonymised data from patients registered at a large network of primary care practices across all regions of England.

3.2 Methods

3.2.1 Study population

Data from 419 primary care practices comprising all patients who had a general practitioner (GP) record between January 2008 and July 2019 were extracted using READ2 or CTV3 codes available in Appendix 9.3. Briefly, the data extraction included age, gender, country of birth, ethnicity, National Health System (NHS) region (i.e., London, Midlands and East, North, South), time registered with the current GP practice, and country of birth. Country of birth was categorised as high (≥8%), intermediate (2-7%), or low (<2%) HBsAg seroprevalence[42]. Referrals to gastroenterology, infectious diseases, or hepatology clinics for specialist follow-up were also extracted. Data extraction was managed by the designated individual Julian Sherlock utilising the list of study specific READ2/CTV3 codes.

The case definition for HBsAg screening was a record of i) recognition of the need for HBsAg testing, or ii) offer of HBsAg testing. Only the first record was considered in the analysis.

The case definition for HBsAg seropositivity was a record of i) history of HBsAg seropositivity or ii) positive HBsAg test result.

Only one test was included in the analysis which allowed for the possible inclusion of both chronic and acute infections.

3.2.2 Socioeconomic and geographical data

Location data, including Indices of Multiple Deprivation (IMD), were derived from the practice postcode. The maps of the prevalence of HBsAg screening and HBsAg seropositivity were

generated by matching practice area to their corresponding local authority (LAD) using data available from the office of national statistics[225]. The prevalence of HBsAg screening per LAD was calculated using the total number of individuals per LAD in the cohort and mapped using the 2017 LAD boundaries available from the office of national statistics[226]. LSOAs that did not match to a LAD in England were removed from the analysis. All maps were created in ArcGIS Pro (Version 2.6 API).

3.2.3 HBsAg screening indicators

Screening indicators included in the analyses were adapted from those in the NICE recommendations[227], according to the availability of suitable codes within the GP records. They comprised country of birth, MSM, current or past IDU, close HBV contact, history of imprisonment, and a recorded diagnosis of a blood-borne or sexually transmitted infection (BB/STI), including hepatitis C virus (HCV), HIV, syphilis, gonorrhoea (GC), scabies, *trichomonas vaginalis* (TV), genital herpes (GH) and human papillomavirus (HPV). Chlamydia was not included as screening results were not recorded. Potential screening indicators of interest that did not have suitable codes within GP records (e.g., having multiple sexual partners) were not included. Screening indicators were considered if they were identified prior to or at the same time as HBsAg screening; if there was no record of HBsAg screening, we considered indicators at any time they were recorded. Pregnancy status during the study period was captured based on published ontologies[228].

3.2.4 Statistical Analysis

Variables were summarised as absolute counts with frequencies or as medians with interquartile ranges (IQR) if categorical or continuous, respectively. Confidence intervals (CI) for prevalence were calculated by Wilson binomial test. In addition to individual variables, cumulative variables were created that considered having ≥1 screening indication (besides MSM and including IDU history, close HBV contact, imprisonment history, syphilis, GC, scabies, TV, GH, HPV, HCV and HIV) or having ≥1 BB/STI record (among syphilis, GC, scabies, TV, GH, HPV, HCV, and HIV). Temporal trends in HBsAg screening were evaluated by counts per year, normalised by the total number of patients registered within that year. Univariate and multivariate logistic regression models were used to explore factors associated with two outcomes: 1) proportion of individuals with a record of HBsAg screening; 2) proportion of individuals with a record of HBsAg seropositivity. For outcome 1, the main analysis excluded records with a history of pregnancy at any time due to the inclusion of

HBsAg screening in routine antenatal booking (which had limited recording in GP files); thus, the gender category for outcome 1 comprised MSM, other men, and women without a pregnancy record. The characteristics of women with a pregnancy record, overall and by screening status, were tabulated separately. For outcome 2, the gender category comprised MSM, other men, and all women. In the main models, multivariable adjustments were approached in two ways: model 1 adjusted for age, gender (as defined above), time registered at current GP, ethnicity, IMD quintile, NHS region, and ≥1 screening indication (among IDU history, close HBV contact, imprisonment history, or at least one BB/STI diagnosis); model 2 adjusted for age, gender (as defined above), time registered at current GP, ethnicity, IMD quintile, NHS region, and the individual screening indications IDU history, close HBV contact, imprisonment history, and at least one BB/STI diagnosis. Adjustment of both time registered at current GP and age was permissible due to the interrupted time of registration within the dataset and registration at any time within the study period. Separate models considered the association between each individual BB/STI diagnosis and the two outcomes of interest after adjusting for age, gender (as defined above), time registered at GP, ethnicity, IMD quintile, NHS region, IDU history, close HBV contact, and imprisonment history; BB/STIs were not reciprocally adjusted. Cross tabulation was used to detect multicolinearity, including co-occurrence of BB/STIs. A sensitivity analysis explored the association between a record of syphilis diagnosis and HBsAg seropositivity, whereby people with both HCV and syphilis records were excluded from the model. All models excluded country of birth due to missing data; in the subset with a recorded country of birth, a two-sample Wilcoxon rank-sum test was used to test for trends in HBsAg screening and HBsAg seropositivity. Univariate logistic regression analysis was used to explore factors associated with a record of referral to specialist care among people with a HBsAg seropositivity record. All statistical analysis was carried out in STATA (Version 14.2 College Station, Texas, United States) and supervised by Dr. Colette Smith and Dr. Giovanni Villa.

3.3 Results

3.3.1 Study population

A total of 6,975,119 records were extracted spanning the period between January 2008 and July 2019. The cohort comprised 3,537,583/6,975,119 (50.7%) women, was ethnically diverse, had a median age of 38 years, and had been registered at their current GP for a median of 10 years by the end of the study period Table 3.1. Overall, 202,407/6,975,119 people (2.9%) had

≥1 HBsAg screening indication recorded (among MSM, IDU history, close HBV contact, imprisonment history or at-least one BB/STI). Individuals from intermediate and high endemicity countries were not included due to low recording. There were 187,242/6,975,119 (2.7%) BB/STI diagnoses, most commonly scabies, HPV, and GH. HCV and HIV had a prevalence of 0.04% (95% CI 0.04-0.04) and 0.001% (95% CI 0.000-0.001), respectively. Demographic and socioeconomic characteristics by screening indication are shown in Table 3.2. The MSM population was predominantly white and largely urban; those with a history of IDU or imprisonment were predominantly white males; close HBV contacts comprised a similar proportion of men and women and were younger, ethnically diverse, and largely urban. For BB/STI diagnoses, syphilis and scabies were recorded in similar proportions of men and women; GC, HCV, and HIV were more common among men; and GH, TV, and HPV were more common among women.

Table 3.1: Characteristics of the study population, total and according to the record of HBsAg screening and HBsAg seropositivity

Characteristic		Total	Record of HBsAg screening		Record of HBsAg seropositivity[a]		HBsAg seroprevalence
			Yes	No	Yes	No	
Total		6,975,119 (100)	192,639 (100)	6,782,480 (100)	8,065 (100)	6,967,054 (100)	0.1 (0.1-0.1)
Gender, n (%)	Women, total	3,537,583 (50.7)	138,108 (71.7)	3,399,475 (50.1)	3,879 (48.1)	3,533,704 (50.7)	0.1 (0.1-0.1)
	Women, no pregnancy record	2,870,055 (41.2)	42,787 (22.2)	2,827,268 (41.7)	1,895 (23.5)	2,868,160 (41.2)	0.1 (0.1-0.1)
	Women, pregnancy record	667,528 (9.6)	95,321 (49.5)	572,207 (8.4)	1,984 (24.6)	665,544 (9.6)	0.3 (0.3-0.3)
	Men, total	3,437,536 (49.3)	54,531 (28.3)	3,383,005(49.9)	4,185 (51.9)	3433350 (49.3)	0.1 (0.1-0.1)
	Men, no MSM record	3,436,356 (49.3)	54,307 (28.2)	3,382,049 (49.9)	4,173 (51.7)	3,432,183 (49.3)	0.1 (0.1-0.1)
	Men, MSM record	1,180 (0.0)	224 (0.1)	956 (0.0)	13 (0.2)	1,167 (0.0)	1.1 (0.1-1.9)
Age, median years (IQR)		38 (24-57)	39 (32-48)	38 (24-57)	44.0 (35.5-54.3)	38.4 (24.2-57.0)	N/A
Time at GP practice, median years (IQR)		10.2 (4.8-18.4)	10.4 (6.0-17.5)	10.2 (4.8-18.5)	7.9 (4.3-12.4)	10.2 (4.8-18.4)	N/A
Ethnicity, n (%)	Asian	519,692 (7.5)	22,044 (11.4)	497,648 (7.3)	2,045 (25.4)	517,647 (7.4)	0.4 (0.4-0.4)
	Black	235,529 (3.4)	11,565 (6.0)	224,964 (3.3)	1,965 (24.4)	234,564 (3.4)	0.8 (0.8-0.9)
	Mixed	107,967 (1.6)	3,108 (1.6)	104,859 (1.6)	309 (3.8)	107,658 (1.6)	0.3 (0.3-0.3)
	Other	99,176 (1.4)	3,806 (2.0)	95,370 (1.4)	357 (4.4)	98,819 (1.4)	0.4 (0.3-0.4)
	White	4,175,022 (59.9)	122,032 (63.4)	4,052,990 (59.8)	2,510 (31.1)	4,172,512 (59.9)	0.1 (0.1-0.1)
	Unknown	1,836,733 (26.3)	30,084 (15.6)	1,806,649 (26.6)	879 (10.9)	1,835,854 (26.4)	0.1 (0.0-0.1)
IMD quintile[b], n (%)	First	1,257,585 (18.0)	47,118 (24.5)	1,210,467 (17.9)	2,986 (37.0)	1,254,599 (18.0)	0.2 (0.2-0.3)
	Second	1,265,469 (18.1)	38,118 (19.8)	1,227,351 (18.1)	2,022 (25.1)	1,263,447 (18.1)	0.2 (0.2-0.2)
	Third	1,292,007 (18.5)	31,858 (16.5)	1,260,149 (18.6)	1,166 (14.5)	1,290,841 (18.5)	0.1 (0.1-0.1)
	Fourth	1,415,766 (20.3)	34,492 (17.9)	1,381,274 (20.4)	889 (11.0)	1,414,877 (20.3)	0.1 (0.1-0.1)
	Fifth	1,505,634 (21.6)	34,719 (18.0)	1,470,915 (21.7)	837 (10.4)	1,504,797 (21.6)	0.1 (0.1-0.1)
	Unknown	238,658 (3.4)	6,334 (3.3)	232,324 (3.4)	165 (2.1)	238,493 (3.4)	0.1 (0.1-0.1)
NHS region, n (%)	London	1,259,823 (18.1)	56,570 (29.4)	1,203,253 (17.7)	3,679 (45.6)	1,256,144 (18.0)	0.3 (0.3-0.3)
	Midlands and East	1,259,531 (18.1)	28,120 (14.6)	1,231,411 (18.2)	1,020 (12.7)	1,258,511 (18.1)	0.1 (0.1-0.1)
	North	1,853,917 (26.6)	42,235 (21.9)	1,811,682 (26.7)	1,553 (19.3)	1,852,364 (26.6)	0.1 (0.1-0.1)
	South	2,601,848 (37.3)	65,714 (34.1)	2,536,134 (37.4)	1,813 (22.5)	2,600,035 (37.3)	0.1 (0.1-0.1)
Location, n (%)	Rural	1,315,162 (18.9)	29,654 (15.4)	1,285,508 (19.0)	507 (6.3)	1,314,655 (18.9)	0.0 (0.0-0.0)
	Urban	5,427,827 (77.8)	156,683 (81.3)	5,271,144 (77.7)	7,398 (91.7)	5,420,429 (77.8)	0.1 (0.1-0.1)
	Unknown	232,130 (3.3)	6,302 (3.3)	225,828 (3.3)	160 (2.0)	231,970 (3.3)	0.1 (0.1-0.1)
≥1 BB/STI diagnosis, n (%)		187,242 (2.7)	8,708 (4.5)	178,534 (2.6)	277 (3.4)	186,965 (2.7)	0.2 (0.1-0.2)
	None	6,773,892 (97.1)	181,847 (94.4)	6,592,045 (97.2)	7,447 (92.3)	6,766,445 (97.1)	0.1 (0.1-0.1)

Screening indication [c], n (%)	≥1	201,227 (2.9)	10,792 (5.6)	190,435 (2.8)	618 (7.7)	200,609 (2.9)	0.3 (0.3-0.3)
	IDU history	9,261 (0.1)	1,077 (0.6)	8,184 (0.1)	124 (1.5)	9,137 (0.1)	1.3 (1.1-1.6)
	Close HBV contact	2,270 (0.0)	876 (0.5)	1,394 (0.0)	62 (0.8)	2,208 (0.0)	2.7 (2.1-3.5)
	Imprisonment history	1,151 (0.0)	57 (0.0)	1,094 (0.0)	4 (0.1)	1,147 (0.0)	0.4 (0.1-0.9)
	Syphilis	1,750 (0.0)	179 (0.1)	1,571 (0.0)	37 (0.5)	1,713 (0.0)	2.1 (1.5-2.9)
	GC	1,282 (0.0)	77 (0.0)	1,205 (0.0)	2 (0.0)	1,280 (0.0)	0.2 (0.0-0.6)
	Scabies	107,686 (1.5)	4,390 (2.3)	103,296 (1.5)	140 (1.7)	107,546 (1.5)	0.1 (0.1-0.2)
	TV	6,806 (0.1)	556 (0.3)	6,250 (0.1)	14 (0.2)	6,792 (0.1)	0.2 (0.1-0.4)
	GH	36,630 (0.5)	2,043 (1.1)	34,587 (0.5)	38 (0.5)	36,592 (0.5)	0.1 (0.1-0.1)
	HPV	37,357 (0.5)	1738 (0.9)	35,619 (0.5)	50 (0.6)	37,307 (0.5)	0.1 (0.1-0.9)
	HCV	2,785 (0.0)	258 (0.1)	2,527 (0.0)	182 (2.3)	2,603 (0.0)	6.5 (5.7-7.5)
	HIV	111 (0.0)	4 (0.0)	107 (0.0)	5 (0.1)	106 (0.0)	4.5 (1.9-10.1)

[a]Record of HBsAg seropositivity at any time; [b]IMD, first, most deprived to fifth, least deprived; [c]Participants may have ≥1 indication. HBsAg= Hepatitis B surface antigen; MSM= Men who have sex with men; GP= General practice; IMD= Index of multiple deprivation; NHS= National health service; IDU= Injecting drug use; BB/STI= Blood borne or sexually transmitted infection; GC= Gonorrhoea; TV= Trichomoniasis; GH= Genital herpes; HPV= Human papillomavirus; HCV= Hepatitis C virus; HIV= Human immunodeficiency virus.

Table 3.2: Characteristics of the study population by HBsAg screening indication

Characteristic		MSM	IDU history	Close HBV contact	Imprisonment history	BB/STI diagnosis							
						Syphilis	GC	Scabies	TV	GH	HPV	HCV	HIV
Total number		1,180	9,261	2,270	1,151	1,750	1,282	107,686	6,806	36,630	37,357	2,785	111
Gender, n (%)	Women, total	NA	2,673 (28.9)	1,175 (51.8)	139 (12.1)	783 (44.7)	485 (37.8)	57,535 (53.4)	6,572 (96.6)	28,024 (76.5)	37,086 (99.3)	997 (35.8)	20 (18.0)
	Women, no pregnancy record	NA	1,643 (17.7)	839 (37.0)	93 (8.1)	462 (26.4)	271 (21.1)	39,339 (36.5)	4,690 (68.9)	17,794 (48.6)	22,928 (61.4)	751 (27.0)	13 (11.7)
	Women, pregnancy record	NA	1,030 (11.1)	336 (14.8)	46 (4.00)	321 (18.3)	214 (16.7)	18,196 (16.9)	1,882 (27.7)	10,230 (27.9)	14,158 (37.9)	246 (8.8)	7 (6.3)
	Men, total	NA	6,588 (71.1)	1,095 (48.2)	1,012 (87.9)	967 (55.3)	797 (62.2)	50,151 (46.6)	234 (3.4)	8,606 (23.5)	271 (0.7)	1,788 (64.2)	91 (82.0)
	Men, no MSM record	NA	6,579 (71.0)	1,095 (48.2)	1,010 (87.8)	962 (55.0)	793 (61.9)	50,099 (46.5)	234 (3.4)	8,594 (23.5)	270 (0.7)	1,787 (62.2)	82 (73.9)
	Men, MSM record	1,180 (100)	9 (0.1)	0 (0.0)	2 (0.2)	5 (0.3)	4 (0.3)	52 (0.1)	0 (0.0)	12 (0.0)	1 (0.0)	1 (0.0)	9 (8.1)
Age, median years (IQR)		35.3 (28.7-47.2)	43.5 (36.6-50.5)	21.9 (10.6-38.0)	43.4 (35.3-52.5)	51.4 (41.1-65.2)	48.4 (32.9-61.6)	37.4 (27.3-53.8)	52.0 (39.2-64.2)	41.9 (32.6-54.4)	35.9 (30.9-44.9)	51.3 (42.6-61.2)	51.2 (44.8-57.8)
Time at GP practice, median years (IQR)		3.3 (1.4-7.6)	9.6 (4.8-14.8)	7.2 (3.9-10.5)	9.0 (4.2-14.4)	12.6 (6.9-20.4)	10.5 (5.1-18.6)	14.5 (6.9-23.5)	16.5 (8.5-25.5)	12.1 (5.7-21.7)	7.4 (3.5-15.9)	9.7 (4.9-17.6)	9.0 (4.8-13.5)
Ethnicity, n (%)	Asian	76 (6.4)	189 (2.0)	546 (24.1)	38 (3.3)	146 (8.3)	48 (3.7)	7,929 (7.4)	347 (5.1)	765 (2.1)	1,493 (4.0)	166 (6.0)	4 (3.6)
	Black	29 (2.5)	245 (2.7)	326 (14.4)	15 (1.3)	286 (16.3)	129 (10.1)	2,392 (2.2)	741 (10.9)	1,070 (2.9)	1,297 (3.5)	59 (2.1)	20 (18.0)
	Mixed	31 (2.6)	133 (1.4)	55 (2.4)	12 (1.0)	40 (2.3)	37 (2.9)	1,245 (1.2)	165 (2.4)	540 (1.5)	685 (1.8)	38 (1.4)	5 (4.5)
	Other	33 (2.8)	67 (0.7)	88 (3.9)	5 (0.4)	30 (1.7)	12 (0.9)	1,043 (1.0)	68 (1.0)	232 (0.6)	430 (1.2)	37 (1.3)	2 (1.8)
	White	926 (78.5)	7,083 (76.5)	975 (43.0)	802 (69.7)	927 (53.0)	845 (65.9)	67,521 (62.7)	4,512 (66.3)	26,070 (71.2)	28,614 (76.6)	1,879 (67.5)	73 (65.8)
	Unknown	85 (7.2)	1,544 (16.7)	280 (12.3)	279 (24.2)	321 (18.3)	211 (16.5)	27,556 (25.6)	973 (14.3)	7,953 (21.7)	4,838 (12.9)	606 (21.8)	7 (6.3)
IMD quintile[b], n (%)	First	377 (32.0)	4,180 (45.1)	1,252 (55.2)	388 (33.7)	504 (28.8)	383 (29.9)	31,141 (28.9)	1,927 (28.3)	5,565 (15.2)	7,695 (20.6)	925 (33.2)	29 (26.1)
	Second	329 (27.9)	1,892 (20.4)	415 (18.3)	196 (17.0)	381 (21.8)	293 (22.9)	21,640 (20.1)	1,777 (26.1)	6,171 (16.9)	7,502 (20.1)	476 (17.1)	43 (38.7)
	Third	207 (17.5)	1,134 (12.2)	197 (8.7)	161 (14.0)	304 (17.4)	193 (15.1)	18,612 (17.3)	1,086 (15.9)	7,125 (19.5)	7,013 (18.8)	410 (14.7)	18 (16.2)
	Fourth	145 (12.3)	946 (10.2)	145 (6.4)	119 (10.3)	255 (14.6)	198 (15.4)	17,826 (16.6)	1,018 (14.9)	8,207 (22.4)	7,318 (19.6)	357 (12.8)	15 (13.5)
	Fifth	101 (8.6)	637 (6.9)	163 (7.2)	56 (4.9)	244 (13.9)	184 (14.4)	15,083 (14.0)	903 (13.3)	8,310 (22.7)	6,869 (18.4)	337 (12.1)	3 (2.7)
	Unknown	21 (1.8)	472 (5.1)	98 (4.3)	231 (20.1)	62 (3.5)	31 (2.4)	3,384 (3.1)	95 (1.4)	1,252 (3.4)	960 (2.6)	280 (10.1)	3 (2.7)
	London	479 (40.6)	1,153 (12.5)	745 (32.8)	27 (2.4)	568 (32.5)	291 (22.8)	13,818 (12.8)	2,006 (29.5)	5,544 (15.1)	9,075 (24.3)	316 (11.4)	34 (30.6)

NHS Region, n (%)	Midlands and East	108 (9.2)	931 (10.1)	219 (9.7)	358 (31.1)	246 (14.1)	167 (13.0)	19,189 (17.8)	707 (10.4)	5,970 (16.0)	5,027 (13.5)	525 (18.9)	2 (1.8)
	North	361 (30.6)	4,574 (49.4)	995 (43.8)	398 (34.6)	352 (20.1)	456 (35.6)	40,119 (37.3)	2,600 (38.2)	9,266 (25.3)	11,782 (31.5)	1,076 (38.6)	6 (5.4)
	South	232 (19.7)	2,603 (28.1)	311 (13.7)	368 (32.0)	584 (33.4)	368 (28.7)	34,560 (32.1)	1,493 (21.9)	15,950 (43.5)	11,473 (30.7)	868 (31.2)	69 (62.2)
Location, n (%)	Rural	64 (5.4)	819 (8.8)	82 (3.6)	166 (14.4)	208 (11.9)	155 (12.1)	16,253 (15.1)	666 (9.8)	7,749 (21.2)	5,023 (13.5)	364 (13.1)	3 (2.7)
	Urban	1,095 (92.8)	468 (5.1)	2,090 (92.1)	755 (65.6)	1,483 (84.7)	1,098 (85.7)	88,194 (81.9)	6,050 (88.9)	27,713 (75.7)	31,385 (84.0)	2,142 (76.9)	106 (95.5)
	Unknown	21 (1.8)	7,974 (86.1)	98 (4.3)	230 (20.0)	59 (3.4)	29 (2.3)	3,239 (3.0)	90 (1.3)	1,168 (3.2)	949 (2.5)	279 (10.0)	2 (1.8)

[a]Participants may have ≥1 indication; [b]IMD, first, most deprived to fifth, least deprived. HBsAg= Hepatitis B surface antigen; BB/STI= Blood borne or sexually transmitted infection; MSM= Men who have sex with men; GP= General practice; IMD= Index of multiple deprivation; NHS= National health service; IDU= Injecting drug use; GC= Gonorrhoea; TV= Trichomoniasis; GH= Genital herpes; HPV= Human papillomavirus; HCV= Hepatitis C virus; HIV= Human immunodeficiency virus.

3.3.2 Patterns of HBsAg screening

A record of HBsAg screening was found in 192,639/6,975,119 (2.8%) people overall and in 11,016/202,407 (5.4%) of those with ≥1 recorded screening indication (MSM, IDU history, close HBV contact, imprisonment history or any BB/STI diagnosis). The distribution of screening across England, with the proportion of those with a screening record in each local authority, is shown in Figure 3.1A. Geographically, those with a screening record were mostly attending practices located in the South and in the most deprived neighbourhoods. HBsAg screening records increased marginally over time (Figure 3.2) Factors associated with HBsAg screening were analysed by univariate and multivariable analysis Table 3.3. After adjustment, the odds of having a record of HBsAg screening were highest in London and for MSM, people with history of IDU, and close HBV contacts. When analysing individual BB/STIs, the adjusted odds of screening were increased for all diagnoses except HIV, and were highest with syphilis (odds ratio [OR] 3.27; 95% CI 2.71-3.95; p<0.01) (Table 3.4) and HCV (OR 3.20; 2.76-3.72; p<0.01) (Table 3.5).

Figure 3.1: Map of HBsAg screening (A) and HBsAg seroprevalence (B) by local authority district

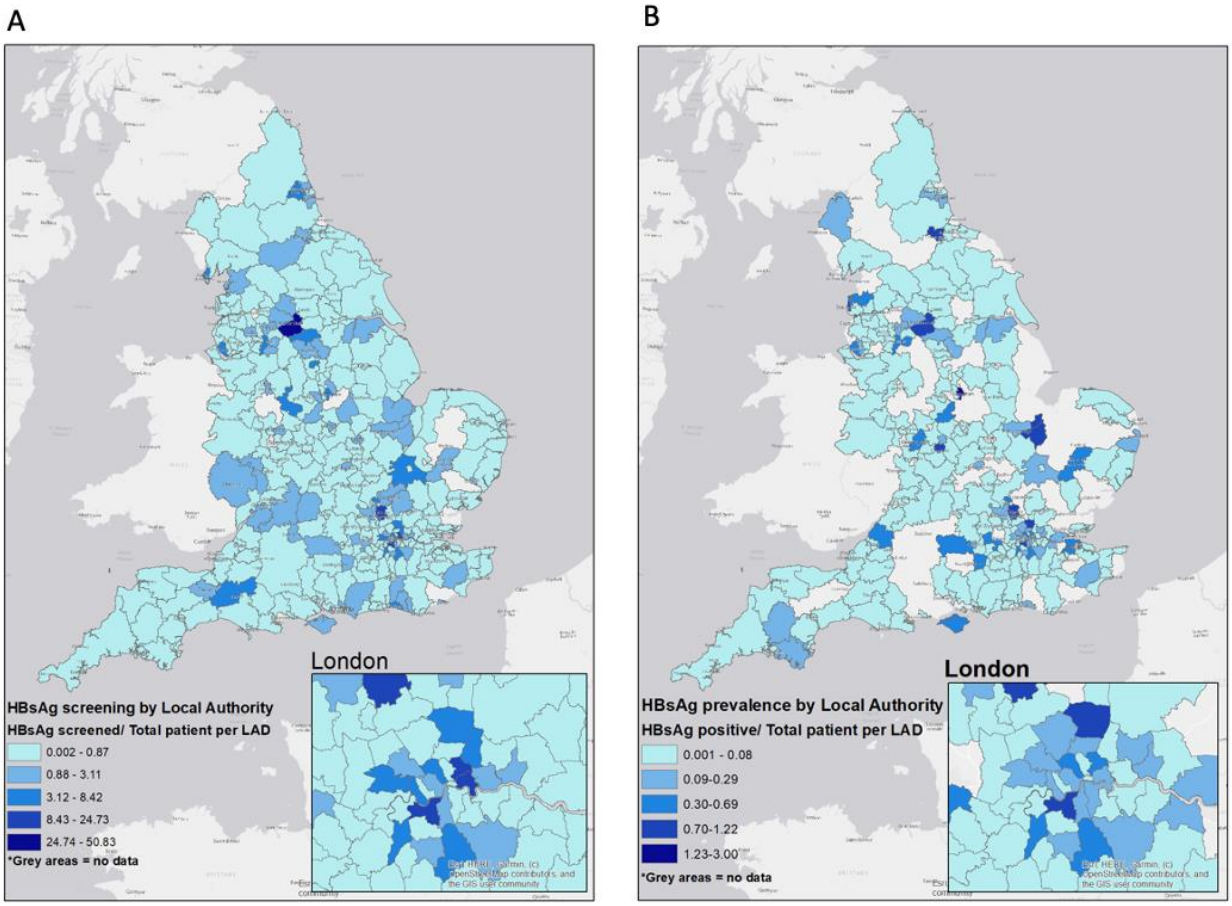

Geospatial analysis of offered HBsAg screening rates and recorded HBsAg seropositivity. HBsAg=Hepatitis B surface antigen; LAD=local authority district. Data in both maps are normalised by the total number of persons recorded as being in each local authority within the cohort. White areas represent LADs with no data. The numbers are presented as percentages.

Figure 3.2: Temporal trends in HBsAg screening records, as the proportion with a record among total registrants

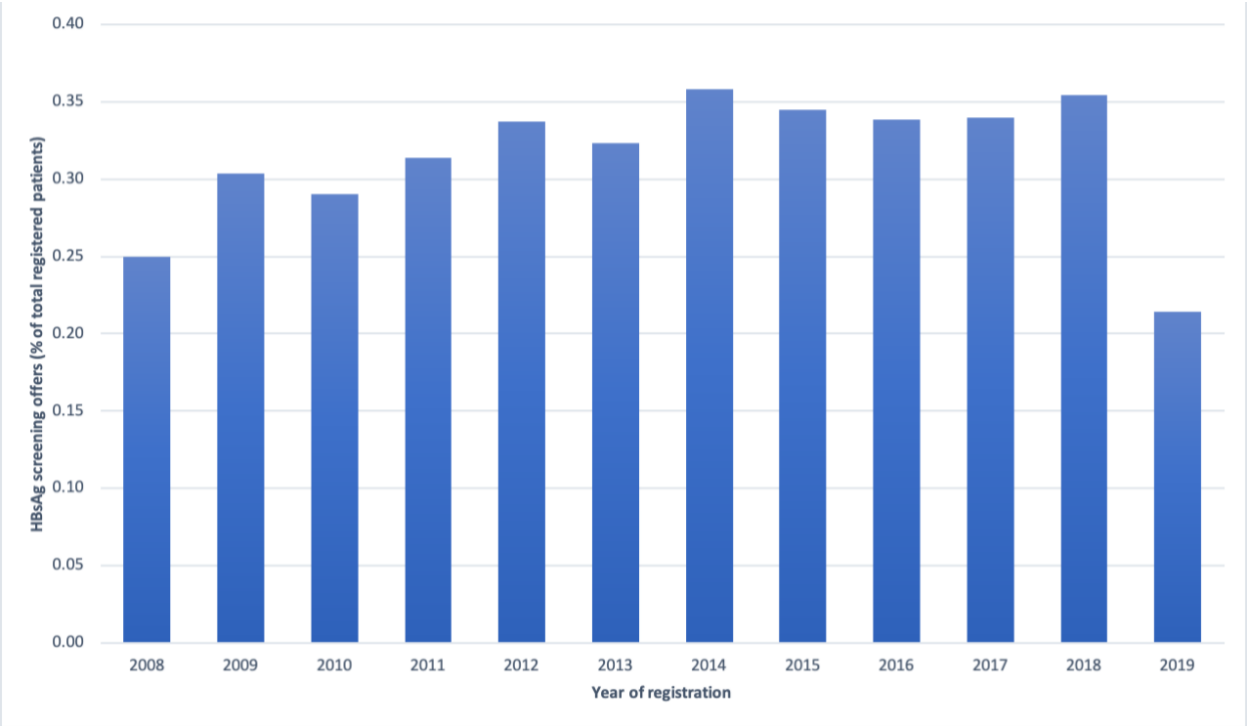

The temporal trends in HBsAg screening records through the study period represented as a percentage of patients offered screening out of the total number of patients registered in the year. HBsAg=hepatitis B surface antigen.

Table 3.3: Factors associated with HBsAg screening[a]

		Univariable			Multivariable Model 1			Multivariable Model 2		
		OR	95% CI	p-value	OR	95% CI	p-value	OR	95% CI	p-value
Gender	Men, no MSM record	REF		<0.01	REF		<0.01	REF		<0.01
	Men, MSM record	14.60	12.6-16.9		9.97	8.57-11.61		10.23	8.79-11.91	
	Women, no pregnancy record	0.90	0.90-0.91		0.92	0.90-0.93		0.93	0.92-0.94	
Age	per 5-year older	1.05	1.05-1.06	<0.01	1.08	1.08-1.08	<0.01	1.08	1.08-1.08	<0.01
Time at GP practice	Per 5-year longer	1.00	1.00-1.01	<0.01	1.02	1.02-1.02	<0.01	1.02	1.02-1.02	<0.01
Ethnicity	White	REF		<0.01	REF		<0.01	REF		<0.01
	Asian	1.86	1.82-1.89		1.25	1.23-1.28		1.25	1.22-1.27	
	Black	2.45	2.39-2.51		1.16	1.13-1.19		1.15	1.12-1.18	
	Mixed	1.16	1.11-1.21		0.90	0.86-0.95		0.90	0.86-0.95	
	Other	1.83	1.76-1.91		1.20	1.15-1.25		1.20	1.15-1.25	
	Unknown	0.49	0.48-0.50		0.56	0.55-0.57		0.56	0.55-0.57	
IMD Quintile[b]	First	REF		<0.01	REF		<0.01	REF		<0.01
	Second	0.71	0.69-0.73		0.69	0.68-0.70		0.69	0.68-0.71	
	Third	0.49	0.49-0.51		0.60	0.59-0.61		0.61	0.59-0.62	
	Fourth	0.40	0.39-0.41		0.57	0.55-0.58		0.57	0.56-0.59	
	Fifth	0.36	0.35-0.37		0.54	0.53-0.56		0.55	0.54-0.56	
	Unknown	0.45	0.44-0.47		0.73	0.70-0.76		0.73	0.70-0.76	
NHS Region	London	REF		<0.01	REF		<0.01	REF		<0.01
	Midlands and West	0.20	0.22-0.23		0.24	0.24-0.25		0.24	0.23-0.25	
	North	0.32	0.31-0.33		0.32	0.62-0.33		0.32	0.31-0.32	
	South	0.23	0.23-0.24		0.29	0.28-0.29		0.28	0.28-0.29	
BB/STI diagnosis	≥1 vs No record	1.49	1.44-1.54	<0.01				1.39	0.34-1.44	<0.01
Screening indication	≥1 vs No record	11.86	11.59-12.46	<0.01	2.06	1.99-2.19	<0.01			
IDU history	Yes vs No record	8.00	7.46-8.57	<0.01				6.99	6.50-7.51	<0.01
Close HBV contact	Yes vs No record	39.32	35.86-43.11	<0.01				38.19	34.63-42.11	<0.01
Imprisonment history	Yes vs No record	2.96	2.22-3.94	<0.01				2.10	1.56-2.84	<0.01
BB/STI diagnosis[c] Syphilis	Yes vs No record	6.34	5.29-7.60	<0.01						
GC	Yes vs No record	2.87	2.14-3.86	<0.01						
Scabies	Yes vs No record	1.21	1.15-1.27	<0.01						
TV	Yes vs No record	3.07	2.69-3.51	<0.01						
GH	Yes vs No record	1.74	1.62-1.88	<0.01						

HPV	Yes vs No record	1.61	1.48-1.75	<0.01
HCV	Yes vs No record	6.07	5.28-6.97	<0.01
HIV	Yes vs No record	2.55	0.94-6.94	0.07

[a]The dataset excluded women who had a pregnancy record at any time (due to opt-out HBsAg testing in routine antenatal care with largely incomplete recording in GP records); [b]IMD, first, most deprived to fifth, least deprived; [c] The adjustment for individual BB/STI diagnoses is presented separately. HBsAg= Hepatitis B surface antigen; MSM= Men who have sex with men; GP= General practice; IMD= Index of multiple deprivation; NHS= National health service; IDU= Injecting drug use; BB/STI= Blood borne or sexually transmitted infection; GC= Gonorrhoea; TV= Trichomoniasis; GH= Genital herpes; HPV= Human papillomavirus; HCV= Hepatitis C virus; HIV= Human immunodeficiency virus; OR= Odds ratio; CI= Confidence interval.

Table 3.4: Adjusted analysis of factors associated with a record of HBsAg screening when considering individuals BB/STI diagnoses

		Multivariable Model 3			Multivariable Model 4			Multivariable Model 5			Multivariable Model 6		
		OR	95% CI	p-value	OR	95% CI	p-value	OR	95% CI	p-value	OR	95% CI	p-value
Gender	Men, no MSM record	REF		<0.01	REF		<0.01	REF		<0.01	REF		<0.01
	Men, MSM record	10.30	8.85-11.97		10.33	8.87-12.03		10.32	8.86-12.01		10.36	8.89-12.06	
	Women, no pregnancy record	0.93	0.92-0.95		0.93	0.92-0.95		0.93	0.92-0.95		0.93	0.92-0.94	
Age	Per 5-year older	1.08	1.08-1.08	<0.01	1.08	1.08-1.08	<0.01	1.08	1.08-1.08	<0.01	1.08	1.08-1.08	<0.01
Time at GP practice	Per 5-year longer	1.02	1.02-1.02	<0.01	1.02	1.02-1.02	<0.01	1.02	1.02-1.02	<0.01	1.02	1.02-1.02	<0.01
Ethnicity	White	REF		<0.01	REF		<0.01	REF		<0.01	REF		<0.01
	Asian	1.24	1.22-1.27		1.24	1.22-1.27		1.24	1.22-1.27		1.24	1.22-1.27	
	Black	1.14	1.11-1.17		1.14	1.12-1.17		1.15	1.12-1.18		1.14	1.11-1.17	
	Mixed	0.90	0.86-0.94		0.90	0.86-0.95		0.90	0.86-0.95		0.90	0.86-0.94	
	Other	1.19	1.14-1.24		1.19	1.14-1.24		1.19	1.14-1.24		1.19	1.14-1.24	
	Unknown	0.56	0.55-0.57		0.56	0.55-0.57		0.56	0.55-0.57		0.56	0.55-0.57	
IMD Quintile[b]	First	REF		<0.01	REF		<0.01	REF		<0.01	REF		<0.01
	Second	0.69	0.68-0.71		0.69	0.68-0.71		0.69	0.68-0.71		0.69	0.68-0.71	
	Third	0.60	0.59-0.62		0.60	0.59-0.62		0.61	0.59-0.62		0.60	0.59-0.62	
	Fourth	0.57	0.56-0.58		0.57	0.56-0.58		0.57	0.56-0.59		0.57	0.56-0.58	
	Fifth	0.55	0.54-0.56		0.55	0.54-0.56		0.55	0.54-0.56		0.55	0.54-0.56	
	Unknown	0.73	0.70-0.76		0.73	0.70-0.76		0.73	0.70-0.76		0.73	0.70-0.76	
NHS Region	London	REF		<0.01	REF		<0.01	REF		<0.01	REF		<0.01
	Midlands and West	0.24	0.23-0.25		0.24	0.23-0.25		0.24	0.23-0.25		0.24	0.23-0.25	
	North	0.32	0.31-0.32		0.32	0.31-0.32		0.32	0.31-0.32		0.32	0.31-0.32	
	South	0.28	0.28-0.29		0.28	0.28-0.29		0.28	0.28-0.29		0.28	0.28-0.29	
IDU	Record vs no record	7.08	6.59-7.61	<0.01	7.08	6.59-7.61	<0.01	7.05	6.56-7.58	<0.01	7.08	6.58-7.60	<0.01
HBV contact	Record vs no record	38.10	34.56-42.02	<0.01	38.11	34.56-42.02	<0.01	38.12	34.57-42.03	<0.01	38.08	34.54-41.99	<0.01
Imprisonment history	Record vs no record	2.13	1.58-2.87	<0.01	2.13	1.58-2.87	<0.01	2.12	1.57-2.86	<0.01	2.13	1.58-2.87	<0.01
Syphilis diagnosis	Record vs no record	3.27	2.71-3.95	<0.01									
GC diagnosis	Record vs no record				1.94	1.44-2.63	<0.01						
Scabies diagnosis	Record vs no record							1.18	1.12-1.24	<0.01			
TV diagnosis	Record vs no record										1.99	1.74-2.80	<0.01

[a]The dataset excluded women who had a pregnancy record at any time (due to opt-out HBsAg testing in routine antenatal care with largely incomplete recording in GP records); [b]IMD, first, most deprived to fifth, least deprived. HBsAg= Hepatitis B surface antigen; BB/STI= Blood borne or sexually transmitted infection; MSM= Men who have sex with men; GP= General practice; IMD= Index of multiple deprivation; NHS= National health service; IDU= Injecting drug use; GC= Gonorrhoea; TV= Trichomoniasis; OR= Odds ratio; CI= Confidence interval.

Table 3.5: (continued) Adjusted analysis of factors associated with a record of HBsAg screening when considering individual BB/STI diagnoses

		Multivariable Model 7			Multivariable Model 8			Multivariable Model 9			Multivariable Model 10		
		OR	95% CI	p-value	OR	95% CI	p-value	OR	95% CI	p-value	OR	95% CI	p-value
Gender	Men, no MSM record	REF		<0.01	REF		<0.01	REF		<0.01	REF		<0.01
	Men, MSM record	10.32	8.87-12.02		10.36	8.90-12.07		10.38	8.91-12.08		10.37	8.90-12.07	
	Women, no pregnancy record	0.93	0.92-0.94		0.93	0.92-0.94		0.93	0.92-0.95		0.93	0.92-0.95	
Age	Per 5-year older	1.08	1.08-1.08	<0.01	1.08	1.08-1.08	<0.01	1.08	1.08-1.08	<0.01	1.08	1.08-1.08	<0.01
Time at GP practice	Per 5-year longer	1.02	1.02-1.02	<0.01	1.02	1.02-1.02	<0.01	1.02	1.02-1.02	<0.01	1.02	1.02-1.02	<0.01
Ethnicity	White	REF		<0.01	REF		<0.01	REF		<0.01	REF		<0.01
	Asian	1.25	1.22-1.27		1.25	1.22-1.27		1.24	1.22-1.27		1.24	1.22-1.27	
	Black	1.15	1.12-1.18		1.15	1.12-1.18		1.15	1.12-1.18		1.15	1.12-1.18	
	Mixed	0.90	0.86-0.95		0.90	0.86-0.95		0.90	0.86-0.95		0.90	0.86-0.95	
	Other	1.19	1.15-1.24		1.19	1.14-1.24		1.19	1.14-1.24		1.19	1.14-1.24	
	Unknown	0.56	0.55-0.57		0.56	0.55-0.57		0.56	0.55-0.57		0.56	0.55-0.57	
IMD Quintile[b]	First	REF		<0.01	REF		<0.01	REF		<0.01	REF		<0.01
	Second	0.69	0.68-0.71		0.69	0.68-0.71		0.69	0.68-0.71		0.69	0.68-0.71	
	Third	0.60	0.59-0.62		0.60	0.59-0.62		0.60	0.59-0.62		0.60	0.59-0.62	
	Fourth	0.57	0.56-0.58		0.57	0.56-0.58		0.57	0.56-0.58		0.57	0.56-0.58	
	Fifth	0.55	0.54-0.56		0.55	0.54-0.56		0.55	0.54-0.56		0.55	0.54-0.56	
	Unknown	0.73	0.70-0.76		0.73	0.70-0.76		0.73	0.70-0.76		0.73	0.70-0.76	
NHS Region	London	REF		<0.01	REF		<0.01	REF		<0.01	REF		<0.01
	Midlands and West	0.24	0.23-0.25		0.24	0.24-0.25		0.24	0.23-0.25		0.24	0.23-0.25	
	North	0.32	0.31-0.32		0.32	0.31-0.32		0.32	0.31-0.32		0.32	0.31-0.32	
	South	0.28	0.28-0.29		0.29	0.28-0.29		0.28	0.28-0.29		0.28	0.28-0.29	
IDU	Record vs no record	7.06	6.57-7.59	<0.01	7.08	6.59-7.61	<0.01	6.57	6.10-7.07	<0.01	7.09	6.60-7.62	<0.01
HBV contact	Record vs no record	38.14	34.59-42.06	<0.01	38.13	34.58-42.04	<0.01	38.06	34.52-41.97	<0.01	38.10	34.55-42.00	<0.01
Imprisonment history	Record vs no record	2.12	1.57-2.86	<0.01	2.13	1.58-2.87	<0.01	1.81	1.33-2.45	<0.01	2.13	1.58-2.87	<0.01
GH diagnosis	Record vs no record	1.77	1.64-1.91	<0.01									
HPV diagnosis	Record vs no record				1.41	1.30-1.54	<0.01						
HCV diagnosis	Record vs no record							3.20	2.76-3.72	<0.01			
HIV diagnosis	Record vs no record										0.89	0.31-2.58	0.84

[a]The dataset excluded women who had a pregnancy record at any time (due to opt-out HBsAg testing in routine antenatal care with largely incomplete recording in GP records); [b]IMD, first, most deprived to fifth, least deprived. HBsAg= Hepatitis B surface antigen; BB/STI= Blood borne or sexually transmitted infection; MSM= Men who have sex with men; GP= General practice;

IMD= Index of multiple deprivation; NHS= National health service; IDU= Injecting drug use; GH= Genital herpes; HPV= Human papillomavirus; HCV= Hepatitis C virus; HIV= Human immunodeficiency virus; OR= Odds ratio; CI= Confidence interval.

3.4 Patterns of HBsAg seropositivity

In the total population, 8,065/6,975,119 had a record of HBsAg seropositivity Table 3.1 yielding an overall HBsAg seroprevalence of 0.12% (95% CI 0.11-0.12). A minority (631/8,065; 7.8%) had ≥1 recorded screening indication. Additionally, those with ≥1 BB/STI diagnosis, was only observed in 277/8,065 (3.4%). The HBsAg seropositive population had a prevalence of 2.30% (95% CI 1.90-2.60) for HCV and 0.06% (95% CI 0.02-0.14) for HIV. The distribution of HBsAg seropositivity across England and in each local authority is shown in Figure 3.1B. Geographically, those with a record of HBsAg seropositivity were mostly attending practices located in London and in the most deprived neighbourhoods. Factors associated with HBsAg seropositivity were analysed by univariate and multivariable analysis Table 3.6. After adjustment, the odds of having a record of HBsAg seropositivity were highest among MSM, people of ethnicities other than white, those with a IDU history, and close HBV contacts. When analysing individual BB/STI diagnoses, the adjusted odds of HBsAg seropositivity were highest for people with a diagnosis of syphilis (Table 3.7), HCV, or HIV (Table 3.8) Among those with both a record of HBsAg seropositivity and a record of syphilis (n=37), 1 also had a recorded diagnosis of GH, 1 of scabies and 3 (8.1%) of HCV, whereas none had a record of GC, TV, HPV, or HIV. In a sensitivity analysis that excluded the 3 people with both a syphilis and HCV, a recorded diagnosis of syphilis remained independently associated with increased odds of HBsAg seropositivity, with an adjusted OR of 5.57 (95% CI 3.97-7.82; $p<0.001$), and with no changes to other findings (not shown).

Table 3.6: Factors associated with a record of HBsAg seropositivity

			Univariable			Multivariable Model 1			Multivariable Model 2		
			OR	95% CI	p-value	OR	95%CI	p-value	OR	95% CI	p-value
Gender		Men, no MSM record	REF		<0.01	REF		<0.01	REF		<0.01
		Men, MSM record	9.16	5.30-15.84		6.78	3.90-11.79		6.83	3.91-11.92	
		Women, no pregnancy record	0.92	0.51-0.57		0.54	0.51-0.57		0.56	0.53-0.59	
		Women, pregnancy record	2.45	2.32-2.59		2.12	2.00-2.24		2.23	2.12-2.35	
Age		per 5-year older	1.05	1.05-1.06	<0.01	1.16	1.15-1.17	<0.01	1.16	1.15-1.17	<0.01
Time at GP practice		per 5-year longer	0.82	0.81-0.83	<0.01	0.82	0.80-0.83	<0.01	0.82	0.81-0.83	<0.01
Ethnicity		White	REF		<0.01	REF		<0.01	REF		<0.01
		Asian	6.57	6.19-6.96		5.56	5.22-5.92		5.54	5.20-5.89	
		Black	13.93	13.13-14.78		9.36	8.75-10.02		9.33	8.72-9.99	
		Mixed	4.77	4.24-5.37		4.75	4.21-5.36		4.77	4.22-5.38	
		Other	6.01	5.37-6.71		4.95	4.42-5.55		4.93	4.40-5.52	
		Unknown	0.80	0.74-0.86		1.09	1.01-1.18		1.09	1.00-1.17	
IMD Quintile[a]		First	REF		<0.01	REF		<0.01	REF		<0.01
		Second	0.67	0.64-0.71		0.75	0.70-0.79		0.75	0.71-0.80	
		Third	0.38	0.35-0.41		0.61	0.57-0.65		0.61	0.57-0.66	
		Fourth	0.26	0.24-0.28		0.52	0.48-0.56		0.53	0.49-0.57	
		Fifth	0.23	0.22-0.25		0.49	0.45-0.53		0.49	0.45-0.53	
		Unknown	0.29	0.25-0.34		0.57	0.48-0.67		0.57	0.48-0.66	
NHS Region		London	REF		<0.01	REF		<0.01	REF		<0.01
		Midlands and East	0.28	0.26-0.30		0.68	0.63-0.73		0.68	0.63-0.73	
		North	0.29	0.27-0.30		0.71	0.66-0.76		0.70	0.66-0.75	
		South	0.24	0.23-0.25		0.74	0.70-0.80		0.74	0.69-0.79	
	BB/STI diagnosis	≥1 vs no record	1.29	1.14-1.45	<0.01				1.22	1.08-1.38	<0.01
Screening indication		≥1 vs no record	13.16	11.43-15.15	<0.01	2.71	2.49-2.95	<0.01			
	IDU	Yes vs no record	11.89	9.95-14.22	<0.01				11.14	9.26-13.40	<0.01
	HBV contact	Yes vs no record	24.43	18.97-31.48	<0.01				12.27	9.44-15.95	<0.01
	Inmate history	Yes vs no record	3.01	1.13-8.05	<0.01				1.71	0.63-4.61	0.29
BB/STI diagnosis[b]	Syphilis	Yes vs no record	18.74	13.5-25.97	<0.01						
	GC	Yes vs no record	1.35	0.34-5.41	0.67						
	TV	Yes vs no record	1.78	1.05-3.01	0.03						

	Scabies	Yes vs no record	1.13	0.95-1.33	0.16
	GH	Yes vs no record	0.90	0.65-1.23	0.50
	HPV	Yes vs no record	1.15	0.88-1.53	0.29
	HCV	Yes vs no record	61.77	53.07-71.91	<0.01
	HIV	Yes vs no record	40.77	16.62-100.00	<0.01

[a]IMD, first, most deprived to fifth, least deprived; [b]The adjustment for individual BB/STI diagnoses is presented separately. HBsAg= Hepatitis B surface antigen; MSM= Men who have sex with men; GP= General practice; IMD= Index of multiple deprivation; NHS= National health service; IDU= Injecting drug use; BB/STI= Blood borne or sexually transmitted infection; GC= Gonorrhoea; TV= Trichomoniasis; GH= Genital herpes; HPV= Human papillomavirus; HCV= Hepatitis C virus; HIV= Human immunodeficiency virus; OR= Odds ratio; CI= Confidence interval.

Table 3.7: Adjusted analysis of factors associated with a record of HBsAg seropositivity when considering individual BB/STI diagnoses

		Multivariable Model 3			Multivariable Model 4			Multivariable Model 5			Multivariable Model 6		
		OR	95% CI	p-value	OR	95% CI	p-value	OR	95% CI	p-value	OR	95% CI	p-value
Gender	Men, no MSM record	REF		<0.01	REF		<0.01	REF		<0.01	REF		<0.01
	Men, MSM record	6.82	3.91-11.89		6.89	3.95-12.02		6.85	3.92-11.95		6.88	3.94-12.01	
	Women, no pregnancy record	0.56	0.53-0.59		0.56	0.53-0.59		0.56	0.53-0.59		0.56	0.53-0.59	
	Women, with pregnancy record	2.24	2.12-2.37		2.24	2.12-2.37		2.24	2.12-2.37		2.24	2.12-2.37	
Age	Per 5-year older	1.16	1.15-1.17	<0.01	1.16	1.15-1.17	<0.01	1.16	1.15-1.17	<0.01	1.16	1.15-1.17	<0.01
Time at GP practice	Per 5-year longer	0.82	0.81-0.83	<0.01	0.82	0.81-0.83	<0.01	0.82	0.81-0.83	<0.01	0.82	0.81-0.83	<0.01
Ethnicity	White	REF		<0.01	REF		<0.01	REF		<0.01	REF		<0.01
	Asian	5.51	5.18-5.87		5.52	5.18-5.88		5.52	5.18-5.88		5.52	5.18-5.88	
	Black	9.25	8.64-9.90		9.32	8.70-9.97		9.33	8.71-9.98		9.32	8.70-9.97	
	Mixed	4.75	4.21-5.35		4.76	4.22-5.37		4.77	4.22-5.38		4.76	4.22-5.38	
	Other	4.90	4.38-5.49		4.91	4.38-5.50		4.92	4.39-5.51		4.91	4.38-5.50	
	Unknown	1.08	1.00-1.17		1.08	1.00-1.17		1.08	1.00-1.17		1.08	1.00-1.17	
IMD Quintile[a]	First	REF		<0.01	REF		<0.01	REF		<0.01	REF		<0.01
	Second	0.75	0.71-0.80		0.75	0.71-0.80		0.75	0.71-0.80		0.75	0.71-0.80	
	Third	0.61	0.57-0.66		0.61	0.57-0.66		0.61	0.57-0.66		0.61	0.57-0.66	
	Fourth	0.53	0.49-0.57		0.52	0.48-0.57		0.53	0.48-0.57		0.52	0.48-0.57	
	Fifth	0.49	0.45-0.53		0.49	0.45-0.53		0.49	0.45-0.53		0.49	0.45-0.53	
	Unknown	0.57	0.48-0.66		0.57	0.48-0.66		0.57	0.48-0.66		0.57	0.48-0.66	
NHS Region	London	REF		<0.01	REF		<0.01	REF		<0.01	REF		<0.01
	Midlands and West	0.68	0.63-0.73		0.68	0.63-0.73		0.78	0.63-0.73		0.68	0.63-0.73	
	North	0.70	0.66-0.75		0.70	0.66-0.75		0.70	0.66-0.75		0.70	0.66-0.75	
	South	0.74	0.69-0.79		0.74	0.69-0.79		0.74	0.69-0.79		0.74	0.69-0.79	
IDU	Record vs no record	11.21	9.32-13.48	<0.01	11.26	9.37-13.53	<0.01	11.20	9.32-13.46	<0.01	11.26	9.37-13.54	<0.01
HBV contact	Record vs no record	12.22	9.40-15.88	<0.01	12.24	9.42-15.91	<0.01	12.25	9.42-15.92	<0.01	12.24	9.42-15.91	<0.01
Imprisonment history	Record vs no record	1.71	0.63-4.64	0.29	1.71	0.63-4.64	0.29	1.71	0.63-4.62	0.29	1.71	0.63-4.63	0.29
Syphilis diagnosis	Record vs no record	5.57	3.97-7.82	<0.01									
GC diagnosis	Record vs no record				0.66	0.16-2.63	0.55						
Scabies diagnosis	Record vs no record							1.17	0.99-1.39	0.06			
TV diagnosis	Record vs no record										0.87	0.51-1.48	0.60

[a]IMD, first, most deprived to fifth, least deprived. HBsAg= Hepatitis B surface antigen; BB/STI= Blood borne or sexually transmitted infection; MSM= Men who have sex with men; GP= General practice; IMD= Index of multiple deprivation; NHS= National health service; IDU= Injecting drug use; GC= Gonorrhoea; TV= Trichomoniasis; OR= Odds ratio; CI= Confidence interval.

Table 3.8: Adjusted analysis of factors associated with a record of HBsAg seropositivity when considering individual BB/STI diagnoses

		Multivariable Model 7			Multivariable Model 8			Multivariable Model 9			Multivariable Model 10		
		OR	95% CI	p-value	OR	95% CI	p-value	OR	95% CI	p-value	OR	95% CI	p-value
Gender	Men, no MSM record	REF		<0.01	REF		<0.01	REF		<0.01	REF		<0.01
	Men, MSM record	6.88	3.95-12.01		6.88	3.94-12.01		7.26	4.17-12.64		6.39	3.64-11.24	
	Women, no pregnancy record	0.56	0.53-0.59		0.56	0.53-0.59		0.56	0.53-0.59		0.56	0.53-0.59	
	Women, with pregnancy record	2.24	2.12-2.37		2.24	2.12-2.37		2.25	2.13-2.38		2.24	2.12-2.37	
Age	Per 5-year older	1.16	1.15-1.17	<0.01	1.16	1.15-1.17	<0.01	1.16	1.15-1.16	<0.01	1.16	1.15-1.17	<0.01
Time at GP practice	Per 5-year longer	0.82	0.81-0.83	<0.01	0.82	0.81-0.83	<0.01	0.82	0.81-0.84	<0.01	0.82	0.81-0.83	<0.01
Ethnicity	White	REF		<0.01	REF		<0.01	REF		<0.01	REF		<0.01
	Asian	5.52	5.18-5.88		5.52	5.18-5.88		5.58	5.24-5.94		5.52	5.19-5.88	
	Black	9.31	8.70-9.97		9.31	8.70-9.97		9.46	8.84-10.13		9.31	8.69-9.96	
	Mixed	4.76	4.22-5.37		4.76	4.22-5.37		4.79	4.24-5.41		4.76	4.22-5.37	
	Other	4.91	4.38-5.50		4.91	4.38-5.50		4.97	4.43-5.57		4.91	4.38-5.51	
	Unknown	1.08	1.00-1.17		1.08	1.00-1.17		1.08	1.00-1.17		1.08	1.00-1.17	
IMD Quintile[a]	First	REF		<0.01	REF		<0.01	REF		<0.01	REF		<0.01
	Second	0.75	0.71-0.80		0.75	0.71-0.80		0.76	0.71-0.80		0.75	0.71-0.80	
	Third	0.61	0.57-0.66		0.61	0.57-0.66		0.62	0.58-0.67		0.61	0.57-0.66	
	Fourth	0.52	0.48-0.57		0.52	0.48-0.57		0.53	0.49-0.58		0.52	0.48-0.57	
	Fifth	0.49	0.45-0.53		0.49	0.45-0.53		0.50	0.46-0.53		0.49	0.45-0.53	
	Unknown	0.57	0.48-0.66		0.57	0.48-0.66		0.55	0.47-0.64		0.57	0.48-0.66	
NHS Region	London	REF		<0.01	REF		<0.01	REF		<0.01	REF		<0.01
	Midlands and West	0.68	0.63-0.73		0.68	0.63-0.73		0.67	0.62-0.72		0.68	0.63-0.73	
	North	0.70	0.66-0.75		0.70	0.66-0.75		0.68	0.64-0.73		0.70	0.66-0.75	
	South	0.74	0.69-0.79		0.74	0.69-0.79		0.74	0.69-0.79		0.74	0.69-0.79	
IDU	Record vs no record	11.26	9.37-13.53	<0.01	11.25	9.36-13.52	<0.01	5.31	4.30-6.55	<0.01	11.20	9.32-13.47	<0.01
HBV contact	Record vs no record	12.24	9.42-15.91	<0.01	12.24	9.42-15.91	<0.01	12.30	9.46-15.99	<0.01	12.25	9.42-15.92	<0.01
Imprisonment history	Record vs no record	1.71	0.63-4.64	0.29	1.71	0.63-0.46	0.29	0.54	0.20-1.51	0.24	1.72	0.64-4.65	0.29
GH diagnosis	Record vs no record	0.94	0.68-1.30	0.72									
HPV diagnosis	Record vs no record				1.03	0.78-1.37	0.81						
HCV diagnosis	Record vs no record							39.46	33.03-47.14	<0.01			
HIV diagnosis	Record vs no record										12.93	4.99-33.46	<0.01

[a]IMD, first, most deprived to fifth, least deprived. HBsAg= Hepatitis B surface antigen; BB/STI= Blood borne or sexually transmitted infection; MSM= Men who have sex with men; GP= General practice; IMD= Index of multiple deprivation; NHS= National health service; IDU= Injecting drug use; GH= Genital herpes; HPV= Human papillomavirus; HCV= Hepatitis C virus; HIV= Human immunodeficiency virus; OR= Odds ratio; CI= Confidence interval.

3.4.1 Population with a pregnancy record

Overall, 667,528 women had a pregnancy record and of these 95,321 (14.3%) had a record of HBsAg screening and 1,984 had a record of HBsAg seropositivity, yielding a seroprevalence of 0.30% (95% CI 0.28-0.31) in this group (Table 3.9). The HBsAg seropositive group comprised similar proportion of women of Asian, Black, or White ethnicity; about half (973/1984, 49.0%) were in London and most (1285/1984, 64.8%) were from deprived neighbourhoods. A small subset (124/1,984; 6.3%) had ≥1 non-pregnancy related screening indication, including 64/1,984 (3.2%) with ≥1 BB/STI diagnosis.

Table 3.9: Characteristics of the population with a record of pregnancy, total and according to the record of HBsAg screening and HBsAg seropositivity

Characteristic			Record of HBV screening		Record of HBV seropositivity[a]	
		Total n, (%)	Yes	No	Yes	No
Total		667,528 (100)	95,321 (100)	572,207 (100)	1,984 (100)	665,544 (100)
Age, median years (IQR)		30.7 (26.0-35.1)	30.8 (26.4-34.9)	30.7 (25.9-35.9)	31.5 (27.5-35.6)	30.7 (26.0-35.1)
Time at GP, median years (IQR)		9.3 (4.9-15.1)	10.8 (6.7-16.6)	9.0 (4.6-14.9)	7.4 (4.1-11.1)	9.3 (4.9-15.1)
Ethnicity, n (%)	Asian	64,801 (9.7)	8,940 (9.4)	55,861 (9.8)	553 (27.9)	64,248 (9.7)
	Black	33,220 (5.0)	3,903 (4.1)	29,317 (5.1)	591 (29.8)	32,629 (4.9)
	Mixed	11,421 (1.7)	1,348 (1.4)	10,073 (1.8)	86 (4.3)	11,335 (1.7)
	Other	10,839 (1.6)	1,292 (1.4)	9,547 (1.7)	71 (3.6)	10,768 (1.6)
	White	432,726 (64.8)	63,161 (66.3)	369,564 (64.6)	521 (26.3)	432,205 (64.9)
	Unknown	114,521 (17.2)	16,677 (17.5)	97,844 (17.1)	162 (8.2)	114,359 (17.2)
IMD quintile.[b] n (%)	First	135,712 (20.3)	17,214 (18.1)	118,498 (20.7)	762 (38.4)	134, 950 (20.3)
	Second	126,751 (19.0)	16,326 (17.1)	110,425 (19.3)	523 (26.4)	126,228 (19.0)
	Third	120,058 (18.0)	16,165 (17.0)	103,893 (18.7)	270 (13.6)	119,788 (18.0)
	Fourth	127,460 (19.1)	20,520 (21.5)	106,940 (18.7)	196 (9.9)	127,264 (19.1)
	Fifth	132,310 (19.8)	21,385 (22.4)	110,925 (19.4)	194 (9.8)	132,116 (19.9)
	Unknown	25,237 (3.8)	3,711 (3.9)	21,526 (3.8)	39 (2.0)	25,198 (3.8)
NHS Region, n (%)	London	135,745 (20.3)	12,888 (13.5)	122,857 (21.5)	973 (49.0)	134,772 (20.3)
	Midlands and East	121,442 (18.2)	18,024 (18.9)	103,418 (18.1)	270 (13.6)	121,172 (18.2)
	North	170,560 (25.6)	20,912 (21.9)	149,648 (26.2)	350 (17.6)	170,210 (25.6)
	South	239,781 (35.9)	43,497 (45.6)	196,284 (34.3)	391 (19.7)	239,390 (36.0)
Location, n (%)	Rural	109,561 (16.4)	18,377 (19.3)	91,184 (15.9)	77 (3.9)	109,484 (16.5)
	Urban	533,364 (79.9)	73,248 (76.8)	460,116 (80.4)	1,868 (94.2)	531,496 (79.9)
	Unknown	24,603 (3.7)	3,696 (3.9)	20,907 (3.7)	39 (2.0)	24,564 (3.7)
	≥1 BB/STI diagnosis	43,295 (6.5)	5,463 (5.7)	37,832 (6.6)	64 (3.2)	43,231 (6.5)
Screening Indication[c], n (%)	≥1	44,709 (6.7)	5,780 (6.1)	38,929 (6.8)	124 (6.3)	44,585 (6.7)
	IDU	1,030 (0.2)	167 (0.2)	863 (0.2)	8 (0.4)	1,022 (0.2)
	HBV contact	336 (0.1)	142 (0.2)	194 (0.0)	25 (1.3)	311 (0.1)
	Inmate history	46 (0.0)	8 (0.0)	38 (0.0)	0 (0.0)	46 (0.1)

	Syphilis	321 (0.1)	50 (0.1)	271 (0.1)	0 (0.0)	321 (0.1)
	GC	214 (0.0)	31 (0.0)	183 (0.0)	0 (0.0)	214 (0.0)
	Scabies	18,196 (2.7)	2,727 (2.9)	15,469 (2.7)	24 (1.2)	18,172 (2.7)
	TV	1,882 (0.3)	330 (0.4)	1,552 (0.3)	4 (0.2)	1,878 (0.3)
	GH	10,230 (1.5)	1,342 (1.4)	8,888 (1.6)	13 (0.7)	10,217 (1.5)
	HPV	14,158 (2.1)	1,168 (1.2)	12,990 (2.3)	25 (1.3)	14,133 (2.1)
	HCV	246 (0.0)	38 (0.0)	208 (0.0)	31 (1.6)	215 (0.0)
	HIV	7 (100.0)	0 (0.0)	7 (100.0)	0 (0.0)	7 (100.0)

[a]Record of HBsAg seropositivity at any time; [b]IMD, first, most deprived to fifth, least deprived; [c]Participants may have ≥1 indication. HBsAg= Hepatitis B surface antigen; GP= General practice; IMD= Index of multiple deprivation; NHS= National health service; IDU= Injecting drug use; BB/STI= Blood borne or sexually transmitted infection; GC= Gonorrhoea; TV= Trichomoniasis; GH= Genital herpes; HPV= Human papillomavirus; HCV= Hepatitis C virus; HIV= Human immunodeficiency virus.

3.5 Population with recorded country of birth

In total, 292,099/6,975,119 (4.2%) individuals had a recorded country of birth (Table 3.10). Among those from countries with intermediate or high HBsAg prevalence, 4,211/49,170 (8.6%) and 916/9,523 (9.6%) respectively had a record of HBsAg screening (vs. 9,431/233,406 [4.0%] for those from a low prevalence country; p<0.01). HBsAg seropositivity was lowest in those born in low HBsAg prevalence countries (0.12%; 95% CI 0.11%-0.14%), higher among those born in countries of intermediate prevalence (0.94%; 95% CI 0.85%-1.02%), and highest among those born in countries of high prevalence (1.91%; 95% CI 1.65%-2.20) (p<0.01).

Table 3.10: Characteristics of participants with recorded country of birth according to HBsAg prevalence in the country

Characteristic		HBsAg prevalence in country of birth		
		Low (<2%)	Intermediate (2-8%)	High (>8%)
Total, n (%)		233,406 (100)	49,170 (100)	9,523 (100)
Record of HBsAg screening	Yes	9,431 (4.0)	4,211 (8.6)	916 (9.6)
	No	223,975 (96.0)	44,959 (91.4)	8,607 (90.4)
Record of HBsAg seropositivity	Yes	290 (0.1)	460 (0.9)	182 (1.9)
	No	233,116 (99.9)	48,710 (99.1)	9,341 (98.1)
Gender, n (%)	Male	108,754 (46.6)	23,135 (47.1)	4,449 (46.7)
	Female	124,652 (53.4)	26,035 (52.9)	5,074 (53.3)
Age, median (IQR)		35.9 (26.4-48.6)	38.2 (30.4-48.0)	40.6 (31.6-50.7)
Time at GP, median years (IQR)		6.3 (2.6-11.1)	5.3 (2.1-9.8)	6.7 (2.8-11.0)
Ethnicity, n (%)	Asian	23,432 (10.0)	20,428 (41.6)	94 (1.0)
	Black	13,355 (5.7)	6,611 (13.5)	7,121 (74.8)
	Mixed	7,581 (3.3)	1,457 (3.0)	513 (5.4)
	Other	8,543 (3.7)	2,331 (4.7)	156 (1.6)
	White	168,180 (72.1)	15,070 (30.7)	1,016 (10.7)
	Unknown	12,315 (5.3)	3,273 (6.7)	623 (6.5)
IMD quintile[a], n (%)	First	82,131 (35.2)	20,260 (41.2)	4,911 (51.6)
	Second	58,878 (25.2)	13,615 (27.7)	2,464 (25.9)
	Third	39,701 (17.0)	6,528 (13.3)	1,241 (13.0)
	Fourth	28,501 (12.2)	4,354 (8.9)	403 (4.2)
	Fifth	18,532 (7.9)	3,461 (7.0)	319 (3.4)
	Unknown	5,663 (2.4)	952 (1.9)	185 (1.9)
NHS Region	London	107,802 (46.2)	27,884 (56.7)	6,064 (63.7)
	Midlands and East	12,932 (5.5)	2,764 (5.6)	524 (5.5)
	North	79,828 (34.2)	10,931 (22.2)	1,901 (20.0)
	South	32,844 (14.1)	7,591 (15.4)	1,034 (10.9)
Location	Rural	9,756 (4.2)	1,285 (2.6)	133 (1.4)
	Urban	218,044 (93.4)	46,961 (95.5)	9,207 (96.7)
	Unknown	5,606 (2.4)	924 (1.9)	183 (1.9)

[a]IMD, first, most deprived to fifth, least deprived. HBsAg= Hepatitis B surface antigen; GP= General practice; IMD= Index of multiple deprivation; NHS= National health service.

3.5.1 Specialist referral

Among those with a record of HBsAg seropositivity, 1,989/8,065 (24.7%) had a record of a referral to secondary care. By univariate analysis, the odds of a referral record were lower in women, those from the most deprived neighbourhoods and those living outside London (Table 3.11).

Table 3.11: Factors associated with a record of referral to specialist care among those with a record of HBsAg seropositivity

		Univariable analysis		
		OR	95% CI	p-value
Gender	Female vs male	0.8	0.7-0.9	<0.01
Age	per 5-year older	0.9	0.9-1.0	0.97
Time at GP	per 5-year longer	0.9	0.9-1.0	0.93
Ethnicity	Non-white vs White	0.9	0.9-1.1	0.70
IMD Quintile[a]	First vs Other	0.8	0.7-0.9	<0.01
NHS Region	Outside London vs London	1.2	1.1-1.3	<0.01
MSM	Yes vs no	0.6	0.1-2.5	0.44
IDU history	Yes vs no	0.8	0.5-1.3	0.34
Close HBV contact	Yes vs no	1.2	0.7-2.0	0.61
Imprisonment history	Yes vs no	3.1	0.4-21.7	0.26
BB/STIs diagnosis	≥1 vs none	1.1	0.8-1.4	0.70

[a]IMD, First, most deprived. HBsAg= Hepatitis B surface antigen; GP= General practice; IMD= Index of multiple deprivation; NHS= National health service; MSM= men who have sex with men; IDU= Injecting drug use; BB/STI= Blood borne/sexually transmitted infection

3.6 Discussion

This study of 6,975,119 patient records from 419 GP surgeries across England found that 2.8% overall had a record of HBsAg screening, increasing to 5.4% among those with ≥1 of the recorded screening indications available for analysis, which included MSM, IDU history of close HBV contact, history of imprisonment, and at least one BB/STI diagnosis. Screening rates remained stable between 2014 and 2018. Without considering women with a pregnancy record, HBsAg screening was most likely among those living in London, MSM, people with history of IDU, close HBV contacts, and people with a recorded diagnosis of syphilis or HCV infection. Country of birth was recorded in only 4.2% of the total population. Those born in countries with intermediate or high HBsAg prevalence, which are a recognised target groups for HBsAg screening, were more likely to have a screening record than those born in low prevalence countries (including the UK); yet less than 10% had a screening record. HBsAg seroprevalence was 0.12% overall. Within the limited data available on country of birth, it

reached 0.94% in those from intermediate prevalence countries and 1.9% among those from high prevalence countries. HBsAg seroprevalence was also substantially higher among MSM (1.1%), people from ethnic minority backgrounds (0.3-0.8%), those with a IDU history (1.3%), close HBV contacts (2.7%), and those with a record of syphilis (2.1%), HCV (6.5%), or HIV (4.5%). Interestingly, HBsAg seropositivity was strongly associated with a record of syphilis, but not with other common STIs including gonorrhoea, genital herpes, or HPV infection. Overall HBsAg screening and seropositivity were highest in the most deprived regions of England.

To our knowledge, this is the most extensive study of HBsAg screening patterns and HBsAg seropositivity in general practice across England. One key strength was the utilisation of data collected from a large and nationally representative network of GP practices, enriching the output of sentinel surveillance of blood-borne viruses[243]. The analysis provides evidence that the likelihood of having a HBsAg testing record increases with commonly recognised HBsAg screening indications. However, it also points to substantial opportunities to increase the offer of HBsAg testing across all the main NICE-endorsed indications we assessed. The findings also guide possible refinements in targeted screening, for instance when considering the independent association we observed between HBsAg seropositivity and a diagnosis of syphilis.

The inclusion of screening indications was dictated by the availability of representative CTV3 and READ2 codes within the dataset; therefore, only screening indications with appropriate coding could be included. As for many large database studies, and as also observed by the sentinel surveillance of blood-borne viruses[243] , the recording was not always complete. In particular, the country of birth was missing from a large portion of the population, preventing a full analysis of HBsAg screening patterns according to HBsAg prevalence in the country of birth. This is despite country of birth being required demographic information for GP registration in England[244]. We were not able to determine if the missing data was due to lack of recording or lack of coding, but this highlights an important area for improvement as highlighted by a recent campaign to improve migrant health care[245]. Although the associations between HBV seropositivity and deprivation was independent of all other modelled factors, we were not able to consider what proportion of migrants from countries of intermediate or high HBsAg prevalence were living in these areas, which may be significant[246].

Within the study population, the prevalence of HIV (0.002%) and HCV (0.04%) fell well below the estimated prevalence for England of 0.16% and 0.20%, respectively[247,248]. This may be attributed to a lack of disclosure of either a known HIV or HCV status or a risk for these infections[249]. It is also possible that those with a record of HBsAg seropositivity had a greater propensity for screening thus inflating the estimates.

Previous studies of HBsAg screening patterns and seroprevalence in GP records in the UK and Europe were limited in generalisability due to the utilisation of only local data[250],[27]. In England, outside of antenatal care, a large fraction of individuals access HBsAg screening via GP surgeries[241]. The RCGP-RSC is one of the largest sentinel research networks in Europe, collecting pseudoanonymised patient records from GP practices across England. A previous study evaluated the RCGP-RSC in its representativeness of the English census and national data on common chronic diseases and found that the database is representative of the English population, with only a small overrepresentation of younger ages and underrepresentation of white ethnicity and deprived people, possibly due to differences in data extraction[252].

Missed opportunities for HBsAg screening among individuals with an indication have been previously highlighted. A study of medical records from general practice in Bristol found that between 2006 and 2013, among 82,561 migrants from countries with HBsAg prevalence $\geq$2% who attended GP practices, only 9,627 (12%) underwent HBsAg testing[250]. We similarly found that among 58,693 individuals born in countries with HBsAg prevalence $\geq$2%, only 5,127 (8.7%) had a HBsAg screening record. Among those with other recorded screening indications (MSM, IDU history, close HBV contact, history of imprisonment, >1 BB/STI diagnosis), a small minority of 5.7% had a record of HBsAg screening. Increasing HBsAg screening in target populations accessing primary care has been consistently cited as a service need both in the UK and globally[251,253,254]. Barriers to provision include incomplete knowledge of HBV among both practitioners and patients, performance pay structure, limited time, and language or cultural challenges[255–257]. Certain populations may receive HBsAg screening as part of care outside of general practice, including GUM clinics, needle exchange and drug misuse clinics, or as part of a prison healthcare service[258–261]. Additionally, practitioners may not offer screening because of low rates of disclosure of risk associated practices[262].

The overall HBsAg seroprevalence of 0.12% in our study was marginally lower than the national estimate of 0.2%[42], but rates were substantially higher among those with certain recorded screening indications including MSM (1.1%), IDU history (1.3%), and close HBV contact (2.7%). Previous UK estimates indicated a HBsAg seroprevalence of 0.2-1.0% for MSM29,[264] and 0.42% for those with a history of IDU[265]. HBsAg seroprevalence among women with a pregnancy record was 0.3% and equal to that of national estimates[266,266]. A record of ≥1 BB/STI diagnosis overall increased by 20% the odds of HBsAg seropositivity; however, the effect was driven by specific associations with a diagnosis of HCV, HIV, syphilis, and marginally scabies. The association between HBV and both HIV and HCV is well recognised and HBsAg screening is recommended for all people with HIV or HCV[267]. A record of syphilis was associated with almost six-fold increase in the odds of HBsAg seropositivity. This is consistent with previous findings [268–270], including those from a systematic review showing that a diagnosis of syphilis was independently associated with a seven-fold increase in the odds of HBsAg seropositivity[271]. Data point to a common mode of transmission via the sexual route. The ongoing syphilis epidemic in the UK affects a large proportion of MSM, but in the last decade it has become more diverse involving heterosexual men and women[272]. National surveillance data from 2018 show that among 111 acute cases of hepatitis B with available information on exposure, over half were likely infected via heterosexual intercourse[237].

Deprivation is quantified in the UK with a weighted score, the Index of Multiple Deprivation which considers levels of income, employment, education, health, crime, barriers to housing and services and living environment with income and employment accounting for almost half of the score[273]. In this study, being registered at a GP practice in the most deprived neighbourhoods in England was independently associated with HBsAg seropositivity. Correspondingly, national surveillance data show that the yearly incidence of acute HBV infection is largely increased in more deprived areas[274].

It is estimated that ~80% of people living with HBV in the UK have not been diagnosed [44,234]. Screening at-risk groups for HBsAg in GP surgeries is recommended by NICE guidelines, and proposed to be cost-effective for populations with HBsAg seroprevalence >1%[275]. Recorded presence of screening indicators increased the likelihood of HBsAg screening in this study; however, there were large gaps in both the recognition (or recording) of such indicators and

the screening offered. Within screening indicators that can be routinely coded within GP datasets, key groups that would benefit from increased HBsAg screening include those from countries with intermediate/high HBV prevalence, MSM, those with a history or current or past IDU, close HBV contacts, and those with a BB/STI diagnosis including HCV, HIV, syphilis, and scabies. Across England, HBV infection is largely a disease of poverty, with the highest prevalence found in the most deprived neighbourhoods. Socioeconomic deprivation also affects HBV-related health outcomes, with higher incidence of HCC than seen in more affluent areas reported in England and Scotland[276,277]. GP surgeries located in deprived areas thus play a key role in ensuring higher rates of HBsAg screening. Checking the vaccination records of children born to mothers with HBV is an additional task, given that large proportion of women with a record of both pregnancy and HBsAg seropositivity were registered at GP practices located in highly deprived areas. Surveillance data indicate that nearly 1 in 4 infants born mothers with HBV have not completed the full HBV vaccination course by the age of one[61,279]. Outside of GP surgeries, guidelines from specialist societies such as the British Association for Sexual Health and HIV (BASHH)[280] could also be strengthened in terms of recommending HBsAg screening for heterosexual men and women with a diagnosis of syphilis.

One key research need is to understand which strategies, including for example electronic flagging systems, may lead to a higher offer of HBsAg screening in primary care, within the boundaries of confidentiality and respect, avoiding contributing to stigma, and considering the recognised barriers to implementation. Further studies are needed to dissect the relationship between a diagnosis of syphilis and HBsAg seropositivity and understand how this differs from that of other common STIs. Additionally, the effect of NHS region and IMD were stable across all models; as such future analysis may wish to patters of screening in individual NHS regions. While acknowledging that referral records might have been incomplete, we found that only approximately 1 in 4 of those with a record of HBsAg seropositivity also had an available referral record, with some evidence of uneven availability based on gender, socio-economic status, and place of residence. Thus, further research is needed to evaluate the current pathways of care for chronic HBV and what action may be required to ensure equality of access.

4 Soluble PD-L1 levels in people living with chronic HBV infection

4.1 Introduction

In 2016, the WHO called for the elimination of viral hepatitis as a public health threat by 2030[281]. This will require robust and targeted HBV screening strategies and access to anti-viral therapies that are often needed for life. In chapter 3 we show that the offer of HBsAg testing to key and at-risk populations was low. Furthermore, in those who had a history of HBsAg seropositivity only a minority were referred to specialist care. The difficulties faced in HBV elimination are similar to HCV which is transmitted by infected blood, found in similar populations, and many infected individuals with chronic HBV infection remain asymptomatic until significant disease develops[282]. Unlike HBV, HCV treatment has been revolutionised by the introduction of direct-acting antivirals (DAAs) which can elicit a curative sustained virological response in over 95% of patients treated in a finite duration[283]. The introduction of DAAs has directly increased the feasibility of HCV elimination. Unfortunately, no such curative therapy yet exists for chronic HBV infection. Instead, of the estimated 12-25% of people living with chronic HBV infection globally are eligible for NUC therapy, only 8% are treated[23,284]. Additionally, stable access to NUC therapy is often needed for life as the estimated HBsAg seroclearence rate is only ~1% annually[86]. Given the currently available interventions, the prospect of HBV elimination may seem bleak. However, the development of a curative therapeutic option is an intensely researched topic. HBV curative therapy strategies are focused on exploitation of immune regulatory pathways, with a focus placed on PD-1/PD-L1 interactions that are characteristically upregulated during chronic infection[173,285,286].

Vigorous innate and adaptive immune responses are key to clearance in acute, self-limited HBV infection[287,288]. However, adequate responses are mainly absent in chronic infection[289]. The heavy antigenic burden during chronic infection triggers persistent T-cell activation driving anergy and exhaustion. This is accompanied by hyperexpression of inhibitory molecules including PD-1 on the surface of effector cells and its natural ligand, PD-L1 expressed on infected hepatocytes as well as nonparenchimal liver cells (e.g., Kupfer cells), and resident and circulating antigen presenting cells and immune cells (primarily NK cells)[83,207]. The binding of PD-L1 to T-cells expressing PD-1 leads to a decrease in antiviral cytokine production, limited clonal expansion and altered T-cell metabolism including a shutdown of glycolysis, gradually leading to T-cell deletion or apoptosis[185,190,202,290]. Promisingly, the induced T-cell anergy and exhausted state is partially reversable in at least

some patients. As such, the PD-1/PD-L1 pathway has become a cornerstone of strategies to functionally cure chronic hepatitis B infection with the aim of reinvigorating HBV directed immune responses and induce sustained immunological control of HBV replication without lifelong treatment[221,291,292].

The PD-L1 molecule exists in a soluble form (sPD-L1). Circulating sPD-L1 exists as a heterogenous population of molecules that, reportedly, differ in both composition and function[293]. PD-L1 can be divided into two broad categories (i) membrane bound PD-L1(mPD-L1), which can be further subdivided into either (a) PD-L1 expressed on the surface of cell membranes e.g., hepatocytes or (b) circulating extracellular vesicle bound PD-L1 (exoPD-L1) which is believed to signal in a similar manner to mPD-L1[294]. The second (ii) broad category of PD-L1 is soluble PD-L1 (sPD-L1) that is produced from two sources (a) proteolytic cleavage of membrane bound forms by either MMPs or ADAMs and (b) alternative splicing of PD-L1 mRNA transcripts resulting in a form of PD-L1 lacking the transmembrane domain[295]. It has recently been highlighted that in certain cancers, sPD-L1 may either reinforce or trigger the PD-1/PD-L1 pathway independently of cell-to-cell contact[296]. The amount of intra-hepatic PD-L1 expression may predict success of anti-PD-L1 therapeutic interventions[297]. However, there are major complications that can arise from liver biopsies preventing routine pre-treatment assessment[298]. Previous studies have suggested that circulating levels of sPD-L1 may mirror cell surface expression[299]and thus may provide an alternative to liver biopsies to identify patients who would benefit from immunotherapy.

sPD-L1 measurement may also serve as a prognostic indicator. Increased levels of sPD-L1 have been associated with adverse outcomes in several forms of cancer, including HCC[296,300–304] Specifically, high levels of sPD-L1 may be a prognostic factor in determining the degree of cirrhosis and progression to HCC[302] Additionally, sPD-L1 levels are increased in certain chronic viral infections such as HIV infection, where sPD-L1 levels have been found to correlate with viraemia, activated $CD8^+$ T-cells and levels of CD14 and may be indirectly increased by HIV proteins[305–307]. sPD-L1 levels have also been found to be raised in chronic HCV infection when compared to healthy individuals[308]. Few studies have evaluated sPD-L1 in chronic hepatitis B infection. In the available literature, increased sPD-L1 levels in people living with chronic HBV is associated with increased inflammation, progression of liver disease, viral load and HBsAg levels[309–311]. However, the measured levels of sPD-L1 and clinical associations from these studies are not consistent.

In this observational study we used paired plasma samples sourced from a diverse and well described cohort of people living with chronic HBV infection and measured sPD-L1 levels with two platforms and explored relationships with clinical and virological factors.

4.2 Methods

4.2.1 Patient Population

Adults living with chronic HBV infection were recruited while attending outpatient clinics at the Royal Liverpool and Broadgreen University Hospital Trust. Plasma was collected from all participants and stored at -80°C until use. Demographic and clinical characteristics were transcribed from the patient record. Virological and biochemical characteristics, including HBV DNA load, HBeAg/anti-HBeAg, ALT, and HBsAg status were measured as part of routine care at Liverpool Clinical Labs, Liverpool, UK. Patients were grouped according to chronic hepatitis B infection phase as described in section 2.2.2 as adapted from the EASL guidelines for the management of chronic hepaitits B[46] [REF]. Briefly, using HBV DNA, HBeAg status, and ALT and defining criteria patients were grouped as HBeAg+ infection, HBeAg+ hepatitis, HBeAg- infection, HBeAg- hepatitis, HBeAg+ hepatitis on NUCs or HBeAg- hepatitis on NUCs. If patients met the criteria of more than one group, an ALT value >40 IU/ml was used as the defining characteristic.

4.2.2 HBeAg and HBsAg Quantification

HBeAg and HBsAg quantification were carried out as described in section 2.5. Briefly, the quantification of HBeAg was carried out with the Roche Elecsys® HBeAg assay (Roche diagnostics, Rotkreuz, Switzerland) on the cobas bioanalyser system according to the manufacturer's instructions on plasma from known HBeAg+ patients with available sample. Quantification was carried out at Roche Diagnostics, Rotkreuz, Switzerland. For quantification, the 1st World Health Organization standard for HBeAg (REF: 129097/12) was sourced from the Paul-Ehrlich-Institute, Langen, Germany. The quantification of HBsAg was carried out with the Roche Elecsys® HBsAg II assay (Roche Diagnostics, Rotkreuz, Switzerland) on the cobas e 801 bioanalyser according to the manufacturer's instructions on plasma from all patients with available sample.

4.2.3 sPD-L1 quantification

sPD-L1 was measured by two platforms as described in section 2.5.1. Briefly, the polyclonal anti-sPD-L1 ELISA based Ella platform (Biotechne® Protein Simple, San Jose, California, USA) (LLOQ=6.90pg/ml; ULOQ=26,300 pg/ml) and the monoclonal anti-sPD-L1 coated bead-based single molecule array (SIMOA) platform (Quanterix™, Billerica Massachusetts, USA) (LLOQ=1.05pg/ml; ULOQ=4,300). Measurements were performed by Microcoat Biotechnology, Starnberger See, Germany in duplicate. Ella used 2 polyclonal antibodies enabling detection of both membrane-bound and sPD-L1, whereas SIMOA uses 2 monoclonal antibodies specifically targeting sPD-L1. Correlation between the two platforms was first evaluated by running a dilution series with recombinant human PD-L1 protein (Abcam, Germany) in duplicate.

4.2.4 Statistical Methods

Variables were summarised with counts and medians with IQRs for categorical and continuous variables, respectively. All continuous variables were log-transformed and resulting coefficients back-transformed and presented as fold-change. Linear regression was used to explore possible relationships between sPD-L1 and clinical characteristics. Kruskal-Wallis with Dunn's multiple comparisons test was used to detect differences in median values between groups. For multivariable models, all univariate factors were included if significant or had a p-value of <0.15. Due to collinearity between HBeAg status and HBV RNA, two models were created where each HBeAg and HBV RNA were adjusted separately. A full sensitivity analysis was performed where possible sPD-L1 outlier values were removed can be found in appendix 9.5. Outliers were determined by calculating values three times above and below the upper and lower quartile ranges. Analyses were performed in STATA version 14 (College Station, Texas, USA) and GraphPad Prism version 9 (San Diego, California, USA).

4.3 Results

4.3.1 Clinical Cohort

From September 2018 to October 2019, 101 people living with chronic HBV infection were recruited from outpatient clinics at the Royal Liverpool and Broadgreen University Foundation Trust in Liverpool, UK of which 97 had available sample for sPD-L1 measurement. Overall, a majority of the cohort was male (58/97,60%) with a median age of 39 years IQR (33-47) and from predominantly Asian ethnic backgrounds (60/97,62%). Patient demographics and characteristics can be found in Table 4.1. Overall, 61/97 (63%) were on NUCs for a median of 2.3 years IQR (1.3-7.6). Most patients had HBV DNA levels lower than the limit of limit

quantification of 10 IU/ml (49/97,51%) and were HBeAg- (71/97,73%). A small proportion of patients showed signs of hepatocyte damage with ALT levels ≥40 IU/ml (19/97,20%). Patients were categorised according to their HBV phase and treatment status. Most patients were HBeAg- hepatitis patients on therapy (43/97,44%) and those with HBeAg- infection (24/97,25%), followed by HBeAg+ hepatitis on therapy, HBeAg+ Infection, HBeAg- hepatitis and HBeAg+ hepatitis (18/97, 19%; 5/97,5%; 4/97, 4%; and 3/97,3%, respectively).

Table 4.1: Patient characteristics of patients included in sPD-L1 analysis

			HBeAg Positive		HBeAg Negative		HBeAg Positive	HBeAg Negative
Characteristic		**Total**	**Infection**	**Hepatitis**	**Infection**	**Hepatitis**	**Hepatitis on NUCs**	**Hepatitis on NUCs**
		N=97	**n=5**	**n=3**	**n=24**	**n=4**	**n=18**	**n=43**
sPD-L1, median pg/ml (Ella) (IQR)		114 (67-238)	146 (129-151)	125 (79-246)	95 (64-194)	107 (84-192)	255 (108-369)	82 (57-157)
sPD-L1, median pg/ml (SIMOA)[a] (IQR)		38 (32-45)	33 (29-33)	52 (48-72)	38 (31-41)	63 (27-70)	39 (31-48)	37 (32-44)
Age, median (years) (IQR)		39 (33-47)	33 (30-38)	28 (27-47)	43 (35-46)	36 (34-41)	36 (25-41)	42 (36-51)
Gender, n (%)	Male	58 (60)	1 (20.0)	2 (66.7)	15 (63)	4 (100.0)	7 (38.9)	29 (67.40
	Female	39 (40)	4 (80.0)	1 (33.3)	9 (38)	0 (0.0)	11 (61.1)	14 (32.6)
Ethnicity, n (%)	Asian	60 (62)	4 (80.0)	2 (66.7)	13 (54.2)	1 (25.0)	16 (88.9)	24 (55.8)
	Black	19 (20)	0 (0.0)	1 (33.3)	7 (29.2)	2 (50.0)	0 (0.0)	9 (20.9)
	White	18 (18)	1 (20.0)	0 (0.0)	4 (16.7)	1 (25.0)	2 (11.1)	10 (23.3)
HBsAg, median log_{10} IU/ml (IQR)[b]		3.2 (2.6-3.8)	4.6 (4.2-4.8)	4.8 (2.8-5.2)	3.3 (2.6-3.6)	4.2 (4.2-4.3)	3.1 (2.7-3.9)	2.9 (2.5-3.5)
HBeAg, median log PEI Units/ml (IQR)[c]		2.5 (0.5-3.0)	3.0 (3.0-3.2)	3.1 (2.6-3.6)	N/A	N/A	1.6 (0.3-2.6)	N/A
HBV DNA, median log_{10} IU/ml (IQR)		1.1 (0.0-3.6)	8.7 (8.4-8.8)	8.4 (7.0-9.4)	3.2 (2.6-4.1)	3.9 (1.8-6.2)	2.8 (0.7-3.9)	0.0 (0.0-0.7)
HBV DNA, n (%)	Below LLOQ	49 (51)	0 (0.0)	0 (0.0)	1 (4.2)	1 (25.0)	7 (38.9)	40 (93.0)
	10-1,999	21 (22)	0 (0.0)	0 (0.0)	10 (41.7)	0 (0.0)	8 (44.4)	3 (7.0)
	2,000-19,999	11 (11)	0 (0.0)	0 (0.0)	6 (25.0)	2 (50.0)	3 (16.7)	0 (0.0)
	≥20,000	16 (17)	5 (100.0)	3 (100.0)	7 (29.2)	1 (25.0)	0 (0.0)	0 (0.0)
HBV RNA Detected, n(%)	Yes	61 (62.9)	5 (100.0)	3 (100.0)	16 (66.7)	4 (100.0)	18 (100.0)	15 (34.9)
	No	36 (37.1)	0 (0.0)	0 (0.0)	8 (33.3)	0 (0.0)	0 (0.0)	28 (65.1)
HBV RNA, median log_{10} copies/ml (IQR)		3.1 (1.7-5.8)	7.0 (6.8-7.4)	7.1 (6.2-8.6)	0.8 (0.0-3.0)	1.6 (0.5-4.7)	5.2 (3.3-6.9)	0.0 (0.0-1.7)
Overall years of therapy in those on NUCs at sampling, median (IQR)		2.3 (1.3-7.6)	N/A	N/A	N/A	N/A	2.2 (1.1-2.9)	3.8 (1.3-9.9)
ALT, median IU/ml (IQR)		25 (19-36)	21 (21-32)	63 (41-186)	23 (18-28)	44 (42-111)	31 (24-46)	23 (17-32)
Raised ALT, n (%)	>40 IU/ml	19 (20.0)	0 (0.0)	3 (100.0)	0 (0.0)	4 (100.0)	6 (33.3)	6 (14.0)

Characteristics of patients included in sPD-L1 analysis characterised by chronic hepatitis B infection phase. Dichotomous and categorical variables represented as counts with percentage, continuous variable presented as medians with inter-quartile ranges. [a]SIMOA measured in n=95 patients [b]HBsAg quantified in n=92 patients [c]HBeAg quantified in n=23 patients

4.3.2 Correlation between assays

The Ella and SIMOA® platforms were used to measure sPD-L1 levels in either base matrix spiked with recombinant sPD-L1 or plasma derived from patients living with chronic hepatitis B infection. A scatter plot of the measured sPD-L1 levels can be found in Figure 4.1. The degree of concordance between resulting sPD-L1 levels measured by the Ella and SIMOA® platforms was determined with linear regression. The two assays were strongly correlated when the sample material analysed was recombinant sPD-L1. Conversely, there was no correlation between sPD-L1 levels determined by the two assays when the sample material was plasma derived from patients living with chronic HBV infection.

Figure 4.1: Comparison of sPD-L1 quantification platforms (A) patient derived sPD-L1 (B)recombinant sPD-L1 protein

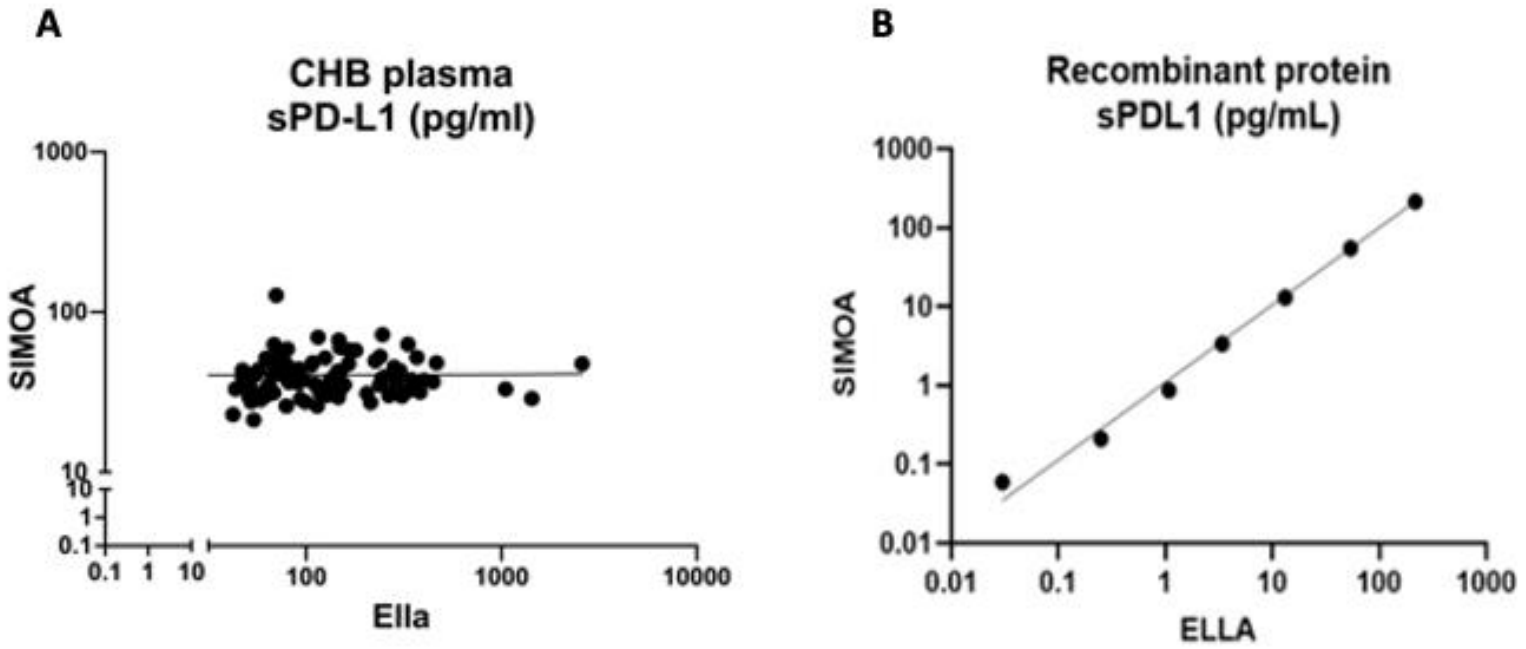

Linear regression analysis was used to compare sPD-L1 measurements with the Ella and SIMOA® platform. sPD-L1 was measured in n=97 patients with the Ella platform and n=95 with SIMOA®. Recombinant sPD-L1 protein dilution series from 0.5 to 500 pg/ml was used.

4.3.3 Variation in sPD-L1 levels across chronic HBV infection phases

sPD-L1 levels measure by the Ella and SIMOA® platforms had an overall median value of 114 pg/ml IQR (67-238) and 38 pg/ml IQR (32-45), respectively. By ELLA (Figure 4.2A), sPD-L1 levels were significantly higher among HBeAg+ patients vs. HBeAg- patients when analysing the population on NUCs (p=0.005). This relationship remained in the sensitivity analysis after excluding potential outliers (appendix 9.5). Levels of sPD-L1 were relatively similar when comparing the other groups (HBeAg+ infection, HBeAg+ hepatitis and HBeAg- infection) (Figure 4.2A). By SIMOA® sPD-L1 levels did not vary significantly between groups. There was a relative elevation in sPD-L1 in patients with HBeAg+ and HBeAg- hepatitis when compared to other chronic HBV infection phases, however these differences were not tested statistically due to the small number of patients in these groups in Figure 4.2B).

Figure 4.2: sPD-L1 quantified by Ella (A) and SIMOA® (B) and grouped by chronic HBV infection phase

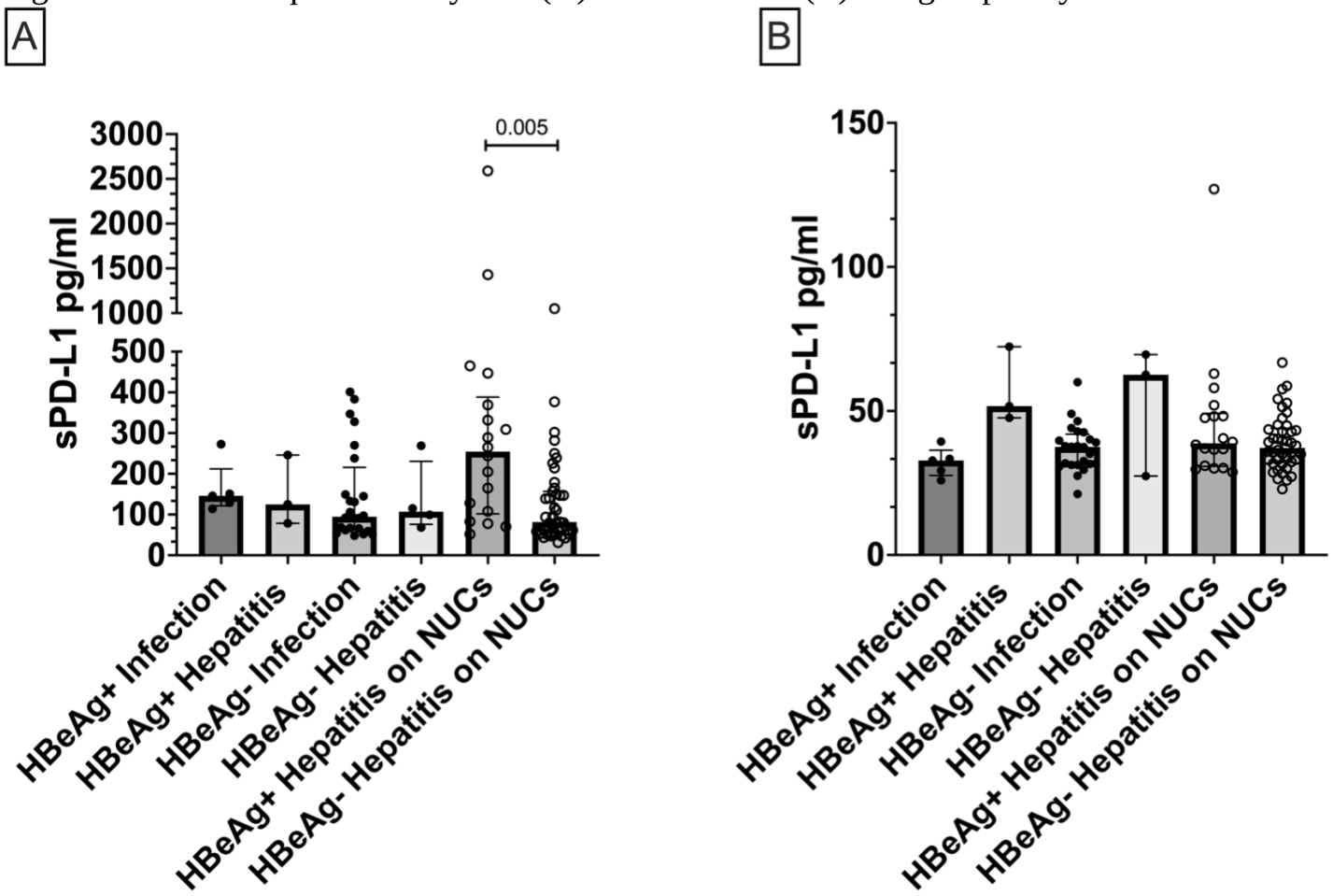

sPD-L1 levels quantified by both Ella and SIMOA® platforms. Differences in medians were calculated with Kruskal-Wallis test and significant differences <0.05 were analysed with Dunn's multiple comparisons test. Due to low numbers, HBeAg +/- hepatitis were excluded from the Kruskal-Wallis analysis.

Factors associated with levels of sPD-L1

Univariate and multivariable analyses were used to explore factors associated with sPD-L1 levels measured by both Ella and SIMOA®. In the univariable analysis, factors associated with sPD-L1 levels measured by the Ella platform were younger age, female gender, HBeAg positivity, and increased HBV RNA load (Table 4.2). Due to collinearity between HBeAg status and HBV RNA, two multivariable models were developed. After adjusting for age, gender, HBeAg status, HBsAg levels, and HBV RNA load, factors associated with sPD-L1 levels measured by the Ella platform were younger age, HBeAg positivity, and female gender.

In the univariable analysis, factors associated with sPD-L1 levels measured by the SIMOA® platform were increased HBsAg, HBV RNA and ALT levels (Table 4.3). After adjusting for HBeAg status, HBsAg levels, HBV RNA load and raised ALT levels, a sole association was detected between sPD-L1 levels measured by SIMOA® and raised ALT levels. An association of borderline significance was also found between sPD-L1 levels and levels of HBsAg.

Table 4.2: Univariate and multivariate factors associated with levels of sPD-L1 fold change (ELLA)

		Univariate			Multivariable 1			Multivariable 2		
Characteristic		FC	95% CI	p-value	FC	95% CI	p-value	FC	95%CI	p-value
Age	Per 5 year older	0.94	0.92-0.97	<0.01	0.95	0.92-0.98	<0.01	0.95	0.92-0.98	<0.01
Gender	Male vs Female	0.84	0.73-0.97	0.02	0.88	0.76-1.01	0.07	0.87	0.75-0.99	0.05
Ethnicity	Asian	1.04	0.86-1.25							
	Black	1.00	0.80-1.27							
	White	REF		0.91						
HBeAg	Positive vs Negative	1.32	1.14-1.54	<0.01	1.21	1.03-1.42	0.02			
HBeAg (PEI/ml)[a]	Per log_{10} increase	0.96	0.83-1.10	0.52						
HBsAg (units/ml)	Per log_{10} increase	1.06	0.98-1.15	0.12	0.99	0.91-1.06	0.69	0.97	0.90-1.06	0.54
HBV DNA (IU/ml)	Per log_{10} increase	1.01	0.98-1.04	0.45						
HBV DNA (IU/ml)	Below LLOQ	REF		0.25						
	10-1,999	1.02	0.85-1.22							
	2,000-19,999	1.27	1.00-1.59							
	$\geq$ 20,000	1.04	0.85-1.27							
HBV RNA (cps/ml)	Per log_{10} increase	1.04	1.01-1.07	<0.01				1.02	0.99-1.06	0.14
On NUCs at sampling	Yes vs no	1.03	0.89-1.19	0.69						
Duration of therapy overall	Per year on NUCs	0.99	0.97-1.01	0.58						
ALT	Per 5 unit increase	1.00	0.99-1.02	0.54						
ALT >40	Yes vs no	1.08	0.91-1.29	0.38						

Univariable and multivariate linear regression factors associated with sPD-L1 levels measured by the Ella platform. [a] HBeAg was quantified in n=23 HBeAg+ patients. Due to collinearity between HBeAg and HBV RNA, two multivariable models were created. Characteristics with p<0.15 were included in the adjusted analysis.

Table 4.3: Univariate and multivariate factors associated with levels of sPD-L1 (SIMOA®)

		Univariate			Multivariable 1		
Characteristic		FC	95% CI	p-value	FC	95%CI	p-value
Age	Per 5 year increase	0.99	0.99-1.01	0.58			
Gender	Male vs Female	1.04	0.98-1.09	0.17			
Ethnicity	Asian	0.94	0.88-1.00				
	Black	0.95	0.88-1.03				
	White	REF		0.16			
HBeAg	Positive vs Negative	1.04	0.99-1.10	0.15	1.00	0.95-1.06	0.88
HBeAg (PEI/ml)[a]	Per log_{10} increase	1.00	0.95-1.07	0.78			
HBsAg (units/ml)	Per log_{10} increase	1.03	1.00-1.06	0.02	1.03	0.99-1.05	0.06
HBV DNA (IU/ml)	Per log_{10} increase	1.00	0.99-1.01	0.27			
HBV DNA (IU/ml)	Below LLOQ	REF		0.74			
	10-1,999	1.01	0.95-1.08				
	2,000-19,999	1.04	0.96-1.13				
	$\geq$ 20,000	1.03	0.96-1.11				
HBV RNA (cps/ml)	Per log_{10} increase	1.01	1.00-1.02	0.02			
On NUCs at sampling	Yes vs no	1.01	0.96-1.07	0.58			
Duration of therapy overall	Per year on NUCs	1.00	0.99-1.01	0.90			
ALT	Per 5 unit increase	1.01	1.00-1.02	<0.01			
ALT >40	Yes vs no	1.13	1.06-1.19	<0.01	1.13	1.06-1.20	<0.01

Univariable and multivariate linear regression factors associated with sPD-L1 levels measured by SIMOA® platform. [a]HBeAg was quantified in n=23 HBeAg+ patients. Due to collinearity between HBeAg and HBV RNA, two multivariable models were created. Characteristics with $p<0.15$ were included in the adjusted analysis.

4.4 Discussion

The exact role and function of sPD-L1 has yet to be fully elucidated. However, it has been postulated that sPD-L1 may potentiate the PD-1/PD-L1 pathway independent of cell-to-cell contact. As such, sPD-L1 will be an important consideration in therapeutic target development and biomarker strategies for the HBV curative programme[202]. In this study we measured the level of sPD-L1 in a heterogenous cohort of 97 people living with chronic HBV infection with two platforms (Ella and SIMOA®), examined the concordance between the two assays and determined factors associated with levels of sPD-L1 measured by both assays. The Ella and SIMOA® platforms only produced concordant results when the sample material was base matrix spiked with recombinant sPD-L1 protein, conversely there was no concordance between the two assays when sPD-L1 was measured in plasma derived from people living with chronic HBV. We found that in the adjusted linear regression analysis the level of sPD-L1 measured by the Ella assay were associated with females, younger age and HBeAg positivity while sPD-L1 measured by the SIMOA® platform was solely associated with increased levels of ALT.

The two assays utilised in this study have different analytical approaches to measuring sPD-L1. The Protein Simple® Ella assay relies upon traditional ELISA technology. Technical specifications of the Ella PD-L1 assay report good correlation (R^2 >0.9) when compared to their cobranded Quantikine® ELISA kit which targets the immunogenic region Phe19-Thr239 of the PD-L1 molecule[312] with a polyclonal anti-PD-L1 antibody. The SIMOA® assay relies upon magnetic beads coated with capture monoclonal antibodies and a fluorescent reporter enzymes to detect single protein analyte molecules[313]. However, the immunogenic region targeted by the SIMOA® is not published. Despite different analytical approaches and clonality of the antibodies, the good correlation between SIMOA® and Ella platform when detecting recombinant sPD-L1 protein suggests they may be detecting colocalised regions when there is a single type of sPD-L1 protein.

Due to the large diversity of sPD-L1 molecules it is reasonable to conclude that the accountable differences in the two assays may be due to measuring different forms of sPD-L1. In a study of 101 patients with lymphoma, exoPD-L1 and sPD-L1 were measured in plasma with both SIMOA® and R&D systems ELISA assay. They found that there was concordance between the SIMOA and Quantikine assays only when exoPD-L1 was measured by the two platforms (r=0.99), however there was no linear relationship found when levels of exoPD-L1 and sPD-L1 were compared (r=0.02)[314]. One explanation for this discordance is that different forms of

PD-L1 may have different immunogenic binding regions resulting from conformational changes that may affect capture antibody binding. Alteration of protein conformation is supported by the previous studies that found sPD-L1 produced via proteolytic cleavage has less PD-1 binding capacity when compared to sPD-L1 produced by alternative splicing[295]. It is also plausible that the clonality of the antibody pairs directly affects the subtype of sPD-L1 measured. In the Ella platform, a polyclonal anti human PD-L1 antibody was used for antigen capture thus may have either a degree of cross-reactivity with PD-L2 or detecting more than one form on sPD-L1[315]. The latter of these two hypotheses may account for the substantially higher limit of detection and dynamic range of the Ella assay compared to SIMOA[316,317].

sPD-L1 may be a potential biomarker for both disease progression and treatment eligibility in a multitude of cancers including non-small cell lung cancer, hepatocellular carcinoma, breast cancer and even used to stratify immunotherapy treatment eligibility such as pembrolizumab and nivolumab[318–320]. However, this study highlights an important finding; there are large discrepancies in quantified levels of sPD-L1 between commercially available (research use only) assays. To our knowledge, there is no currently available assay for sPD-L1 that has been validated for diagnostic use. Assays for measuring membrane bound PD-L1 in tissue, have been developed as companion test ("essential for the safe and effective use of a corresponding drug or biological product" [321] or co-diagnostic tests (non-essential but may be used to stratify therapy eligibility) for cancer therapeutics. A systematic review of 26 primary studies evaluating PD-L1 immunohistochemistry found that there was poor agreement between PD-L1 antibodies and no defined threshold for PD-L1 positivity[297]. The data presented expand this notion to also include sPD-L1 measurement. Currently, there are several molecules in early development with the aim of reinvigorating the immune response of people living with chronic HBV infection. Several of these clinical trials specifically target PD-L1 and measure sPD-L1 levels as an exploratory biomarker [292]; thus it may seem possible that future immunotherapies for chronic hepatitis B infection may rely on preselection of patients based on baseline sPD-L1 levels. As indicated in this analysis, assays employed for selection or monitoring patients for which sPD-L1 is a predictor of interest will need to be validated and broadly standardized.

We found that HBeAg positivity was associated with a 32% increase in sPD-L1 when measured by the Ella platform. HBeAg positivity is often associated with high levels of HBV DNA, HBV RNA and decreased immune responses[46]. However, the association found between sPD-L1 and HBeAg was independent of levels of HBV replication. The role of the HBeAg molecule itself

is debated. It is an accessory protein not crucial for viral replication as exemplified in pre-core mutant HBV infection that is characterised by high levels of HBV replication with no production of HBeAg[46]. Studies have suggested that HBeAg may be directly tolerogenic and thus may play a role in the classical exhausted T-cell phenotype described in chronic HBV infection[322,323]. The mechanism by which circulating HBeAg induces a tolerogenic state in T-cells is not well understood but there is evidence to suggest that HBeAg may direct the upregulation of PD-L1, eventually leading to T-cell deletion[207,324]. Interestingly, we did not find that higher serum levels of HBeAg were associated with increased levels of sPD-L1, suggesting that HBeAg positivity may have been a proxy for immune status. Our findings conflict with some previous studies. In a cross-sectional cohort of a diverse population of 273 people living with chronic HBV infection, sPD-L1 was quantified using the mlbio®(Shanghai, China) ELISA assay. They found that sPD-L1 was associated with HBsAg level and HBV DNA but found no association with HBeAg positivity. However, the results of this study should be interpreted with caution as no attempt was made to adjust for confounding factors, and there is limited comparability between sPD-L1 assays as highlighted in this study[310]. The association found in this analysis between HBeAg positivity and sPD-L1 levels may have important implications for treatment eligibility. A study of *ex vivo* PBMCs from people living with chronic HBV infection found that those who had already seroconverted HBeAg and had low levels of HBV DNA had more robust T-cell responses following blockade with anit-PD-L1 antibodies[325] suggesting that immunotherapies may provide greater therapeutic benefit to HBeAg- individuals that have lower levels of sPD-L1.

HBV-associated liver damage is not the direct consequence of virus cytotoxicity and instead is a result of host immune responses. ALT is exuded from damaged hepatocytes into the blood and measured clinically as a surrogate marker of immune mediated damage. Previous studies found that sPD-L1 levels were positively associated with increased ALT levels regardless of HBeAg positivity and may predict disease progression[311,326]. It may seem counter intuitive that sPD-L1, which is associated with immune tolerance, is positively associated with ALT levels. One possible explanation is that the subtype of sPD-L1 associated with ALT levels is not functional. For example, *in vitro* studies have shown that HBV, via the HBx protein, is able to induce the expression of matrix metalloprotease-9 (MMP-9), an important enzyme in the degradation of extracellular matrix and cleavage of membrane bound PD-L1 (mPD-L1) to form sPD-L1[327,328]. Functional studies have suggested that the PD-1 binding region is removed when sPD-L1 is produced via MMP-9 proteolytic cleavage thus removing inhibition of T-cell

effector function and favouring a more inflammatory environment[328,329]. It is due to this association between MMPs and PD-L1 cleavage, that expression of these proteases is implicated in resistance to immunomodulators targeting the PD-1/L1 pathway[330]. sPD-L1 molecules may also act as antagonists to conventional PD-L1. An *in-vitro* study which evaluated mPD-L1 and sPD-L1, generated via alternative splicing, and their effect on the T-cell compartment. They found that when $CD8^+$ cells were challenged with mPD-L1, there was a significant decrease in proliferation and production of cytolytic molecules. However, when $CD8^+$ cells were challenged with sPD-L1, there was no decrease in proliferation or cytokine production. Upon further evaluation, they found that in this context, the sPD-L1 molecule acted antagonistically, effectively blocking the suppressive capacity of the PD-1/PD-L1 pathway. The antagonistic function was reversed with the addition of anti-PD-L1 antibodies. It should be noted that the authors carefully controlled for confounding by blocking exosome production, which may have produced circulating PD-L1 like membrane forms[331]. However, there is a need for further research to pinpoint the exact mechanisms sPD-L1 may contribute to or fail to dampen, inflammatory processes.

Detection of sPD-L1 without discrimination of subtype, may be helpful in the context of new immunotherapies targeting the PD-1/L1 pathway. For example, a recent phase 1 study evaluating a novel locked nucleic acid single stranded oligonucleotide specific for PD-L1 mRNA (RO7191863) in virologically suppressed patients with chronic HBV infection found that sPD-L1 levels (by tSIMOA®) declined in parallel with a decline in serum HBsAg and a raise in ALT[292]. This suggests a peripheral decline in measured sPD-L1 may prove to be an important biomarker for evaluating favourable responses to novel therapeutic agents.

There are limitations to this study. First, the study design could be optimised in the future to include healthy controls and prospective sampling. Previous studies have shown that sPD-L1 levels are increased in people living with chronic HBV infection compared to healthy controls and can vary over time especially after the introduction of NUC therapy[311,326]. The largest improvement to this study would be to incorporate differentiation of sPD-L1 subtypes. This has been accomplished previously in several studies with various approaches including multiplex detection of both PD-L1 and CD63 or CD82 to identify exoPD-L1[331] or detection of the glycosylated forms of sPD-L1. N-glycosylated PD-L1 and sPD-L1 has been shown to be the most stable version of the molecule and may directly increase the ability of sPD-L1 to bind to PD-1[332,333]. The sequestration of sPD-L1 molecules with the ability to bind PD-1 may be

monitored in peripheral plasma utilising adapted ELISA platforms[334]. However, with this technique it may prove difficult to prevent binding to other subtypes of sPD-L1 if measured using patient samples. To our knowledge, no studies have differentiated splice variant sPD-L1 versus proteolytically cleaved subtypes of sPD-L1 *in vivo*, it has been suggested that splice variants of sPD-L1 naturally dimerize thus possibly allowing for exclusion based on molecular weight[295]. Future investigations examining the relationship between sPD-L1 levels and circulating lymphocytes may provide insight as to which immune cells may be affected by sPD-L1.

Despite discovery of the PD-1/PD-L1 pathway in 1992, there are still many unanswered questions of the divisive role of sPD-L1. How sPD-L1 is associated with circulating T-cell compartments is not well researched and should be evaluated in future studies as this would possibly infer the function of different subtypes. As discussed previously, sPD-L1 levels have been associated with different disease phases, however this has not taken into account the subtypes of sPD-L1 and future studies should evaluate if there are dominate sub-types at different timepoints as this may affect their role. Clinically, anti-PD-L1 therapy, approached through either antibody mediated or RNA targeting therapeutics may not be effective alone in reinvigorating the immune response in people living with chronic HBV infection[335,336]. Importantly, this study provides the first head-to-head comparison of sPD-L1 quantification in a well described and heterogenous cohort of people living with chronic HBV infection and highlights the discrepancies in detection of sPD-L1 when using different assays.

5 Peripheral lymphocyte PD-1 expression and correlations with novel and traditional parameters and hepatitis B infection disease state

5.1 Introduction

Programmed cell death 1 (PD-1) is a cell surface receptor that is broadly expressed on the surface of T-cells, B-cells, NK-cells, and other myeloid populations[202]. PD-1, in addition to playing a key role in immune homeostasis, through its interaction with the ligand PD-L1, is thought to modulate the outcome of HBV infection by inducing a state of anergy in both the innate and adaptive responses, leading to established chronicity[337,338]. The mechanisms that contribute to the impaired immune recognition and failed clearance of HBV are not fully understood but are likely to include multiple immune system changes including; imbalanced cytokine expression patterns, altered epigenetic profile of lymphocytes, and modified metabolic regulation, in addition to the upregulation of inhibitory immune markers[150,339–341]. Several studies have previously examined the *ex vivo* expression levels of PD-1 in people living with chronic HBV infection with different disease profiles[82,342–345]. However, within these studies, there is inconsistency in the correlates between virological and biochemical parameters and disease phase status.

T-lymphocytes that have undergone MHC specialisation for HBV peptides are subjected to continuous rounds of antigen induced activation. It is currently thought that due to chronic *de novo* activation, subsets of CD8 T-cells exist in a state of either partial and reversable functional impairment, termed non-terminally exhausted or have progressed past a tipping point where they can no longer return to their previous capacity and are termed terminally exhausted. A variety of parameters have been proposed to differentiate the different effector states. A previous study on *ex-vivo* T-lymphocytes from patients with HCV, which may have a similar T-cell antigen induced exhaustion immunopathology, identified a CD8 subset TCF-1$^+$ CD127$^+$ PD-1$^+$ that had characteristics of both memory and exhaustion. Upon stimulation *in vitro* with viral peptides, the TCF-1$^+$CD127$^+$PD-1$^+$ subset expanded. However, after antigen exposure the CD8$^+$ T-cell subset lost expression of TCF1 and CD127 but retained high levels of PD-1. Functional experiments suggested that the CD8$^+$ subset TCF-1$^+$CD127$^+$PD-1$^+$ may represent a non-terminally exhausted population while the TCF1$^-$CD127$^-$PD-1$^+$ population represented a terminally exhausted state[194]. Further studies suggested that the co-expression of ectonucleotidase CD39, may further characterize the subpopulation of CD8$^+$ T-cells that are terminally exhausted[346,347]. Disruption of the PD-1/PD-L1 pathway with antibody-based

therapies has the potential for reinvigoration of the immune responses by lymphocytes that are not terminally exhausted. Early clinical studies have demonstrated that rescuing non-terminally exhausted lymphocytes is possible by targeting the PD-1/PD-L1 pathway[220,348]. It is important to understand the correlations between exhausted T-cells and other novel and traditional clinical parameters, as they may be important in selecting suitable patients for future curative trials[349].

It is hypothesised that circulating soluble PD-L1 (sPD-L1) may have multiple immune regulatory functions and may also prompt activation of the PD-1/PD-L1 pathway without direct cell-to-cell contact[295,350]. In chapter 4, we provided background information on sPD-L1 and a detailed analysis of the levels of circulating soluble PD-L1 (sPD-L1) in different phases of chronic HBV infection. The correlation between sPD-L1 levels and PD-1 expression on circulating immune cells during chronic HBV infection has not been studied. The aim of this hypothesis-generating study was to investigate possible associations between peripheral PD-1 expression on a broad selection of T-cell and NK-cell populations and both clinical parameters and levels of sPD-L1 in patients in different stages of chronic HBV infection.

5.2 Methods

5.2.1 Study Population and sampling

The cohort of participants were asked to join this observational study while attending routine care appointments for chronic hepatitis B at the Royal Liverpool University Hospital in Liverpool, United Kingdom as described in section 1.1.2. Briefly, pseudoanonymised demographic data and treatment history were collected from the patient's medical records. Virological markers including HBV DNA, HBeAg, qualitative HBsAg and biochemical markers including the levels of ALT, bilirubin and platelets were measured as part of routine care in samples either collected on the day of recruitment or measured within the two weeks prior to recruitment as part of routine care. Routine virological and biochemical measures were conducted at either Liverpool Clinical Laboratories, Liverpool UK or at the University of Liverpool as described in section 1.1.2. Samples for research were collected and transferred to the Institute of Infection and Global Health and processed as described in section 1.2. Non-routine biomarkers including the level of sPD-L1, quantitative HBsAg and quantitative HBeAg were measured on research samples as described in section 2.5.

Patients with chronic HBV infection were categorised according to levels of HBV DNA and ALT as well as HBeAg status according to cut-off values adapted from the EASL guidelines as described in section 2.2.2. Briefly, patients were categorised into six groups including those with HBeAg+ infection, HBeAg+ hepatitis, HBeAg- hepatitis, HBeAg- infection and those with HBeAg+/- hepatitis and receiving NUC therapy.

5.2.2 Cell preparation and cryopreservation

Cells were prepared as described in section 2.3.2. Briefly, 30ml of whole blood was split equally into two 50ml Falcon tubes containing 13ml of pre-warmed RPMI1640 (Gibco). The K_2EDTA tubes were then washed with 2ml of RPMI 1640 to remove any remaining blood. The whole blood + RPMI mixture was then carefully layered on top of 15ml of Lymphoprep in a fresh 50ml Falcon tube. The layered diluted blood and Lymphoprep tube was then centrifuged at 800xg 20°C for 15 minutes with full acceleration and no break. PBMCs were carefully harvested by aspiration from the resulting interface between the diluted plasma and underlying Lymphoprep with Pasteur pipettes. The PBMCs were then washed twice by resuspending in 50ml of R-10 media and centrifuged at 400xg for 10 minutes (full acceleration and deceleration). The PBMCs were then resuspended in 10ml of R-10 media. The PBMCs were counted as described in section 2.3.3. A total of $1.2x10^7$ cells were removed for use in fresh flow cytometry. The remaining cells were then cryopreserved for future studies as described in section 2.3.2.

5.2.3 Flow Cytometry

5.2.3.1 Panel and cell staining

The flow-cytometry panel used was designed to include broad detection of immune cell subsets including total $CD8^+$ and $CD4^+$ T-cells, NK cells ($CD3\text{-}CD56^+$) and to determine the expression of PD-1 on each of those cell types. A separate panel was included to explore non-terminally and terminally exhausted $CD8^+$ T-cell phenotypes, as described by Wieland et.al in the context of chronic HCV infection and defined as $CD127^+TCF1^+PD\text{-}1^+$ for non-terminally exhausted and $CD127^-TCF1^-PD\text{-}1^+CD39^+$ for terminally exhausted. Optimal antibody concentration was determined by titration on archived cryopreserved PBMCs. Staining was completed as described in section 2.4.1.

5.2.3.2 Lymphocyte population gating and analysis considerations

The identification of lymphocyte populations and representative gating diagram are detailed in section 2.4.1.6. Briefly, fluorescence minus one controls (FMO) were used to identify positive populations that had indiscriminate separation including total $CD56^+$ cells, PD-1, TCF-1, and CD127 populations. The use of FMO controls was not necessary for $CD45^+$, $CD3^+$, $CD4^+$ and $CD8^+$ populations.

In order to standardise the percentage of lymphocyte populations are reported as a proportion of total $CD45^+$ cells. The percentage of PD-1^+ was measured on each parent cell population and also reported as a proportion of the total $CD45^+$ population. Non-terminally and terminally exhausted $CD8^+$ T-cells ($CD127^+TCF1^+PD\text{-}1^+$) ($CD127^-CDF1^-PD\text{-}1^+CD39^+$), respectively are reported as a proportion of total $CD8^+$ T-cells.

5.2.3.3 Statistical Analysis

The characteristics of the study population were represented as counts for dichotomous variables and median with interquartile ranges for continuous variables. The percentage of lymphocyte subsets and the percentage PD-1$^+$ lymphocytes were presented as median with IQRs. The median percentage of lymphocyte subsets and percentage PD-1$^+$ were compared between clinical phases, differences in the medians were explored with Kruskal-Wallis test for and paired with Dunn's post-hoc test for individuals p-values. Potential relationships between clinical characteristics and cellular data were explored with Spearman correlation analysis and presented as a correlation matrix. The correlations with significant findings were represented with scatter plots. Categorical clinical characteristics such as HBeAg, treatment status and those with raised ALT values (>40 IU/ml) as defined by EASL guidelines[46] were explored with either Fisher's exact test for dichotomous variables, and Kruskal-Wallis with the Dunn's post-hoc test for grouped categorical variables. Significant findings from the Spearman correlation analysis were further assessed by dividing patients into two groups using the median percentage PD-1$^+$ into those above and below the median of the overall population for the respective parameter or cell-type. This was indicated as either high percentage (groups I) or low percentage (Group II); differences between the two groups were explored with Fisher's exact test. As non-terminally exhausted T-cells are thought to shift toward a terminally exhausted, therefore non-terminally to terminally exhausted CD8$^+$T-cells were expressed as a ratio by dividing the frequency of non-terminally exhausted by terminally exhausted and expressed as relative frequency. A ratio of >1 indicated a greater proportion of non-terminally exhausted CD8+ cells, conversely a ratio of <1 indicated more terminally exhausted CD8+ cells. Due to the exploratory nature of this study, no p-value corrections were performed, thus p-values should only be considered indicative of possible associations. Statistical analysis was completed with STATA version 14 (College Station, TX, USA) and GraphPad Prism 9 for Mac (La Jolla, California, USA). Patients were categorised by HBV disease as described in section 2.1.2.

5.3 Results

5.3.1 Study Population

From September 2018 to October 2019, 101 patients with chronic HBV infection were recruited from outpatient clinics at the Royal Liverpool and Broadgreen University Foundation Trust, Liverpool, UK. Peripheral blood mononuclear cells (PBMCs) from 101 patients were isolated from whole blood and stained with two flow-cytometry panels; the first captured PD-

1 expression on total CD4+, CD8+, CD56+ cells and the second, CD8+ cells classed as non-terminally exhausted (CD127+ TCF1+ PD-1+) or terminally exhausted (CD127- TCF1- CD39+ PD-1+).

Overall, 3/101 (3%) patients were removed entirely from the analysis and 7/101 (7%) were removed from the exhaustion panel alone due to inadequate or failed staining. Demographic and clinical characteristics of the 98 patients included in the analysis according to their HBV infection and disease status can be found in Table 5.1. Just over half were male, a large proportion were from Asian ethnic backgrounds, and the median age was 39 years and overall, 62/98 (63.3%) patients were receiving NUC therapy and had a median time on therapy at recruitment of 3 years (IQR 1-7). In patients with a detectable viral load, the median HBV DNA level was 3,564 IU/ml (IQR 477-7,229). Overall, 28/98 (28.6%) of patients were HBeAg positive, of whom 23 had an available sample for HBeAg quantification; the median HBeAg level was 257.1 PEI U/ml (IQR 4.8-851.5). A total of 82 patients had an available sample for HBsAg quantification, with a median level of 1,797 IU/ml (IQR 477 - 6,208).

Table 5.1: Patient characteristics by chronic HBV infection and treatment status

Characteristic		**Total**[a]	HBeAg+		HBeAg-		HBeAg+	HBeAg-
			Infection	**Hepatitis**	**Infection**	**Hepatitis**	**Hepatitis on NUCs**	**Hepatitis on NUCs**
		N=98	**n=6**	**n=3**	**n=22**	**n=5**	**n=19**	**n=43**
Age, median years(IQR)		39 (32-46)	30.5 (29-37)	27 (26-46)	43 (35-46)	35 (34-37)	35 (24-41)	42 (35-50)
Gender, n (%)	Male	56 (57)	1 (16.7)	2 (66.7)	13 (59.1)	5 (100.0)	7 (36.8)	28 (65.1)
	Female	42 (43)	5 (83.3)	1 (33.3)	9 (40.9)	0 (0.0)	12 (63.2)	15 (34.9)
Ethnicity, n (%)	Asian	63 (64)	5 (83.3)	2 (66.7)	13 (59.1)	1 (25.0)	17 (89.5)	25 (58.1)
	Black	17 (17)	0 (0.0)	1 (33.3)	6 (27.3)	2 (40.0)	0 (0.0)	8 (18.6)
	White	18 (18)	1 (16.7)	0 (0.0)	3 (13.6)	2 (40.0)	2 (10.5)	10 (23.3)
sPD-L1 (Ella), median pg/ml (IQR)		114 (67-239)	146 (129-151)	125 (79-246)	102 (67-238)	99 (69-115)	255 (108-369)	81 (57-150)
sPD-L1 (SIMOA), median pg/ml (IQR)		38 (32-45)	33 (29-33)	52 (48-72)	38 (32-43)	51 (34-66)	39 (31-48)	36 (32-43)
HBsAg, median log_{10} IU/ml (IQR)[b]		3.3 (2.7-3.8)	4.6 (4.2-4.8)	4.8 (2.8-5.2)	3.3 (3.1-3.6)	4.2 (-2.3-4.3)	3.2 (2.7-4.1)	2.9 (2.5-3.5)
HBeAg, median log10 PEI U/ml (IQR)[c]			3.0 (2.9-3.2)	3.1 (2.6-3.6)	N/A	N/A	1.6 (0.3-2.6)	N/A
HBV DNA, median log10 IU/ml (IQR)		1.0 (0.0-3.4)	8.7 (8.4-8.9)	8.2 (7.0-9.4)	3.2 (2.5-4.0)	3.3 (1.3-6.2)	2.6 (0.7-3.9)	0.0 (0.0-0.7)
HBV DNA, n (%)	Not Detected	28 (29)	0.0 (0.0)	0.0 (0.0)	0.0 (0.0)	1 (20.0)	3 (15.8)	24 (55.8)
	<LLOQ	18 (18)	0.0 (0.0)	0.0 (0.0)	1 (4.6)	0.0 (0.0)	2 (10.5)	15 (34.9)
	10-1,999	23 (24)	0.0 (0.0)	0.0 (0.0)	12 (54.6)	1 (20.0)	6 (31.6)	4 (9.3)
	2,000-19,999	12 (12)	0.0 (0.0)	0 (0.0)	5 (22.7)	2 (40.0)	5 (26.3)	0 (0.0)
	≥20,000	17 (17)	6 (100.0)	3 (100.0)	4 (18.2)	1 (20.0)	3 (15.8)	0 (0.0)
HBV RNA, n(%)	Detected	62 (63)	6 (100.0)	1 (100)	15 (68.2)	5 (100.0)	19 (100)	15 (34.9)
	Not detected	35 (36)	0 (0.0)	0 (0.0)	7 (31.8)	0 (0.0)	0 (0.0)	28 (65.1)
On NUCs, n(%)	Yes	62 (63)	0 (0.0)	0.0 (0.0)	0.0 (0.0)	0.0 (0.0)	19 (100.0)	43 (100.0)
	No	36 (37)	6 (100.0)	3 (100.0)	22 (100.0)	5 (100.0)	0.0 (0.0)	0.0 (0.0
Duration of NUCs at sampling, median years (IQR)		3 (1-7)	N/A	N/A	N/A	N/A	2.2 (1.1-2.9)	3.3 (1.3-9.9)
Previous IFN exposure, n(%)		19 (10)	0 (0.0)	1 (33.3)	0 (0.0)	1 (20.0)	3 (15.8)	5 (11.6)
ALT, median (IQR)		25 (19)	21.5 (21-32)	63 (41-186)	23 (17-28)	42 (42-45)	29 (22-46)	23 (17-32)
ALT >40 IU/ml, n(%)	Yes		0 (0.0)	3 (100.0)	0 (100.0)	4 (80.0)	6 (31.6)	6 (14.0)

	No		6 (100.0)	0 (0.0)	0 (0.0)	1 (20.0)	13 (68.4)	37 (86.0)
Bilirubin umol/L, median (IQR)		8 (6-13)	12 (7-17)	15 (12-23)	8 (6-13)	10 (9-14)	7 (5-9)	7 (6-13)
Platelets $x10^9$/L , median (IQR)		215 (179-264)	260 (224-308)	174 (164-303)	214 (182-247)	193 (156-227)	227 (184-280)	212 (173-243)

[a] Both the intracellular and exhaustion phenotyping panels failed in n=3 patients and were excluded from the analysis [b] Quantified in those with available sample n=86 [c] Quantified in those with available sample n=23, NUCs=nucleos(t)ide therapy, sPD-L1=soluble PD-L1, HBsAg=hepatitis B surface antigen, HBeAg=hepatitis B e antigen, LLOQ=lower limit of quantification, IFN=interferon, ALT=alanine transaminase

5.3.2 Distribution of PD-1$^+$ lymphocytes

The percentages of each immune cell subset and the associated percent PD-1$^+$ can be found in Table 5.2. Overall, CD4+ and CD8+ T-cells showed the highest proportion of PD-1 positivity.

Table 5.2: PD-1 expression by lymphocyte population

Cell Type	***Proportion of CD45$^+$ (%)***	***Proportion PD-1$^+$ (%)***
CD4$^+$	33.4 (26.2-37.2)	7.5 (5.8-9.6)
CD8$^+$	19.6 (15.5-24.6)	3.6 (2.5-4.8)
CD3$^-$ CD56$^+$dim	10.3 (7.1-15.1)	0.02 (0.01 -0.05)
CD3$^-$ CD56$^+$ bright	0.4 (0.3-0.5)	0.0 (0.0-0.0)
CD3$^-$ CD56$^+$ total	10.7 (7.4-15.7)	0.02 (0.01-0.05)
CD8$^+$ Subset [b]	***Proportion CD8$^+$(%)***	
Non-terminally exhausted CD8+	0.15 (0.04-0.52)	-
Terminally exhausted CD8+	0.10 (0.02-0.27)	-

[a]Lymphocyte population frequencies represented as a proportion of total CD45$^+$ cells; values are medians with IQR.[b]PD-1 positivity is part of the phenotypic definition of non-terminally and terminally exhausted CD8$^+$ T-cells, thus they are not presented as a proportion PD-1$^+$. Non-terminally exhausted=CD127$^+$TCF1$^+$PD1$^+$, terminally exhausted= CD127$^-$TCF1$^-$PD1$^+$CD39$^+$

5.3.3 PD-1 expression by HBV infection and treatment status

All subjects were classified by infection and treatment status as described in Table 5.1. Both the percentage of lymphocyte types and the percentage of PD-1+ cells were analysed. The groups HBeAg+ hepatitis and HBeAg- hepatitis had limited numbers and were not included in the statistical analysis. In the analysis of those with HBeAg+ infection, HBeAg- infection, HBeAg+ on NUCs and HBeAg- on NUCs, the proportion of immune cell subsets remained relatively consistent across disease phases, including CD4$^+$ CD8$^+$, CD3$^-$CD56$^+$ total, CD3$^-$ CD56$^+$dim and CD3$^-$CD56$^+$ bright cells (Figure 5.1). Greater variation was observed when considering the percentage of PD-1$^+$ lymphocytes. The percentage of PD-1$^+$ lymphocytes was significantly elevated in the total CD56$^+$ compartment in HBeAg- infection. Within the CD56$^+$ compartment, cells dimly expressing CD56 also showed significantly increased percentage PD-1$^+$ in those with HBeAg- infection when compared to HBeAg$^+$ infection and those on NUCs (Figure 5.2).

The percentage of terminally exhausted CD8+ T-cells was highest in the HBeAg+ and HBeAg- hepatitis populations and decreased in HBeAg+ and HBeAg- infection populations; however,

the differences were not significant (Figure 5.3a). A similar pattern was found in those with a non-terminally exhausted phenotype (Figure 5.3b).

Figure 5.1: Percentage of lymphocyte subsets across HBV disease phases

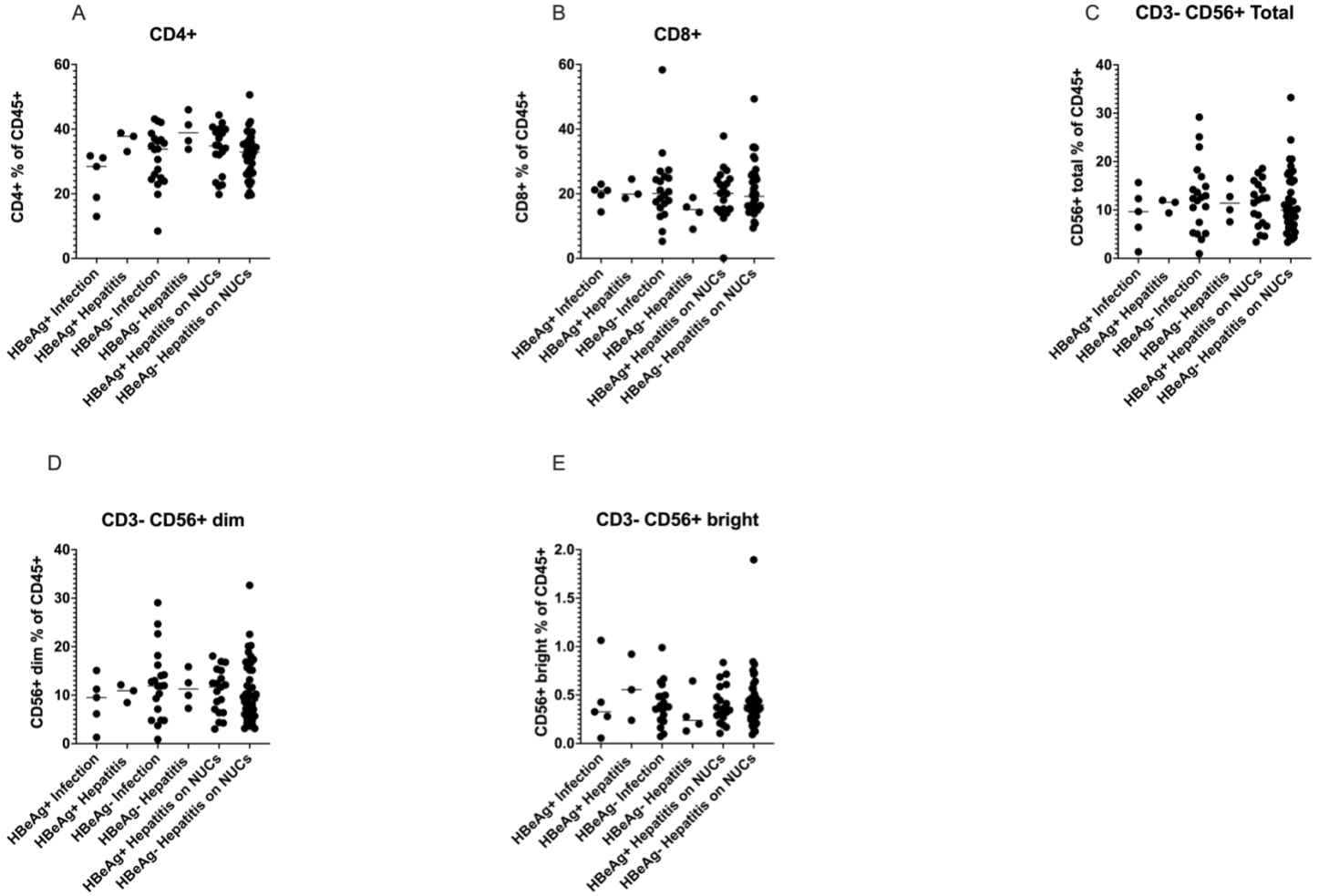

Comparison of lymphocyte subset frequencies by chronic HBV infection phase. The Kruskal-Wallis test was applied to detect differences in the proportion of lymphocyte subsets between chronic HBV infection phase, HBeAg^{+}hepatitis and HBeAg-hepatitis were excluded from the Kruskal-Wallis test due to low numbers and only included in the graph for visual comparison.

Figure 5.2: Percentage of PD-1+ lymphocyte subsets across HBV disease phases

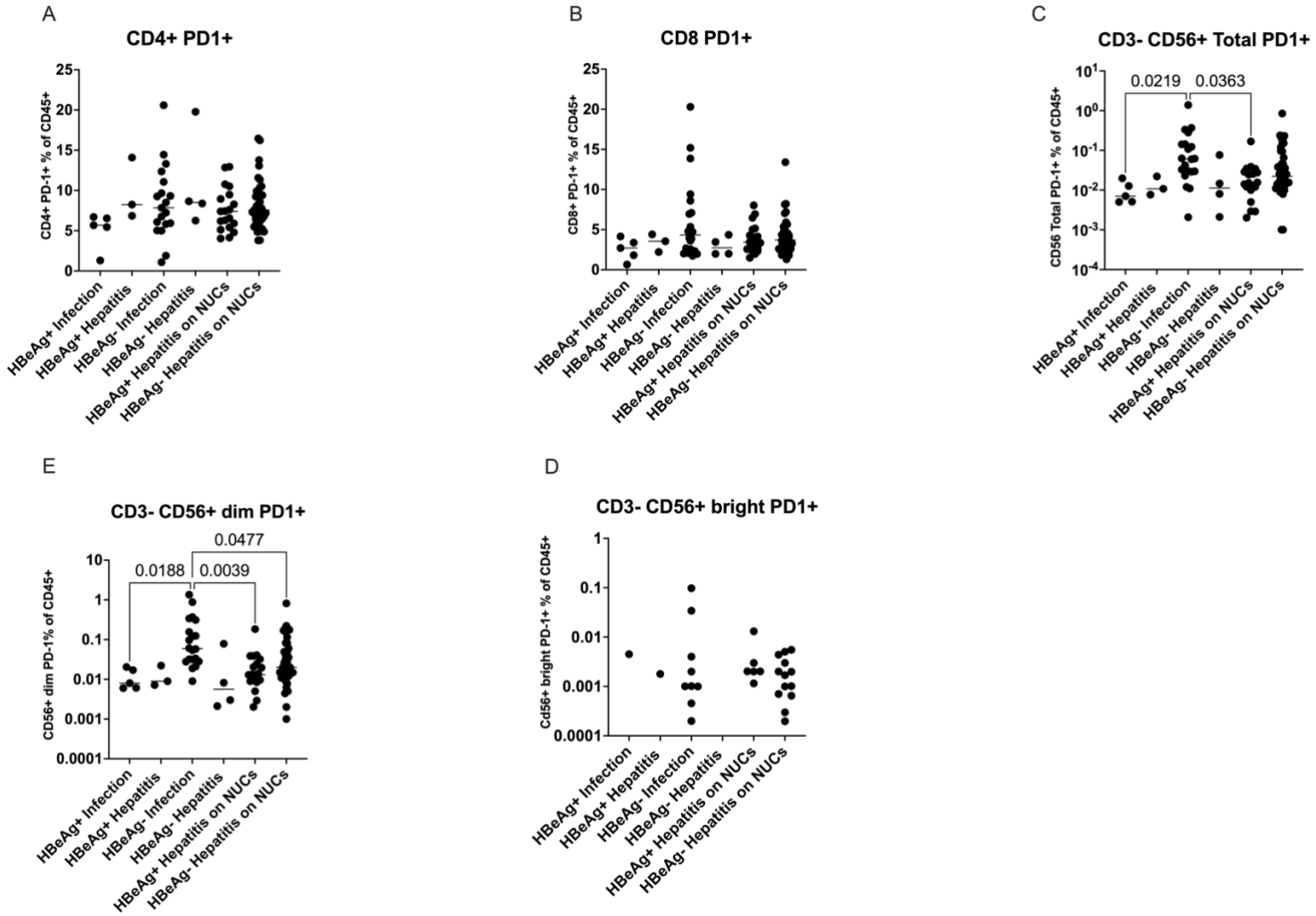

Comparison of PD-1 expressing lymphocyte subsets frequencies by chronic HBV infection phase. The Kruskal-Wallis test was applied to detect differences in the proportion of lymphocyte subsets between chronic HBV infection phase, HBeAg^{+}hepatitis and HBeAg-hepatitis were excluded

from the Kruskal-Wallis test due to low numbers and only included in the graph for visual comparison. The Dunn's multiple comparisons post-hoc test was applied if a significant results $p<0.05$ was found in the Kruskal-Wallis analysis. Due to only a small proportion of patients with PD-1^+ expression within the $CD56^+$ bright population, not all patients are represented in Figure 2D.

Figure 5.3: Terminally and non-terminally exhausted CD8+ T-cells across HBV disease phases

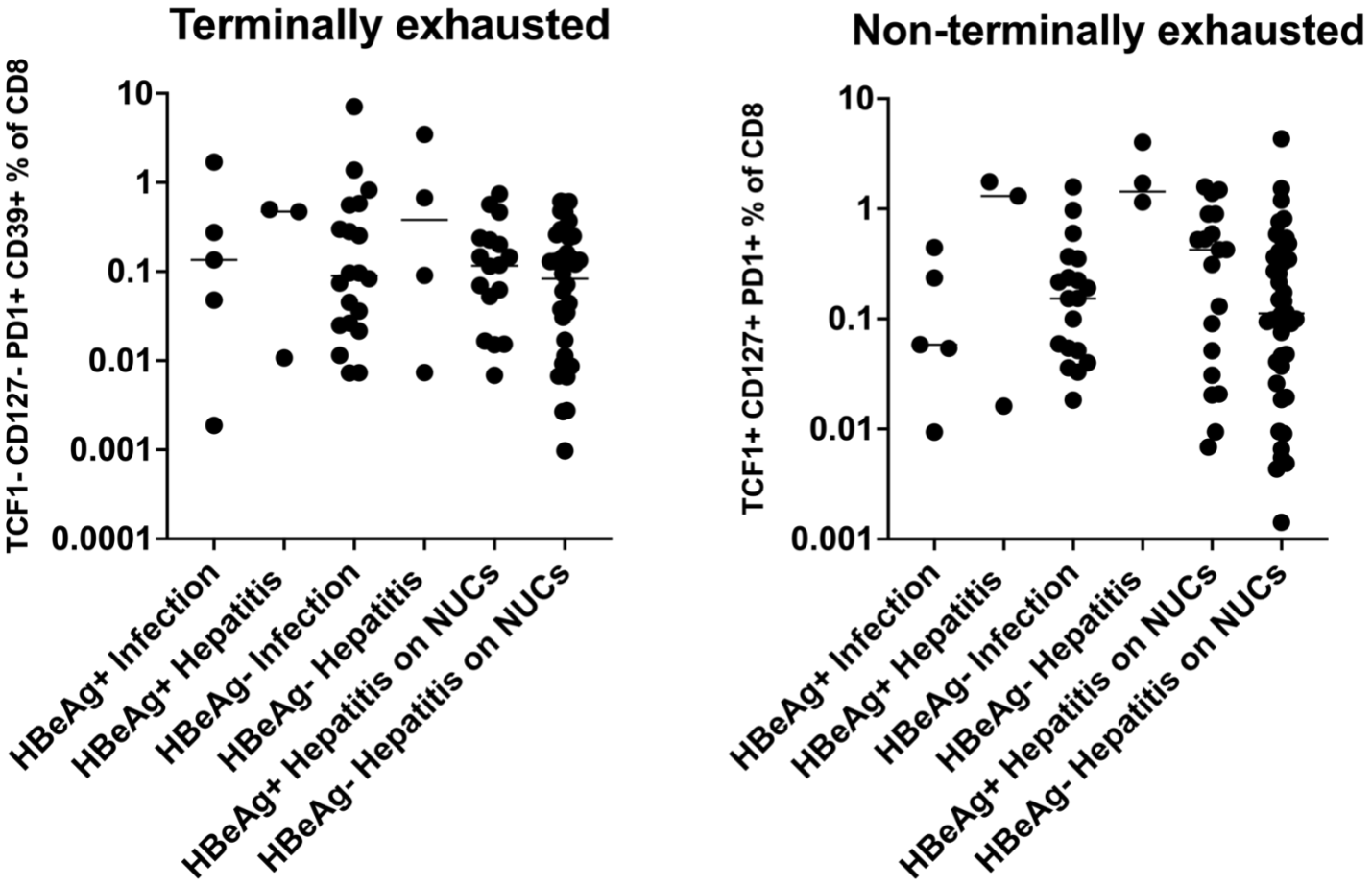

Comparison of PD-1 expressing lymphocyte subsets frequencies by chronic HBV infection phase. The Kruskal-Wallis test was applied to detect differences in the proportion of terminally and non-terminally exhausted $CD8^+$ T-cell subsets between chronic HBV infection phase, $HBeAg^+$ hepatitis and HBeAg- hepatitis were excluded from the Kruskal-Wallis test due to low numbers and only included in the graph for visual comparison

5.3.4 Relationship between lymphocyte populations and clinical characteristics

Potential relationships between the percentage of PD-1 positive lymphocytes and clinical characteristics were explored by Spearman correlation for continuous variables and either Kruskal-Wallis or Ficher's exact for grouped variables. Only those with significant findings are presented.

By Spearman, an inverse correlation was found between the percent PD-1^+ $CD4^+$ and PD-1^+CD8^+ T-cells and platelet counts (Table 5.3). Within the $CD8^+$compartment, the percentage of non-terminally and terminally exhausted $CD8^+$ cells were positively correlated with raised levels of ALT. The correlations found in the Spearman analysis were represented graphically in (Figure 5.4).

When ethnic backgrounds were considered, those from Asian backgrounds had a higher percentage of PD-1^+CD4^+ T-cells when compared to those from both Black and White backgrounds (Table 5.4). The effect of HBeAg status was unremarkable except within the $CD56^+$ compartment where HBeAg- patients had a lower percentage of PD-$1^+CD3^-CD56^+$ cells compared to those who were $HBeAg^+$ (Table 5.5).

Associations between cellular PD-1 and sPD-L1

To explore potential relationships between lymphocyte membrane bound PD-1 and levels of sPD-L1 we used Spearman correlation analysis. A positive and significant association was found between sPD-L1 measured with the SIMOA platform and the percentage of PD-1^+ $CD4^+$ T-cells ($r=0.22$; $p=0.04$) (Table 5.3). A scatter plot of the positive correlation between sPD-L1 levels and the percentage of PD-1^+ $CD4^+$ T-cells and plotted in (Figure 5.4F).

Table 5.3: Spearman correlation matrix of lymphocyte type and PD-1+ lymphocytes with clinical characteristics

	HBeAg PEI U/ml	sPD-L1 (Ella)	sPD-L1 (SIMOA)	ALT IU/ml	Platelets x10^9/L
$CD4^+$ $PD\text{-}1^+$			0.2		-0.2
$CD8^+PD\text{-}1^+$					-0.1
$CD56^+$ Total $PD\text{-}1^+$					
$CD56^+$ bright $PD\text{-}1^+$					
$CD56^+$ dim $PD\text{-}1^+$					
$TCF1^+$ $CD127^+$ $PD\text{-}1^+$				0.3	
$TCF1^-$ $CD127^-$ $PD\text{-}1^+$ $CD39^+$				0.3	
$CD4^+$	-0.5	0.3			
$CD8^+$					
$CD56^+$ Total					
$CD56^+$ bright					
$CD56^+$ dim					

Spearman correlation of lymphocyte populations and continuous clinical characteristics. Spearman correlation value (r) presented in each box. Red hues represent positive correlations and blue hues represent negative correlations. Only variables with correlation with a p-value of <0.05 are presented in emboldened boxes. The full Spearman correlation matrix with 95% confidence intervals and p-values can be found in appendix files. Dichotomous and categorial explanatory variable analyses are shown in individual tables; non-significant dichotomous and categorical tables for non-significant results can be found in the appendix files. HBsAg=hepatitis B surface antigen, HBeAg=hepatitis E antigen, PEI=Paul-Ehrlich Institute units, sPD-L1=soluble PD-L1, ALT= alanine transaminase.

Table 5.4: The variation in the percentage of PD-1+CD4+ T-cells by ethnic background

Ethnicity	N	Rank Sum	p-value
Asian	63	2762.0	0.03
Black	17	974.0	
White	18	1115.0	
Dunn's Pairwise Comparison			
	Asian	Black	
Black	-1.73 p=0.04		
White	-2.38 p=0.01	-0.48 p=0.31	

Table 5.5: Percentage of PD-1+ lymphocytes by HBeAg status

Cell Type	HBeAg- n=70	HBeAg+ n=28	p-value
$CD4^+$ $PD1^+$	7.80 (6.08-9.91)	6.63 (5.43-8.61)	0.09
$CD8^+$ $PD1^+$	3.80 (2.48-5.36)	3.36 (2.34-4.21)	0.19
$CD56^+$ Total $PD1^+$	0.03 (0.01-0.10)	0.01 (0.01-0.03)	<0.01*
$CD56^+$ bright $PD1^+$	0.00 (0.00-0.00)	0.00 (0.00-0.00)	0.87
$CD56^+$ dim $PD1^+$	0.03 (0.01-0.10)	0.01 (0.01-0.02)	<0.01*
Non-terminally exhausted $CD8^+$	0.14 (0.04-0.39)	0.31 (0.03-0.89)	0.30
Terminally exhausted $CD8^+$	0.09 (0.01-0.27)	0.13 (0.02-0.27)	0.49

Comparison of the median proportion of PD-1 expressing lymphocytes by HBeAg status. Differences were calculated with Fisher's exact test.

Figure 5.4: Scatter plots of relationships found to be significant in the correlation analysis of lymphocytes and clinical characteristics.

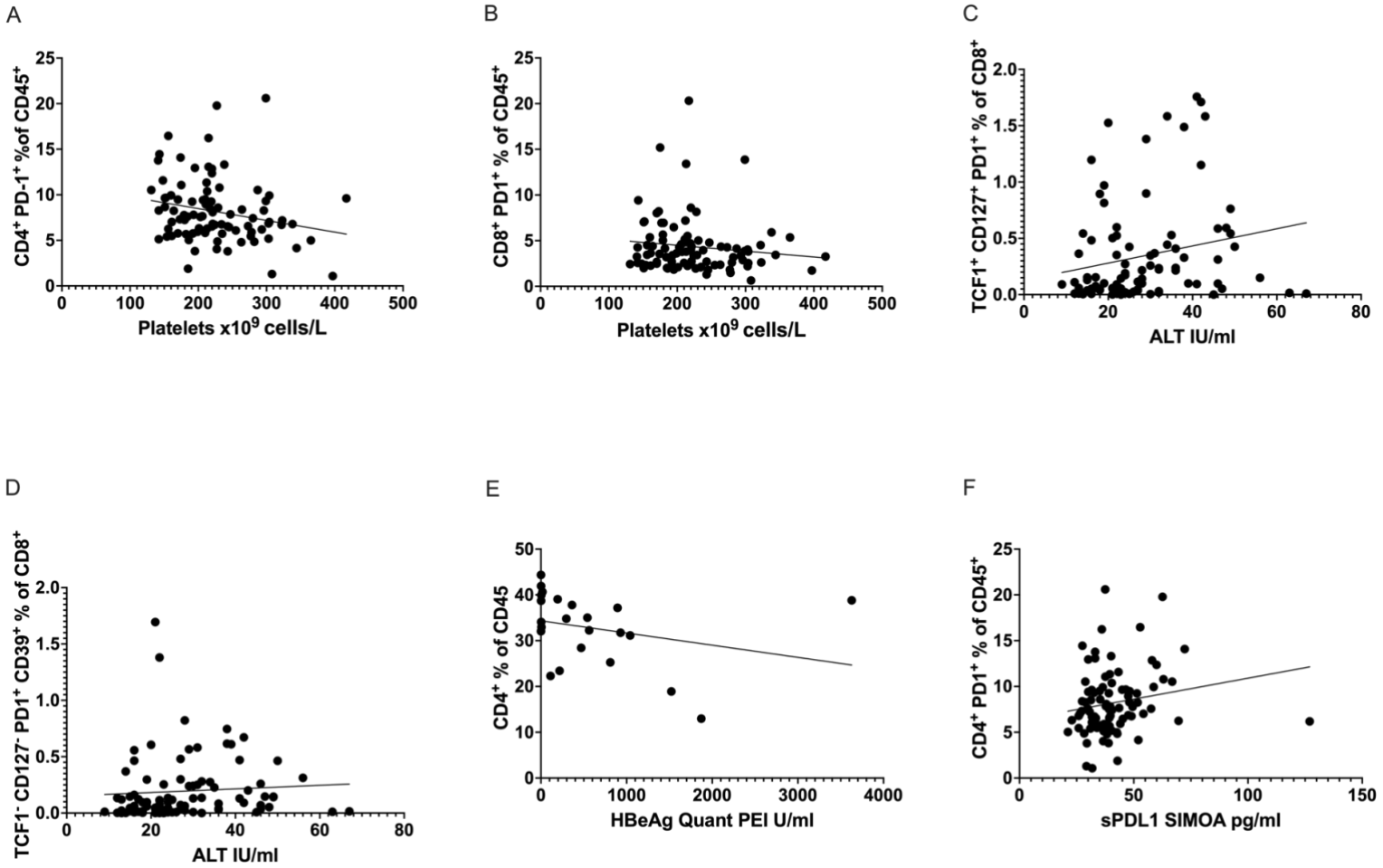

Scatter plots of correlations found to be significant between lymphocytes and clinical parameters in the correlation matrix analysis (Table 5.3). Lines are for to describe overall trends and not a representation of regression analysis.

Analysis of patients grouped by percentage of lymphocyte populations

To further assess the relationships detected between the lymphocyte populations and clinical characteristics, patients were divided into two groups using the median percentage PD-1$^+$ positive into those above and below the overall median of cell subset as defined in Table 5.2. Differences were explored with Fisher's exact test. Within the CD4$^+$ compartment, patients with an increased percentage of PD-1$^+$ CD4$^+$ cells also had higher levels of sPD-L1 when measured by Ella, raised ALT levels (>40 IU/ml) and decreased platelet counts. Except for ALT, these findings support those found in the correlation analysis. Within the CD8$^+$ compartment, the previous finding that the percentage of PD-1$^+$total CD8$^+$ cells being negatively correlated with platelets was no longer supported. However, when considering patients with an increased percentage of non-terminally exhausted CD8$^+$ T-cells they also had increased levels of ALT (>40IU/ml), supporting the correlation findings. Although not detected in the correlation analysis, patients with a higher percentage of terminally exhausted CD8$^+$ T-cells also had increased levels of sPD-L1 (measured by Ella).

Table 5.6: Clinical parameters in study participants with percentage PD-1+ CD4+ cells above or below the median of the overall study population

Characteristic	Total N=98	Group I (high) n=49	Group II (low) n=49	p-value
Age median years (IQR)	39 (32-46)	39 (33-47)	39 (32-45)	0.83
qHBsAg median IU/ml (IQR)	1797 (477-6367	1946 (537-10206)	1515 (389-5457)	0.27
qHBeAg median PEI U/ml (IQR)	297 (3-894)	17 (3-217)	686 (112-1042)	0.06
Time on NUCs median years IQR	3 (1-7)	2 (1-6)	3 (1-8)	0.52
sPD-L1 median pg/ml (IQR) (Ella)	114 (67-239)	125 (72-250)	94 (51-151)	0.14
sPD-L1 median pg/ml (IQR) (SIMOA)	38 (32-45)	39 (33-49)	36 (31-41)	**0.03***
HBV RNA median log_{10} copies/ml (IQR)	2 (0-4)	0.5 (0-3)	2 (0-6)	0.06
HBV DNA median IU/ml (IQR)	14 (1-5823)	5 (1-861)	318 (1-15440)	0.12
ALT median IU/ml (IQR)	25 (19-36)	24 (19-42)	25 (18-32)	0.40
ALT >40 U/L, n (%)	19 (100)	14 (74)	5 (26)	**0.02***
Platelets median $x10^9$/L (IQR)	215 (179-264)	207 (170-227)	234 (192-293)	**<0.01***

Patients were classed as either having a percentage of lymphocytes expressing PD-1 above or below the median percentage of the overall cell population as reported in Table5.2. Demographic and clinical characteristics were tabulated accordingly. Fisher's exact test was used to explore differences between the two groups.

Table 5.7: Clinical parameters in study participants with median percentage of PD-1+ CD8+ T-cells above or below the median of the overall study population

Characteristic	Total N=98	Group I (high) n=49	Group II (low) n=49	p-value
Age median years (IQR)	39 (32-46)	39 (32-45)	38 (33-46)	0.59
qHBsAg median IU/ml (IQR)	1797 (477-6367)	1787 (594-7654)	1946 (350-6208)	0.69
qHBsAg median PEI U/ml (IQR)	297 (3-894)	206 (4-420)	470 (3-930)	0.40
Time on NUCs median years (IQR)	3 (1-7)	3 (1-5)	2 (1-10)	0.54
sPD-L1 median pg/ml (IQR) (Ella)	114 (67-239)	106 (67-226)	116 (67-245)	0.87
sPD-L1 median pg/ml (IQR) (SIMOA)	38 (32-45)	39 (31-45)	37 (32-45)	0.97
HBV RNA median log_{10}copies/ml (IQR)	2 (0-4)	0.5 (0-3)	2 (0-5)	0.15
HBV DNA median IU/ml (IQR)	14 (1-5823)	12 (1-5823)	18 (1-4254)	0.59
ALT median IU/ml (IQR)	25 (19-36)	25 (18-36)	24 (19-32)	0.62
Raised ALT >40, n (%)	19 (100)	11 (58)	8 (42)	0.61
Platelets median $x10^9$/L (IQR)	215 (179-264)	212 (179-238)	224 (185-278)	0.41

Patients were classed as either having a percentage of lymphocytes expressing PD-1 above or below the median percentage of the overall cell population as reported in table 5.2. Demographic and clinical characteristics were tabulated accordingly. Fisher's exact test was used to explore differences between the two groups.

Table 5.8: Clinical parameters in study participants with median percentage non-terminally exhausted CD8+ T-cells above or below the median of the overall study population

Characteristic	Total N=98	Group I (high) n=50	Group II (low) n=48	p-value
Age median years (IQR)	39 (32-46)	37 (32-45)	40 (34-46)	0.38
qHBsAg median IU/ml (IQR)	1797 (477-6367	1806 (440-13394)	1650 (504-5313)	0.50
qHBeAg median PEI U/m (IQR)*	297 (3-894)	217 (3-562)	420 (17-930)	0.46
Time on NUCs years (IQR)	3 (1-7)	3 (2-7)	2 (1-7)	0.46
sPD-L1 median pg/ml (IQR) (Ella)	114 (67-239)	133 (72-269)	98 (62-161)	0.13
sPD-L1 median pg/ml (IQR) (SIMOA)	38 (32-45)	38 (32-47)	38 (31-44)	0.58
HBV RNA median log_{10}copies/ml (IQR)	2 (0-4)	2 (0-4)	0.5 (0-3)	0.53
HBV DNA median IU/ml (IQR)	14 (1-5823)	166 (5-8886)	5 (1-1927)	0.15
ALT median IU/ml (IQR)	25 (19-36)	30 (21-38)	23 (17-28)	**0.02***
Raised ALT >40, n(%)	19 (100)	12 (63)	7 (37)	0.30
Platelets median $x10^9$/L (IQR)	215 (179-264)	214 (179-287)	219 (182-251)	0.88

Patients were classed as either having a percentage of lymphocytes expressing PD-1 above or below the median percentage of the overall cell population as reported in table 5.2. Demographic and clinical characteristics were tabulated accordingly. Fisher's exact test was used to explore differences between the two groups.

Table 5.9: Clinical parameters in study participants with median percentage of terminally exhausted CD8+ T-cells above or below the median of the overall study population

Characteristic	Total N=98	Group I (high) n=51	Group II (low) n=47	p-value
Age median years (IQR)	39 (32-46)	38 (29-50)	39 (33-44)	0.97
qHBsAg median IU/ml (IQR)	1797 (477-6367	1515 (348-7669)	2045 (702-6208)	0.38
qHBeAg median PEI U/ml (IQR)	297 (3-894)	206 (3-809)	543 (6.2-894)	0.71
Time on NUCs years (IQR)	3 (1-7)	3 (2-8)	2 (1-5)	0.18
sPD-L1 median pg/ml (IQR) (Ella)	114 (67-239)	142 (81-272)	91.3 (62-157)	**0.02***
sPD-L1 median pg/ml (IQR) (SIMOA)	38 (32-45)	39 (32-48)	37 (31-43)	0.17
HBV RNA median log_{10}copies/ml (IQR)	2 (0-4)	1 (0-5)	2 (0-4)	0.89
HBV DNA median IU/ml (IQR)	14 (1-5823)	16 (1-2432)	10 (1-10208)	0.87
ALT median IU/ml (IQR)	25 (19-36)	29 (20-39)	23 (18-32)	0.09
Raised ALT >40, n(%)	19 (100)	12 (63)	7 (37)	0.32
Platelets median $x10^9$/L (IQR)	215 (179-264)	220 (170-287)	212 (186-247)	0.91

Patients were classed as either having a percentage of lymphocytes expressing PD-1 above or below the median percentage of the overall cell population as reported in table 5.2. Demographic and clinical characteristics were tabulated accordingly. Fisher's exact test was used to explore differences between the two groups.

Non-terminal and terminally exhausted CD8+ cells

To understand the relationship between non-terminally and terminally exhausted $CD8^+$ T-cells, the ratio of non-terminally to terminally exhausted CD8+ cells was calculated. A ratio of >1 indicates a greater proportion of non-terminally exhausted CD8+ cells and <1 showed more terminally exhausted CD8+ cells. In all clinical phases, the ratio of non-terminally exhausted cells and terminally exhausted cells was >1. However, those with HBeAg- infection had a depressed ratio when compared to other clinical phases indicating a propensity toward terminally exhausted cells (Figure 5.5).

Figure 5.5: Ratio of non-terminally to terminally exhausted CD8+ cells by HBV clinical phase

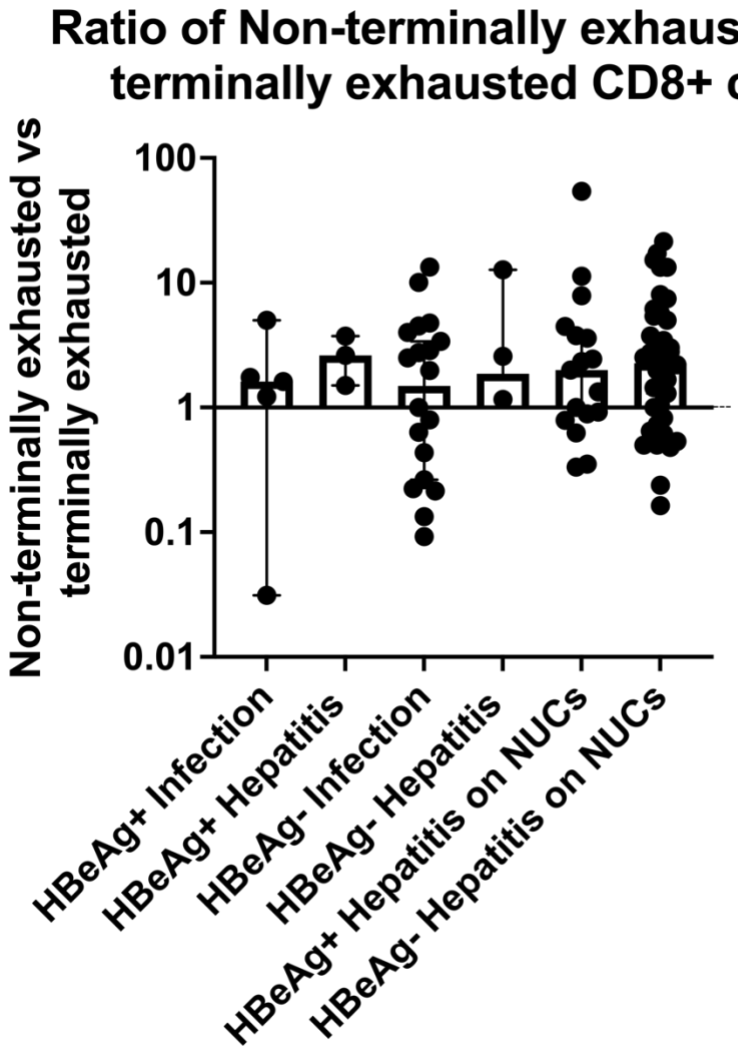

The ratio of non-terminally to terminally exhausted CD8+ cells was calculated. A ratio of >1 indicates a greater proportion of non-terminally exhausted CD8+ cells and <1 showed more terminally exhausted CD8+ cells.

5.4 Discussion

This hypothesis-generating study provides a characterisation of the proportion of PD-1 positivity in the global lymphocyte population from 98 well defined patients with differing chronic HBV infection and treatment status. The levels of circulating leukocyte populations were in line with published reference ranges and aligned with specific ranges for the majority Chinese ethnicity found in this population[351,352]. We found some evidence that circulating levels of sPD-L1 correlated with global levels of PD-1$^+$ lymphocytes. Specifically, the proportion of PD-1 expressing CD4$^+$ T-cells was positively correlated with the level of sPD-L1 measured by SIMOA while the percentage of terminally exhausted cells was found moderately increased in those with high levels of sPD-L1 by Ella. Interestingly, we found an inverse correlation between the percentage of PD-1$^+$ cells and platelet count. We observed few of the percentage of global PD-1$^+$ lymphocyte populations varying by chronic HBV infection phase.

We found a positive correlation between sPD-L1 and CD4$^+$ T-cells expressing PD-1 that was supported in the median expression analysis. Increased levels of sPD-L1 are correlated with poor immune control and poor outcomes in some cancers, suggesting a suppressive and possibly a pathogenic role[208,353]. The positive association between sPD-L1 levels and the percentage of PD-1 positive CD4$^+$ T-cells has been noted in the context of sepsis and septic shock[354]. CD4$^+$T-cells are the major supporters of CD8$^+$ and B-cell responses, providing multiple potentiating signals, enabling effector function[355] and may play a direct role in the immune response against HBV, dependent on their expression of cytokines such as TNF-a or IFN-y[355]. CD4$^+$ cell responsiveness, however, is likely modulated by the level of inhibitory signals such as PD-1/PD-L1[355]. This is supported by directly *ex vivo* studies that show that PD-L1 blockade increases CD4$^+$T-cell production of IFN-y and TNF-a[356]. Our data suggest that the cellular expression levels of PD-1 may be mechanistically tied to the levels of circulating sPD-L1 found in the periphery, enriching the current body of evidence. We also found a modest association in the median expression analysis between sPD-L1 levels measured with SIMOA and terminally exhausted CD8$^+$ T-cells. Several *in vitro* studies have shown that sPD-L1 can deliver both suppressive and proapoptotic signals to CD4$^+$ and CD8$^+$ T-cells[295,350]. Some of the strongest evidence for sPD-L1 inducing lymphocyte dysfunction via peripheral interactions comes from studies in a melanoma model, which found that injection of sPD-L1 decreased trafficking of CD8$^+$ T-cells and their proliferative ability when the CD8$^+$ cells expressed PD-1[353]. Additionally, this study found that higher sPD-L1 levels prior to commencing anti-PD-1

therapy was associated with failed treatment response. However, this study did not examine effects on the $CD4^+$compartment. Further studies are needed to clarify that the associations presented in this study directly impact the function of the lymphocytes and if, among other factors, sPD-L1 can be used as an indicator in preselecting patients for anti-PD-1 or anti-PD-L1 HBV curative studies.

An inverse correlation was observed between the percentage of PD-1 $CD4^+$ T-cells (and to a lesser extent PD-1 positive $CD8^+$) and platelet count, which was supported in the median expression analysis. Platelets account for the second largest proportion of cells in circulation. Few studies have examined the relationship between platelets and immunoregulatory processes in the context of chronic HBV infection however, it is becoming increasingly recognized that platelets may be important modulators of both innate and adaptive immune functions[357–359]. A similar trend was observed in an *in vitro* study of PBMCs isolated from head and neck cancer patients; it was demonstrated that the presence of platelets significantly decreased PD-1 expression on $CD4^+$T-cells, decreased proliferation of both $CD4^+$ and $CD8^+$T-cells and decreased production of pro-inflammatory cytokines[360]. In the same study, it was also found that platelets were bound more frequently to activated T-cells with higher levels of PD-1. To our knowledge, the data presented in this chapter is the first description of this association in the context of chronic HBV infection. It is hypothesized that T-cell aggregation with platelets may result in a greater propensity for pro-inflammatory effector functions. Indeed, a large cohort study of 122,200 individuals with a HBsAg positivity rate of 4.0%, found that HBsAg positivity was independently associated with thrombocytopenia (defined as <150,000 platelets/ul) with the strongest association found in those with evidence of raised ALT levels, suggesting decreased platelets may provide an environment favouring inflammatory processes[361]. Nevertheless, it could also be argued that platelets bound to already functionally anergic lymphocytes may further propagate immune dysfunction. Evidence that platelet-lymphocyte aggregates may have a pathogenic role is presented in a study which found that anti-platelet therapy decreased liver platelet-lymphocyte complexes in a transgenic HBV mouse model, which increased overall survival and decreased the severity of liver fibrosis and incidence of hepatocellular carcinoma[362,363]. The interaction was further highlighted in a modelling study which found that alongside liver fibrosis stage, HBeAg status and HBV DNA load, platelet levels were central to the equation in estimating levels of circulating HBsAg levels[364]. Whether the role of platelets is pathogenic or homeostatic in the context of HBV

infection will likely prove complex to decipher. It is clear, however, that the relationship warrants further investigation.

There are limitations to this study. Firstly, our flow cytometry staining protocol was not specific for HBV-restricted T-cells targeted toward the major HBV epitopes (HBcAg, HBsAg, and pol) but instead measured PD-1 expression on global populations. Two studies elegantly described that HBV specific T-cells with differing epitope specificities exhibit greater exhaustion profile, increased PD-1 expression and decreased differentiation when targeted toward polymerase versus core and varied by disease phase[215,365]. Future studies on the samples collected in the work described in this chapter will likely include assessment of HBV-specific responses, however, it was not possible to conduct this work due to COVID restrictions. Furthermore, it has been demonstrated that these cell types are only present at high frequencies in acute infection versus only very low frequencies when derived from individuals with chronic infection and lower still as a proportion of the peripheral population[187,366]. Additionally, due to limitation in the staining panel, we were not able to include a viability dye. This may have skewed population percentages by including dead cells which may adversely bind fluorophores. However, this was partially mitigated by using fresh PBMCs immediately after isolation and utilising AOPI viability stain to calculate cell dilutions prior to staining procedures. It is also possible that immune cell subtypes that are important in the pathogenesis of chronic HBV infection may not egress in large numbers from the intrahepatic compartment and would thus only be observable from tissue retrieved from the liver[366]. Due to the technical difficulty and potential side effects of invasive procedures, examination of cells from the intrahepatic compartment was not possible within this study. This suggests that a possible reason we did not see substantial differences between disease phase was the lack of HBV specific lymphocytes detected. This has limited previous research to focus only on patients with low levels of HBV replication, which have been found to have the most detectable HBV specific T-cells[187]. Though care was taken to exclude patients who may have conditions known to upregulate peripheral PD-1 levels, the PD-1/PD-L1 pathway is widely linked to T-cell activation status and thus, many associations with HBV characteristics may have been masked due to non-specific upregulations of PD-1. Due to limitations of flow cytometry and fluorophore spectral overlap, global CD4, CD8 and NK populations were measured without probing into individual subsets e.g. effector and memory subsets or measuring the level of lymphocyte associated PD-L1, which is addressed in chapter 6. Due to the natural history of chronic HBV infection, several HBV disease phase groups were underpowered, namely those

in the HBeAg+ infection category which is normally linked to HBV infection in younger people[367]. Lastly, due to time and ethics constraints, we were not able to recruit a healthy volunteer cohort for comparison of immunological parameters, thus comparisons presented are only between chronic HBV infection phases. Future studies should include a healthy control population to determine baseline expression levels of both phenotypic markers and inhibitory markers.

In this hypothesis-generating study, we found evidence of several relationships between PD-1 expression on the surface of lymphocytes and peripheral factors and clinical characteristics adding to the continually evolving evidence of the complex interplay between the immune response and chronic HBV infection. Specifically, we found that $CD4^+$ cells expressing PD-1 correlate with levels of sPD-L1 measured by the SIMOA assay and levels of platelets. While this study has limitations, there are potentially important relationships that warrant further investigation.

6 Deep Immunophenotyping of peripheral PBMCs from people living with chronic HBV

6.1 Introduction

Interrogation of single-cells with high-dimensional platforms like mass cytometry time of flight (CyTOF) has allowed for data-driven exploration of immunophenotypes without considering antigen specificity. CyTOF utilises metal isotopes as the equivalent of flow cytometry fluorophores and can host over 40 markers with negligible channel spill over[368]. One of the first studies by Brugger et al. utilised a high-dimensional non-antigen specific approach to identify a unique lymphocyte signature that predicted AIDS-free survival among people living with HIV[369]. A key analysis technique used alongside CyTOF by Brugger et al was a powerful supervised machine learning tool called cluster identification, characterization and regression (CITRUS). CITRUS analysis allows for the identification of cell signatures that would be overlooked with traditional bivariate gating[369]. Since then, this approach has been simplified and used to identify predictive lymphocyte signatures in several disease specific instances[370–372]. The use of CyTOF coupled with CITRUS machine has the potential to shed light on the complex host-virus interplay in chronic hepatitis B infection.

In chapter 5, we found that global $CD4^+$T-cells expressing PD-1 and global terminally exhausted $CD8^+$ T-cells were positively correlated with levels of sPD-L1 when measured by the SIMOA platform. These findings suggest a role for sPD-L1 in peripheral T-cell dysfunction patients living with chronic HBV infection. These findings were technically limited and did not explore subsets within each T-cell compartment. Additionally, we did not explore the expression of membrane bound PD-L1 which is postulated as a potential source of the proteolytically cleaved isoform of sPD-L1. PD-1/PD-L1 directed T-cell dysfunction in chronic hepatitis B infection is propagated by continued antigen exposure. HBsAg is found in quantities several fold higher than other HBV viral products. Quantification levels of HBsAg may provide utility by correlating with disease phase and therapeutic intervention outcomes[373–375]. HBsAg-specific T-cells are a rare population, possibly due to large-scale deletion after continued antigen exposure and subsequent activation cycles[376,377]. Identification of a T-cell subset associated with HBsAg control may be advantageous as future curative therapies may rely on both antigen reduction and immune rescue[378]. Identification of T-cell subsets in peripheral blood would be favourable by avoiding the necessity of invasive procedures.

In this study, we utilised CyTOF deep immunophenotyping paired with a novel supervised machine learning algorithm (CITRUS) with the aim of elucidating a T-cell signature in peripheral blood that was predictive of patients with increased levels of sPD-L1 and HBsAg. Additionally, we re-evaluated the study population to further investigate the relationships between clinical characteristics and lymphocyte subsets described in chapter 5.

6.2 Methods

6.2.1 PBMC preparation

Cells were retrieved from liquid nitrogen. Briefly, cells were quickly thawed in a 37°C water bath and resuspended in 10ml of R-10 kept at 4°C. The DMSO containing media was removed by centrifugation. The resulting cell pellet was resuspended in R-10 media prewarmed to 37°C and aliquoted into a 12-well plate. The cells were then allowed to rest for one hour at 37°C and 5% CO_2. After 1 hr the cells were carefully scraped and aspirated from the 12-well plate. The wells were washed until no cells appeared after observing with bright field microscopy. The cell suspension was then centrifuged at 400xg for 10 minutes and the supernatant removed. The PBMCs were then resuspended in 1ml of prewarmed RPMI 1640 and counted as described in section 2.3.3.

6.2.2 Cell counting

The PBMCs were counted as described in section 1.2.4. Briefly, 20ul of stock PBMC was removed and diluted 1:1 with ViaStain™ and mixed well. A Cellometer® slide was loaded with 20ul of the PBMC ViaStain™ mixture and inserted into the Cellometer® Auto 1000 and counted under fluorescence with live/dead discrimination. Only the live cell count was used for dilution calculations.

6.2.3 Anti-CD45 Cadmium isotope barcoding

A cell viability of $\geq$80% was required for the MAXPAR staining procedure. The PBMCs were resuspended at a concentration of $1x10^6$/ml if three samples were barcoded and $1.5x10^6$ if two samples were barcoded, in MAXPAR cell staining buffer (MCSB). The PBMCs were then briefly pelleted by centrifugation at 300xg and resuspended in 50ul of cold MCSB. Fc-block was added at a volume of 5ul and incubated for 5 minutes at room temperature. MCSB supplemented with 1 test (1ul) of anti-human anti-CD45 bound to cadmium isotope 106, 110 or 111 was then added to the cell-Fc-block suspension and incubated for 30 minutes at room temperature. The PBMCs were then washed with, 1ml of cold MCSB and centrifuged at 500xg

for 10 mins. The wash was repeated for three cycles to ensure removal of excess anti-CD45 barcoding antibody. All patient samples were then combined into a single tube and resuspended in 50ul of cold MCSB.

6.2.4 Maxpar Direct Immune Profiling Assay and healthy controls

The Maxpar Direct Immune Profiling Assay (MDIPA) was selected to minimise intersample and interrun variability[229]. The cadmium isotope labelled anti-CD45 PBMCs were supplemented with 5ul of Fc-block and incubated for 10 minutes at room temperature. PBMCs were then stained as according to the manufacturer's requirements as detailed in section 2.4.2.2. and acquired as described in section 1.3.2.3.

Healthy control data for five patients processed with the MDIPA kit were sourced from Fluidigm®. As these data were part of the kit validation studies, age and gender matching were not possible. These data also did not contain PD-1/PD-L1 markers thus healthy controls could only be used to describe the relationship with lymphocyte parent populations.

6.2.5 Quality control and bivariate gating

The quality of the mass cytometry data was assessed and automatically normalised with Fluidigm® Maxpar Pathsetter® software. Bivariate gating was conducted in FlowJo® and guided by the Fluidigm technical note *Approach to Bivariate Analysis of Data Acquired Using the Maxpar Direct Immune Profiling Assay*[230] where most positive signals are considered for cells $>10^1$ percent positive. A brief description of the markers used to identify lymphocyte subsets in available in Appendix 9.4. Within the CD4 and CD8 T-cell subsets, naive (T_{naive}), central memory (T_{CM}), effector memory (T_{EM}), and terminal memory (T_{TM}) were identified.

6.2.6 Statistical analysis

The analysis for this study was approached stepwise. 1) Sub-populations of T-lymphocytes and those expressing PD-1 and PD-L1 were compared between chronic hepatitis B infection phases. 2) If no significant differences were detected between phases, all patients were analysed irrespective of clinical phase with correlation analysis. 3) CITRUS analysis was used to identify potential stratifying lymphocyte signatures based on sPD-L1 level and HBsAg levels 4) Any potential lymphocyte signature would be examined and described with analysis lines 1 & 2.

6.2.6.1 Patient Characteristics

The characteristics of the patients included in the analysis were summarised with counts and percentages for categorial and dichotomous variables and as median and inter-quartile range (IQR) for continuous variables. Patients were categorised based on chronic hepatitis B infection phase as described in 2.2.2., Briefly patients were grouped as those with HBeAg+ infection (EPI), HBeAg+ hepatitis (EPH), HBeAg- infection (ENI), HBeAg- hepatitis (ENH) and EPH or ENH receiving NUC therapy. Either Mann-Whitney or Kuskal-Wallis with Dunn's multiple comparison post-hoc test were used for exploration of median differences between healthy controls and people living with chronic hepatitis B and between chronic hepatitis B infection phases. Those with EPI, EPH, ENH were excluded from the analysis due to low numbers. Spearman correlation was used to explore relationships between lymphocyte population and patient characteristics.

6.2.6.2 CITRUS machine learning pipeline

CITRUS supervised machine learning pipeline used was adapted from[231] and an overview visualised in Figure 6.1. There is no known clinically relevant cut-off for sPD-L1 levels that are assay specific, therefore sPD-L1 levels were grouped as above or below the assays respective median. For the HBsAg analysis a cut-off of 1,000 IU/ml was used.

Figure 6.1: Analysis pipeline for CITRUS algorithm and downstream analysis

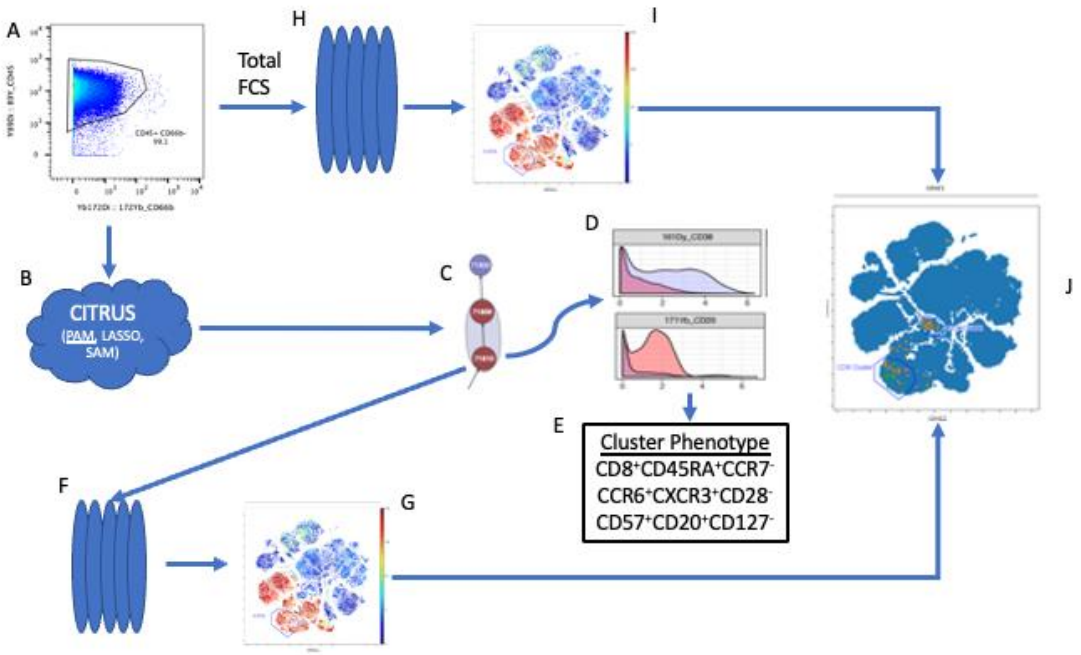

Flow diagram of the analysis pipeline used to identify T-lymphocyte signatures of both sPD-L1 and HBsAg models and the downstream analysis plan used verify features of both models (A) Bi-variate gating was used to identify positive and negative populations in Cytobank as described in the Fluidigm provided technical note to train the CITRUS algorithm[230] (B) Individual files were included in the CITRUS algorithm for both sPD-L1 and HBsAg modelling. (C) The cluster node featuring the false discovery rate constrained (FDRC) models were identified by histograms with a positive signal that was greater for the cluster than the background (D) The combination of positive signals in the FDRC model resulted in the cluster phenotype (E) The individual FCS files of the main cluster were exported and concatenated (F). t-SNE analysis was then used to visualise similarities in T-cell signatures identified in the CITRUS algorithm (G). The global bivariate gated .fcs files (A) were then concatenated (H) and run through the t-SNE with the same parameters as the cluster (I). The two t-SNE maps were then overlaid to visualise similarities in lymphocyte compartments between the CITRUS identified sPD-L1 and HBsAg T-cell signatures.

Model Parameter Definitions*:*

Adapted from *How to configure and run a Citrus analysis*[379]

- **Minimum cluster size**: parameter in CITRUS analysis that determines the number of clusters that will be in the final model; where a smaller minimum cluster size results in an increase in the number of clusters which, due to statistical multiple testing, decreases the power of the model.
- **Cross validation folds**: Cross validation is the process of subdividing the data set into random arbitrary training and testing sets that are used to construct the best model that predicts the group the sample belongs to. This process is repeated for each parameter included in the model. A cross validation of 5 is considered robust while a cross validation of 1 implies no cross validation has occurred.
- **Cross validation error rate**: The proportion of models that incorrectly predicts outcome selected for a patient. The desired cross validation error rate is less than 50%.
- **False discovery rate**: The number of times a feature (or marker) is spuriously included in a model. A false discovery rate of <5% is generally considered ideal.
- **False discover rate constrained model**: A predictive model that includes all the markers with a given outcome and still be below the set false discovery rate.

6.2.7 CITRUS Model Parameters

The largest lymphocyte population, $CD45^{+}CD66b^{-}$, was used as the sampled population to increase the strength of the analysis. The phenotypic markers used for cluster identification in the CITRUS models are described in Table 6.1. The model parameters were guided by Cytobank support[379] and are detailed in Table 6.2. The number of events were normalized to the default of 2,500 events. To minimize potential false discovery, sequential models were run beginning with a false discovery rate of 1% and increased in increments of 1% to a maximum of 10% until a significant model was produced below the false discovery rate. Models were not attempted beyond a false discovery rate of 10% as they would be considered unreliable.

Table 6.1: Clustering markers included in CITRUS analysis

Marker (Clustering markers)	Metal Isotope
CD196 (CCR6)	141Pr
CD123 (IL-3 receptor)	143Nd
CD19	144Nd
CD4	145Nd
CD8a	146Nd
CD11c	147Sm
CD16	148Nd
CD45RO	149SM
CD45RA	150Nd
CD161	151Eu
CD194 (CCR4)	152Sm
CD25 (IL-2 receptor)	153Eu
CD27	154Sm
CD57	155Gd
CD183 (CXCR3)	156Gd
CD185 (CXCR5)	158Gd
CD28	160Gd
CD38	161Dy
CD56 (NCAM)	163Dy
TCRgd	164Dy
CD294	166Er
CD197 (CCR7)	167Er
CD14	168Er
CD20	171Yb
CD66b	172Yb
HLA-DR	173Yb
IgD	174Yb
CD127 (IL-7 receptor)	176Yb
Stratifying markers[a]	
PD-1	175Lu
PD-L1	159Tb

Markers considered in the clustering algorithm. [a]Markers with median positive signal serve to differentiate between stratifying cell populations identified with the clustering markers.

Table 6.2: CITRUS model parameters

Parameter	sPD-L1 (Ella)	sPD-L1 (SIMOA)	Quantitative HBsAg
Population sampled	CD45+CD66b-[a]	CD45+CD66b-[a]	CD45+CD66b-[a]
Events sampled per file	2,500	2,500	2,500
Minimum cluster size (%)	5	5	5
Cross validation folds	5	5	5
False discovery rate (%)	1	10	10

The parameters used to build the CITRUS models adapted from Cytobank support[379]
[a]lymphocytes, dendritic cells and monocytes

In total, PBMCs from 30 people living with chronic HBV infection were included for deep immunoprofiling, their characteristics can be found in Table 6.3. Overall, a slight majority were female (17/30, 57%) with a median age of 41 IQR (32-47) and predominantly from Asian ethnic background (19/30, 63%). Most patients were HBeAg- (22/30, 73%) and the population had a median HBV DNA viral load of 1.2 $\log_{10}$ IU/ml (IQR 0.0-3.3). HBV RNA was detectable in 21/30 (70%) patients, with an overall HBV RNA load of median 1.4 $\log_{10}$ copies/ml (IQR, 0.0-4.3). NUC therapy was administered to 19/30 (63.3%) patients for a median of 5 years (IQR 2-11). Few (5/30, 17%) patients had ALT values greater than 40 IU/ml.

Table 6.3: Characteristics of patients included in CyTOF analysis

Characteristic		Total n=30
Age median years (IQR)		41 (32-47)
Sex, n (%)	Female	17 (57)
	Male	13 (43)
Ethnicity, n (%)	Asian	19 (63)
	Black	5 (17)
	White	6 (20)
HBeAg, n (%)	Positive	8 (27)
	Negative	22 (73)
HBsAg, median IU/ml (IQR)[a]		3.3 (2.8-3.9)
HBV DNA, median log_{10} IU/ml (IQR)[b]		3.1 (1.1-3.9)
HBV RNA detected, n (%)	Yes	21 (70.0)
	No	9 (30.0)
HBV RNA, median log_{10} copies/ml (IQR)[c]		3.0 (0.8-5.2)
On NUC therapy, n (%)	Yes	19 (63.3)
	No	11 (37)
Duration of NUC therapy , median years (IQR) [d]		5 (2-11)
ALT, median IU/ml (IQR)		23 (17-36)
ALT >40 U/ml, n (%)	Yes	5 (17)
	No	25 (83)
Platelets, median count $x10^9$ cells/mm^3 (IQR)		224 (180-296)

Clinical characteristics of patients included in the CyTOF analysis. [a] Quantified in n=29 [b] In those with detectable DNA [c] In those with detectable RNA [d] Duration of therapy overall among those treated regardless of NUC type. HBeAg= Hepatitis B e antigen, HBsAg=Hepatitis B surface antigen, NUC=nucleos(t)ide therapy, ALT=alanine transaminase

6.3 Results

6.3.1 CITRUS modelling of sPD-L1 and qHBsAg

Cluster analysis was used to elucidate non-conventional stratifying cell phenotypes that could not be easily identified with traditional bi-variate gating and had the utility of predicting patients with increased sPD-L1 levels or HBsAg levels $\geq$1000 IU/ml. One patient did not have quantified HBsAg levels thus the total patients included was n=29.

Model error rate plots for models developed for sPD-L1 measured by Ella and SIMOA platforms and qHBsAg levels are available in Figures 6.2. 6.3, 6.4, respectively. The model error rate plots presented provide an overall evaluation of the stability of the cluster models evaluated during the CITRUS analysis. Each blue point represents a different model analysed in the CITRUS algorithm. The number of clusters being evaluated by the algorithm (the number of model features) is on the top x-axis. The number of cross-validation folds is plotted on the y-axis and represents the model's predictive accuracy; <50% is desirable. The cv.fdr.constrained model (yellow triangle) represents the best predictive model that falls below the set false discovery rate <10%. Only the qHBsAg and Ella sPD-L1 models had a cross validation error rates <50% and resulted significant and reliable models. Models of sPD-L1 levels determined by the SIMOA platform did not yield a significant predictive model and thus excluded from further analysis (Figure 6.3). The lowest false discovery rate that yielded a significant model was 1% for the sPD-L1 (Ella) model and 10% for the HBsAg model.

Figure 6.2: model error rate plot for the CITRUS analysis of sPD-L1 levels measured by Ella

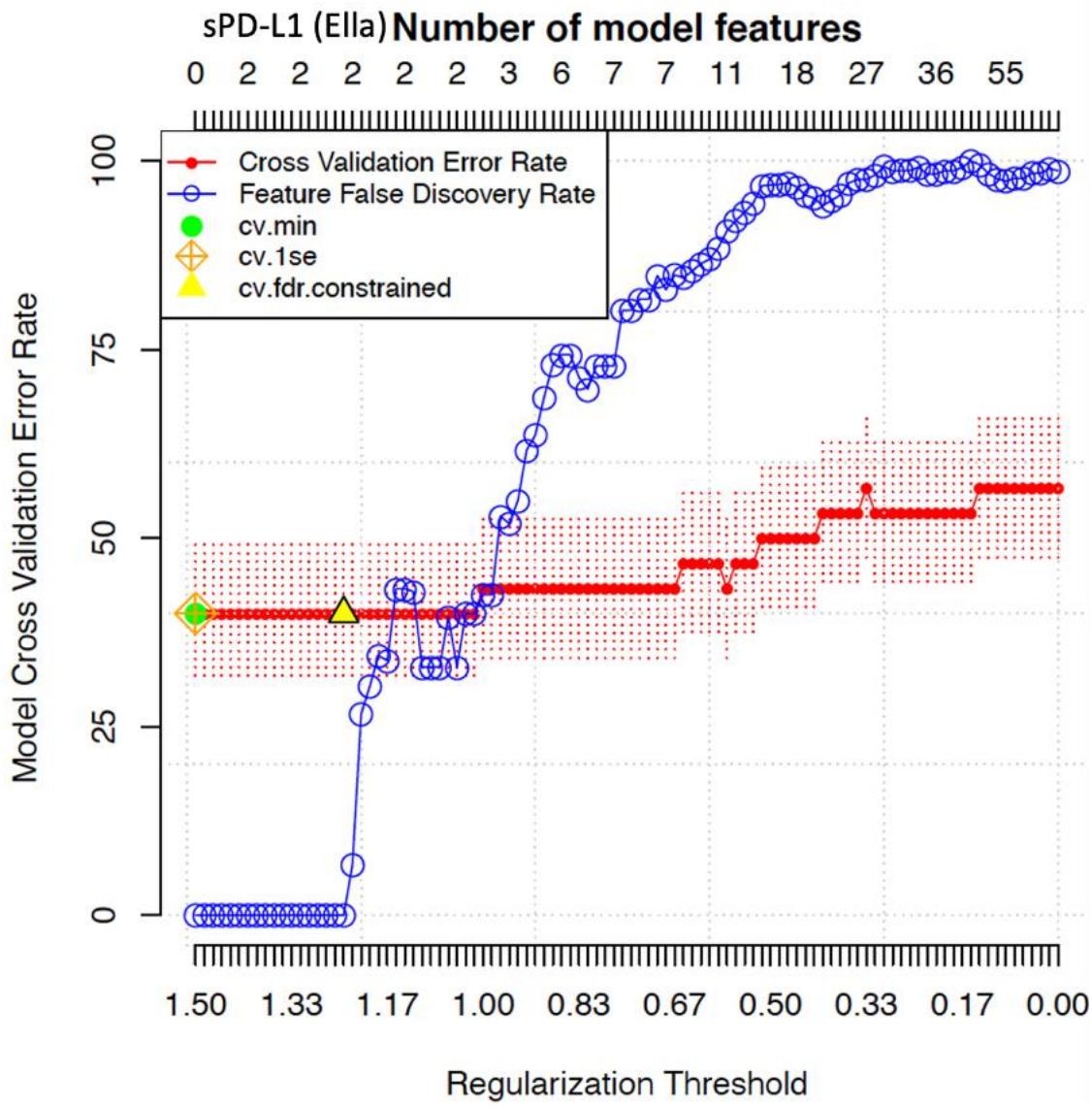

The model error rate graph for the sPD-L1 (Ella) model. This graph provides a depiction of the stability of the models created during the CITRUS analysis. Each blue point represents a different model analysed in the CITRUS algorithm. The number of clusters being evaluated by the algorithm (the number of model features) is on the top x-axis. The number of cross-validation folds is plotted on the y-axis and represents the models predictive accuracy; <50% is desirable. The cv.fdr.constrained model (yellow triangle) represents the best predictive model that falls below the set false discovery rate <10%.

Figure 6.3: Model error rate plot for the CITRUS analysis of sPD-L1 levels measured by SIMOA

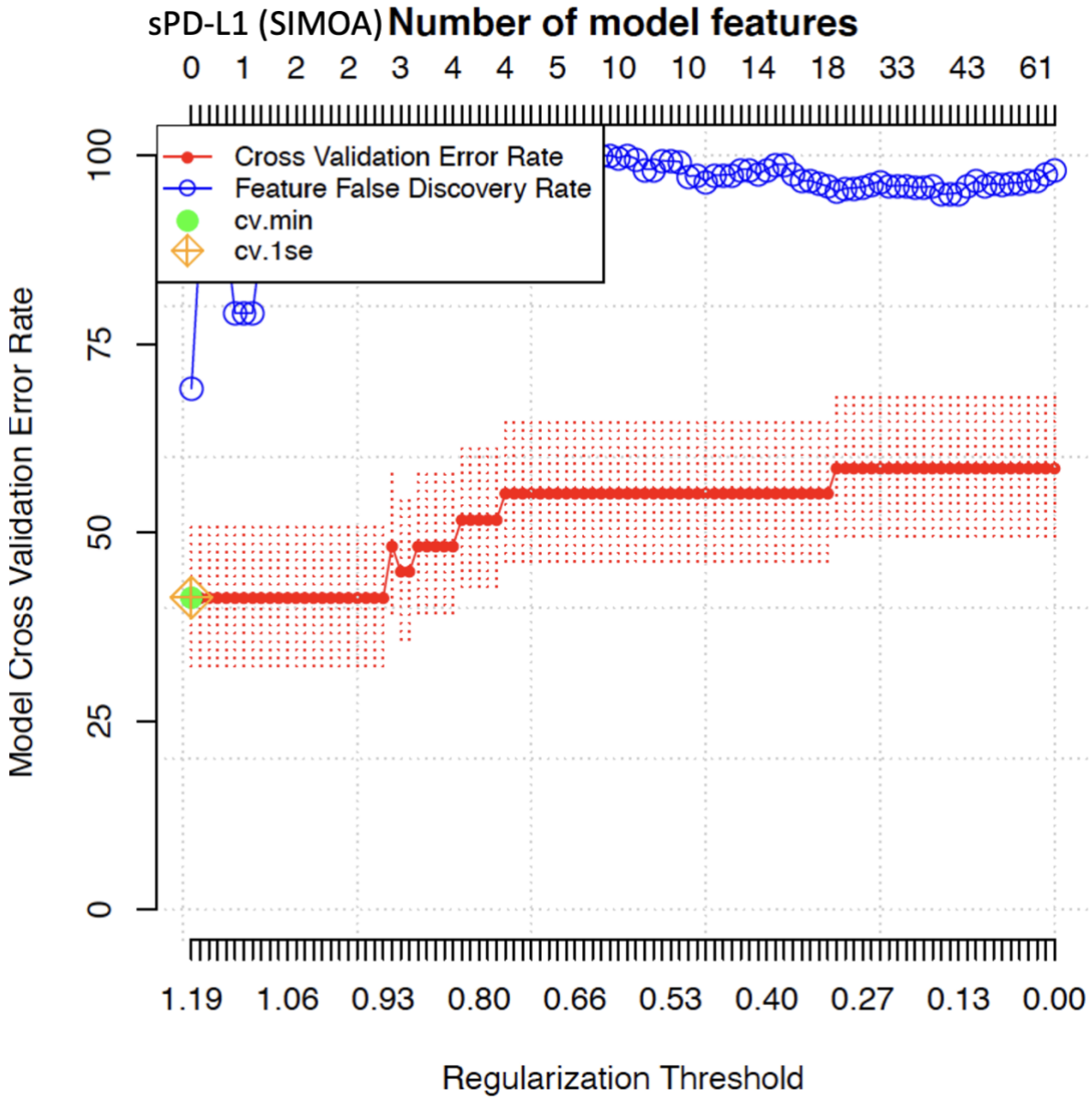

The model error rate graph for the sPD-L1 (SIMOA) model. Each blue point represents a different model analysed in the CITRUS algorithm. *This graph provides a depiction of the stability of the models created during the CITRUS analysis.* The number of clusters being evaluated by the algorithm (the number of model features) is on the top x-axis. The number of cross-validation folds is plotted on the y-axis and represents the models predictive accuracy; <50% is desirable. The cv.fdr.constrained model (yellow triangle) represents the best predictive model that falls below the set false discovery rate <10%.

Figure 6.4: Model error rate plot for the CITRUS analysis of qHBsAg levels

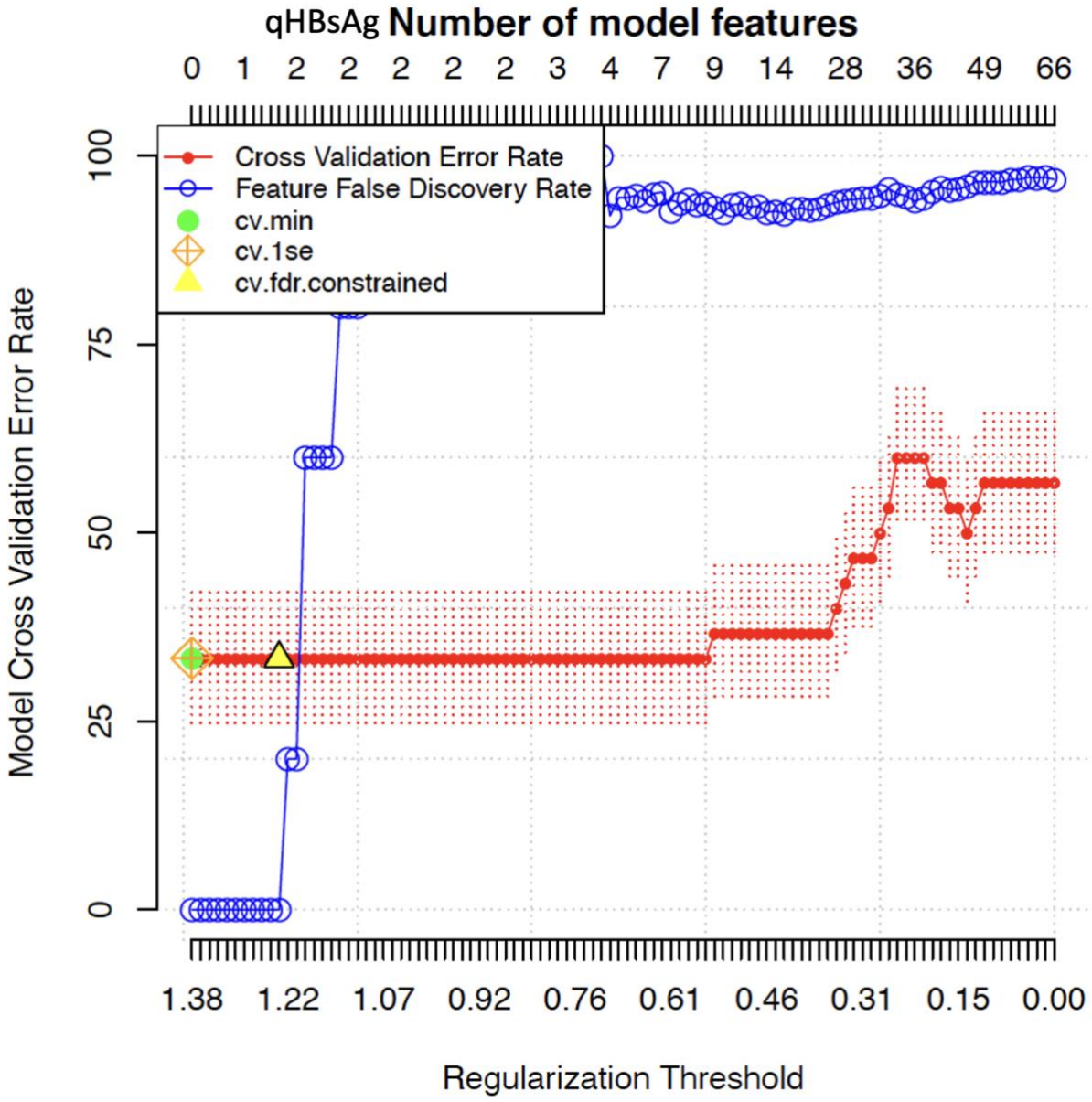

The model error rate graph for the qHBsAg model. Each blue point represents a different model analysed in the CITRUS algorithm. This graph provides a depiction of the stability of the models created during the CITRUS analysis. The number of clusters being evaluated by the algorithm (the number of model features) is on the top x-axis. The number of cross-validation folds is plotted on the y-axis and represents the models predictive accuracy; <50% is desirable. The cv.fdr.constrained model (yellow triangle) represents the best predictive model that falls below the set false discovery rate <10%.

Demographic and clinical characteristics tabulated by modelling group (HBsAg greater or less than 1,000 IU/ml or sPD-L1 greater or less than the median (Ella) is described in Table 6.4 and Table 6.5, respectively.

Table 6.4: Characteristics of HBsAg groups for CITRUS analysis

Characteristic Total		HBsAg <1000 n=10	HBsAg ≥1000 n=19
Age, median years (IQR)			
Sex, n (%)	Male	4 (40.0)	10 (53.0)
	Female	6 (60.0)	9 (47.0)
Ethnicity, n (%)	Asian	10 (10.0)	9 (47.0)
	Black	0 (0.0)	4 (21.0)
	White	0 (0.0)	6 (32.0)
HBeAg, n (%)	Negative	7 (70.0)	14 (74.0)
	Positive	3 (30.0)	5 (26.3)
HBsAg, median IU/ml (IQR)		308 (180-702)	3,912 (1,946-16,500)
HBV DNA log_{10} IU/ml, median (IQR)[a]		0.0 (0.0-1.0)	2.9 (0.5 – 3.5)
HBV DNA IU/ml, n (%)	≤10	9 (90.0)	6 (32.0)
	11-1999	1 (10.0)	11 (58.0)
	≥2,000	0 (0.0)	2 (11.0)
HBV RNA detected, n (%)	No	4 (40.0)	6 (32.0)
	Yes	6 (60.0)	13 (68.0)
HBV RNA, median log_{10} copies/ml (IQR)[b]		0.8 (0.0-2.8)	1.9 (0.0-5.2)
On NUC therapy, n (%)	No	1 (10.0)	10 (53.0)
	Yes	9 (90.0)	9 (47.0)
Duration of NUC therapy, median years (IQR)		7.6 (2.7-10.5)	1.5 (1.3-7.4)
ALT, median IU/ml (IQR)		20 (17-35)	32 (21-38)
ALT >40 U/ml, n(%)	No	8 (80.0)	16 (84.0)
	Yes	2 (20.0)	3 (16.0)
Platelets, median count $x10^9$ cells/mm^3 (IQR)		194 (173-231)	234 (182-299)

[a] In those with detectable HBV DNA [b] In those with detectable HBV RNA. Characteristics of patients included in the CITRUS analysis grouped by HBsAg level.

Table 6.5: Characteristics of sPD-L1 groups for CITRUS analysis

Characteristic Total		sPD-L1 <114 pg/ml n=11	sPD-L1 ≥114 pg/ml n=19
Age, median years (IQR)			
Sex, n (%)	Male	4 (36.0)	10 (53.0)
	Female	7 (64.0)	9 (47.0)
Ethnicity, n (%)	Asian	9 (82.0)	10 (53.0)
	Black	2 (18.0)	3 (16.0)
	White	0 (0.0)	6 (32.0)
HBeAg, n (%)	Negative	8 (73.0)	14 (74.0)
	Positive	3 (27)	5 (26.0)
HBsAg, median IU/ml (IQR)		1958 (180-16,500)	1867 (949-7,654)
HBV DNA log_{10} IU/ml, median (IQR)[a]		2.9 (0.0-4.3)	1.0 (0.0-3.2)
HBV DNA IU/ml, n (%)	≤10	5 (45)	11 (58)
	11-1999	5 (45)	7 (37)
	≥2,000	1 (10)	1 (5)
HBV RNA detected, n (%)	No	3 (27)	7 (37)
	Yes	8 (73)	12 (63)
HBV RNA median log_{10} copies/ml, (IQR)[b]		0.5 (0.0-4.0)	1.7 (0.0-4.4)
On NUC therapy, n (%)	No	5 (45)	6 (32)
	Yes	6 (55)	13 (68)
Duration of NUC therapy, median years (IQR)		2.1 (1.1-5.1)	7.6 (2.2-10.9)
ALT, median IU/ml (IQR)		32 (17-36)	23 (19-38)
ALT >40 U/ml, n (%)	No	9 (82)	16 (84)
	Yes	2 (18)	3 (16)
Platelets, median count $x10^9$ cells/mm^3 (IQR)\		234 (180-303)	212 (173-282)

[a] In those with detectable HBV DNA [b] In those with detectable HBV RNA.

Cluster feature relation trees representing the relationship between cluster nodes obtained from PAM modelling of sPD-L1 and qHBsAg are depicted in Figures 6.5 and 6.6, respectively. Modelling of sPD-L1 by Ella identified two nodal clusters (71810 and 71808) where PD-1 positive cells were significantly predictive of patients with increased levels of sPD-L1 (Figure 10a). Only cluster 71808 was considered for further analysis to ensure discrete populations were captured. When considering the modelling of qHBsAg levels $\geq$1000 IU/ml, only one nodal cluster (71805) was identified where PD-1 positivity was predictive of increased levels (figure 10b). No T-cell signatures were identified where PD-L1 levels were predictive.

Figure 6.5: Cluster relation trees for sPD-L1(Ella) model

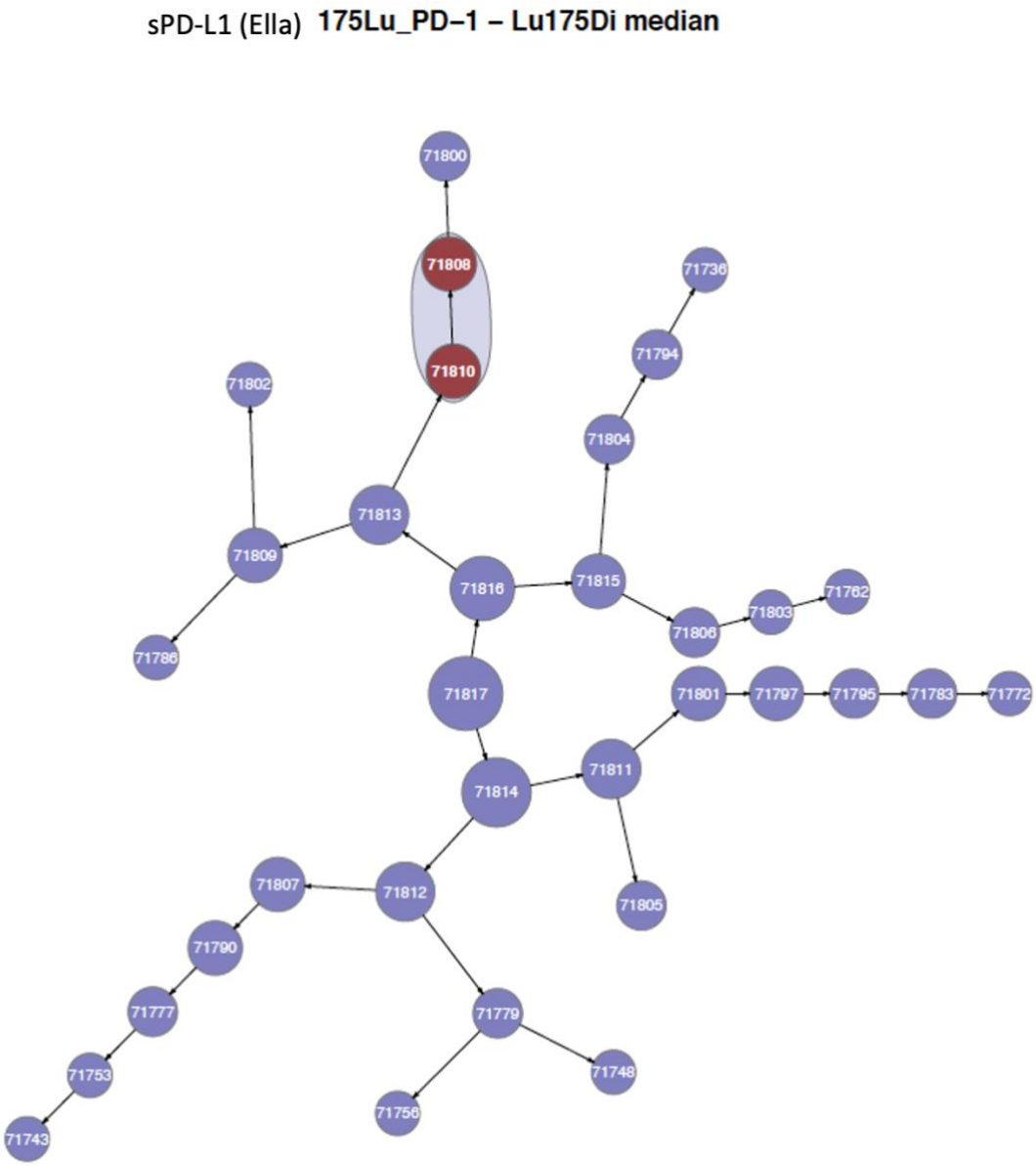

Cluster tree depicting the relationship between the clustering phenotypic markers included in the CITRUS analysis. Each circle is representative of one cluster. The size of the circle is representative of the connection between nodes, larger circles are parents of the smaller connected child node. All events in the child cluster are also within the parent. The red nodes represent the clusters that produced significant models in the CITRUS analysis. The numbers present on the nodes are identifiers.

Figure 6.6: Cluster relation trees for qHBsAg model

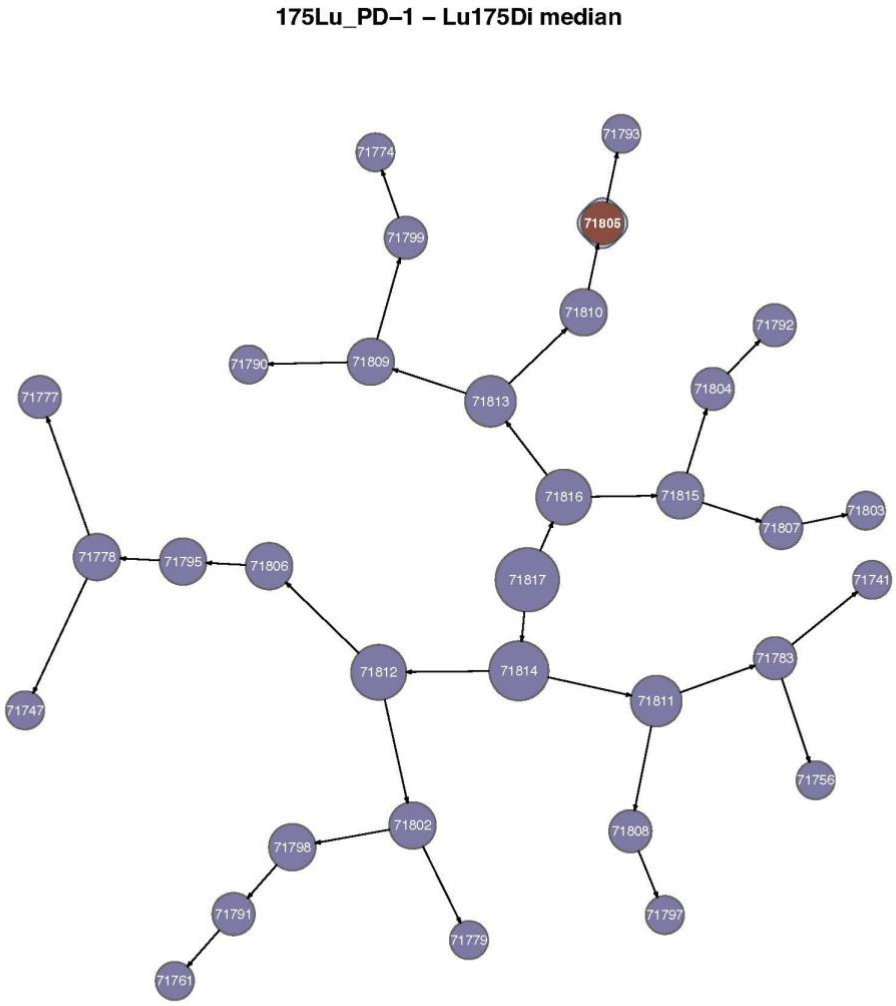

Cluster tree depicting the relationship between the clustering phenotypic markers included in the CITRUS analysis. Each circle is representative of one cluster. The size of the circle is representative of the connection between nodes i.e. larger circles are parents of the smaller connected child node. All events in the child cluster are also within the parent. The red nodes represent the clusters that produced significant models in the CITRUS analysis. The numbers present on the nodes are identifiers.

The markers expressed on the cell types identified in the sPD-L1 and HBsAg models are represented by the positive peaks in the histograms depicted below in figures 6.7, 6.8,6.9 and 6.10.

Figure 6.7: Histogram of cluster features found in the predictive HBsAg model

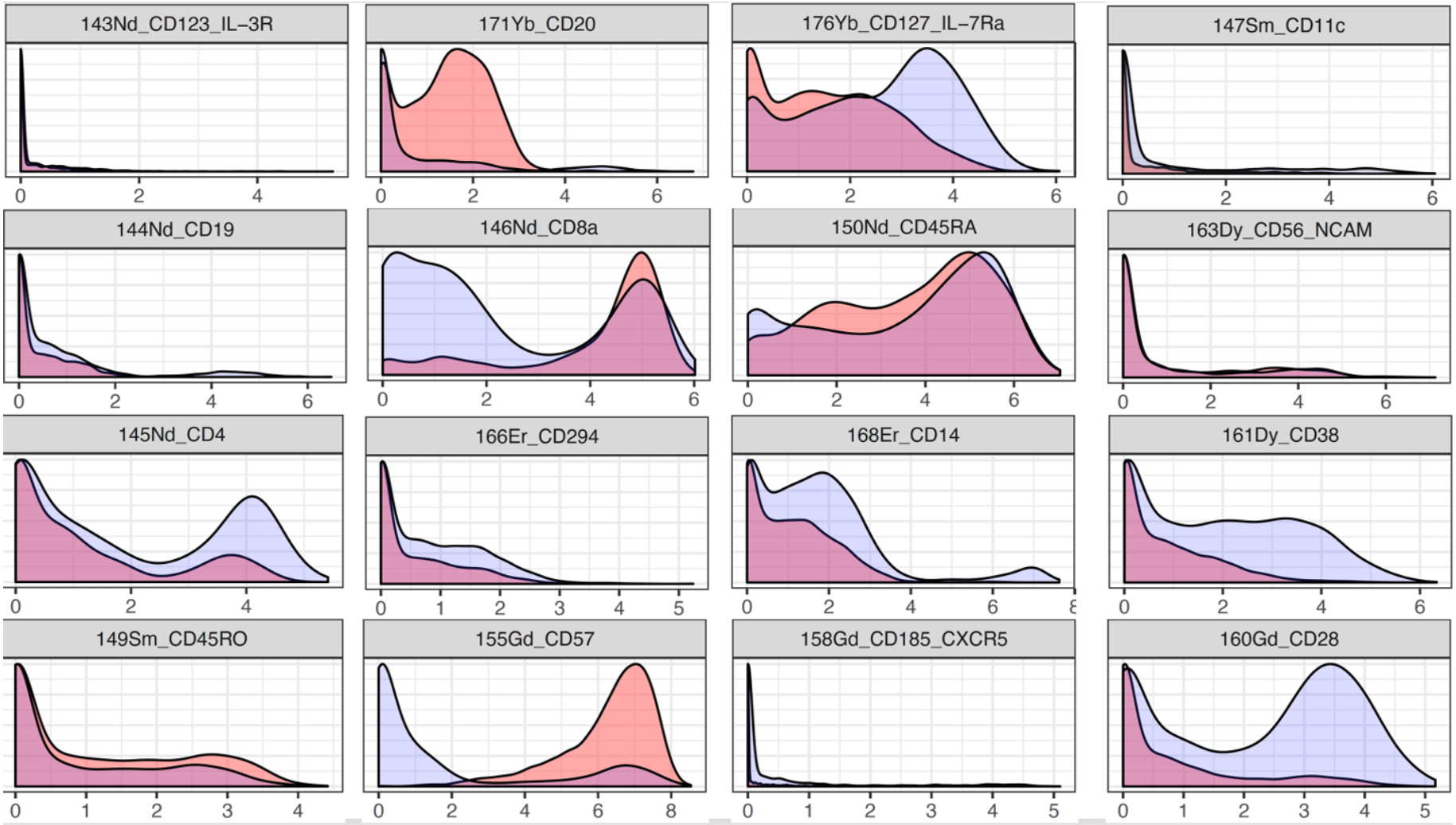

Cluster feature histogram of node 71805. Each histogram represents a feature of the lymphocyte signature proposed by the CITRUS model. The blue peaks represent the background signal while the orange peaks represent positive. Feature cluster markers are labelled for each histogram.

Figure 6.8 (cont) Histogram of cluster features found in the predictive HBsAg model

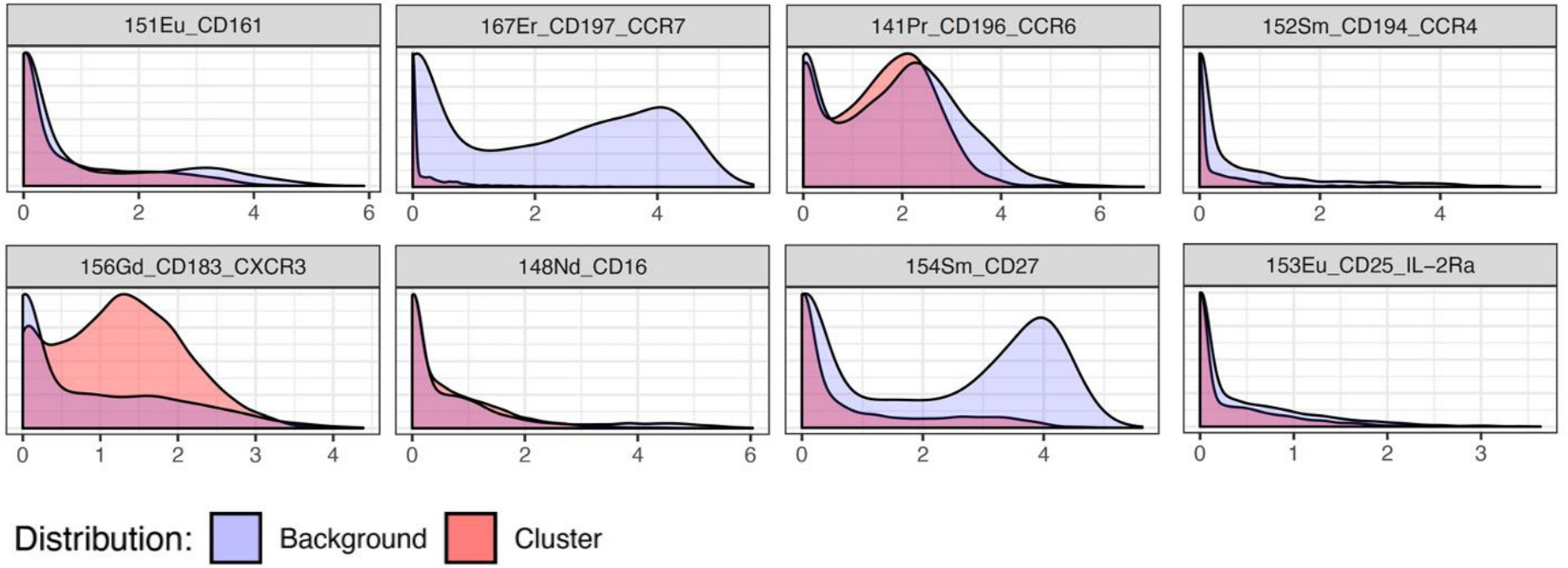

Cluster feature histogram of node 71805. Each histogram represents a feature of the lymphocyte signature proposed by the CITRUS model. The blue peaks represent the background signal while the orange peaks represent positive. Feature cluster markers are labelled for each histogram.

Figure 6.9: Histogram of cluster features found in the predictive sPD-L1 (Ella) model

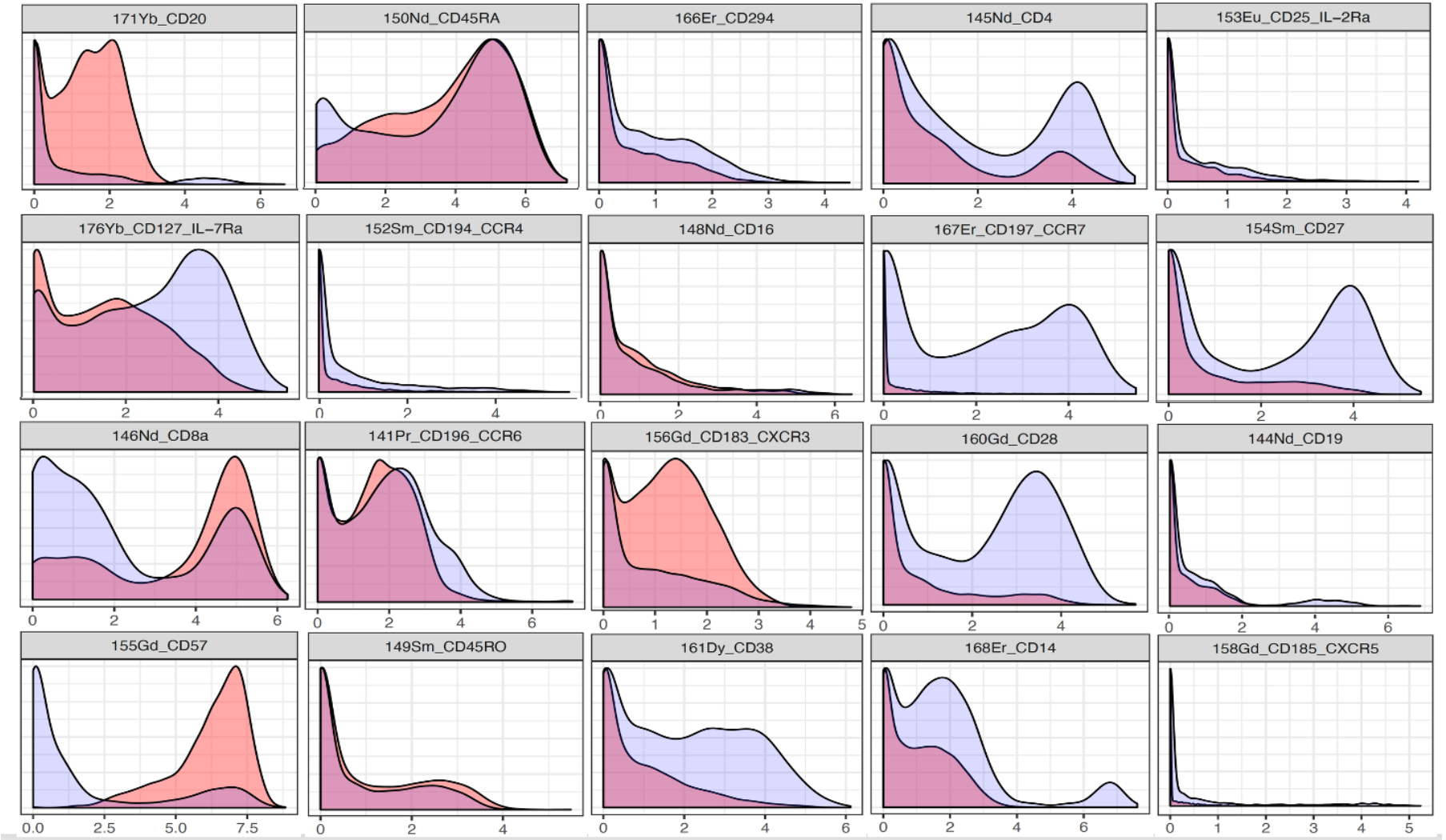

Cluster feature histogram of nodes 71808. Each histogram represents a feature of the lymphocyte signature proposed by the CITRUS model. The blue peaks represent the background signal while the orange peaks represent positive. Feature cluster markers are labelled for each histogram.

Figure 6.10: (cont) Histogram of cluster features found in the predictive sPD-L1 (Ella) model

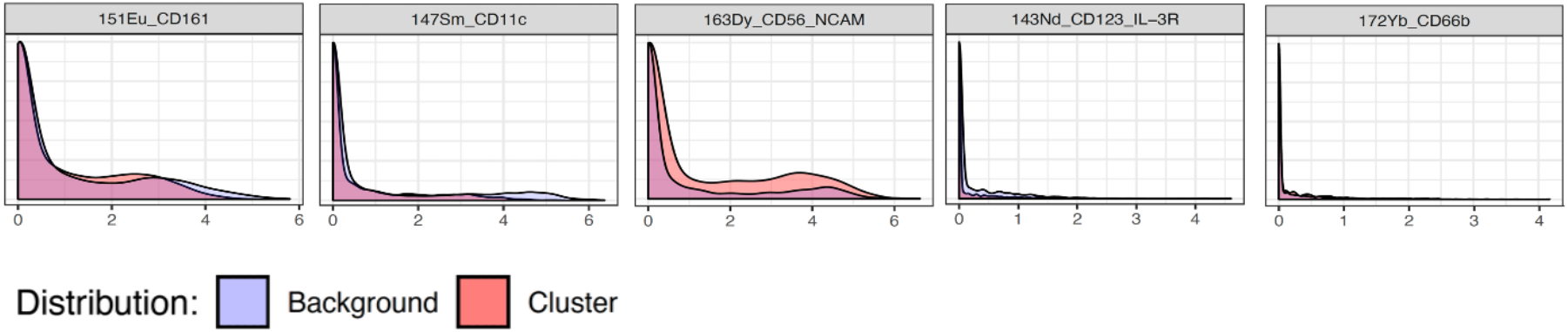

Cluster feature histogram of nodes 71808. Each histogram represents a feature of the lymphocyte signature proposed by the CITRUS model. The blue peaks represent the background signal while the orange peaks represent positive. Feature cluster markers are labelled for each histogram.

Analysis of the histograms revealed the phenotype in the sPD-L1 model was $CD8^{+}CD45RA^{+}CCR7^{-}CCR6^{+}CXCR3^{+}CD28^{-}CD57^{+}CD20^{+}CD127^{-}$. The phenotype identified in the HBsAg model was identical to that identified in the sPD-L1 model $CD8^{+}CD45RA^{+}CCR7^{-}CCR6^{+}CXCR3^{+}CD28^{-}CD57^{+}CD20^{+}CD127^{-}$. CD4 expression appeared in both clusters, however the background was higher than the expression level as highlighted in (Figure 14) and thus the CD4 cluster was excluded.

6.3.2 Cluster Phenotype and associations

The median level of PD-1 expression was considered the discriminatory factor for cluster identification. The plots in figure 6.11 shows increased PD-1 expression on the cluster identified in the CITRUS analysis for both the sPD-L1 and HBsAg models. PD-1 was significantly raised on the cell type identified in both those with high levels of HBsAg (p=0.02) and high levels of sPD-L1 (p=0.04).

Figure 6.11: PD-1 expression as the discriminatory marker for sPD-L1 (A) and HBsAg (B) clusters

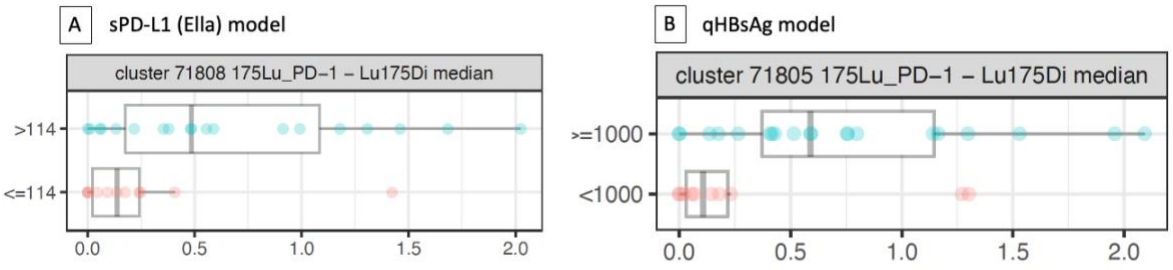

Box and whisker plots showing PD-1 expression as the discriminatory marker on the cluster identified during CITRUS analysis.

To visualise the similarity between the sPD-L1 and HBsAg clusters identified in CITRUS analysis, dimension reduction t-SNE analysis was conducted with concatenated cluster fcs files from each patient and overlaid in Figure 6.12. The clusters identified by PAM analysis were highlighted. Discrete clusters were identified for both 71805 and 71808 but split between CD8 and CD4 compartments. Due to the earlier indication that CD4 expression was mainly background, the CD4 compartment was not considered for further analysis. This decision was confirmed when analysing the histograms in figure 14. To support the inclusion of each feature marker in the proposed novel T-cell phenotype, the relative expression of each feature marker was represented in individual t-SNE heatmaps in Figures 6.13,6.14,6.15.

Figure 6.12: t-SNE analysis of qHBsAg and sPD-L1 cluster overlaid on global lymphocyte population compartments.

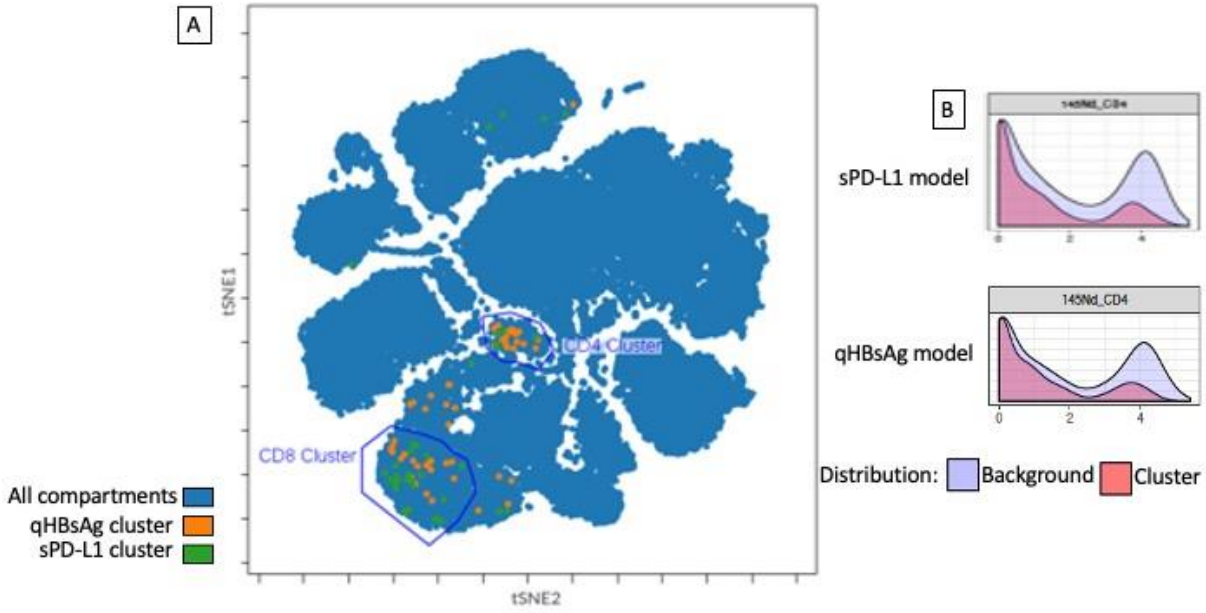

a)t-SNE analysis of sPD-L1 cluster (71808) and HBsAg cluster (71805) overlaid on t-SNE analysis of total ungated populations. (b) Exclusion of the CD4 sub-cluster due to background staining rather than positive population

Figure 6.13: t-SNE heatmap of individual cluster markers

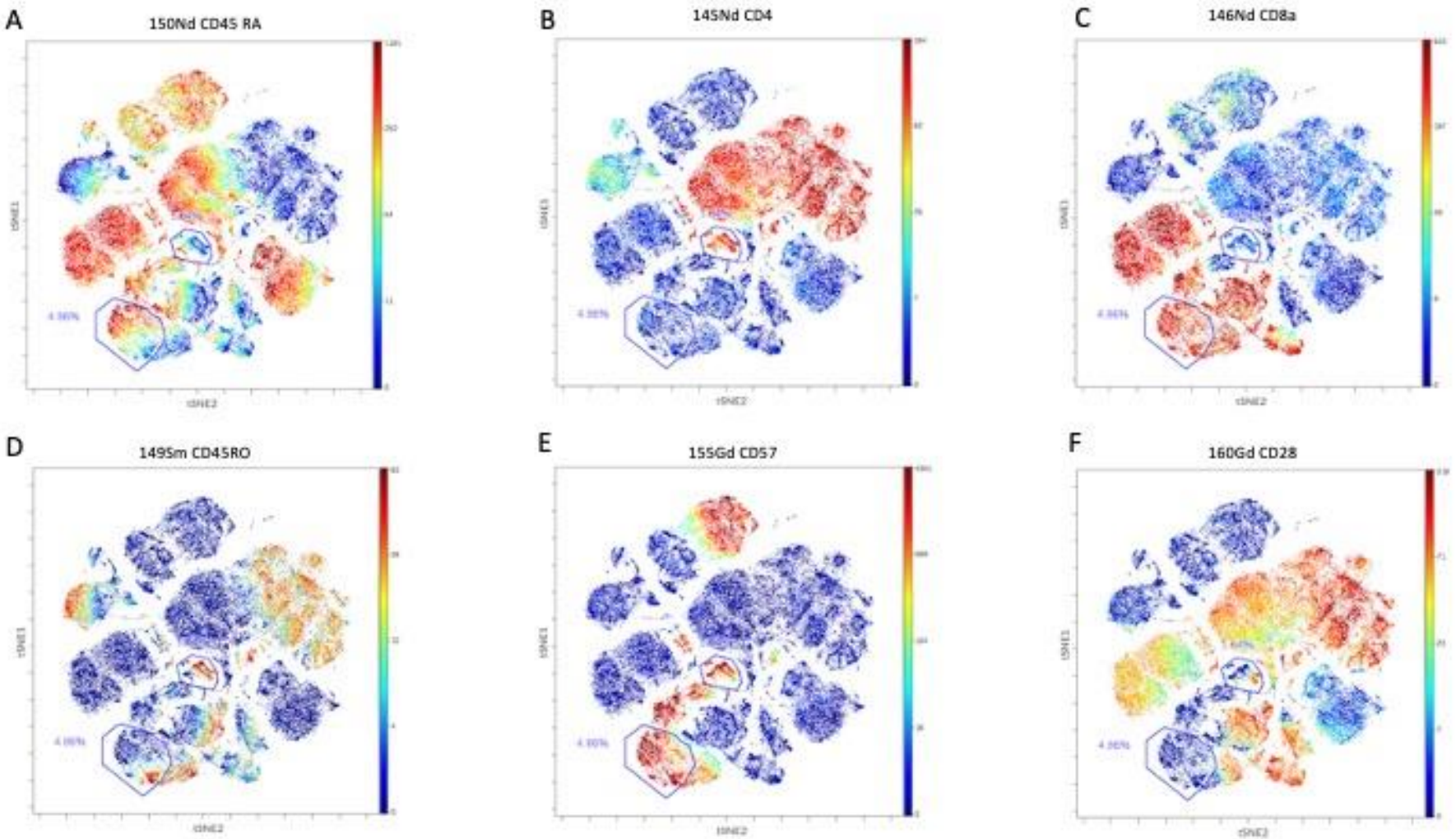

Individual t-SNE heatmap diagrams depicting the relative expression of each cluster feature marker. The individual clusters are circled; the larger circle represents the CD8 cluster and the smaller represents the CD4 cluster. Red hues represent high expression and blue represent low expression.

Figure 6.14: (cont) t-SNE heatmap of cluster markers

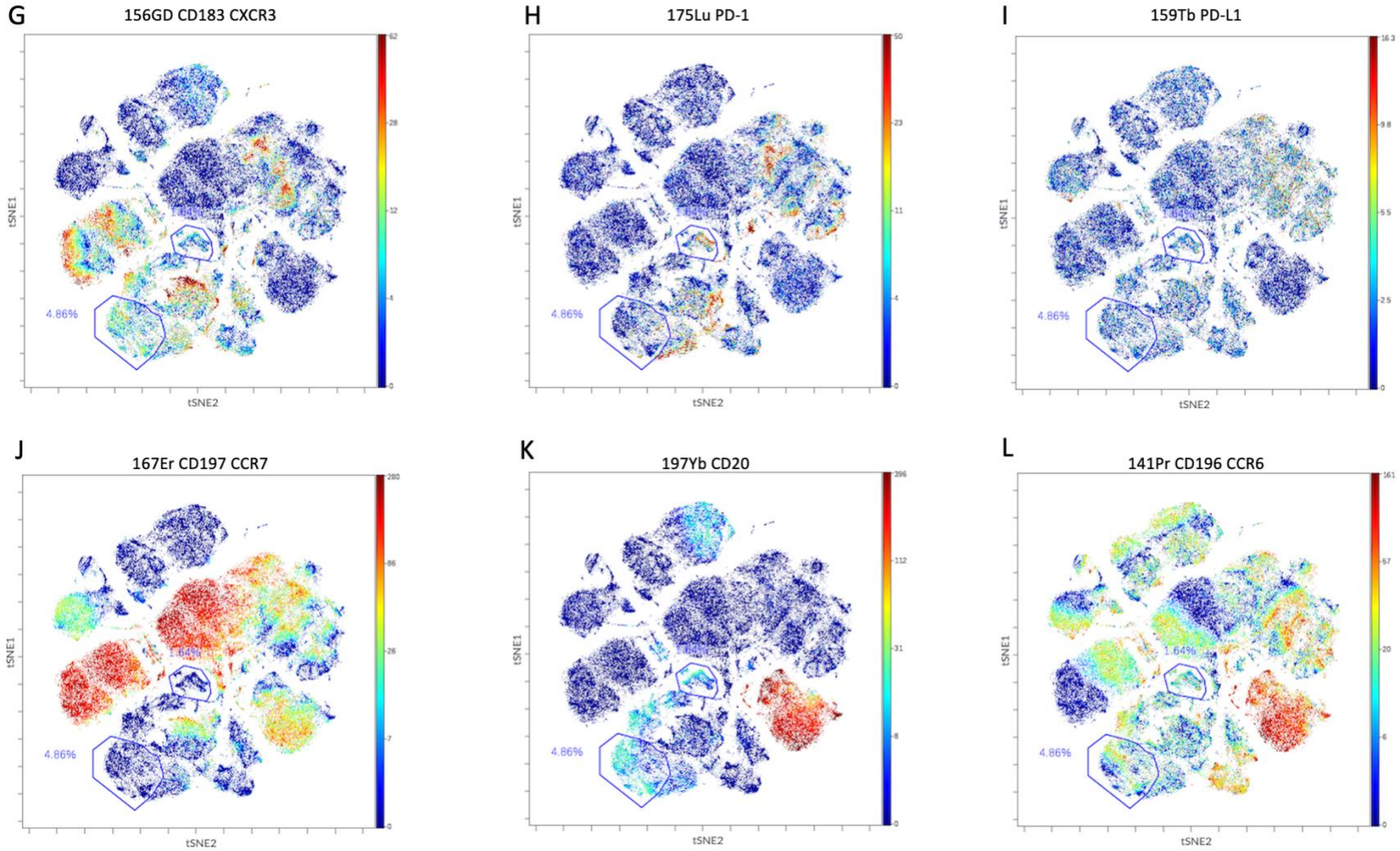

Individual t-SNE heatmap diagrams depicting the relative expression of each cluster feature marker. The individual clusters are circled; the larger circle represents the CD8 cluster and the smaller represents the CD4 cluster. Red hues represent high expression and blue represent low expression.

Figure 6.15: (cont) t-SNE heatmap of cluster markers

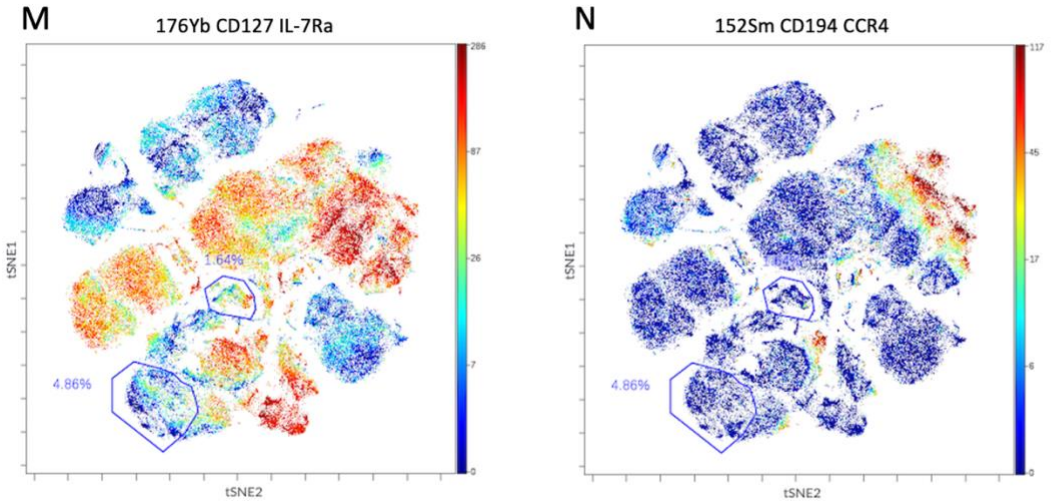

Figure 15c: Individual t-SNE heatmap diagrams depicting the relative expression of each cluster feature marker. The individual clusters are circled; the larger circle represents the CD8 cluster and the smaller represents the CD4 cluster. Red hues represent high expression and blue represent low expression.

The cell cluster phenotype $CD8^{+}CD45RA^{+}CCR7^{-}CCR6^{+}CXCR3^{+}CD28^{-}CD57^{+}CD20^{+}CD127^{-}$ identified in the CITRUS and t-SNE analysis was isolated in individual patients as described in the representative gating diagram in Figure 6.16.

Figure 6.16: Representative gating diagram for identification of T-cell signature

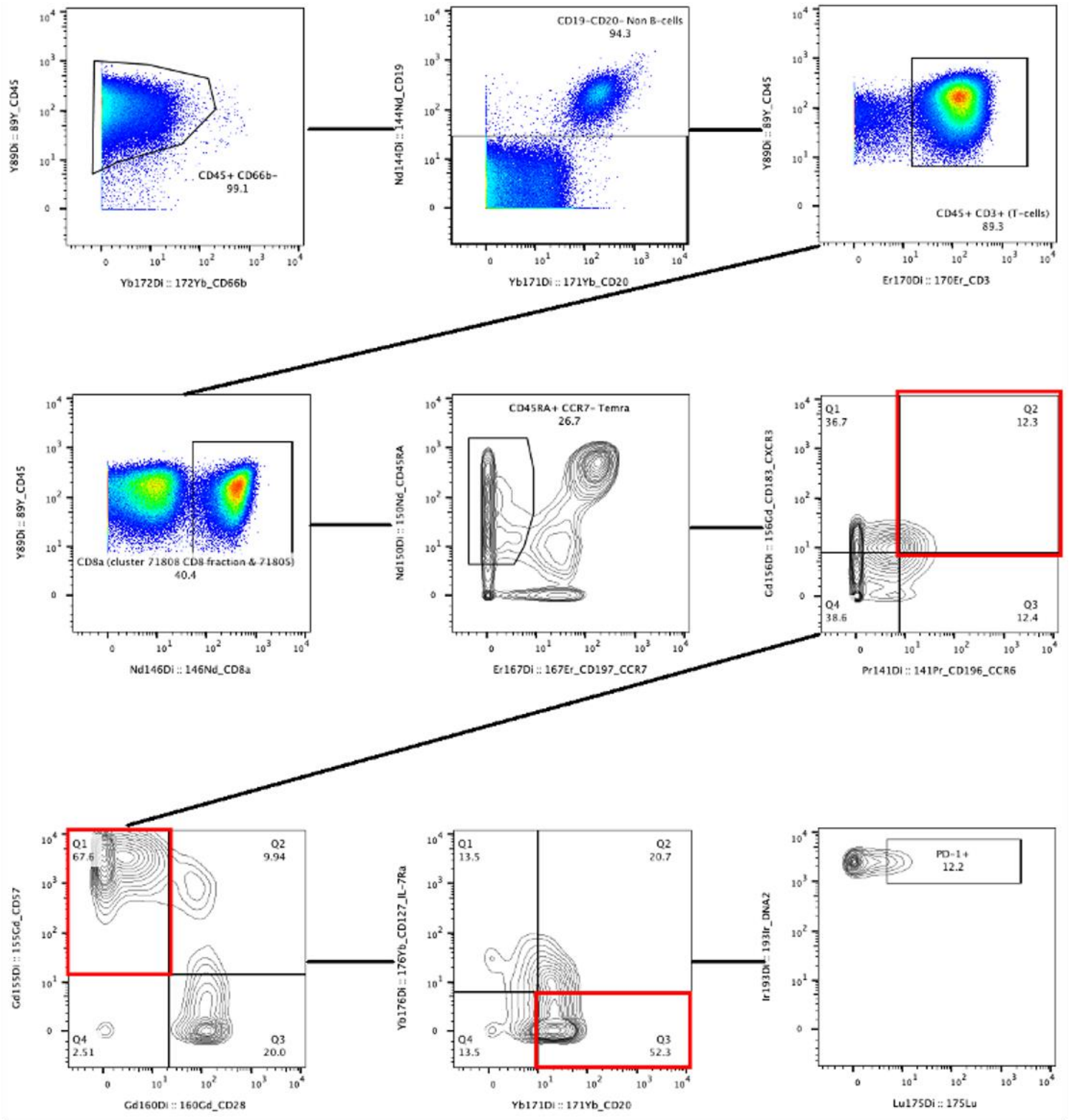

Representative gating diagram used to isolate the novel T-cell cluster in each individual patient. Red outlies represent the parent population for subsequent gates

When compared to healthy donors, the median frequency of the cluster phenotype was higher in those with chronic hepatitis B infection (p=0.0119) (Figure 6.17). The endpoints considered in the CITRUS model were compared with the gated phenotype in individual patients, the proportion of PD-1^+ cluster cells were significantly increased in those with higher levels of sPD-L1(p=0.0264). Similarly, the proportion of PD-1^+ cluster was increased in chronic hepatitis B infection patients with higher levels of circulating HBsAg though only of borderline significance (p=0.0559) (Figure 6.18).

Figure 6.17: T-cell signature phenotype in chronic hepatitis B infection and healthy controls

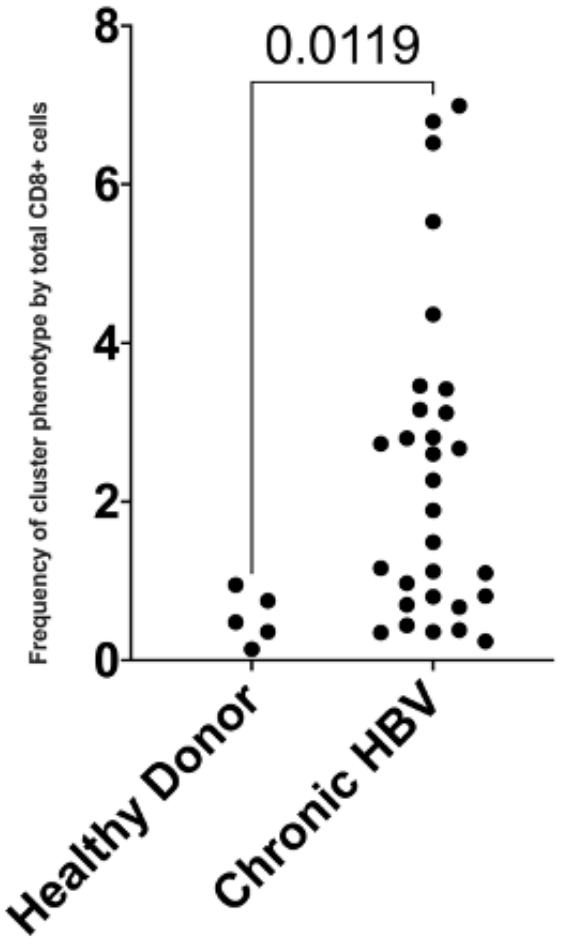

Differences in T-cell cluster between healthy controls and those with chronic hepatitis B infection.

Figure 6.18: Frequency of PD-1+ T-cell signature phenotype by CITRUS model groups

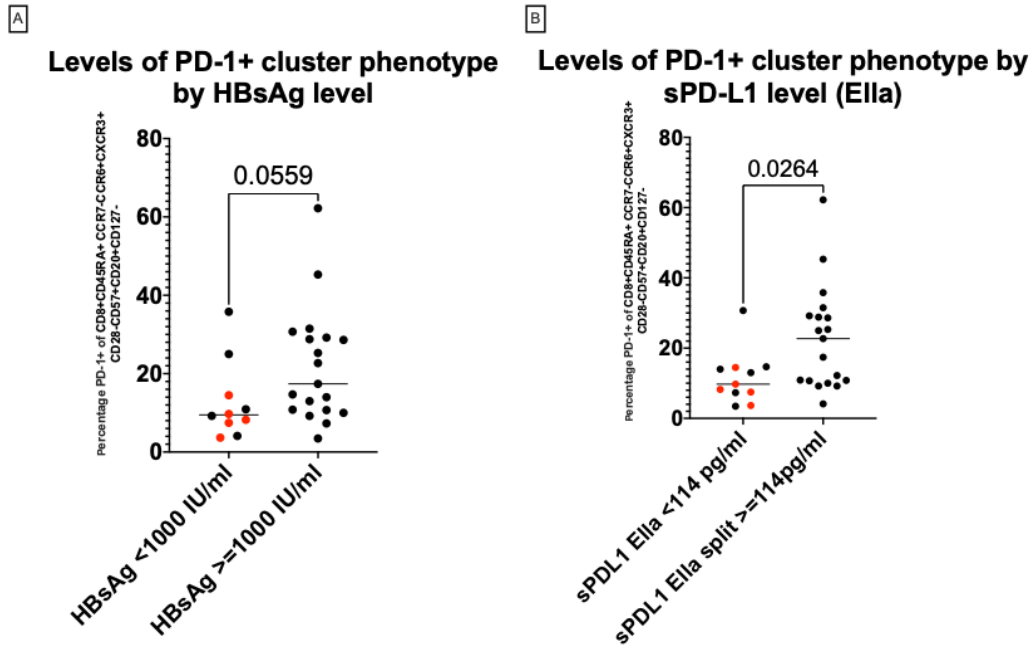

Differences in the proportion of the novel T-cell PD-1 positivity grouped by the predictors used in the CITRUS analysis. Medians represented as horizontal line, P-values calculated with Mann-Whitney U. Red circles represent the same patient in each analysis.

6.3.3 T-lymphocyte populations expression of PD-1 and PD-L1 and relationship with clinical characteristics

The percentage of traditional T-cell compartment populations and the proportion found to be the be positive for PD-1 and PD-L1 are summarised in Table 6.6. Expression of PD-1 was the highest on CD4 cells overall, specifically on terminal and effector memory CD4 cells. Within the CD8 compartment, the effector memory and central memory cells had the highest PD-1 expression. Only a small proportion of both naïve CD4 and CD8 cells had detectable PD-1 expression, as expected. PD-L1 expression was highest on central memory cells of both the CD4 and CD8 compartments. Due to the relatively low level of expression of PD-L1, gating was not reliable in the overall CD4 and CD8 population.

Table 6.6: PD-1/PD-L1 on lymphocyte populations

Lymphocyte population	Proportion of parent	% PD-1+	% PD-L1+
Total $CD4^{a}$	56.2 (47.7 – 63)	15.6 (12.1 – 20.4)	N/A
$CD4_{naive}$	40.8 (30.9 – 45.6)	2.8 (1.6 – 4.3)	3.3 (2.5 – 4.2)
$CD4_{CM}$	7.0 (5.0 – 9.5)	12.2 (10.6 – 16.1)	23.9 (20.3 – 27.2)
$CD4_{EM}$	28.2 (23.0 – 33.5)	38.0 (34.2 – 43.2)	14.2 (12.2 – 16.8)
$CD4_{TM}$	11.1 (8.3 – 16.9)	39.5 (35.0 – 46.8)	20.4 (18.8 – 24.9)
Total $CD8^{b}$	39.2 (29.6 – 43.6)	14.3 (11.9 – 20.3)	N/A
$CD8_{naive}$	42.9 (28.2 – 51.7)	2.1 (0.9 – 3.5)	2.0 (1.4 – 2.5)
$CD8_{CM}$	0.3 (0.2 – 0.6)	26.3 (22.5 – 31.2)	16.4 (10.8 – 18.9)
$CD8_{EM}$	27.1 (21.7 – 32.3)	30.4 (26.7 – 40.0)	9.2 (7.4 – 10.3)
$CD8_{TM}$	20.5 (13.3 – 31.7)	14.9 (8.1 – 24.6)	4.6 (3.5 – 7.1)

Cellular proportions expressing PD-1 and PD-L1. Due to low expression levels, PD-L1 was not reliable on total $CD4^{+}$ or $CD8^{+}$ T-cells. All figures represented as median (IQR).[a,b] Proportion of total $CD45^{+}CD3^{+}$

6.3.4 CD4 and CD8 compartments versus healthy controls and chronic HBV infection phase

Healthy controls were immunoprofiled using the MDIPA deep immunoprofiling assay at Fluidigm® central labs and compared with immunoprofiling of patients with chronic HBV infection in and detailed in Figure 6.19. No demographic information was provided for the healthy participants and PD-1/PD-L1 expression was not included. The proportion of $CD4_{naive}$, $CD4_{EM}$ and $CD4_{TM}$ or $CD8_{naive}$, $CD8_{CM}$ or $CD8_{EM}$ did not deviate significantly from the proportions found in healthy controls. PBMCs from patients living with chronic HBV infection had a lower frequency of $CD4_{CM}$ and a higher frequency of $CD8_{TE}$ though only of borderline significance (Figure 6.19 and Figure 6.20). When analysed by chronic hepatitis B infection phase, the proportion of naive, central memory, effector memory and terminal memory cells in both the CD4 and CD8 compartment remained consistent in Figures 6.21 and 6.23. Increased PD-L1 expression on central and effector memory CD4 T-cells was found in those with HBeAg+ hepatitis and on therapy when compared to those with HBeAg- infection (Figure 6.22 and 6.24). No other relationships were detected between PD-1 or PD-L1 expressing cells in the CD4 or CD8 T-cell compartments. Due to the limited variation observed, all patients were explored collectively regardless of clinical phase in subsequent correlation analysis.

Figure 6.19: Comparison of CD4 subsets in those living with chronic hepatitis B infection vs healthy controls

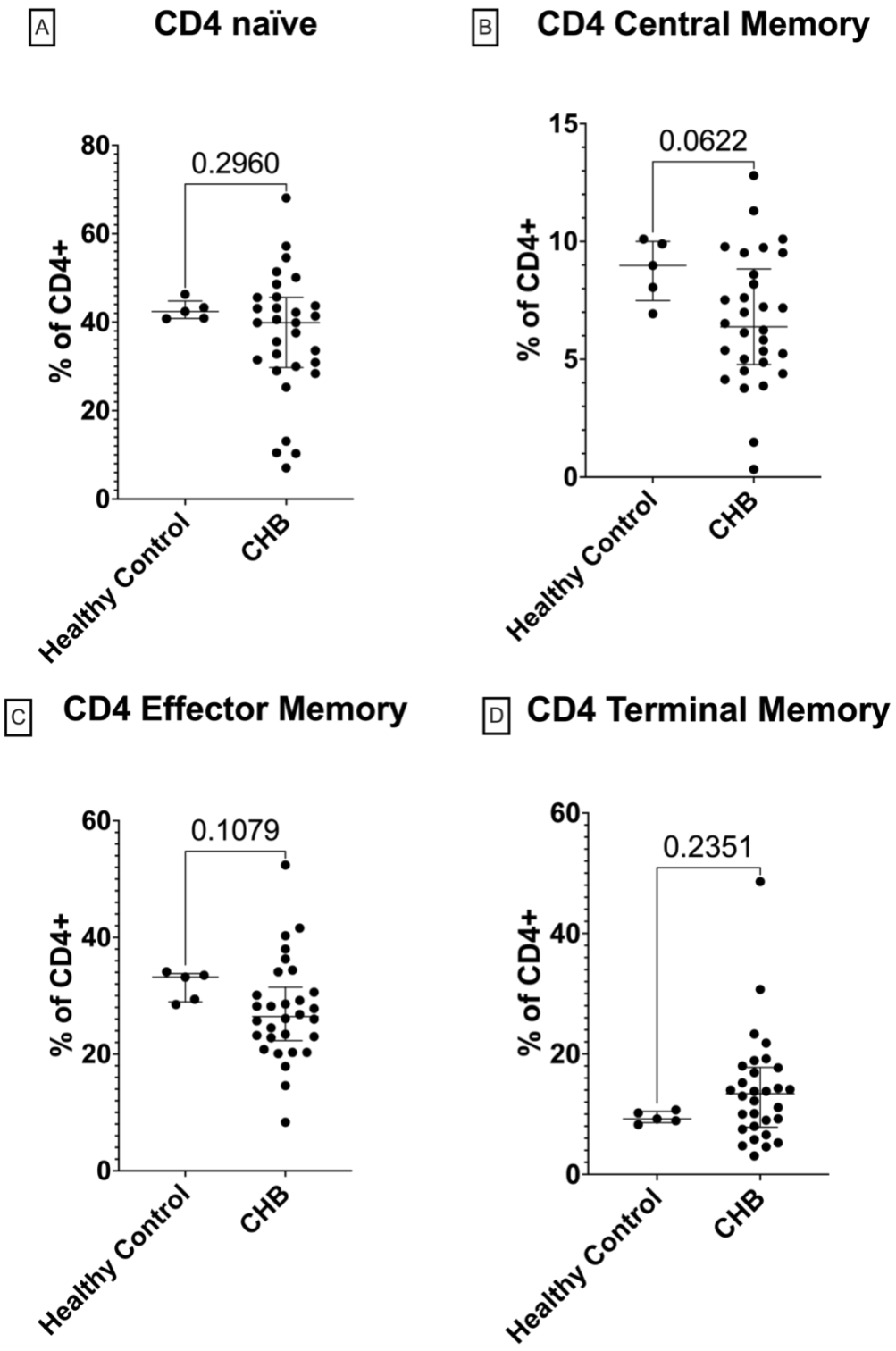

Comparison of $CD4^+$ sub-populations between healthy controls and people with chronic hepatitis B infection. Differences were calculated with Mann-Whitney U. Medians with 95% CIs represented by horizontal lines

Figure 6.20: Comparison of CD8 subsets in those living with chronic hepatitis B infection vs healthy controls

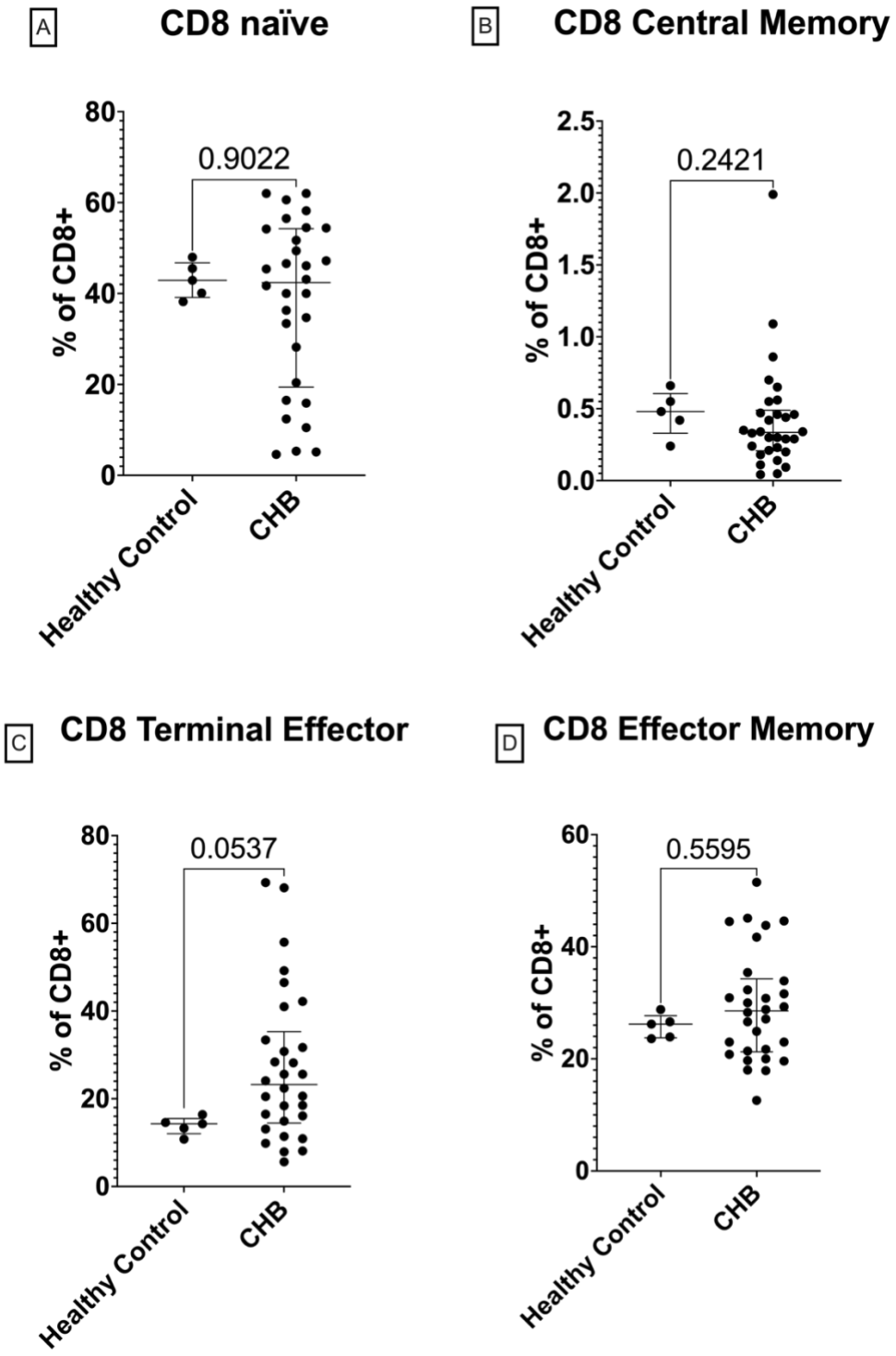

Comparison of $CD8^+$ sub-populations between healthy controls and people with chronic hepatitis B infection. Differences were calculated with Mann-Whitney U. Medians with 95% CIs represented with horizontal lines.

Figure 6.21: Comparison of CD4 subsets grouped by chronic hepatitis B infection phase

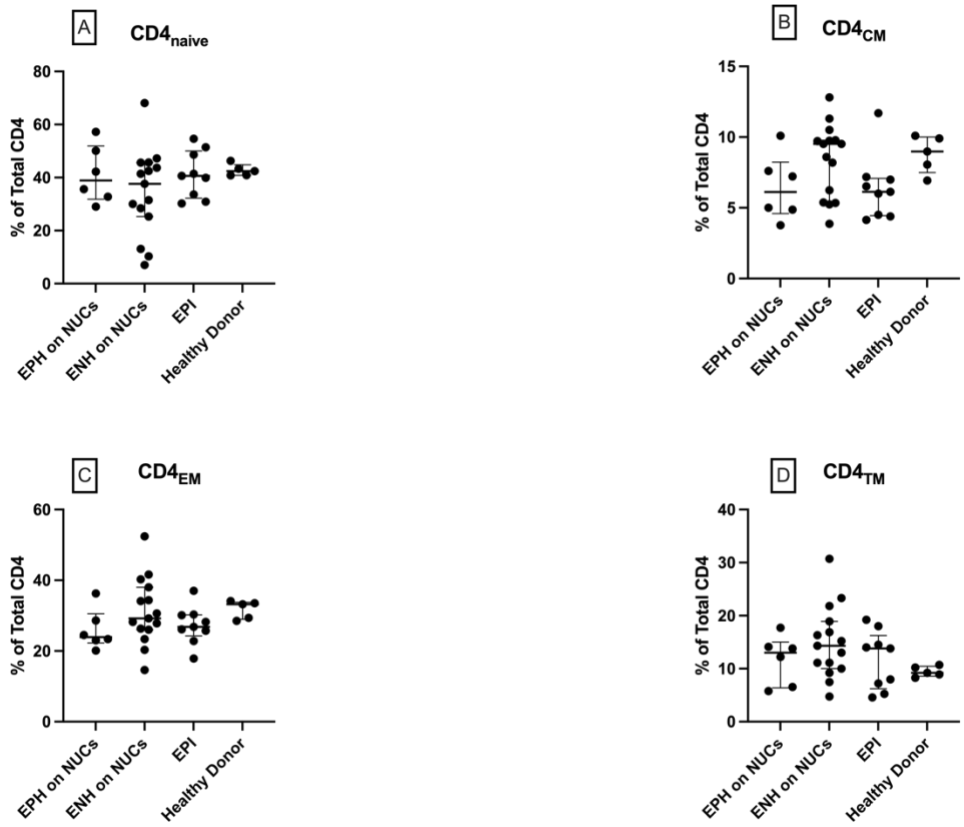

Comparison of $CD4^+$ sub-populations between chronic hepatitis B infection phases. Differences were calculated with Kruskal-Wallis. Disease phases with too few patients for statistical testing were removed.

Figure 6.22: Comparison of PD-1+ and PD-L1+ CD4 compartments grouped by chronic hepatitis B infection phase

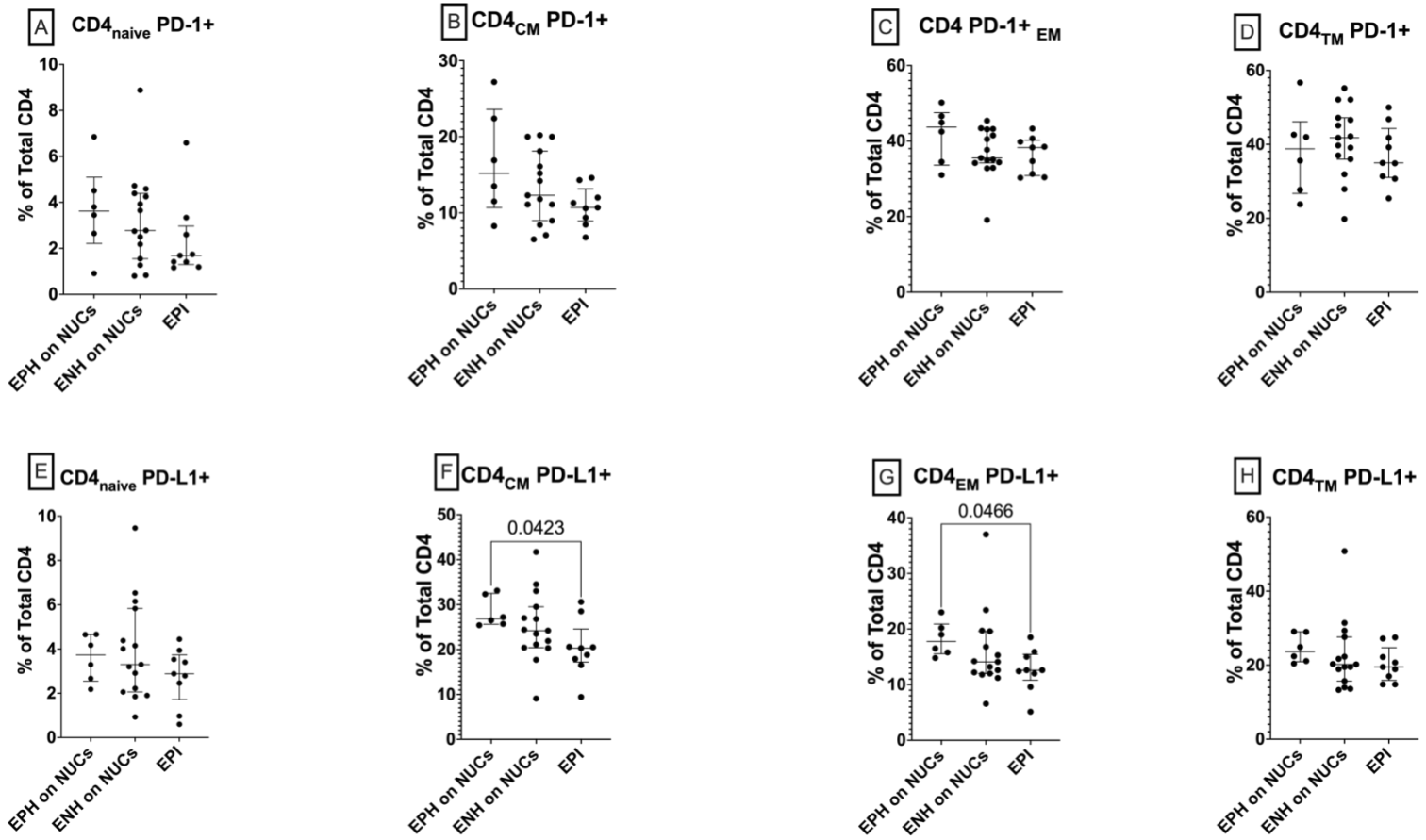

Comparison of PD-1 and PD-L1 positive $CD4^+$ subsets between chronic hepatitis B infection phases. Differences were calculated with Kruskal-Wallis paired with Dunn's multiple comparisons post-hoc test. Disease phases with too few patients for statistical testing were removed.

Figure 6.23: Comparison of CD8+subsets grouped by chronic hepatitis B infection phase

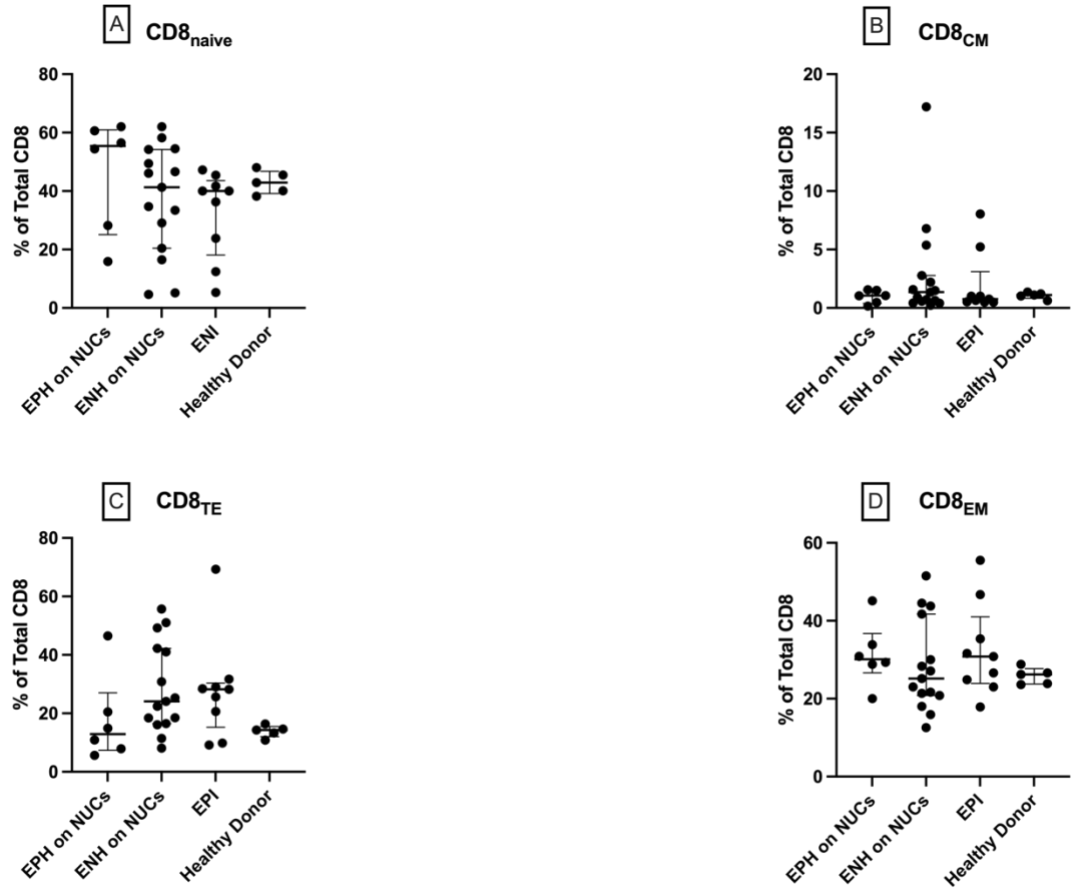

Comparison of $CD8^+$ sub-populations between chronic hepatitis B infection phases. Differences were calculated with Kruskal-Wallis. Disease phases with too few patients for statistical testing were removed

Figure 6.24: Comparison of PD-1+ and PD-L1+ CD8 subsets by chronic hepatitis B infection phase

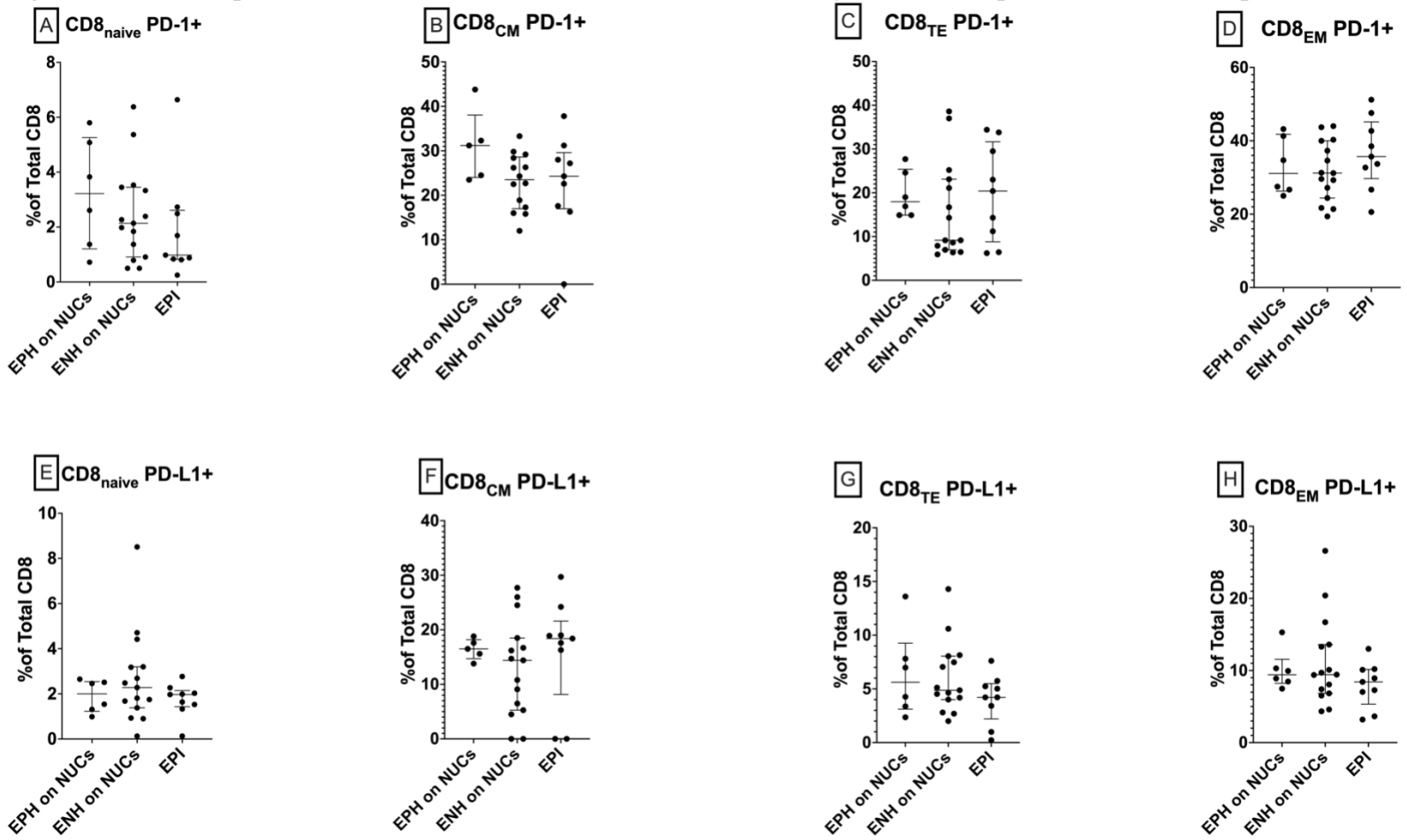

Comparison of PD-1 and PD-L1 positive $CD8^+$ subsets between chronic hepatitis B infection phases. Differences were calculated with Kruskal-Wallis. Disease phases with too few patients for statistical testing were removed.

6.3.5 T-cell compartment and correlations with clinical parameters

Differences in the percentage of T-lymphocyte subsets, including those expressing PD-1 and PD-L1, between clinical characteristics were explored with Spearman correlation. The resulting Spearman correlation matrix can be found in Table 6.7. Only relationships with significant differences are presented.

Table 6.7: Spearman correlation of PD-1 and PD-L1 positive CD4 and CD8 T-cell subsets with clinical characteristics

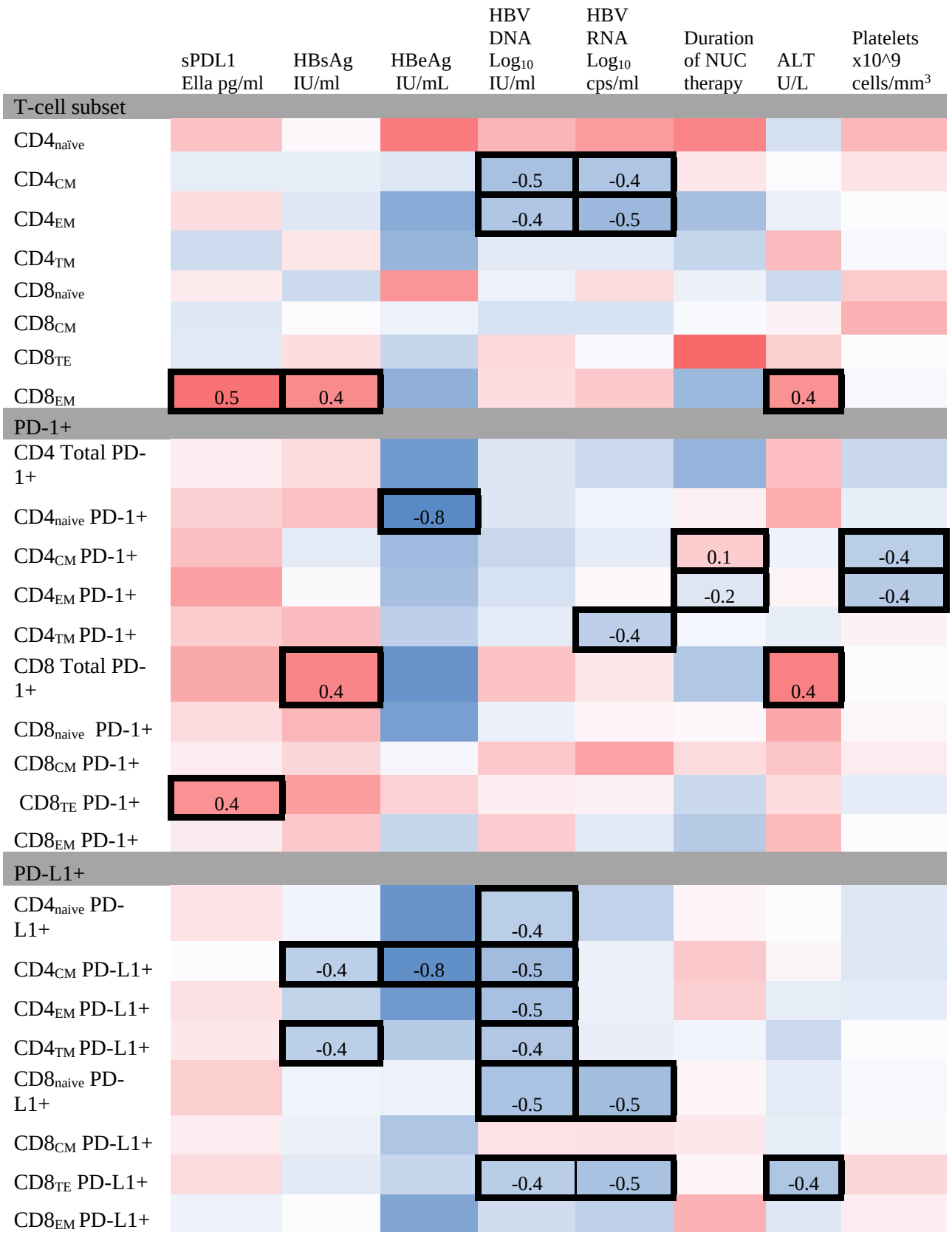

Correlation matrix with Spearman correlation values (r). Only relationships with significant differences (<0.05) are presented and emboldened. The full correlation matrix with all r values, 95% confidence intervals and P-values can be found in online appendix files.

Spearman correlation analysis of T-lymphocyte populations found that the proportion of $CD4_{CM}$ and $CD4_{EM}$ cells were inversely correlated with both HBV DNA and HBV RNA. Within the CD8 compartment, $CD8_{EM}$ were positively correlated with levels of sPD-L1 measured by the Ella platform. $CD8_{EM}$ cells were also positively correlated with HBsAg and ALT levels.

The proportion of PD-1 positive $CD4_{CM}$ and $CD4_{EM}$ subsets were inversely correlated with platelet count. Within the CD8 compartment, only the total PD-1 positive CD8 T-cells were positively correlated with both the level of HBsAg and ALT.

Most correlations with PD-L1 positive cells were limited to the CD4 compartment. Similarly, the proportion of PD-L1 positive $CD4_{naive,}$ $CD4_{CM}$, $CD4_{EM}$ and $CD4_{TM}$ were inversely correlated with HBV DNA levels. An inverse correlation was detected between the proportion of PD-L1 positive $CD4_{CM}$ and HBeAg and HBsAg levels. Negative correlations were detected between the proportion of PD-L1 positive $CD8_{naïve}$ and $CD8_{TE}$ and levels of HBV DNA and HBV RNA. Additionally, PD-L1+ $CD8_{TE}$ were negatively correlated with ALT levels.

6.4 Discussion

This study provides a detailed immune profile of 30 people living with chronic HBV infection and associated PD-1 and PD-L1 expression. We propose a novel T-cell phenotype, $CD8^{+}CD45RA^{+}CCR7^{-}CCR6^{+}CXCR3^{+}CD28^{-}CD57^{+}CD20^{+}CD127^{-}$, identified with novel supervised machine learning algorithms, that is elevated in patients living with chronic HBV infection when compared to healthy donors and is predictive of those with HBsAg levels >1000 IU/ml and sPD-L1 $\geq$114pg/ml measured by Ella. Total PD-1 expression on lymphocyte populations showed similar trends as previously discussed in Chapter 5 including further evidence of an inverse correlation between $PD\text{-}1^{+}$ $CD4^{+}$ T-cells and circulating platelets particularly in the central and effector memory subsets.

This detailed immune profiling experiment utilized the heavily validated Fluidigm® MaxPar Direct Deep Immune Profiling assay utilises CyTOF mass cytometry[229] . This standardised and assay allowed us to explore deep subpopulations of lymphocytes without multiple panels which was a limiting factor in chapter 5. As a result, we were able to further characterise the relationship between $PD\text{-}1^{+}CD4^{+}$ T-cells and the level of circulating platelets, specifically in the $CD4^{+}_{CM}$ and $CD4^{+}_{EM}$ compartments. The $CD4^{+}_{CM}$ and $CD4^{+}_{EM}$ are thought to serve separate functions; the $CD4^{+}_{EM}$ travel to peripheral sites of inflammation and produce pro-inflammatory cytokines while $CD4^{+}_{CM}$ cells likely travel to secondary lymphoid organs to await antigen rechallenge[380]. However, both $CD4^{+}_{CM}$ and $CD4^{+}_{EM}$ originate from naïve $CD4^{+}$ cells that have undergone initial T-cell receptor signalling and remain in circulation[380]. In chapter 5 the relationship between $PD\text{-}1^{+}$ T-cells and platelets was discussed. The findings of a large cohort study of 122,000 individuals found a greater prevalence of HBsAg among those with low levels of platelets and high ALT levels[361]. The negative association described between $PD\text{-}1^{+}$ $CD4^{+}_{CM}$ and $CD4^{+}_{EM}$ and platelets may further support the hypothesis that platelets shift the balance toward a more pro-inflammatory state, potentially driven by $CD4^{+}_{CM}$ and $CD4^{+}_{EM}$. However, within this cohort, there was a low prevalence of transaminitis thus no strong conclusions can be drawn.

In the preliminary analysis, bivariate gating was used to identify common T-cell subsets. We were able to use machine learning algorithms to elucidate a novel phenotype, $CD8^{+}CD45RA^{+}CCR7^{-}CCR6^{+}CXCR3^{+}CD28^{-}CD57^{+}CD20^{+}CD127^{-}$. Furthermore, the percentage of $PD\text{-}1^{+}$ positivity on the novel cell type was associated with increased levels of both HBsAg and sPD-L1 measured by Ella. No significantly predictive models were identified

for sPD-L1 measured by SIMOA or membrane bound PD-L1. The cluster phenotype identified in both the HBsAg and sPD-L1 (Ella) models show several unique marker combinations not typically investigated in T-cell phenotyping.

First, $CD20^+$ T-cells are a recent field of investigation. CD20 is a prototypical B-cell marker. It was once thought $CD3^+CD20^+$ cells were only detected due to issues with flow cytometry compensation[381]. However, they have since been confirmed to be a true population and may account for approximately 3-5% of the total T-cell compartment[382]. T-cells may acquire CD20 expression through trogocytosis of $CD20^+$ from B-cells[383]. The phenotype we describe agrees with previous studies that suggest $CD20^+$ T-cells are primarily found in CD8 compartment and are deficient in CCR7; however, our findings diverge from previous studies in that phenotype we described expresses RA instead of RO[382]. $CD3^+CD20^+$ cells have been described in autoimmune diseases such as rheumatoid arthritis, multiple sclerosis and psoriasis[384–387]. $CD20^+$ T-cells have been identified as a potential reservoir for HIV transcripts that are expanded in HIV patients with ongoing viremia and depleted in those on long term suppressive ART[388] . Functional studies have shown that $CD20^+$ T-cells often mirror that of inflammatory effector memory cells producing IFN-y and IL-17 but with decreased homing ability and altered adhesion capacity[385,389,390]. Coincidentally, the expression of CD20 on T-cells could make them a target for anti-CD20 therapies[383]. Depletion of $CD20^+$ T-cells with Rituximab has been described in those with multiple sclerosis[391]. It is well known that in patients with previous chronic hepatitis B infections that administration of anti-CD20 therapies increases the risk of viral reactivation, in some cases up to 55% in HBsAg+ individuals[392]. With the data presented in this study, this suggests that $CD20^+$ T-cells may play a partial role in the immune control of HBV carriers.

Second, $CD8^+CD28^-CD57^+$ cells are described in diseases that promote long-term immune activation[393]. Our results are in line with a previous finding that $CD28^-$CD8 cell are enriched in people with chronic HBV infection when compared to healthy controls. However, this study diverges from our findings as we did not find an associated between the phenotype and HBV DNA[394]. In normal CD8 activation pathways CD28 is crucial in supplying co-stimulatory signals to complete T-cell/MHC activation pathways[393]. Over periods of chronic immune activation, CD28 expression is curtailed and is followed by the emergence of CD57[394] .Functionally, T-cell expressing CD57 can produce potent cytotoxic molecules like IFN-y, granzyme B and perforin yet do not proliferate readily[395]. Expression of CD57 on T-cells has

previously been associated with older age and but increasingly investigates in the context of chronic infection and cancers[395–398]. Recently, an elegant experiment of CD8 exhaustion among different chronic HBV infection phases found that the frequency of $CD57^+$ expression was significantly higher among cells also expressing markers of immune exhaustion including PD-1, KLRG1, EOMES, TCF-1, BCL-2, and TOX[189]. Our study strengthens these findings and expands them to also include the markers identified in the novel T-cell phenotype described. Similar trends have been described in HIV, CMV, malaria and lung cancer and particularly among the TEMRA subset as we also describe[397,399,400].

Thirdly, CD8+CD45RA+RO-CCR7-, referred to as the CD8 terminal effector cells re-expressing RA(Temra), are highly differentiated effector CD8 cells[401]. Increases in the Temra subset of CD8 T-cells is associated with chronic infections such as CMV, HCV and HIV[402–404]. Despite their highly differentiated state, the CD8 Temra subset can produce potent inflammatory and regulatory cytokines including IL-15 and are associated with immune control of HIV[403,404] suggesting the importance of the Temra subset in coordinating the adaptive immune response and antigen rechallenge. Despite this, CD8 Temra are often found expressing high levels of inhibitory markers such as PD-1[402] as is the case with the phenotype we report. Previous reports suggest that CD8 Temra population should be interpreted with caution as they have been found to expand with increased age and may indicate senescence[405,406].

Finally, in the T-cell phenotype presented, we found increases in CCR6 and CXCR3 in the absence of CD127. Chemokines and their receptors are important in the chemotaxis of lymphocytes to tissue compartments from the periphery. For example, Ye Htun et al found that CCR6 and CXCR3 mediated CD8 recruitment to the liver of mice with hepatic injury and inflammation and facilitate binding the sinusoidal endothelium[407]. While the importance of CCR6 and CXCR3 in homing expression has documented, few studies have examined their expression in the context of chronic HBV infection. A study by Mullins et al found that in activated CD8 cells from melanoma patients receiving therapeutic vaccination, $CD8^+$ T-cells double positive for CCR6 and CXCR3 were associated with increased survival rates, suggesting that this cell subset may play a role in control of chronic disease[408]. However, a study of PBMCs isolated from patients with autoimmune vasculitis found that CCR6/$CXCR3^+$ T-cells were associated with poor prognosis and disease progression[409]. Additionally, CCR6/$CXCR3^+$ T-cells have been shown to be readily infected by HIV and act as a reservoir for replication despite suppressive ART[410,411].These data indicate that the role

of CCR6/CXCR3^{+} CD8^{+} cells may be disease specific and their role in chronic HBV infection should be further investigated. Low or absent CD127 expression (IL-7 receptor), has become associated with chronic antigen stimulation and an exhausted T-cell phenotype. We previously included CD127^{-} CD8^{+} T-cells as part of our previous definition of terminally exhausted cells. T-cells deficient in CD127, which is generally associated with a memory phenotype, are unable to be stimulated by IL-7 and in turn are unable to self-renew[412–414]. Given the increase of both CCR6 and CXCR3 and deficiency of CD127, previous studies would suggest this combination is associated with memory CD8 cells capable of homing to tissue sites but with signs of antigen induced exhaustion and limited expansion abilities.

Overall, the cell phenotype identified by high-dimensional machine learning algorithms shows signs of terminal differentiation with memory capabilities and elements of immune exhaustion. Unsurprisingly, many of the cluster phenotype markers have been associated with pro-inflammatory immune activation and cytotoxic activity in chronic infections and diseases such as HIV, HCV, CMV, cancers and autoimmune diseases but are often co-expressed with inhibitory markers such as PD-1. To our knowledge this is the first time many of these markers have been reported in the context of chronic hepatitis B infection.

The proportion of PD-1 positivity on the novel T-cell phenotype was predictive of both patients with increased levels HBsAg and sPD-L1. This may suggest that immunosuppressive mechanisms in chronic HBV pathogenesis may be more systemic and in addition to that of the hepatic compartment[414]. The correlations with sPD-L1 and clinical parameters in addition to broad lymphocyte compartments was discussed in detail in chapters 5 and 6. However, in this deep analysis of T-cell compartments, we did not find the same association with PD-1^{+} CD4^{+} cells and sPD-L1. This discrepancy may be due to this population including a relatively low proportion of individuals or differences in gating analysis. In a recent phase 1 study evaluating the safety and PK of a novel PD-L1 mRNA silencing molecule, it was found that after 3 doses, HBsAg levels and sPD-L1 levels declined accompanied by an increase in ALT however, sPD-L1 was only associated when measured with the SIMOA platform but not the Ella platform[291]. This may suggest that the T-cell phenotype identified in this study that was predictive of sPD-L1 levels by Ella and not SIMOA may be T-cells with elements of exhaustion that cannot be rescued by immunotherapies.

This study has limitations. First, as discussed in chapter 5, we did not include HBV specific responses and only considered global populations. Previous studies have shown that PD-1 expression is expressed highly on HBV-specific T-cells that that may not be mirrored on global populations[375,415]. The detection of global immune cell signatures that provide distinct associations of clinically relevant outcomes should remain a goal in research as this would provide utility in that it is more efficient, reproducible and not limited and patient specific HLA types. However, due to the associations detected, future studies would benefit from also observing antigen specific cells to confirm if the cluster phenotype described in this study is in associated with Env specific cells. Second, due to the expense of the assay used, we were not able to include all participants which limits the generalizability of these findings. Instead, this study was heavily populated by those who were on long-term NUC therapy and therefore may not be representative of the immunological status of those with high level of HBV replication and minimal to moderate hepatic inflammation. This is highlighted by the low proportion of participants included in this analysis that had raised ALT levels (>40 IU/ml) and the low number of HBeAg + hepatitis/ infection which prevented us from drawing any strong conclusions from HBeAg quantification. Due to the requirements of the CITRUS algorithm, at least 10 samples were needed in each group thus the limited number of participants included in this study prevented the comparison of HBV disease phases and other virological outcomes. The CITRUS algorithm relies on certain parameters selected by the user. While care was taken to optimize the parameters utilised in the CITRUS analysis, due to the false discovery rate of up to 10%, some associations may be spurious and currently there is no method for adjustment for other parameters. Ideally to strengthen the findings, the false discovery rate and cross-validation error rate would be lowered to 1% for all models. Additionally, only 2,500 events were used for modelling, this small population was used as not all samples had equal events recorded thus some samples were heavily down sampled. Third, the healthy volunteer data provided by Fluidigm did not contain the data for PD-1 and PD-L1 expression or demographics which excluded them from some of the analysis.

We highlights findings that warrant further investigation. To increase the generalizability of the study, further recruitment is necessary. Specifically, recruitment should be targeted at increasing both the HBeAg+ infection and hepatitis groups that would likely require multicentre recruitment due to the low proportion of patients with the disease profile. Further recruitment should also aim to increase the diversity of the ethnic backgrounds represented as well as healthy volunteers as HLA types vary between ethnic backgrounds and a majority of

HBV research is concentrated around the expression of HLA A*0102[375]. Experimentally, to confirm the association found between HBsAg and the T-cell signature identified in cluster analysis, the T-cells expressing the signature should be sorted from the global T-cell population and then assessed for HBV specificity, including all major HBV epitopes. Due to the limited frequencies of both HBV-specific cells and the cluster signature, evaluating this population may prove technically difficult and may be approached in two ways. First, *in-vitro* expansion of directly *ex-vivo* PBMCs stimulated with HBV peptide pools for at least 10 days has been used in most studies to detect these rarer populations[216]. However, this technique has its limitations as *in-vitro* expansion requires relatively long cell culture times coupled with stimulatory molecules which alter the phenotype of the cells recovered. Second, a more recent technique suggests utilizing magnetic based purification system that captures HBV-specific cells from the peripheral population[216]. Evaluation of the functional capacity of the CD8 cluster signature would be crucial to confirm the association of the phenotypic features with function. Particularly, due to the multitude of effector features, functional experiments would aim to assess the production of IFN-y, TNF-a, IL-15 and IL-17 and ideally should be coupled PD-1 blockade. Though PD-1 is often the major checkpoint inhibitor described on exhausted T-cell, future studies should also include markers associated with exhausted phenotypes such as KLRG1, T-bet, EOMES, CLTA-4 and TOX[186,416].

This study applied a complex panel of immune markers with mass cytometry to examine PD-1 and PD-L1 expression on global deep cell subsets in a select group of people living with chronic HBV infection and explored associations with clinical and virological characteristics. Additionally, we utilized a novel machine learning technique (CITRUS) to identify a CD8 T-cell signature that phenotypically showed signs of memory and effector capability coupled with markers of immune senescence and exhaustion. PD-1 expression on the global CD8 cluster signature identified was both predictive and linearly associated in patients with high levels of both HBsAg and sPD-L1. Although these findings need to be confirmed within the HBV-specific T-cell population, we provide evidence of a CD8 T-cell subset, detected in the global T-cell population, that is associated with clinically relevant parameters.

7 General discussion and future directions

The scale of the HBV epidemic and the burden of HBV-related disease are substantial, yet our current understanding of disease pathogenesis and immunological control is incomplete. Although researching a cure for chronic HBV infection is in focus, the success of any potential curative therapeutic approach will be limited by the vast population of undiagnosed individuals living with HBV. In our analysis of the Oxford RCGP-RSC primary care database, we found increased odds of HBsAg seropositivity, the marker of a current infection, among several well-recognised indicator populations, supporting their continued inclusion in national screening guidance. However, we also found evidence that the screening practices in English primary care may not be optimal. Only 5.4% of those with 1 recorded screening indication, including MSM, those with a history of IDU, close HBV contact or imprisonment, and those with 1 BB/STI diagnosis, had a record of being offered HBsAg screening. It is likely this finding is mirrored internationally. A recent report from the European Centre for Disease Control and Prevention found that only 4 countries in the European region have diagnosed at least 50% of those living with chronic HBV infection[417]. Gauging the success of HBV screening programmes is difficult where data recording about denominators is partial. This limited our analysis of screening and HBsAg seropositivity among people from medium or high HBV endemicity countries for example, a population for whom HBsAg testing is recommended by NICE, as only 4.2% of the 6,975,119 GP records included a recorded country of birth. This unexpected, yet important finding highlights the urgent need for both improved data collection and the improvement of migrant healthcare practices[418]. Socioeconomic deprivation was strongly associated with increased HBsAg seropositivity. The imbalance between primary care resource allocation and healthcare needs has been described since 1971[419]. We provide further evidence that a shift from population-based funding allocation to deprivation weighted allocation would better align with regional differences in healthcare need[420]. Importantly, this finding further provides an indication for targeted HBsAg screening in areas of high socioeconomic deprivation. Finally, among several recorded STIs, we found an independent association between HBsAg seropositivity and a diagnosis of syphilis that provides a clear indication for adopting HBsAg testing in people with such a diagnosis regardless of other recognised risk factors.

Chronic HBV infection often only show signs of disease after people have been living with the infection for decades. The underlying mechanism driving virus control vs. the progressive

development of liver disease is considered primarily immunological and is only partially reflected by the currently available clinical markers. New biomarkers for HBV characterisation and which do not require invasive liver sampling are warranted. sPD-L1 has been posed as a diagnostic marker in certain cancers and as a prognostic marker following anti-cancer immunotherapy. Some of these approaches have been trialled in patients living with HBV[295,296,306] but few studies have systematically evaluated sPD-L1 biology in this context. There is also little consistency in published studies of the measure of sPD-L1. Perhaps providing an insight as to one reason for discrepant findings in the literature, we described largely contrasting findings when two different platforms for sPD-L1 quantification (either Ella or SIMOA) were used, possibly reflecting the detection of different sPD-L1 forms, which per se may reflect different pathogenic pathways. Correlation of sPD-L1 with routine virological parameters varied also by platform; increased sPD-L1 levels by Ella were independently associated with female sex, HBeAg positivity and younger age, while sPD-L1 levels measured with the SIMOA platform were associated with increased ALT levels. One important conclusion from this work is that for sPD-L1 to be a viable biomarker for disease stratification and therapeutic monitoring, detection of sPD-L1 will need to be broadly standardised and validated in diverse populations. The associations found in this study do provide grounds for continued investigation of sPD-L1 in the context of chronic HBV infection. It will be essential for future studies to dissect if different sub-types of sPD-L1 are being detected and if different sub-types of sPD-L1 have different mechanistic characteristics.

It is possible that some forms of sPD-L1 influence T-cell responses via interaction with cell surface expression of PD-1, as demonstrated *in vitro*[293]. This has yet to be demonstrated in HBV infection. Therefore, we characterised the global T-cell compartment with broad phenotypic markers and measured PD-1 expression on lymphocyte subsets. We found that levels of sPD-L1 (measured by SIMOA) showed a moderate positive correlation with levels of expression of PD-1 on $CD4^+$ T-cells. $CD4^+$ T-cells are major orchestrators of cytotoxic $CD8^+$ T-cell responses and B-cell activation and they participate in crosstalk with the innate immune compartment[421]. The current dogma of immune impairment in chronic HBV infection focuses on exhaustion of the effector $CD8^+$ T-cell compartment. We found no evidence of correlations between this compartment and sPD-L1 levels, however. Our findings provide justification for further studies into the role of $CD4^+$ T-cells in HBV pathogenesis.

Our analysis of global PD-1 expression and routine clinical parameters revealed an inverse correlation between PD-1 expressing $CD4^+$ and $CD8^+$ T-cells and circulating platelets. The relationship between lymphocytes expressing PD-1 and platelets has been described previously in other systemic inflammatory conditions and it is suggested this interaction may play an immunosuppressor role[357359]. There is evidence that platelets express PD-L1 and the concentration of PD-L1 positive platelets may be representative of membrane bound PD-L1 expression[422]. One possible mechanism that explains the negative correlation between PD-1 positive lymphocytes and total platelets is ongoing activation of the PD-1 pathway by PD-L1 positive platelets leading to deletion of the PD-1 positive T-cells. Importantly, previous studies have found that PD-L1 positive platelets may be predictive of response to immunotherapy, like sPD-L1[415,416]. Future studies are needed to determine the role of platelets in the PD-1/L1 pathway and immunopathology in chronic HBV infection.

The immune response to HBV is highly dynamic in nature. Advances in cytometry and user-friendly machine learning platforms have allowed for broad and deep characterisation of single cells to provide greater resolution of the peripheral lymphocyte phenotypes. When considering the broad $CD4^+$ T-cell population, we found a positive relationship between PD-1 expression and levels of sPD-L1. However, a deeper understanding of this relationship was required. Therefore, we employed deep immunophenotyping with CyTOF, coupled with novel machine learning algorithms, to detect cell subsets that may be linked to sPD-L1 levels and would not be detected with conventional flow-cytometry. We found that PD-1 expression on $CD8^+CD45_{RA}^+CCR7^-$ $CCR6^+CXCR3^+CD28^-CD57^+CD20^+CD127^-$ T-cells was associated with increased levels of sPD-L1 and increased HBsAg levels in patients with chronic HBV infection. Though we lacked functional assays to characterise the novel phenotype, previous studies suggest that $CD8^+$ T-cells displaying this combination of markers are both highly differentiated and capable of effector function, while also likely heavily exhausted[390,393,402]. A detailed functional characterisation of this novel cell type is warranted. Additionally, identification of this population within T-lymphocytes specific for HBV antigens would be key to understanding their potential role. As previously discussed, the HBV-specific pool of lymphocytes is heterogenous in nature and those with HBsAg specificity are often very low in frequency, potentially due to deletion after continuous activation by HBsAg antigen loads[417].

In summary, within the past decade, there have been substantial strides in development of new therapeutic and potentially curative options for people living with chronic HBV infection. This

thesis aimed to highlight the dual aspect of potential barriers to the implementation and discovery of future curative therapies for people with the infection. It should not be understated that the scale of the HBV epidemic globally is greatly concerning. However, the current framework is inadequate to initiate the required cascade of care, as we have described in a large quasi-representative analysis of primary-care HBV testing data. Clinical characterisation of known people living with HBV is inexact and new, non-invasive, parameters are needed. We evaluated sPD-L1, a novel biomarker that has showed promise in predicting disease outcome and immunotherapeutic monitoring. However, we found large inter-assay variation in detection ranges between two commercially available platforms (Ella and SIMOA). The differences continued in associations with routine biomarkers and in associations with cellular levels of PD-1. The complexity of the immune response to HBV is difficult to define using traditional laboratory and analysis techniques. Utilising deep immunophenotyping and machine learning algorithms, we were able to identify a novel T-cell signature in peripheral blood that was able to predict patients that had high antigen loads or high levels of sPD-L1, depending on the PD-1 expression level of this population. This provides a potential pathway to understanding the immune response without the variability of tetramer staining or liver tissue harvest.

Improvements to the existing framework for HBsAg screening and development of curative therapies also need support from positive social changes. The people currently living with HBV do not have an equal level of advocacy compared to those living with other chronic conditions, yet the stigma associated with HBV is strong and often overlooked[418]. Future programmes are needed to decrease the stigma of those living with HBV, like that of the large-scale multinational studies for HCV and HIV that have made great strides in normalising public opinion[419].

8 References

1. Viruses, I. C. on T. of. *Virus Taxonomy: The classification and nomenclature of viruses: The 9th Report of the ICTV*. https://talk.ictvonline.org/ictv-reports/ictv_9th_report/ (2011).
2. Organization, W. H. Hepatitis B Fact Sheet. Preprint at https://www.who.int/en/news-room/fact-sheets/detail/hepatitis-b (2021).
3. Nayagam, S. *et al.* Requirements for global elimination of hepatitis B: a modelling study. *Lancet Infect Dis* **16**, 1399–1408 (2016).
4. Suh, A., Brosius, J., Schmitz, J. & Kriegs, J. O. The genome of a Mesozoic paleovirus reveals the evolution of hepatitis B viruses. *Nat Commun* **4**, 1791 (2013).
5. Datta, S. Excavating new facts from ancient Hepatitis B virus sequences. *Virology* **549**, 89–99 (2020).
6. Krause-Kyora, B. *et al.* Neolithic and medieval virus genomes reveal complex evolution of hepatitis B. *Elife* **7**, (2018).
7. Sherlock, S. Landmark perspective: Landmarks in viral hepatitis. *JAMA* **252**, 402–406 (1984).
8. Blumberg, B. S. Polymorphisms of the Serum Proteins and the Development of Iso-Precipitins in Transfused Patients. *Bull N Y Acad Med* **40**, 377–386 (1964).
9. Blumberg, B. S., Gerstley, B. J., Hungerford, D. A., London, W. T. & Sutnick, A. I. A serum antigen (Australia antigen) in Down's syndrome, leukemia, and hepatitis. *Ann Intern Med* **66**, 924–931 (1967).
10. Gerlich, W. H. Medical virology of hepatitis B: how it began and where we are now. *Virol J* **10**, 239 (2013).
11. Blumberg, B. S. Australia antigen and the biology of hepatitis B. *Science (1979)* **197**, (1977).
12. Bancroft, W. H., Mundon, F. K. & Russell, P. K. Detection of additional antigenic determinants of hepatitis B antigen. *J Immunol* **109**, 842–848 (1972).
13. Okamoto, H. *et al.* Typing hepatitis B virus by homology in nucleotide sequence: comparison of surface antigen subtypes. *J Gen Virol* **69 (Pt 10)**, 2575–2583 (1988).
14. Araujo, N. M., Teles, S. A. & Spitz, N. Comprehensive Analysis of Clinically Significant Hepatitis B Virus Mutations in Relation to Genotype, Subgenotype and Geographic Region. *Front Microbiol* **11**, 616023 (2020).
15. Torres, C., Fernandez, M. D., Flichman, D. M., Campos, R. H. & Mbayed, V. A. Influence of overlapping genes on the evolution of human hepatitis B virus. *Virology* **441**, 40–48 (2013).
16. Kramvis, A., Kew, M. & Francois, G. Hepatitis B virus genotypes. *Vaccine* **23**, 2409–2423 (2005).
17. Tatematsu, K. *et al.* A genetic variant of hepatitis B virus divergent from known human and ape genotypes isolated from a Japanese patient and provisionally assigned to new genotype J. *J Virol* **83**, 10538–10547 (2009).
18. Yu, H. *et al.* Molecular and phylogenetic analyses suggest an additional hepatitis B virus genotype 'I'. *PLoS One* **5**, e9297 (2010).
19. Liu, Z., Zhang, Y., Xu, M., Li, X. & Zhang, Z. Distribution of hepatitis B virus genotypes and subgenotypes: A meta-analysis. *Medicine (Baltimore)* **100**, e27941 (2021).

20. Andernach, I. E., Nolte, C., Pape, J. W. & Muller, C. P. Slave trade and hepatitis B virus genotypes and subgenotypes in Haiti and Africa. *Emerg Infect Dis* **15**, 1222–1228 (2009).
21. Andernach, I. E., Hubschen, J. M. & Muller, C. P. Hepatitis B virus: the genotype E puzzle. *Rev Med Virol* **19**, 231–240 (2009).
22. Velkov, S., Ott, J. J., Protzer, U. & Michler, T. The global hepatitis B virus genotype distribution approximated from available genotyping data. *Genes (Basel)* **9**, (2018).
23. Organization, W. H. *Global hepatitis report*. https://www.who.int/publications/i/item/9789241565455 (2017).
24. Organization, W. H. *Hepatitis B*. *Fact Sheets* https://www.who.int/news-room/fact-sheets/detail/hepatitis-b (2022).
25. Moed, S. & Zaman, M. H. Towards better diagnostic tools for liver injury in low-income and middle-income countries. *BMJ Glob Health* **4**, e001704 (2019).
26. Stockdale, A. J. *et al.* Diagnostic performance evaluation of hepatitis B e antigen rapid diagnostic tests in Malawi. *BMC Infect Dis* **21**, 487 (2021).
27. Aberra, H. *et al.* The WHO guidelines for chronic hepatitis B fail to detect half of the patients in need of treatment in Ethiopia. *J Hepatol* **70**, 1065–1071 (2019).
28. Brunetto, M. R. *et al.* Hepatitis B surface antigen serum levels help to distinguish active from inactive hepatitis B virus genotype D carriers. *Gastroenterology* **139**, 483–490 (2010).
29. Global Burden of Disease Liver Cancer, C. *et al.* The Burden of Primary Liver Cancer and Underlying Etiologies From 1990 to 2015 at the Global, Regional, and National Level: Results From the Global Burden of Disease Study 2015. *JAMA Oncol* **3**, 1683–1691 (2017).
30. DALYs, G. B. D. & Collaborators, H. Global, regional, and national disability-adjusted life-years (DALYs) for 333 diseases and injuries and healthy life expectancy (HALE) for 195 countries and territories, 1990-2016: a systematic analysis for the Global Burden of Disease Study 2016. *Lancet* **390**, 1260–1344 (2017).
31. Howell, J. *et al.* A global investment framework for the elimination of hepatitis B. *J Hepatol* **74**, (2021).
32. Foundation, H. B. Immigration and International Issues. vol. 2022 https://www.hepb.org/resources-and-support/know-your-rights/immigration-and-international-issues/ (2022).
33. Smith-Palmer, J. *et al.* Impact of Stigma on People Living with Chronic Hepatitis B. *Patient Relat Outcome Meas* **11**, 95–107 (2020).
34. Freeland, C. *et al.* Cure everyone and vaccinate the rest: The patient perspective on future hepatitis B treatment. *J Viral Hepat* **28**, 1539–1544 (2021).
35. Szmuness, W. *et al.* Hepatitis B vaccine: demonstration of efficacy in a controlled clinical trial in a high-risk population in the United States. *N Engl J Med* **303**, (1980).
36. Beasley, R. P. & Hwang, L. Y. Immunogenicity of hepatitis B virus vaccine (Heptavax-B)--response of healthy adults. *West J Med* **140**, 731–734 (1984).
37. Public Health England. Immunisation against infectious disease (the “Green Book”). in *Immunisation against infectious disease (the “Green Book”)* (2017).
38. Keating, G. M. & Noble, S. Recombinant hepatitis B vaccine (Engerix-B): a review of its immunogenicity and protective efficacy against hepatitis B. *Drugs* **63**, 1021–1051 (2003).

39. Lemoine, M., Thursz, M., Njie, R. & Dusheiko, G. Forgotten, not neglected: Viral hepatitis in resource-limited settings, recall for action. *Liver International* **34**, (2014).
40. Wang, C. & Cui, F. Expanded screening for chronic hepatitis B virus infection in China. *Lancet Glob Health* **10**, e171–e172 (2022).
41. Lemoine, M. *et al.* Acceptability and feasibility of a screen-and-treat programme for hepatitis B virus infection in The Gambia: the Prevention of Liver Fibrosis and Cancer in Africa (PROLIFICA) study. *Lancet Glob Health* **4**, e559-67 (2016).
42. World Health Organization. WHO chronic HBV infections (prevalence of HBsAg) dashboard. http://whohbsagdashboard.com/ (2015).
43. Polaris Observatory, C. Global prevalence, treatment, and prevention of hepatitis B virus infection in 2016: a modelling study. *Lancet Gastroenterol Hepatol* **3**, 383–403 (2018).
44. World Health Organization. *Hepatitis B Fact Sheet*. https://www.who.int/en/news-room/fact-sheets/detail/hepatitis-b (2020).
45. Candotti, D., Assennato, S. M., Laperche, S., Allain, J. P. & Levicnik-Stezinar, S. Multiple HBV transfusion transmissions from undetected occult infections: revising the minimal infectious dose. *Gut* **68**, 313–321 (2019).
46. European Association for the Study of the Liver. Electronic address, easloffice easloffice eu & European Association for the Study of the, L. EASL 2017 Clinical Practice Guidelines on the management of hepatitis B virus infection. *J Hepatol* **67**, 370–398 (2017).
47. Nelson, N. P., Jamieson, D. J. & Murphy, T. v. Prevention of Perinatal Hepatitis B Virus Transmission. *J Pediatric Infect Dis Soc* **3 Suppl 1**, S7–S12 (2014).
48. Zhou, Y. H. Evidence against in utero transmission of hepatitis B virus. *Nat Rev Gastroenterol Hepatol* **18**, 445 (2021).
49. Terrault, N. A., Cheung, K. W., Levy, M. T. & Jourdain, G. Reply to 'Evidence against in utero transmission of hepatitis B virus'. *Nat Rev Gastroenterol Hepatol* **18**, 445–446 (2021).
50. Wieland, S., Thimme, R., Purcell, R. H. & Chisari, F. v. Genomic analysis of the host response to hepatitis B virus infection. *Proc Natl Acad Sci U S A* **101**, 6669–6674 (2004).
51. Dunn, C. *et al.* Temporal analysis of early immune responses in patients with acute hepatitis B virus infection. *Gastroenterology* **137**, 1289–1300 (2009).
52. Wang, H. & Ryu, W. S. Hepatitis B virus polymerase blocks pattern recognition receptor signaling via interaction with DDX3: implications for immune evasion. *PLoS Pathog* **6**, e1000986 (2010).
53. Chen, J. *et al.* Hepatitis B virus polymerase impairs interferon-alpha-induced STA T activation through inhibition of importin-alpha5 and protein kinase C-delta. *Hepatology* **57**, 470–482 (2013).
54. Isogawa, M., Robek, M. D., Furuichi, Y. & Chisari, F. v. Toll-like receptor signaling inhibits hepatitis B virus replication in vivo. *J Virol* **79**, 7269–7272 (2005).
55. Ferrari, C. *et al.* Cellular immune response to hepatitis B virus-encoded antigens in acute and chronic hepatitis B virus infection. *J Immunol* **145**, 3442–3449 (1990).
56. Bertoletti, A. & Kennedy, P. T. F. HBV antiviral immunity: not all CD8 T cells are born equal. *Gut* **68**, 770–773 (2019).
57. Webster, G. J. *et al.* Incubation phase of acute hepatitis B in man: dynamic of cellular immune mechanisms. *Hepatology* **32**, 1117–1124 (2000).

58. Kappus, M. R. & Sterling, R. K. Extrahepatic manifestations of acute hepatitis B virus infection. *Gastroenterol Hepatol (N Y)* **9**, 123–126 (2013).
59. McMahon, B. J. *et al.* Acute hepatitis B virus infection: relation of age to the clinical expression of disease and subsequent development of the carrier state. *J Infect Dis* **151**, 599–603 (1985).
60. Wang, C. Y., Zhao, P., Liu, W. W. & Acute Liver Failure Study, T. Acute liver failure caused by severe acute hepatitis B: a case series from a multi-center investigation. *Ann Clin Microbiol Antimicrob* **13**, 23 (2014).
61. Rehermann, B., Ferrari, C., Pasquinelli, C. & Chisari, F. v. The hepatitis B virus persists for decades after patients' recovery from acute viral hepatitis despite active maintenance of a cytotoxic T-lymphocyte response. *Nat Med* **2**, 1104–1108 (1996).
62. Hoofnagle, J. H. Reactivation of hepatitis B. *Hepatology* **49**, S156-65 (2009).
63. Cholongitas, E., Haidich, A. B., Apostolidou-Kiouti, F., Chalevas, P. & Papatheodoridis, G. v. Hepatitis B virus reactivation in HBsAg-negative, anti-HBc-positive patients receiving immunosuppressive therapy: a systematic review. *Ann Gastroenterol* **31**, 480–490 (2018).
64. Zhou, K., Contag, C., Whitaker, E. & Terrault, N. Spontaneous loss of surface antigen among adults living with chronic hepatitis B virus infection: a systematic review and pooled meta-analyses. *Lancet Gastroenterol Hepatol* **4**, 227–238 (2019).
65. Kennedy, P. T. F. *et al.* Preserved T-cell function in children and young adults with immune-tolerant chronic hepatitis B. *Gastroenterology* **143**, 637–645 (2012).
66. Rackaityte, E. & Halkias, J. Mechanisms of Fetal T Cell Tolerance and Immune Regulation. *Front Immunol* **11**, 588 (2020).
67. Zhu, S. *et al.* Antiviral therapy in hepatitis B virus-infected children with immune-tolerant characteristics: A pilot open-label randomized study. *J Hepatol* **68**, 1123–1128 (2018).
68. Bertoletti, A. & Kennedy, P. T. The immune tolerant phase of chronic HBV infection: new perspectives on an old concept. *Cell Mol Immunol* **12**, 258–263 (2015).
69. Maini, M. K. *et al.* The role of virus-specific CD8(+) cells in liver damage and viral control during persistent hepatitis B virus infection. *J Exp Med* **191**, 1269–1280 (2000).
70. Mason, W. S. *et al.* HBV DNA Integration and Clonal Hepatocyte Expansion in Chronic Hepatitis B Patients Considered Immune Tolerant. *Gastroenterology* **151**, 986-998 e4 (2016).
71. Geginat, J., Sallusto, F. & Lanzavecchia, A. Cytokine-driven proliferation and differentiation of human naive, central memory, and effector memory CD4(+) T cells. *J Exp Med* **194**, 1711–1719 (2001).
72. Wang, H. Y. *et al.* Distinct hepatitis B virus dynamics in the immunotolerant and early immunoclearance phases. *J Virol* **84**, 3454–3463 (2010).
73. Kollmann, T. R., Levy, O., Montgomery, R. R. & Goriely, S. Innate immune function by Toll-like receptors: distinct responses in newborns and the elderly. *Immunity* **37**, 771–783 (2012).
74. Phillips, S. *et al.* CD8(+) T cell control of hepatitis B virus replication: direct comparison between cytolytic and noncytolytic functions. *J Immunol* **184**, 287–295 (2010).
75. Sitia, G. *et al.* MMPs are required for recruitment of antigen-nonspecific mononuclear cells into the liver by CTLs. *J Clin Invest* **113**, 1158–1167 (2004).

76. Jeng, W. J., Sheen, I. S. & Liaw, Y. F. Hepatitis B virus DNA level predicts hepatic decompensation in patients with acute exacerbation of chronic hepatitis B. *Clin Gastroenterol Hepatol* **8**, 541–545 (2010).
77. Vanwolleghem, T. *et al.* Re-evaluation of hepatitis B virus clinical phases by systems biology identifies unappreciated roles for the innate immune response and B cells. *Hepatology* **62**, 87–100 (2015).
78. Chen, Y. C., Chu, C. M. & Liaw, Y. F. Age-specific prognosis following spontaneous hepatitis B e antigen seroconversion in chronic hepatitis B. *Hepatology* **51**, 435–444 (2010).
79. Suslov, A. *et al.* Transition to HBeAg-negative chronic hepatitis B virus infection is associated with reduced cccDNA transcriptional activity. *J Hepatol* **74**, 794–800 (2021).
80. Hui, C. K. *et al.* Sustained disease remission after spontaneous HBeAg seroconversion is associated with reduction in fibrosis progression in chronic hepatitis B Chinese patients. *Hepatology* **46**, 690–698 (2007).
81. Zeng, D. W. *et al.* HBeAg-negative chronic hepatitis patients should be monitored more strictly: a cross-sectional retrospective study on antiviral treatment-naive patients. *J Med Virol* **87**, 1682–1688 (2015).
82. Boni, C. *et al.* Characterization of hepatitis B virus (HBV)-specific T-cell dysfunction in chronic HBV infection. *J Virol* **81**, 4215–4225 (2007).
83. Fisicaro, P. *et al.* Pathogenetic Mechanisms of T Cell Dysfunction in Chronic HBV Infection and Related Therapeutic Approaches. *Front Immunol* **11**, 849 (2020).
84. Wenjin, Z., Chuanhui, P., Yunle, W., Lateef, S. A. & Shusen, Z. Longitudinal fluctuations in PD1 and PD-L1 expression in association with changes in anti-viral immune response in chronic hepatitis B. *BMC Gastroenterol* **12**, 109 (2012).
85. Invernizzi, F., Viganò, M., Grossi, G. & Lampertico, P. The prognosis and management of inactive HBV carriers. *Liver International* **36**, 100–104 (2016).
86. Yeo, Y. H. *et al.* Factors Associated With Rates of HBsAg Seroclearance in Adults With Chronic HBV Infection: A Systematic Review and Meta-analysis. *Gastroenterology* **156**, 635-646 e9 (2019).
87. Xiong, S. *et al.* Longitudinal characterization of phenotypic profile of T cells in chronic hepatitis B identifies immune markers associated with HBsAg loss. *EBioMedicine* **69**, 103464 (2021).
88. Liu, Y., Jiang, M., Xue, J., Yan, H. & Liang, X. Serum HBV RNA quantification: useful for monitoring natural history of chronic hepatitis B infection. *BMC Gastroenterol* **19**, 53 (2019).
89. Gozlan, Y. *et al.* HBV-RNA, Quantitative HBsAg, Levels of HBV in Peripheral Lymphocytes and HBV Mutation Profiles in Chronic Hepatitis B. *Viruses* **14**, (2022).
90. Gupta, S., Govindarajan, S., Fong, T. L. & Redeker, A. G. Spontaneous reactivation in chronic hepatitis B: patterns and natural history. *J Clin Gastroenterol* **12**, 562–568 (1990).
91. Loomba, R. & Liang, T. J. Hepatitis B Reactivation Associated With Immune Suppressive and Biological Modifier Therapies: Current Concepts, Management Strategies, and Future Directions. *Gastroenterology* **152**, 1297–1309 (2017).
92. Carman, W. F. *et al.* Mutation preventing formation of hepatitis B e antigen in patients with chronic hepatitis B infection. *Lancet* **2**, 588–591 (1989).

93. Okamoto, H. *et al.* Hepatitis B virus with mutations in the core promoter for an e antigen-negative phenotype in carriers with antibody to e antigen. *J Virol* **68**, 8102–8110 (1994).
94. Wu, J. F., Ni, Y. H., Chen, H. L., Hsu, H. Y. & Chang, M. H. The impact of hepatitis B virus precore/core gene carboxyl terminal mutations on viral biosynthesis and the host immune response. *J Infect Dis* **209**, 1374–1381 (2014).
95. Lok, A. S., Akarca, U. & Greene, S. Mutations in the pre-core region of hepatitis B virus serve to enhance the stability of the secondary structure of the pre-genome encapsidation signal. *Proc Natl Acad Sci U S A* **91**, 4077–4081 (1994).
96. Zeng, G., Gill, U. S. & Kennedy, P. T. F. Prioritisation and the initiation of HCC surveillance in CHB patients: lessons to learn from the COVID-19 crisis. *Gut* **69**, 1907–1912 (2020).
97. Yao, K. *et al.* Distribution and clinical characteristics of patients with chronic hepatitis B virus infection in the grey zone. *J Viral Hepat* **28**, 1025–1033 (2021).
98. Bonacci, M. *et al.* Anti-viral therapy can be delayed or avoided in a significant proportion of HBeAg-negative Caucasian patients in the Grey Zone. *Aliment Pharmacol Ther* **47**, 1397–1408 (2018).
99. Lau, K. C. K., Burak, K. W. & Coffin, C. S. Impact of Hepatitis B Virus Genetic Variation, Integration, and Lymphotropism in Antiviral Treatment and Oncogenesis. *Microorganisms* **8**, (2020).
100. British National Formulary. Hepatitis Treatment Summary. (2022).
101. Udompap, P. & Kim, W. R. Development of Hepatocellular Carcinoma in Patients With Suppressed Viral Replication: Changes in Risk Over Time. *Clin Liver Dis (Hoboken)* **15**, 85–90 (2020).
102. Chen, C. J. *et al.* Risk of hepatocellular carcinoma across a biological gradient of serum hepatitis B virus DNA level. *JAMA* **295**, 65–73 (2006).
103. Howell, J., Chan, H. L. Y., Feld, J. J., Hellard, M. E. & Thompson, A. J. Closing the Stable Door After the Horse Has Bolted: Should We Be Treating People With Immune-Tolerant Chronic Hepatitis B to Prevent Hepatocellular Carcinoma? *Gastroenterology* **158**, 2028–2032 (2020).
104. McNaughton, A. L., Lemoine, M., van Rensburg, C. & Matthews, P. C. Extending treatment eligibility for chronic hepatitis B virus infection. *Nature Reviews Gastroenterology and Hepatology* vol. 18 Preprint at https://doi.org/10.1038/s41575-020-00398-x (2021).
105. Hadziyannis, S. J., Sevastianos, V., Rapti, I., Vassilopoulos, D. & Hadziyannis, E. Sustained responses and loss of HBsAg in HBeAg-negative patients with chronic hepatitis B who stop long-term treatment with adefovir. *Gastroenterology* **143**, 629-636 e1 (2012).
106. Liu, Y. *et al.* Hepatitis B Virus Virions Produced Under Nucleos(t)ide Analogue Treatment Are Mainly Not Infectious Because of Irreversible DNA Chain Termination. *Hepatology* **71**, 463–476 (2020).
107. Maasoumy, B. *et al.* HBV-RNA Co-amplification May Influence HBV DNA Viral Load Determination. *Hepatol Commun* **4**, 983–997 (2020).
108. Wang, J. *et al.* Serum hepatitis B virus RNA is encapsidated pregenome RNA that may be associated with persistence of viral infection and rebound. *J Hepatol* **65**, 700–710 (2016).

109. Tu, T., Budzinska, M. A., Shackel, N. A. & Urban, S. HBV DNA Integration: Molecular Mechanisms and Clinical Implications. *Viruses* **9**, (2017).
110. Lythgoe, K. A., Lumley, S. F., Pellis, L., McKeating, J. A. & Matthews, P. C. Estimating hepatitis B virus cccDNA persistence in chronic infection. *Virus Evol* **7**, (2021).
111. Lok, A. S. *et al.* Durability of Hepatitis B Surface Antigen Loss With Nucleotide Analogue and Peginterferon Therapy in Patients With Chronic Hepatitis B. *Hepatol Commun* **4**, 8–20 (2020).
112. Stadler, D. *et al.* Interferon-induced degradation of the persistent hepatitis B virus cccDNA form depends on ISG20. *EMBO Rep* **22**, e49568 (2021).
113. Perrillo, R. P. *et al.* A randomized, controlled trial of interferon alfa-2b alone and after prednisone withdrawal for the treatment of chronic hepatitis B. The Hepatitis Interventional Therapy Group. *N Engl J Med* **323**, 295–301 (1990).
114. Ye, J. & Chen, J. Interferon and Hepatitis B: Current and Future Perspectives. *Front Immunol* **12**, 733364 (2021).
115. Cossart, Y. E. & Field, A. M. Virus-like particles in serum of patients with Australia-antigen-associated hepatitis. *Lancet* **1**, 848 (1970).
116. Venkatakrishnan, B. & Zlotnick, A. The Structural Biology of Hepatitis B Virus: Form and Function. *Annu Rev Virol* **3**, (2016).
117. Luckenbaugh, L., Kitrinos, K. M., Delaney, W. E. th & Hu, J. Genome-free hepatitis B virion levels in patient sera as a potential marker to monitor response to antiviral therapy. *J Viral Hepat* **22**, 561–570 (2015).
118. Delius, H., Gough, N. M., Cameron, C. H. & Murray, K. Structure of the hepatitis B virus genome. *J Virol* **47**, 337–343 (1983).
119. Hu, J. & Liu, K. Complete and Incomplete Hepatitis B Virus Particles: Formation, Function, and Application. *Viruses* **9**, (2017).
120. Tsukuda, S. & Watashi, K. Hepatitis B virus biology and life cycle. *Antiviral Res* **182**, 104925 (2020).
121. Marchetti, A. L. & Guo, H. New Insights on Molecular Mechanism of Hepatitis B Virus Covalently Closed Circular DNA Formation. *Cells* **9**, (2020).
122. Siddiqui, A., Jameel, S. & Mapoles, J. Transcriptional control elements of hepatitis B surface antigen gene. *Proc Natl Acad Sci U S A* **83**, 566–570 (1986).
123. Bulla, G. A. & Siddiqui, A. Negative regulation of the hepatitis B virus pre-S1 promoter by internal DNA sequences. *Virology* **170**, 251–260 (1989).
124. Golsaz-Shirazi, F. *et al.* Localization of immunodominant epitopes within the “a” determinant of hepatitis B surface antigen using monoclonal antibodies. *Arch Virol* **161**, (2016).
125. Rinker, F. *et al.* Quantitation of large, middle and small hepatitis B surface proteins in HBeAg-positive patients treated with peginterferon alfa-2a. *Liver Int* **40**, 324–332 (2020).
126. Yan, H. *et al.* Sodium taurocholate cotransporting polypeptide is a functional receptor for human hepatitis B and D virus. *Elife* **1**, e00049 (2012).
127. Ni, Y., Sonnabend, J., Seitz, S. & Urban, S. The pre-s2 domain of the hepatitis B virus is dispensable for infectivity but serves a spacer function for L-protein-connected virus assembly. *J Virol* **84**, 3879–3888 (2010).
128. Moolla, N., Kew, M. & Arbuthnot, P. Regulatory elements of hepatitis B virus transcription. *J Viral Hepat* **9**, 323–331 (2002).

129. Nassal, M. The arginine-rich domain of the hepatitis B virus core protein is required for pregenome encapsidation and productive viral positive-strand DNA synthesis but not for virus assembly. *J Virol* **66**, 4107–4116 (1992).
130. Tan, Z. *et al.* The interface between hepatitis B virus capsid proteins affects self-assembly, pregenomic RNA packaging, and reverse transcription. *J Virol* **89**, 3275–3284 (2015).
131. Rabe, B., Vlachou, A., Pante, N., Helenius, A. & Kann, M. Nuclear import of hepatitis B virus capsids and release of the viral genome. *Proc Natl Acad Sci U S A* **100**, 9849–9854 (2003).
132. Lan, Y. T., Li, J., Liao, W. & Ou, J. Roles of the three major phosphorylation sites of hepatitis B virus core protein in viral replication. *Virology* **259**, 342–348 (1999).
133. Lubyova, B. & Weber, J. Posttranslational modifications of HBV core protein. *Acta Virol* **64**, 177–186 (2020).
134. Messageot, F., Salhi, S., Eon, P. & Rossignol, J. M. Proteolytic processing of the hepatitis B virus e antigen precursor. Cleavage at two furin consensus sequences. *J Biol Chem* **278**, 891–895 (2003).
135. Slagle, B. L. & Bouchard, M. J. Role of HBx in hepatitis B virus persistence and its therapeutic implications. *Curr Opin Virol* **30**, 32–38 (2018).
136. Lin, X., Yuan, Z. H., Wu, L., Ding, J. P. & Wen, Y. M. A single amino acid in the reverse transcriptase domain of hepatitis B virus affects virus replication efficiency. *J Virol* **75**, 11827–11833 (2001).
137. McNaughton, A. L. *et al.* Insights From Deep Sequencing of the HBV Genome-Unique, Tiny, and Misunderstood. *Gastroenterology* **156**, 384–399 (2019).
138. Urban, s. New insights into hepatitis B and hepatitis delta virus entry. *Future Medicine* **3**, (2008).
139. Iwamoto, M. *et al.* Epidermal growth factor receptor is a host-entry cofactor triggering hepatitis B virus internalization. *Proc Natl Acad Sci U S A* **116**, 8487–8492 (2019).
140. Herrscher, C. *et al.* Hepatitis B virus entry into HepG2-NTCP cells requires clathrin-mediated endocytosis. *Cell Microbiol* **22**, e13205 (2020).
141. Harrison, S. C. Viral membrane fusion. *Virology* **479–480**, 498–507 (2015).
142. Chojnacki, J., Anderson, D. A. & Grgacic, E. v. A hydrophobic domain in the large envelope protein is essential for fusion of duck hepatitis B virus at the late endosome. *J Virol* **79**, 14945–14955 (2005).
143. Rabe, B., Glebe, D. & Kann, M. Lipid-mediated introduction of hepatitis B virus capsids into nonsusceptible cells allows highly efficient replication and facilitates the study of early infection events. *J Virol* **80**, 5465–5473 (2006).
144. Sodeik, B. Mechanisms of viral transport in the cytoplasm. *Trends Microbiol* **8**, 465–472 (2000).
145. Kann, M., Schmitz, A. & Rabe, B. Intracellular transport of hepatitis B virus. *World J Gastroenterol* **13**, 39–47 (2007).
146. Wei, L. & Ploss, A. Hepatitis B virus cccDNA is formed through distinct repair processes of each strand. *Nat Commun* **12**, 1591 (2021).
147. Yang, W. & Summers, J. Infection of ducklings with virus particles containing linear double-stranded duck hepatitis B virus DNA: illegitimate replication and reversion. *J Virol* **72**, 8710–8717 (1998).

148. Zhao, L. H. *et al.* Genomic and oncogenic preference of HBV integration in hepatocellular carcinoma. *Nat Commun* **7**, 12992 (2016).
149. Edman, J. C., Gray, P., Valenzuela, P., Rall, L. B. & Rutter, W. J. Integration of hepatitis B virus sequences and their expression in a human hepatoma cell. *Nature* **286**, 535–538 (1980).
150. Hong, X., Kim, E. S. & Guo, H. Epigenetic regulation of hepatitis B virus covalently closed circular DNA: Implications for epigenetic therapy against chronic hepatitis B. *Hepatology* **66**, 2066–2077 (2017).
151. Zhang, Y. *et al.* Transcription of hepatitis B virus covalently closed circular DNA is regulated by CpG methylation during chronic infection. *PLoS One* **9**, e110442 (2014).
152. Belloni, L. *et al.* Nuclear HBx binds the HBV minichromosome and modifies the epigenetic regulation of cccDNA function. *Proc Natl Acad Sci U S A* **106**, 19975–19979 (2009).
153. Decorsiere, A. *et al.* Hepatitis B virus X protein identifies the Smc5/6 complex as a host restriction factor. *Nature* **531**, 386–389 (2016).
154. Bartenschlager, R., Junker-Niepmann, M. & Schaller, H. The P gene product of hepatitis B virus is required as a structural component for genomic RNA encapsidation. *J Virol* **64**, 5324–5332 (1990).
155. Bartenschlager, R. & Schaller, H. Hepadnaviral assembly is initiated by polymerase binding to the encapsidation signal in the viral RNA genome. *EMBO J* **11**, 3413–3420 (1992).
156. Pollack, J. R. & Ganem, D. Site-specific RNA binding by a hepatitis B virus reverse transcriptase initiates two distinct reactions: RNA packaging and DNA synthesis. *J Virol* **68**, 5579–5587 (1994).
157. Yao, Y. *et al.* RNA-Binding Motif Protein 24 (RBM24) Is Involved in Pregenomic RNA Packaging by Mediating Interaction between Hepatitis B Virus Polymerase and the Epsilon Element. *J Virol* **93**, (2019).
158. Lanford, R. E., Kim, Y. H., Lee, H., Notvall, L. & Beames, B. Mapping of the hepatitis B virus reverse transcriptase TP and RT domains by transcomplementation for nucleotide priming and by protein-protein interaction. *J Virol* **73**, 1885–1893 (1999).
159. Wang, G. H. & Seeger, C. The reverse transcriptase of hepatitis B virus acts as a protein primer for viral DNA synthesis. *Cell* **71**, 663–670 (1992).
160. Watanabe, T. *et al.* Involvement of host cellular multivesicular body functions in hepatitis B virus budding. *Proc Natl Acad Sci U S A* **104**, 10205–10210 (2007).
161. Tuttleman, J. S., Pourcel, C. & Summers, J. Formation of the pool of covalently closed circular viral DNA in hepadnavirus-infected cells. *Cell* **47**, 451–460 (1986).
162. Kock, J. *et al.* Generation of covalently closed circular DNA of hepatitis B viruses via intracellular recycling is regulated in a virus specific manner. *PLoS Pathog* **6**, e1001082 (2010).
163. Bai, L. *et al.* Extracellular Hepatitis B Virus RNAs Are Heterogeneous in Length and Circulate as Capsid-Antibody Complexes in Addition to Virions in Chronic Hepatitis B Patients. *J Virol* **92**, (2018).
164. Shen, S. *et al.* Biogenesis and molecular characteristics of serum hepatitis B virus RNA. *PLoS Pathog* **16**, e1008945 (2020).
165. Prakash, K. *et al.* High serum levels of pregenomic RNA reflect frequently failing reverse transcription in hepatitis B virus particles. *Virol J* **15**, 86 (2018).

166. Liu, S., Zhou, B., Valdes, J. D., Sun, J. & Guo, H. Serum Hepatitis B Virus RNA: A New Potential Biomarker for Chronic Hepatitis B Virus Infection. *Hepatology* **69**, 1816–1827 (2019).
167. Wieczorek, M. *et al.* Major Histocompatibility Complex (MHC) Class I and MHC Class II Proteins: Conformational Plasticity in Antigen Presentation. *Front Immunol* **8**, (2017).
168. Neefjes, J., Jongsma, M. L. M., Paul, P. & Bakke, O. Towards a systems understanding of MHC class I and MHC class II antigen presentation. *Nat Rev Immunol* **11**, 823–836 (2011).
169. Münz, C. Antigen Processing for MHC Class II Presentation via Autophagy. *Front Immunol* **3**, (2012).
170. Sauer, R. T. & Baker, T. A. AAA+ proteases: ATP-fueled machines of protein destruction. *Annu Rev Biochem* **80**, 587–612 (2011).
171. Mak, T. W. & Saunders, M. E. *The immune response*. vol. 1 (Academic Press, 2006).
172. Zak, K. M. *et al.* Structural Biology of the Immune Checkpoint Receptor PD-1 and Its Ligands PD-L1/PD-L2. *Structure* **25**, 1163–1174 (2017).
173. Hoogeveen, R. C. & Boonstra, A. Checkpoint Inhibitors and Therapeutic Vaccines for the Treatment of Chronic HBV Infection. *Front Immunol* **11**, 401 (2020).
174. Cosman, D. *et al.* ULBPs, novel MHC class I-related molecules, bind to CMV glycoprotein UL16 and stimulate NK cytotoxicity through the NKG2D receptor. *Immunity* **14**, 123–33 (2001).
175. Jiang, J., Natarajan, K. & Margulies, D. H. MHC Molecules, T cell Receptors, Natural Killer Cell Receptors, and Viral Immunoevasins-Key Elements of Adaptive and Innate Immunity. *Adv Exp Med Biol* **1172**, 21–62 (2019).
176. Kaufmann, S. H. E. & Parida, S. K. Tuberculosis in Africa: Learning from Pathogenesis for Biomarker Identification. *Cell Host Microbe* **4**, 219–228 (2008).
177. Zheng, M. & Tian, Z. Liver-Mediated Adaptive Immune Tolerance. *Front Immunol* **10**, 2525 (2019).
178. Osei-Bordom, D., Bozward, A. G. & Oo, Y. H. The hepatic microenvironment and regulatory T cells. *Cell Immunol* **357**, 104195 (2020).
179. Mueller, S. N. & Ahmed, R. High antigen levels are the cause of T cell exhaustion during chronic viral infection. *Proc Natl Acad Sci U S A* **106**, 8623–8628 (2009).
180. Wherry, E. J., Blattman, J. N., Murali-Krishna, K., van der Most, R. & Ahmed, R. Viral persistence alters CD8 T-cell immunodominance and tissue distribution and results in distinct stages of functional impairment. *J Virol* **77**, 4911–4927 (2003).
181. Zajac, A. J. *et al.* Viral immune evasion due to persistence of activated T cells without effector function. *J Exp Med* **188**, 2205–2213 (1998).
182. Fuller, M. J. *et al.* Cutting edge: emergence of CD127high functionally competent memory T cells is compromised by high viral loads and inadequate T cell help. *J Immunol* **174**, 5926–5930 (2005).
183. Lodolce, J. P. *et al.* IL-15 receptor maintains lymphoid homeostasis by supporting lymphocyte homing and proliferation. *Immunity* **9**, 669–676 (1998).
184. Wherry, E. J., Barber, D. L., Kaech, S. M., Blattman, J. N. & Ahmed, R. Antigen-independent memory CD8 T cells do not develop during chronic viral infection. *Proc Natl Acad Sci U S A* **101**, 16004–16009 (2004).
185. Schurich, A. *et al.* Distinct Metabolic Requirements of Exhausted and Functional Virus-Specific CD8 T Cells in the Same Host. *Cell Rep* **16**, 1243–1252 (2016).

186. Fan, R. *et al.* T-bet expression in CD8+ T cells associated with chronic hepatitis B virus infection. *Virol J* **13**, 14 (2016).
187. Schuch, A. *et al.* Phenotypic and functional differences of HBV core-specific versus HBV polymerase-specific CD8+ T cells in chronically HBV-infected patients with low viral load. *Gut* **68**, 905–915 (2019).
188. Wang, Y. *et al.* The Transcription Factor TCF1 Preserves the Effector Function of Exhausted CD8 T Cells During Chronic Viral Infection. *Front Immunol* **10**, 169 (2019).
189. Heim, K. *et al.* TOX defines the degree of CD8+ T cell dysfunction in distinct phases of chronic HBV infection. *Gut* (2020) doi:10.1136/gutjnl-2020-322404.
190. Peppa, D. *et al.* Up-regulation of a death receptor renders antiviral T cells susceptible to NK cell-mediated deletion. *J Exp Med* **210**, 99–114 (2013).
191. Lenardo, M. J. Fas and the art of lymphocyte maintenance. *J Exp Med* **183**, 721–724 (1996).
192. Green, D. R. Fas Bim boom! *Immunity* **28**, 141–143 (2008).
193. Yoo, Y. G. & Lee, M. O. Hepatitis B virus X protein induces expression of Fas ligand gene through enhancing transcriptional activity of early growth response factor. *J Biol Chem* **279**, 36242–36249 (2004).
194. Wieland, D. *et al.* TCF1(+) hepatitis C virus-specific CD8(+) T cells are maintained after cessation of chronic antigen stimulation. *Nat Commun* **8**, 15050 (2017).
195. Acuto, O. & Michel, F. CD28-mediated co-stimulation: a quantitative support for TCR signalling. *Nat Rev Immunol* **3**, 939–951 (2003).
196. Gamez-Diaz, L. & Grimbacher, B. Immune checkpoint deficiencies and autoimmune lymphoproliferative syndromes. *Biomed J* **44**, 400–411 (2021).
197. Diniz, M. O. *et al.* NK cells limit therapeutic vaccine-induced CD8(+)T cell immunity in a PD-L1-dependent manner. *Sci Transl Med* **14**, eabi4670 (2022).
198. Ishida, Y., Agata, Y., Shibahara, K. & Honjo, T. Induced expression of PD-1, a novel member of the immunoglobulin gene superfamily, upon programmed cell death. *EMBO J* **11**, 3887–3895 (1992).
199. Agata, Y. *et al.* Expression of the PD-1 antigen on the surface of stimulated mouse T and B lymphocytes. *Int Immunol* **8**, 765–772 (1996).
200. Bally, A. P. R. *et al.* PD-1 Expression during Acute Infection Is Repressed through an LSD1-Blimp-1 Axis. *J Immunol* **204**, 449–458 (2020).
201. Sheppard, K. A. *et al.* PD-1 inhibits T-cell receptor induced phosphorylation of the ZAP70/CD3zeta signalosome and downstream signaling to PKCtheta. *FEBS Lett* **574**, 37–41 (2004).
202. Sharpe, A. H. & Pauken, K. E. The diverse functions of the PD1 inhibitory pathway. *Nat Rev Immunol* **18**, 153–167 (2018).
203. Thibult, M. L. *et al.* PD-1 is a novel regulator of human B-cell activation. *Int Immunol* **25**, 129–137 (2013).
204. Vari, F. *et al.* Immune evasion via PD-1/PD-L1 on NK cells and monocyte/macrophages is more prominent in Hodgkin lymphoma than DLBCL. *Blood* **131**, 1809–1819 (2018).
205. Li, M. *et al.* HBcAg induces PD-1 upregulation on CD4+T cells through activation of JNK, ERK and PI3K/AKT pathways in chronic hepatitis-B-infected patients. *Lab Invest* **92**, 295–304 (2012).
206. Tzeng, H. T. *et al.* PD-1 blockage reverses immune dysfunction and hepatitis B viral persistence in a mouse animal model. *PLoS One* **7**, e39179 (2012).

207. Sun, Y. *et al.* Hepatitis B virus-triggered PTEN/beta-catenin/c-Myc signaling enhances PD-L1 expression to promote immune evasion. *Am J Physiol Gastrointest Liver Physiol* **318**, G162–G173 (2020).
208. Bailly, C., Thuru, X. & Quesnel, B. Soluble Programmed Death Ligand-1 (sPD-L1): A Pool of Circulating Proteins Implicated in Health and Diseases. *Cancers (Basel)* **13**, (2021).
209. Niu, M., Liu, Y., Yi, M., Jiao, D. & Wu, K. Biological Characteristics and Clinical Significance of Soluble PD-1/PD-L1 and Exosomal PD-L1 in Cancer. *Front Immunol* **13**, 827921 (2022).
210. Frigola, X. *et al.* Soluble B7-H1: differences in production between dendritic cells and T cells. *Immunol Lett* **142**, 78–82 (2012).
211. Khan, M., Zhao, Z., Arooj, S., Fu, Y. & Liao, G. Soluble PD-1: Predictive, Prognostic, and Therapeutic Value for Cancer Immunotherapy. *Front Immunol* **11**, 587460 (2020).
212. Mahoney, K. M. *et al.* Soluble PD-L1 as an early marker of progressive disease on nivolumab. *J Immunother Cancer* **10**, (2022).
213. Gill, U. S., Pallett, L. J., Kennedy, P. T. F. & Maini, M. K. Liver sampling: a vital window into HBV pathogenesis on the path to functional cure. *Gut* **67**, 767–775 (2018).
214. Khakpoor, A. *et al.* Spatiotemporal Differences in Presentation of CD8 T Cell Epitopes during Hepatitis B Virus Infection. *J Virol* **93**, (2019).
215. Hoogeveen, R. C. *et al.* Phenotype and function of HBV-specific T cells is determined by the targeted epitope in addition to the stage of infection. *Gut* **68**, 893–904 (2019).
216. Cao, K. *et al.* Differentiation between African populations is evidenced by the diversity of alleles and haplotypes of HLA class I loci. *Tissue Antigens* **63**, 293–325 (2004).
217. Ellis, J. M. *et al.* Frequencies of HLA-A2 alleles in five U.S. population groups. Predominance Of A*02011 and identification of HLA-A*0231. *Hum Immunol* **61**, 334–340 (2000).
218. Heim, K., Hensel, N., Hofmann, M. & Thimme, R. Tetramer enrichment for HBV-specific CD8+ T-cells. *International Coalition to Eliminate HBV* (2020).
219. Chen, L. & Han, X. Anti-PD-1/PD-L1 therapy of human cancer: past, present, and future. *J Clin Invest* **125**, 3384–3391 (2015).
220. Gane, E. *et al.* Anti-PD-1 blockade with nivolumab with and without therapeutic vaccination for virally suppressed chronic hepatitis B: A pilot study. *J Hepatol* **71**, 900–907 (2019).
221. ClinicalTrials.gov. A Phase II Study of Subcutaneously Injected PD-L1 Antibody ASC22 in Chronic Hepatitis B Patients - NCT04465890. Preprint at (2020).
222. McPherson, K. A. *et al.* Person-centred language and HIV research: a cross-sectional examination of stigmatising terminology in medical literature. *Sex Transm Infect* (2022) doi:10.1136/sextrans-2021-055391.
223. NHS Digital. Read Codes: Terminology and Classification. *https://digital.nhs.uk/services/terminology-and-classifications/read-codes*.
224. Department for Communities and Local Government. *The English Index of Multiple Deprivation (IMD) 2015 – Guidance*. https://assets.publishing.service.gov.uk/government/uploads/system/uploads/attachment_data/file/464430/English_Index_of_Multiple_Deprivation_2015_-_Guidance.pdf (2015).

225. Office for National Statistics. Local Authority Districts (December 2016) Names and Codes in the United Kingdom. Preprint at https://data.gov.uk/dataset/9b9e026f-02e7-4481-ab2b-cf19e3b9ea61/local-authority-districts-december-2016-names-and-codes-in-the-united-kingdom (2016).
226. Office for National Statistics. *Local Authority Districts (December 2017) Full Clipped Boundaries in Great Britain*. https://geoportal.statistics.gov.uk/datasets/ae90afc385c04d869bc8cf8890bd1bcd_1/explore (2017).
227. National Institutes for Care and Health Excellence. *Hepatitis B and C testing: people at risk of infection*. https://www.nice.org.uk/guidance/ph43 (2013).
228. Liyanage, H., Williams, J., Byford, R. & de Lusignan, S. Ontology to identify pregnant women in electronic health records: primary care sentinel network database study. *BMJ Health Care Inform* **26**, (2019).
229. Bagwell, C. B. *et al.* Multi-site reproducibility of a human immunophenotyping assay in whole blood and peripheral blood mononuclear cells preparations using CyTOF technology coupled with Maxpar Pathsetter, an automated data analysis system. *Cytometry B Clin Cytom* **98**, 146–160 (2020).
230. Fluidigm. *Approach to Bivariate Analysis of Data Acquired Using the Maxpar Direct Immune Profiling Assay*. https://www.imc.unibe.ch/unibe/portal/fak_medizin/micro_imc/content/e987276/e1010628/ApproachtoBivariateAnalysis_TechnicalNote400248B1.pdf (2019).
231. Kimball, A. K. *et al.* A Beginner's Guide to Analyzing and Visualizing Mass Cytometry Data. *J Immunol* **200**, 3–22 (2018).
232. van Bommel, F. *et al.* Serum hepatitis B virus RNA levels as an early predictor of hepatitis B envelope antigen seroconversion during treatment with polymerase inhibitors. *Hepatology* **61**, 66–76 (2015).
233. World Health Organization. Hepatitis B Fact Sheet. Preprint at https://www.who.int/en/news-room/fact-sheets/detail/hepatitis-b (2021).
234. Polaris Observatory, C. Global prevalence, treatment, and prevention of hepatitis B virus infection in 2016: a modelling study. *Lancet Gastroenterology and Hepatology* **3**, 383–403 (2018).
235. Nayagam, S. *et al.* Requirements for global elimination of hepatitis B: a modelling study. *Lancet Infectious Diseases* **16**, 1399–1408 (2016).
236. World Health Organization. *COMBATING HEPATITIS B AND C TO REACH ELIMINATION BY 2030 MAY 2016 ADVOCACY BRIEF*.
237. Public Health England. *Acute Hepatitis B (England): annual report for 2018*. *Health Protection Report* vol. 13 https://assets.publishing.service.gov.uk/government/uploads/system/uploads/attachment_data/file/877344/hpr3019_ct-hbv18_V3.pdf (2018).
238. Health Protection Agency. *Migrant Health: Infectious diseases in non-UK born populations in the UK*. (2011).
239. Burton, A. *et al.* The landscape of hepatocellular carcinoma in the UK in the past 20 years: the HCCUK/NCRAS partnership. *NCRI Cancer Conference* Preprint at (2019).
240. Public Health England. *Guidance on the hepatitis B antenatal screening and selective neonatal immunisation pathway*. https://www.gov.uk/government/publications/hepatitis-b-antenatal-screening-and-

selective-neonatal-immunisation-pathway/guidance-on-the-hepatitis-b-antenatal-screening-and-selective-neonatal-immunisation-pathway--2 (2021).
241. Public Health England. *Annual report from the sentinel surveillance of blood borne virus testing in England 2019*. *Health Protection Report* vol. 15 https://assets.publishing.service.gov.uk/government/uploads/system/uploads/attachment_data/file/954334/hpr0221_sentBBV_main-report_v2.pdf (2021).
242. RCGP Research and Surveillane Centre (RSC). *https://www.rcgp.org.uk/clinical-and-research/our-programmes/research-and-surveillance-centre.aspx*.
243. Public Health England. *Annual report from the sentinel surveillance study of blood borne virus testing in England: data for January to December 2018*. *Health Protection Report* vol. 10 (2020).
244. National Health Service. Form GMS1. https://www.gov.uk/government/publications/gms1 (2019).
245. Ciftci, Y. & Blane, D. N. Improving GP registration and access for migrant health. *British Journal of General Practice* **72**, 56–57 (2022).
246. Allsopp Sigona N. Phillimore J., J. Poverty among refugees and asylum seekers in the UK: An evidence and policy review. *IRiS Working Paper Series* **1/2014**, (2014).
247. Aghaizu, A. *et al.* HIV in the UK 2016 report. (2016).
248. Public Health England. *Hepatitis C in London: 2019 report*. (2019).
249. Nyblade, L. *et al.* Stigma in health facilities: why it matters and how we can change it. *BMC Med* **17**, 25 (2019).
250. Evlampidou, I. *et al.* Low hepatitis B testing among migrants: a cross-sectional study in a UK city. *British Journal of General Practice* **66**, e382-91 (2016).
251. Bielen, R. *et al.* Assessing testing rates for viral hepatitis B and C by general practitioners in Flanders, Belgium: a registry-based study. *BMJ Open* **9**, e026464 (2019).
252. Correa, A. *et al.* Royal College of General Practitioners Research and Surveillance Centre (RCGP RSC) sentinel network: a cohort profile. *BMJ Open* **6**, e011092 (2016).
253. Bechini, A. *et al.* The role of the general practitioner in the screening and clinical management of chronic viral hepatitis in six EU countries. *Journal of Preventative Medicine & Hygeine* **57**, E51-60 (2016).
254. Evlampidou, I. *et al.* Low hepatitis B testing among migrants: A cross-sectional study in a UK city. *British Journal of General Practice* **66**, e382–e391 (2016).
255. Sweeney, L. *et al.* Informing the design of a national screening and treatment programme for chronic viral hepatitis in primary care: qualitative study of at-risk immigrant communities and healthcare professionals. *BMC Health Serv Res* **15**, 97 (2015).
256. Roche, R. *et al.* What do primary care staff know and do about blood borne virus testing and care for migrant patients? A national survey. *BMC Public Health* **21**, 336 (2021).
257. Richmond, J. A., Sasadeusz, J. & Temple-Smith, M. The Role of Primary Health Care in Hepatitis B Testing and Management: A Case Study. *J Community Health* **43**, 38–47 (2018).
258. British Association for Sexual Health and HIV (BASHH). *2017 interim update of the 2015 BASHH National Guidelines for the Management of the Viral Hepatitides*. https://www.bashhguidelines.org/media/1161/viral-hepatitides-2017-update-18-12-17.pdf (2017).

259. Clutterbuck, D. *et al.* 2016 United Kingdom national guideline on the sexual health care of men who have sex with men. *Int J STD AIDS* 956462417746897 (2018) doi:10.1177/0956462417746897.
260. National Institutes for Health and Care Excellence. *Introducing a blood borne virus testing facility within a substance misuse harm reduction service*. (2014).
261. House of Commons. *Prison Health*. https://publications.parliament.uk/pa/cm201719/cmselect/cmhealth/963/963.pdf (2018).
262. Brooks, H. *et al.* Sexual orientation disclosure in health care: a systematic review. *British Journal of General Practice* **68**, e187–e196 (2018).
263. Price, H., Salimee, S. & Coelho, D. Prevalence of hepatitis B and hepatitis C in a UK genitourinary medicine clinic. *Int J STD AIDS* **28**, 238–241 (2017).
264. European Center for Disease Control. *Systematic review on hepatitis B and C prevalence in the EU/EEA*. https://www.ecdc.europa.eu/sites/default/files/media/en/publications/Publications/systematic-review-hepatitis-B-C-prevalence.pdf (2015).
265. Public Health England. *Shooting Up: infections among people who inject drugs in the UK*. https://www.gov.uk/government/publications/shooting-up-infections-among-people-who-inject-drugs-in-the-uk (2018).
266. Public Health England. *Annual Report from the sentinel surveillance of blood borne virus testing in England: data for January to December 2018*. *Health Protection Report* https://assets.publishing.service.gov.uk/government/uploads/system/uploads/attachment_data/file/857311/hpr0120_SNTNL-BBVs.pdf (2020).
267. NICE. Hepatitis B and C testing: people at risk of infection. Preprint at https://www.nice.org.uk/guidance/ph43 (2013).
268. Bielen, R. *et al.* Assessing testing rates for viral hepatitis B and C by general practitioners in Flanders, Belgium: a registry-based study. *BMJ Open* **9**, e026464 (2019).
269. Marseille, E. *et al.* Hepatitis B prevalence association with sexually transmitted infections: a systematic review and meta-analysis. *Sex Health* **18**, 269–279 (2021).
270. Xiao, Y. *et al.* Factors associated with syphilis infection: a comprehensive analysis based on a case-control study. *Epidemiol Infect* **144**, 1165–1174 (2016).
271. Marseille, E. *et al.* Hepatitis B prevalence association with sexually transmitted infections: a systematic review and meta-analysis. *Journal of Sexual Health* **18**, 269–279 (2021).
272. Public Health England. *Tracking the syphilis epidemic in England: 2010 to 2019*. https://assets.publishing.service.gov.uk/government/uploads/system/uploads/attachment_data/file/956716/Syphilis_Action_Plan_Metrics_2010_to_2019_report.pdf (2021).
273. Department for Communities and Local Governments. English indices of deprivation 2015 - GOV.UK. https://www.gov.uk/government/statistics/english-indices-of-deprivation-2015 (2015).
274. Public Health England. *Liver disease profiles: statistical commentary, April 2018*. https://www.gov.uk/government/statistics/liver-disease-profiles-april-2018-update/liver-disease-profiles-statistical-commentary-april-2018 (2018).

275. Martin, N. K. *et al.* Chronic hepatitis B virus case-finding in UK populations born abroad in intermediate or high endemicity countries: an economic evaluation. *BMJ Open* **9**, e030183 (2019).
276. Mohammed, M. S., Ferrier, G., Abouda, G. & Corless, L. Socio-economic deprivation significantly impacts clinical management and survival in hepatocellular carcinoma. *J Hepatol* **68**, 623–625 (2018).
277. Curran, C., Stanley, A. J., Barclay, S. T., Priest, M. & Graham, J. The association between deprivation and the incidence and survival of patients with hepatocellular carcinoma in the West of Scotland. *Expert Reviews in Gastroenterology and Hepatology* **15**, 1427–1433 (2021).
278. Public Health England. *Quarterly vaccination coverage statistics for children aged up to five years in the UK (COVER programme): January to March 2019*. *Health Protection Report* https://assets.publishing.service.gov.uk/government/uploads/system/uploads/attachment_data/file/812968/hpr2219_COVER.pdf (2019).
279. Keeble, S., Quested, J., Barker, D., Varadarajan, A. & Shankar, A. G. Immunization of babies born to HBsAg positive mothers: An audit on the delivery and completeness of follow up in Norfolk and Suffolk, United Kingdom. *Human Vaccines and Immunotherapy* **11**, 1153–1156 (2015).
280. British Association for Sexual Health and HIV. *BASHH Clinical Efffectiveness Group guidance on tests for Sexually Transmitted Infections*. (2015).
281. Organization, W. H. *Global Health Sector Strategy on Viral Hepatitis*. *Toward Ending Viral Hepatitis* https://apps.who.int/iris/bitstream/handle/10665/246177/who?sequence=1 (2016).
282. Organization, W. H. *Hepatitis C Fact Sheet*. https://www.who.int/news-room/fact-sheets/detail/hepatitis-c (2022).
283. Falade-Nwulia, O. *et al.* Oral Direct-Acting Agent Therapy for Hepatitis C Virus Infection: A Systematic Review. *Ann Intern Med* **166**, 637–648 (2017).
284. Tan, M. *et al.* Estimating the proportion of people with chronic hepatitis B virus infection eligible for hepatitis B antiviral treatment worldwide: a systematic review and meta-analysis. *Lancet Gastroenterol Hepatol* **6**, 106–119 (2021).
285. Lim, S. G., Agcaoili, J., de Souza, N. N. A. & Chan, E. Therapeutic vaccination for chronic hepatitis B: A systematic review and meta-analysis. *J Viral Hepat* **26**, 803–817 (2019).
286. Hu, J., Protzer, U. & Siddiqui, A. Revisiting Hepatitis B Virus: Challenges of Curative Therapies. *J Virol* **93**, (2019).
287. Fisicaro, P. *et al.* Early kinetics of innate and adaptive immune responses during hepatitis B virus infection. *Gut* **58**, 974–982 (2009).
288. Maini, M. K. *et al.* Direct ex vivo analysis of hepatitis B virus-specific CD8(+) T cells associated with the control of infection. *Gastroenterology* **117**, 1386–1396 (1999).
289. Bertoletti, A. & Gehring, A. J. The immune response during hepatitis B virus infection. *J Gen Virol* **87**, 1439–1449 (2006).
290. Ferrando-Martinez, S. *et al.* Functional Exhaustion of HBV-Specific CD8 T Cells Impedes PD-L1 Blockade Efficacy in Chronic HBV Infection. *Front Immunol* **12**, 648420 (2021).

291. Wang Cui Yimin. Xie Yao et al., Guiqiang. NUCLEOS(T)IDE ANALOGS TREATMENT: INTERIM RESULTS FROM A PHASE IIb CLINICAL TRIAL. *The Liver Meeting* Preprint at (2021).
292. Geretti, A. M. *et al.* LIVER-DIRECTED TARGETING OF PD-L1 WITH RO7191863, A LOCKED NUCLEIC ACID, IN CHRONIC HEPATITIS B: FIRST REPORT OF PHASE 1 TOLERABILITY, PHARMACOKINETICS, AND PHARMACODYNAMICS. *The Liver Meeting* Preprint at https://www.natap.org/2021/AASLD/AASLD_153.htm (2021).
293. Bailly, C., Thuru, X. & Quesnel, B. Soluble Programmed Death Ligand-1 (sPD-L1): A Pool of Circulating Proteins Implicated in Health and Diseases. *Cancers (Basel)* **13**, (2021).
294. Xie, F., Xu, M., Lu, J., Mao, L. & Wang, S. The role of exosomal PD-L1 in tumor progression and immunotherapy. *Mol Cancer* **18**, 146 (2019).
295. Mahoney, K. M. *et al.* A secreted PD-L1 splice variant that covalently dimerizes and mediates immunosuppression. *Cancer Immunol Immunother* **68**, 421–432 (2019).
296. Han, B. *et al.* The clinical implication of soluble PD-L1 (sPD-L1) in patients with breast cancer and its biological function in regulating the function of T lymphocyte. *Cancer Immunol Immunother* **70**, 2893–2909 (2021).
297. Udall, M. *et al.* PD-L1 diagnostic tests: a systematic literature review of scoring algorithms and test-validation metrics. *Diagn Pathol* **13**, 12 (2018).
298. Neuberger, J. *et al.* Guidelines on the use of liver biopsy in clinical practice from the British Society of Gastroenterology, the Royal College of Radiologists and the Royal College of Pathology. *Gut* **69**, 1382–1403 (2020).
299. Chen, Y. *et al.* Development of a sandwich ELISA for evaluating soluble PD-L1 (CD274) in human sera of different ages as well as supernatants of PD-L1+ cell lines. *Cytokine* **56**, 231–238 (2011).
300. Buderath, P. *et al.* Soluble Programmed Death Receptor Ligands sPD-L1 and sPD-L2 as Liquid Biopsy Markers for Prognosis and Platinum Response in Epithelial Ovarian Cancer. *Front Oncol* **9**, 1015 (2019).
301. Yang, J. *et al.* Plasma levels of soluble programmed death ligand 1 (sPD-L1) in WHO II/III nasopharyngeal carcinoma (NPC): A preliminary study. *Medicine (Baltimore)* **98**, e17231 (2019).
302. Finkelmeier, F. *et al.* High levels of the soluble programmed death-ligand (sPD-L1) identify hepatocellular carcinoma patients with a poor prognosis. *Eur J Cancer* **59**, 152–159 (2016).
303. Zhu, X. & Lang, J. Soluble PD-1 and PD-L1: predictive and prognostic significance in cancer. *Oncotarget* **8**, 97671–97682 (2017).
304. Mocan, T. *et al.* Serum levels of soluble programmed death-ligand 1 (sPD-L1): A possible biomarker in predicting post-treatment outcomes in patients with early hepatocellular carcinoma. *Int Immunopharmacol* **94**, 107467 (2021).
305. Leon-Flores, A., del Rio Estrada, P. M., Alvarez-Garcia, L. X., Piten-Isidro, E. & Reyes-Teran, G. Increased levels of soluble co-stimulatory molecule PD-L1 (B7-H1) in the plasma of viraemic HIV-1(+) individuals. *Immunol Lett* **203**, 70–79 (2018).
306. Planes, R. *et al.* HIV-1 Tat protein induces PD-L1 (B7-H1) expression on dendritic cells through tumor necrosis factor alpha- and toll-like receptor 4-mediated mechanisms. *J Virol* **88**, 6672–6689 (2014).
307. Avendano-Ortiz, J. *et al.* Soluble PD-L1: a potential immune marker for HIV-1 infection and virological failure. *Medicine (Baltimore)* **99**, e20065 (2020).

308. Yamagiwa, S. *et al.* Increase of Soluble Programmed Cell Death Ligand 1 in Patients with Chronic Hepatitis C. *Int J Med Sci* **14**, 403–411 (2017).
309. Xuan Hoan, N. *et al.* Association of PD-L1 gene polymorphisms and circulating sPD-L1 levels with HBV infection susceptibility and related liver disease progression. *Gene* **806**, 145935 (2022).
310. RM, K. *et al.* Serum Soluble Programmed Death Ligand 1 is Correlated with HBsAg Level and Nucleos(t)ide Analogue Therapy in Chronic Hepatitis B. *Japanese Journal of Gastroenterology and Hepatology* **6**, (2021).
311. Xia, J. *et al.* Profiles of serum soluble programmed death-1 and programmed death-ligand 1 levels in chronic hepatitis B virus-infected patients with different disease phases and after anti-viral treatment. *Aliment Pharmacol Ther* **51**, 1180–1187 (2020).
312. Bio-techne. Human PD-L1/B7-H1 Antibody Product Datasheet. vol. 2022 https://www.bio-techne.com/p/antibodies/human-pd-l1-b7-h1-antibody-2340d_mab1562 (2022).
313. Rissin, D. M. *et al.* Single-molecule enzyme-linked immunosorbent assay detects serum proteins at subfemtomolar concentrations. *Nat Biotechnol* **28**, 595–599 (2010).
314. Li, J. W. *et al.* Clinical significance of circulating exosomal PD-L1 and soluble PD-L1 in extranodal NK/T-cell lymphoma, nasal-type. *Am J Cancer Res* **10**, 4498–4512 (2020).
315. Bio-techne. Human PD-L1/B7-H1 antibody.
316. R&D systems. *Simple Plex assay for the detection of human B7-H1/PD-L1 in serum and plasma (EDTA/Heparin)*. (2017).
317. Quanterix. Simoa PD-L1 Discovery Kit. vol. 2022 https://www.quanterix.com/wp-content/uploads/2020/12/PD-L1-SR-X-Data-Sheet.pdf (2017).
318. Zhou, J. *et al.* Soluble PD-L1 as a Biomarker in Malignant Melanoma Treated with Checkpoint Blockade. *Cancer Immunol Res* **5**, 480–492 (2017).
319. Kim, H. J., Park, S., Kim, K. J. & Seong, J. Clinical significance of soluble programmed cell death ligand-1 (sPD-L1) in hepatocellular carcinoma patients treated with radiotherapy. *Radiother Oncol* **129**, 130–135 (2018).
320. Wang, L. *et al.* Serum levels of soluble programmed death ligand 1 predict treatment response and progression free survival in multiple myeloma. *Oncotarget* **6**, 41228–41236 (2015).
321. Food and Drug Administration. *List of Cleared or Approved Companion Diagnostic Devices (In Vitro and Imaging Tools)*. (2022).
322. Kramvis, A., Kostaki, E. G., Hatzakis, A. & Paraskevis, D. Immunomodulatory Function of HBeAg Related to Short-Sighted Evolution, Transmissibility, and Clinical Manifestation of Hepatitis B Virus. *Front Microbiol* **9**, 2521 (2018).
323. Chen, M. *et al.* Immune tolerance split between hepatitis B virus precore and core proteins. *J Virol* **79**, 3016–3027 (2005).
324. Tian, Y., Kuo, C. F., Akbari, O. & Ou, J. H. Maternal-Derived Hepatitis B Virus e Antigen Alters Macrophage Function in Offspring to Drive Viral Persistence after Vertical Transmission. *Immunity* **44**, 1204–1214 (2016).
325. Ferrando-Martinez, S. *et al.* HBeAg seroconversion is associated with a more effective PD-L1 blockade during chronic hepatitis B infection. *JHEP Rep* **1**, 170–178 (2019).
326. Xuan Hoan, N. *et al.* Association of PD-L1 gene polymorphisms and circulating sPD-L1 levels with HBV infection susceptibility and related liver disease progression. *Gene* **806**, 145935 (2022).

327. Chung, T. W., Lee, Y. C. & Kim, C. H. Hepatitis B viral HBx induces matrix metalloproteinase-9 gene expression through activation of ERK and PI-3K/AKT pathways: involvement of invasive potential. *FASEB J* **18**, 1123–1125 (2004).
328. Dezutter-Dambuyant, C. *et al.* A novel regulation of PD-1 ligands on mesenchymal stromal cells through MMP-mediated proteolytic cleavage. *Oncoimmunology* **5**, e1091146 (2016).
329. Li, Y., Liu, H. & Xu, L. Expression of MMP-9 in different degrees of chronic hepatitis B and its correlation with inflammation. *Exp Ther Med* **16**, 4136–4140 (2018).
330. Orme, J. J. *et al.* ADAM10 and ADAM17 cleave PD-L1 to mediate PD-(L)1 inhibitor resistance. *Oncoimmunology* **9**, 1744980 (2020).
331. Ng, K. W. *et al.* Soluble PD-L1 generated by endogenous retroelement exaptation is a receptor antagonist. *Elife* **8**, (2019).
332. Benicky, J. *et al.* PD-L1 Glycosylation and Its Impact on Binding to Clinical Antibodies. *J Proteome Res* **20**, (2021).
333. Li, C. W. *et al.* Glycosylation and stabilization of programmed death ligand-1 suppresses T-cell activity. *Nat Commun* **7**, (2016).
334. Takeuchi, M. *et al.* Soluble PD-L1 with PD-1-binding capacity exists in the plasma of patients with non-small cell lung cancer. *Immunol Lett* **196**, (2018).
335. Bunse, T., Kosinska, A. D., Michler, T. & Protzer, U. PD-L1 Silencing in Liver Using siRNAs Enhances Efficacy of Therapeutic Vaccination for Chronic Hepatitis B. *Biomolecules* **12**, (2022).
336. Orme, J. J. *et al.* Therapeutic plasma exchange clears circulating soluble PD-L1 and PD-L1-positive extracellular vesicles. *J Immunother Cancer* **8**, (2020).
337. Jubel, J. M., Barbati, Z. R., Burger, C., Wirtz, D. C. & Schildberg, F. A. The Role of PD-1 in Acute and Chronic Infection. *Front Immunol* **11**, 487 (2020).
338. Watanabe, T., Bertoletti, A. & Tanoto, T. A. PD-1/PD-L1 pathway and T-cell exhaustion in chronic hepatitis virus infection. *J Viral Hepat* **17**, 453–458 (2010).
339. Zhong, S., Zhang, T., Tang, L. & Li, Y. Cytokines and Chemokines in HBV Infection. *Front Mol Biosci* **8**, 805625 (2021).
340. Bertoletti, A. & Gehring, A. J. Immune therapeutic strategies in chronic hepatitis B virus infection: virus or inflammation control? *PLoS Pathog* **9**, e1003784 (2013).
341. Barili, V. *et al.* Metabolic regulation of the HBV-specific T cell function. *Antiviral Res* **185**, 104989 (2021).
342. Sung, P. S. *et al.* Ex vivo Detection and Characterization of Hepatitis B Virus-Specific CD8(+) T Cells in Patients Considered Immune Tolerant. *Front Immunol* **10**, 1319 (2019).
343. Ye, P. *et al.* Programmed death-1 expression is associated with the disease status in hepatitis B virus infection. *World J Gastroenterol* **14**, 4551–4557 (2008).
344. Peng, G. *et al.* PD-1 upregulation is associated with HBV-specific T cell dysfunction in chronic hepatitis B patients. *Mol Immunol* **45**, 963–970 (2008).
345. Yong, Y. K. *et al.* Hyper-Expression of PD-1 Is Associated with the Levels of Exhausted and Dysfunctional Phenotypes of Circulating CD161(++)TCR iValpha7.2(+) Mucosal-Associated Invariant T Cells in Chronic Hepatitis B Virus Infection. *Front Immunol* **9**, 472 (2018).
346. Gupta, P. K. *et al.* CD39 Expression Identifies Terminally Exhausted CD8+ T Cells. *PLoS Pathog* **11**, e1005177 (2015).

347. Fang, F. *et al.* Expression of CD39 on Activated T Cells Impairs their Survival in Older Individuals. *Cell Rep* **14**, 1218–1231 (2016).
348. El-Khoueiry, A. B. *et al.* Nivolumab in patients with advanced hepatocellular carcinoma (CheckMate 040): an open-label, non-comparative, phase 1/2 dose escalation and expansion trial. *Lancet* **389**, 2492–2502 (2017).
349. Zhou, Z. Y., Liu, S. R., Xu, L. B., Liu, C. & Zhang, R. Clinicopathological and Prognostic Value of Programmed Cell Death 1 Expression in Hepatitis B Virus-related Hepatocellular Carcinoma: A Meta-analysis. *J Clin Transl Hepatol* **9**, 889–897 (2021).
350. Frigola, X. *et al.* Identification of a soluble form of B7-H1 that retains immunosuppressive activity and is associated with aggressive renal cell carcinoma. *Clin Cancer Res* **17**, 1915–1923 (2011).
351. Valiathan, R. *et al.* Reference ranges of lymphocyte subsets in healthy adults and adolescents with special mention of T cell maturation subsets in adults of South Florida. *Immunobiology* **219**, 487–496 (2014).
352. Wei, B. *et al.* Reference ranges of T lymphocyte subsets by single-platform among healthy population in southwest China. *BMC Immunol* **22**, 80 (2021).
353. Chen, G. *et al.* Exosomal PD-L1 contributes to immunosuppression and is associated with anti-PD-1 response. *Nature* **560**, 382–386 (2018).
354. Zhao, Y., Jia, Y., Li, C., Shao, R. & Fang, Y. Predictive Value of Soluble Programmed Death-1 for Severe Sepsis and Septic Shock during the First Week in an Intensive Care Unit. *Shock* **51**, (2019).
355. Crawford, A. *et al.* Molecular and transcriptional basis of CD4(+) T cell dysfunction during chronic infection. *Immunity* **40**, 289–302 (2014).
356. Jacobi, F. J. *et al.* OX40 stimulation and PD-L1 blockade synergistically augment HBV-specific CD4 T cells in patients with HBeAg-negative infection. *J Hepatol* **70**, 1103–1113 (2019).
357. Hottz, E. D., Bozza, F. A. & Bozza, P. T. Platelets in Immune Response to Virus and Immunopathology of Viral Infections. *Front Med (Lausanne)* **5**, 121 (2018).
358. Seifert, U. & Greinacher, A. Platelets modulate T-cell activity. *Blood* **138**, 358–360 (2021).
359. Chapman, L. M. *et al.* Platelets present antigen in the context of MHC class I. *J Immunol* **189**, 916–923 (2012).
360. Polasky, C., Wendt, F., Pries, R. & Wollenberg, B. Platelet Induced Functional Alteration of CD4(+) and CD8(+) T Cells in HNSCC. *Int J Mol Sci* **21**, (2020).
361. Joo, E. J., Chang, Y., Yeom, J. S., Lee, Y. G. & Ryu, S. Hepatitis B infection is associated with an increased incidence of thrombocytopenia in healthy adults without cirrhosis. *J Viral Hepat* **24**, 253–258 (2017).
362. Sitia, G. *et al.* Antiplatelet therapy prevents hepatocellular carcinoma and improves survival in a mouse model of chronic hepatitis B. *Proc Natl Acad Sci U S A* **109**, E2165-72 (2012).
363. Maini, M. K. & Schurich, A. Platelets harness the immune response to drive liver cancer. *Proc Natl Acad Sci U S A* **109**, 12840–12841 (2012).
364. Hsu, C. W., Liang, K. H., Lin, C. L., Wang, T. H. & Yeh, C. T. Platelet counts modulate the quantitative relationship between hepatitis B viral DNA and surface antigen concentrations: a cross-sectional study of hematological, histological and viral factors. *BMC Infect Dis* **17**, 9 (2017).

365. Schuch, A. *et al.* Phenotypic and functional differences of HBV core-specific versus HBV polymerase-specific CD8+ T cells in chronically HBV-infected patients with low viral load. *Gut* **68**, 905–915 (2019).
366. Gill, U. S. *et al.* Fine needle aspirates comprehensively sample intrahepatic immunity. *Gut* **68**, 1493–1503 (2019).
367. Bertoletti, A. & Kennedy, P. T. The immune tolerant phase of chronic HBV infection: new perspectives on an old concept. *Cell Mol Immunol* **12**, 258–263 (2015).
368. Spitzer, M. H. & Nolan, G. P. Mass Cytometry: Single Cells, Many Features. *Cell* **165**, 780–791 (2016).
369. Bruggner, R. v, Bodenmiller, B., Dill, D. L., Tibshirani, R. J. & Nolan, G. P. Automated identification of stratifying signatures in cellular subpopulations. *Proc Natl Acad Sci U S A* **111**, E2770-7 (2014).
370. Jaeger, N. *et al.* Single-cell analyses of Crohn's disease tissues reveal intestinal intraepithelial T cells heterogeneity and altered subset distributions. *Nat Commun* **12**, 1921 (2021).
371. Knaus, H. A. *et al.* Signatures of CD8+ T cell dysfunction in AML patients and their reversibility with response to chemotherapy. *JCI Insight* **3**, (2018).
372. Mpande, C. A. M. *et al.* Immune profiling of Mycobacterium tuberculosis-specific T cells in recent and remote infection. *EBioMedicine* **64**, 103233 (2021).
373. Tseng, T. C. & Kao, J. H. Clinical utility of quantitative HBsAg in natural history and nucleos(t)ide analogue treatment of chronic hepatitis B: new trick of old dog. *J Gastroenterol* **48**, 13–21 (2013).
374. Liu, J. *et al.* Serum Levels of Hepatitis B Surface Antigen and DNA Can Predict Inactive Carriers With Low Risk of Disease Progression. *Hepatology* **64**, 381–389 (2016).
375. Wu, S., Luo, W., Wu, Y., Chen, H. & Peng, J. HBsAg quantification predicts off-treatment response to interferon in chronic hepatitis B patients: a retrospective study of 250 cases. *BMC Gastroenterol* **20**, 121 (2020).
376. Rivino, L. *et al.* Hepatitis B virus–specific T cells associate with viral control upon nucleos(t)ide-analogue therapy discontinuation. *Journal of Clinical Investigation* **128**, 668–681 (2018).
377. Pallett, L. J. & Maini, M. K. Liver-resident memory T cells: life in lockdown. *Semin Immunopathol* (2022) doi:10.1007/s00281-022-00932-w.
378. Moini, M. & Fung, S. HBsAg Loss as a Treatment Endpoint for Chronic HBV Infection: HBV Cure. *Viruses* **14**, (2022).
379. Hesler, J. How to configure and run a CITRUS analysis. vol. 2022 https://support.cytobank.org/hc/en-us/articles/226678087-How-to-Configure-and-Run-a-CITRUS-Analysis (2021).
380. Pepper, M. & Jenkins, M. K. Origins of CD4(+) effector and central memory T cells. *Nat Immunol* **12**, 467–471 (2011).
381. Henry, C. *et al.* CD3+CD20+ cells may be an artifact of flow cytometry: comment on the article by Wilk et al. *Arthritis Rheum* **62**, 2561–3; author reply 2563-5 (2010).
382. Schuh, E. *et al.* Features of Human CD3+CD20+ T Cells. *J Immunol* **197**, 1111–1117 (2016).
383. Sumida, T. S. & O'Connor, K. C. Identity thieves: T cells steal CD20 from B cells but mark themselves for certain death. *Sci Immunol* **7**, eabq7242 (2022).
384. Du, F. H., Mills, E. A. & Mao-Draayer, Y. Next-generation anti-CD20 monoclonal antibodies in autoimmune disease treatment. *Auto Immun Highlights* **8**, 12 (2017).

385. Holley, J. E. *et al.* CD20+inflammatory T-cells are present in blood and brain of multiple sclerosis patients and can be selectively targeted for apoptotic elimination. *Mult Scler Relat Disord* **3**, 650–658 (2014).
386. Eggleton, P. *et al.* Frequency of Th17 CD20+ cells in the peripheral blood of rheumatoid arthritis patients is higher compared to healthy subjects. *Arthritis Res Ther* **13**, R208 (2011).
387. Niu, J. *et al.* Dissection of a circulating CD3(+) CD20(+) T cell subpopulation in patients with psoriasis. *Clin Exp Immunol* **192**, 206–212 (2018).
388. Serra-Peinado, C. *et al.* Expression of CD20 after viral reactivation renders HIV-reservoir cells susceptible to Rituximab. *Nat Commun* **10**, 3705 (2019).
389. Vlaming, M. *et al.* CD20 positive CD8 T cells are a unique and transcriptionally-distinct subset of T cells with distinct transmigration properties. *Sci Rep* **11**, 20499 (2021).
390. Chen, Q., Yuan, S., Sun, H. & Peng, L. CD3(+)CD20(+) T cells and their roles in human diseases. *Hum Immunol* **80**, 191–194 (2019).
391. Palanichamy, A. *et al.* Rituximab efficiently depletes increased CD20-expressing T cells in multiple sclerosis patients. *J Immunol* **193**, 580–586 (2014).
392. Tsutsumi, Y. *et al.* Hepatitis B virus reactivation with a rituximab-containing regimen. *World J Hepatol* **7**, 2344–2351 (2015).
393. Strioga, M., Pasukoniene, V. & Characiejus, D. CD8+ CD28- and CD8+ CD57+ T cells and their role in health and disease. *Immunology* **134**, 17–32 (2011).
394. Li, X. *et al.* Changes of costimulatory molecule CD28 on circulating CD8+ T cells correlate with disease pathogenesis of chronic hepatitis B. *Biomed Res Int* **2014**, 423181 (2014).
395. Huang, B. *et al.* CD8(+)CD57(+) T cells exhibit distinct features in human non-small cell lung cancer. *J Immunother Cancer* **8**, (2020).
396. Weng, N. P., Akbar, A. N. & Goronzy, J. CD28(-) T cells: their role in the age-associated decline of immune function. *Trends Immunol* **30**, 306–312 (2009).
397. Frimpong, A. *et al.* Phenotypic Evidence of T Cell Exhaustion and Senescence During Symptomatic Plasmodium falciparum Malaria. *Front Immunol* **10**, 1345 (2019).
398. Focosi, D., Bestagno, M., Burrone, O. & Petrini, M. CD57+ T lymphocytes and functional immune deficiency. *J Leukoc Biol* **87**, 107–116 (2010).
399. Bengsch, B. *et al.* Epigenomic-Guided Mass Cytometry Profiling Reveals Disease-Specific Features of Exhausted CD8 T Cells. *Immunity* **48**, 1029-1045 e5 (2018).
400. Hoji, A., Connolly, N. C., Buchanan, W. G. & Rinaldo Jr., C. R. CD27 and CD57 expression reveals atypical differentiation of human immunodeficiency virus type 1-specific memory CD8+ T cells. *Clin Vaccine Immunol* **14**, 74–80 (2007).
401. Verma, K. *et al.* Human CD8+ CD57- TEMRA cells: Too young to be called 'old'. *PLoS One* **12**, e0177405 (2017).
402. Shen, T. *et al.* PD-1 expression on peripheral CD8+ TEM/TEMRA subsets closely correlated with HCV viral load in chronic hepatitis C patients. *Virol J* **7**, 310 (2010).
403. Pangrazzi, L. *et al.* Increased IL-15 Production and Accumulation of Highly Differentiated CD8(+) Effector/Memory T Cells in the Bone Marrow of Persons with Cytomegalovirus. *Front Immunol* **8**, 715 (2017).
404. Meraviglia, S. *et al.* T-Cell Subsets (TCM, TEM, TEMRA) and Poly-Functional Immune Response in Patients with Human Immunodeficiency Virus (HIV) Infection and Different T-CD4 Cell Response. *Ann Clin Lab Sci* **49**, 519–528 (2019).

405. Herndler-Brandstetter, D. *et al.* The impact of aging on memory T cell phenotype and function in the human bone marrow. *J Leukoc Biol* **91**, 197–205 (2012).
406. Goronzy, J. J. & Weyand, C. M. Successful and Maladaptive T Cell Aging. *Immunity* **46**, 364–378 (2017).
407. Oo, Y. H. *et al.* CXCR3-dependent recruitment and CCR6-mediated positioning of Th-17 cells in the inflamed liver. *J Hepatol* **57**, 1044–1051 (2012).
408. Mullins, I. *et al.* Expression of CCR6 and CXCR3 by activated CD8+ T lymphocytes following immunotherapeutic vaccination correlates with enhanced survival. *Cancer Res* **64**, 323–324 (2004).
409. Liao, Z. *et al.* Altered circulating CCR6(+)and CXCR3(+) T cell subsets are associated with poor renal prognosis in MPO-ANCA-associated vasculitis. *Arthritis Res Ther* **23**, 194 (2021).
410. Gosselin, A. *et al.* Peripheral blood CCR4+CCR6+ and CXCR3+CCR6+CD4+ T cells are highly permissive to HIV-1 infection. *J Immunol* **184**, 1604–1616 (2010).
411. Khoury, G. *et al.* Persistence of integrated HIV DNA in CXCR3 + CCR6 + memory CD4+ T cells in HIV-infected individuals on antiretroviral therapy. *AIDS* **30**, 1511–1520 (2016).
412. Kared, H., Saeed, S., Klein, M. B. & Shoukry, N. H. CD127 expression, exhaustion status and antigen specific proliferation predict sustained virologic response to IFN in HCV/HIV co-infected individuals. *PLoS One* **9**, e101441 (2014).
413. Wherry, E. J. & Kurachi, M. Molecular and cellular insights into T cell exhaustion. *Nat Rev Immunol* **15**, 486–499 (2015).
414. Saeidi, A. *et al.* T-Cell Exhaustion in Chronic Infections: Reversing the State of Exhaustion and Reinvigorating Optimal Protective Immune Responses. *Front Immunol* **9**, 2569 (2018).
415. Hinterleitner, C. *et al.* Platelet PD-L1 reflects collective intratumoral PD-L1 expression and predicts immunotherapy response in non-small cell lung cancer. *Nat Commun* **12**, 7005 (2021).
416. Rolfes, V. *et al.* PD-L1 is expressed on human platelets and is affected by immune checkpoint therapy. *Oncotarget* **9**, 27460–27470 (2018).
417. le Bert, N. *et al.* Effects of Hepatitis B Surface Antigen on Virus-Specific and Global T Cells in Patients With Chronic Hepatitis B Virus infection. *Gastroenterology* **159**, 652–664 (2020).
418. Mokaya, J. *et al.* A blind spot? Confronting the stigma of hepatitis B virus (HBV) infection - A systematic review. *Wellcome Open Res* **3**, 29 (2018).
419. Matthews, P. C. *et al.* A call for advocacy and patient voice to eliminate hepatitis B virus infection. *Lancet Gastroenterol Hepatol* **7**, 282–285 (2022).

9 Appendix

9.1 Favourable ethical opinion

NHS
Health Research Authority

Yorkshire & The Humber - South Yorkshire Research Ethics Committee
NHSBT Newcastle Blood Donor Centre
Holland Drive
Newcastle upon Tyne
NE2 4NQ

Telephone: 0207 1048091

Please note: This is the favourable opinion of the REC only and does not allow you to start your study at NHS sites in England until you receive HRA Approval

17 July 2018

Professor Anna Maria Geretti
Professor of Virology and Infectious Diseases, University of Liverpool, Honorary Consultant in Infectious Diseases and Clinical Lead of the ID Hepatitis Service, Royal Liverpool University Hospital
University of Liverpool
Institute of Infection and Global Health
Ronald Ross Building
Liverpool L69 7BE

Dear Professor Geretti

Study title:	**INTERFACE: The interplay between HBV infection and the PD-1/PD-L1 pathway of immune modulation**
REC reference:	**18/YH/0286**
Protocol number:	**UoL0001386**
IRAS project ID:	**245799**

The Proportionate Review Sub-committee of the Yorkshire & The Humber - South Yorkshire Research Ethics Committee reviewed the above application via correspondence.

We plan to publish your research summary wording for the above study on the HRA website, together with your contact details. Publication will be no earlier than three months from the date of this favourable opinion letter. The expectation is that this information will be published for all

A Research Ethics Committee established by the Health Research Authority

studies that receive an ethical opinion but should you wish to provide a substitute contact point, wish to make a request to defer, or require further information, please contact hra.studyregistration@nhs.net outlining the reasons for your request. Under very limited circumstances (e.g. for student research which has received an unfavourable opinion), it may be possible to grant an exemption to the publication of the study.

Ethical opinion

On behalf of the Committee, the sub-committee gave a **favourable ethical opinion** of the above research on the basis described in the application form, protocol and supporting documentation, subject to the conditions specified below.

Conditions of the favourable opinion

The REC favourable opinion is subject to the following conditions being met prior to the start of the study.

Management permission must be obtained from each host organisation prior to the start of the study at the site concerned.

Management permission should be sought from all NHS organisations involved in the study in accordance with NHS research governance arrangements. Each NHS organisation must confirm through the signing of agreements and/or other documents that it has given permission for the research to proceed (except where explicitly specified otherwise).

Guidance on applying for HRA and HCRW Approval (England and Wales)/ NHS permission for research is available in the Integrated Research Application System, www.hra.nhs.uk or at http://www.rdforum.nhs.uk.

Where a NHS organisation's role in the study is limited to identifying and referring potential participants to research sites ("participant identification centre"), guidance should be sought from the R&D office on the information it requires to give permission for this activity.

For non-NHS sites, site management permission should be obtained in accordance with the procedures of the relevant host organisation.

Sponsors are not required to notify the Committee of management permissions from host organisations.

Registration of Clinical Trials

All clinical trials (defined as the first four categories on the IRAS filter page) must be registered on a publically accessible database. This should be before the first participant is recruited but no later than 6 weeks after recruitment of the first participant.

There is no requirement to separately notify the REC but you should do so at the earliest opportunity e.g. when submitting an amendment. We will audit the registration details as part of the annual progress reporting process.

To ensure transparency in research, we strongly recommend that all research is registered but for non-clinical trials this is not currently mandatory.

If a sponsor wishes to request a deferral for study registration within the required timeframe, they should contact hra.studyregistration@nhs.net. The expectation is that all clinical trials will be registered, however, in exceptional circumstances non registration may be permissible with prior agreement from the HRA. Guidance on where to register is provided on the HRA website.

It is the responsibility of the sponsor to ensure that all the conditions are complied with before the start of the study or its initiation at a particular site (as applicable).

Ethical review of research sites

The favourable opinion applies to all NHS sites taking part in the study, subject to management permission being obtained from the NHS/HSC R&D office prior to the start of the study (see "Conditions of the favourable opinion").

Extract from Minutes

Social or scientific value; scientific design and conduct of the study

Members stated that Question 2b of the IRAS form said 'no' to using existing samples but queried the African bloods in relation to this. It is detailed that ethics approval has already been obtained for these, however the REC enquired whether there was any documentation available for this.

It was confirmed that this had been an error and should have been 'yes'.

Members queried the rationale for no Patient and Public Involvement (Question A14 on the IRAS form).

It was stated that as this was a basic science study, involvement of the public in the study design would not have been feasible. The study design was simple in that patients were asked to donate blood samples for basic science investigations of their immune response to hepatitis B. The applicant had not undertaken an evaluation of patients' opinion on the laboratory-based experimental procedures that would be undertaken, as this was not considered to be in scope. However the applicant would be available to provide information to patients who may have questions in relation to the general theme of hepatitis B cure. A sentence had been added to the PIS to indicate that investigators would be available to answer questions about the general research area concerning hepatitis B.

Members queried Question A54 of the IRAS form which referred to external peer review however the peer review form attached was not very comprehensive.

It was confirmed that the University of Liverpool standard procedure for obtaining peer review had been followed, which was a requirement for obtaining sponsorship approval. This was completed by two academics without direct involvement in the study. The peer review submission to the sponsor was submitted.

Recruitment arrangements and access to health information, and fair participant selection

Question A31 of the IRAS form states that 1 hour from approaching participant to consent. The REC stated that this was inadequate time for participants to decide.

It was appreciated that 1 hour may be insufficient for some patients to make a decision however this had been extended to 48 hours. However, it was envisaged that patients who elected to wait past their time in clinic before making a decision would be deferred to the next clinic visit to avoid a study- specific visit which would be inconvenient to patients.

Favourable risk benefit ratio; anticipated benefit/risks for research participants (present and future)

The Committee noted Question A22 of the IRAS form and queried whether there was additional venepuncture or whether taking additional tubes of blood from a single puncture was taking place.

The applicant stated that whole venous blood would be collected utilising the vacutainer blood collection system, wherein there was only a single venepuncture from which multiple tubes could be filled. There would be no need for multiple punctures.

Care and protection of research participants; respect for potential and enrolled participants' welfare and dignity

The REC required that the study be registered on a publicly accessible database (Question A50 of the IRAS form).

The applicant had consulted the University of Liverpool Research Office and been advised that the data from this study would be deposited on the publically accessible University of Liverpool data depository. It had been advised that there was no other suitable registry based on the non-interventional nature of this study.

Informed consent process and the adequacy and completeness of participant information

Members stated that the Consent Form was not clear about the Opt Out of preferably Opt In for the genetic testing and requested that this be re-written.

It was stated that the testing of genes involved with HBV control was solely designated as an opt-in sub-study with participants who wished to be involved and was stated as an opt-in study in the consent form and reflected on the PIS. Participants who do not wish to opt-in to the sub-study would still allowed to participate in the general study. This had been reworded for clarity on the Consent Form.

Members noted that Question A13 stated 50 mls however the PIS stated 40 mls of blood. Clarification was requested on this and amendments to the PIS if required.

It was confirmed that this was a typographical error. It was planned to collect 50ml of whole blood during the recruitment process and the PIS had been revised accordingly.

Approved documents

The documents reviewed and approved were:

Document	*Version*	*Date*
Covering letter on headed paper [Cover Letter]		25 June 2018
Evidence of Sponsor insurance or indemnity (non NHS Sponsors only) [Insurance]		27 July 2017
GP/consultant information sheets or letters [GP Letter]	1	08 June 2018
IRAS Application Form [IRAS_Form_27062018]		27 June 2018
IRAS Checklist XML [Checklist_11072018]		11 July 2018
Letter from sponsor [Sponsor Approval]		31 May 2018
Other [Stored Sample EC]	1	30 January 2018
Other [Stored Sample EC]	1	25 July 2018
Other [Response Cover Letter]	1	10 July 2018
Participant consent form [Consent Form]	3	10 July 2018
Participant information sheet (PIS) [Patient Information Sheet]	3	10 July 2018
Referee's report or other scientific critique report [Peer Review Evidence]		23 April 2018
Referee's report or other scientific critique report [Peer Review Evidence]		24 April 1918
Research protocol or project proposal [Protocol]	5.1	25 June 2018
Summary CV for Chief Investigator (CI) [AMG CV]		03 April 2017
Summary CV for student [HBV CV]		01 June 2018
Summary CV for supervisor (student research) [AMG CV]		03 April 2017

Membership of the Proportionate Review Sub-Committee

The members of the Sub-Committee who took part in the review are listed on the attached sheet.

Statement of compliance

The Committee is constituted in accordance with the Governance Arrangements for Research Ethics Committees and complies fully with the Standard Operating Procedures for Research Ethics Committees in the UK.

After ethical review

Reporting requirements

The attached document "After ethical review – guidance for researchers" gives detailed guidance on reporting requirements for studies with a favourable opinion, including:

- Notifying substantial amendments
- Adding new sites and investigators
- Notification of serious breaches of the protocol
- Progress and safety reports
- Notifying the end of the study

The HRA website also provides guidance on these topics, which is updated in the light of changes in reporting requirements or procedures.

User Feedback

The Health Research Authority is continually striving to provide a high quality service to all applicants and sponsors. You are invited to give your view of the service you have received and the application procedure. If you wish to make your views known please use the feedback form available on the HRA website:
http://www.hra.nhs.uk/about-the-hra/governance/quality-assurance/

HRA Training

We are pleased to welcome researchers and R&D staff at our training days – see details at http://www.hra.nhs.uk/hra-training/

With the Committee's best wishes for the success of this project.

18/YH/0286	**Please quote this number on all correspondence**

Yours sincerely

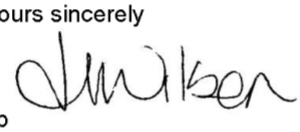

pp
Dr David Broomhead
Chair

Email: nrescommittee.yorkandhumber-southyorks@nhs.net

Enclosures:	*List of names and professions of members who took part in the review*
	"After ethical review – guidance for researchers"
Copy to:	Mr Alex Astor
	Mrs Heather Rogers, Governance Administrator Research Development & Innovation Royal Liverpool University Hospital

9.2 HRA approval

Ymchwil Iechyd a Gofal Cymru
Health and Care Research Wales

NHS
Health Research Authority

Professor Anna Maria Geretti
Professor of Virology and Infectious Diseases
University of Liverpool
Institute of Infection and Global Health
L69 7BE

Email: hra.approval@nhs.net
Research-permissions@wales.nhs.uk

20 July 2018

Dear Professor Geretti

HRA and Health and Care Research Wales (HCRW) Approval Letter

Study title:	**INTERFACE: The interplay between HBV infection and the PD-1/PD-L1 pathway of immune modulation**
IRAS project ID:	**245799**
Protocol number:	**UoL0001386**
REC reference:	**18/YH/0286**
Sponsor	**University of Liverpool**

I am pleased to confirm that **HRA and Health and Care Research Wales (HCRW) Approval** has been given for the above referenced study, on the basis described in the application form, protocol, supporting documentation and any clarifications received. You should not expect to receive anything further relating to this application.

How should I continue to work with participating NHS organisations in England and Wales?
You should now provide a copy of this letter to all participating NHS organisations in England and Wales, as well as any documentation that has been updated as a result of the assessment.

Following the arranging of capacity and capability, participating NHS organisations should **formally confirm** their capacity and capability to undertake the study. How this will be confirmed is detailed in the "*summary of assessment*" section towards the end of this letter.

You should provide, if you have not already done so, detailed instructions to each organisation as to how you will notify them that research activities may commence at site following their confirmation of capacity and capability (e.g. provision by you of a 'green light' email, formal notification following a site initiation visit, activities may commence immediately following confirmation by participating organisation, etc.).

It is important that you involve both the research management function (e.g. R&D office) supporting each organisation and the local research team (where there is one) in setting up your study. Contact details of the research management function for each organisation can be accessed here.

IRAS project ID	245799

How should I work with participating NHS/HSC organisations in Northern Ireland and Scotland?
HRA and HCRW Approval does not apply to NHS/HSC organisations within the devolved administrations of Northern Ireland and Scotland.

If you indicated in your IRAS form that you do have participating organisations in either of these devolved administrations, the final document set and the study wide governance report (including this letter) has been sent to the coordinating centre of each participating nation. You should work with the relevant national coordinating functions to ensure any nation specific checks are complete, and with each site so that they are able to give management permission for the study to begin.

Please see IRAS Help for information on working with NHS/HSC organisations in Northern Ireland and Scotland.

How should I work with participating non-NHS organisations?
HRA and HCRW Approval does not apply to non-NHS organisations. You should work with your non-NHS organisations to obtain local agreement in accordance with their procedures.

What are my notification responsibilities during the study?
The document "*After Ethical Review – guidance for sponsors and investigators*", issued with your REC favourable opinion, gives detailed guidance on reporting expectations for studies, including:

- Registration of research
- Notifying amendments
- Notifying the end of the study

The HRA website also provides guidance on these topics, and is updated in the light of changes in reporting expectations or procedures.

I am a participating NHS organisation in England or Wales. What should I do once I receive this letter?
You should work with the applicant and sponsor to complete any outstanding arrangements so you are able to confirm capacity and capability in line with the information provided in this letter.

The sponsor contact for this application is as follows:

Name: Harrison Austin
Email: Harrison.Austin@liverpool.ac.uk

Who should I contact for further information?
Please do not hesitate to contact me for assistance with this application. My contact details are below.

Your IRAS project ID is **245799**. Please quote this on all correspondence.

Yours sincerely,

Steph Blacklock
Senior Assessor

IRAS project ID	245799

Email: hra.approval@nhs.net

Copy to: *Mr Alex Astor, Sponsor Contact*
Mrs Heather Rogers, Governance Administrator Research Development & Innovation Royal Liverpool University Hospital, Lead R&D Contact

IRAS project ID	245799

List of Documents

The final document set assessed and approved by HRA and HCRW Approval is listed below.

Document	*Version*	*Date*
Covering letter on headed paper [Cover Letter]		25 June 2018
Evidence of Sponsor insurance or indemnity (non NHS Sponsors only) [Insurance]		27 July 2017
GP/consultant information sheets or letters [GP Letter]	1	08 June 2018
HRA Schedule of Events [SOE]	1	20 July 2018
HRA Statement of Activities [SOA]	1	20 July 2018
IRAS Application Form [IRAS_Form_27062018]		27 June 2018
Letter from sponsor [Sponsor Approval]		31 May 2018
Other [Stored Sample EC]	1	30 January 2018
Other [Response Cover Letter]	1	10 July 2018
Participant consent form [Consent Form]	3	10 July 2018
Participant information sheet (PIS)	4	20 July 2018
Referee's report or other scientific critique report [Peer Review Evidence]		23 April 2018
Referee's report or other scientific critique report [Peer Review Evidence]		24 April 1918
Research protocol or project proposal [Protocol]	5.1	25 June 2018
Summary CV for Chief Investigator (CI) [AMG CV]		03 April 2017
Summary CV for student [HBV CV]		01 June 2018
Summary CV for supervisor (student research) [AMG CV]		03 April 2017

IRAS project ID	245799

Summary of assessment

The following information provides assurance to you, the sponsor and the NHS in England and Wales that the study, as assessed for HRA and HCRW Approval, is compliant with relevant standards. It also provides information and clarification, where appropriate, to participating NHS organisations in England and Wales to assist in assessing, arranging and confirming capacity and capability.

Assessment criteria

Section	Assessment Criteria	Compliant with Standards	Comments
1.1	IRAS application completed correctly	Yes	No comments
2.1	Participant information/consent documents and consent process	Yes	Participant Information Sheet updated to V4 in order to comply with GDPR legislation and HRA standards regarding human tissue.
3.1	Protocol assessment	Yes	No comments
4.1	Allocation of responsibilities and rights are agreed and documented	Yes	Statement of Activities and Schedule of Events provided.
4.2	Insurance/indemnity arrangements assessed	Yes	No comments
4.3	Financial arrangements assessed	Yes	Consumables provided to site via Statement of Activities.
5.1	Compliance with the Data Protection Act and data security issues assessed	Yes	No comments
5.2	CTIMPS – Arrangements for compliance with the Clinical Trials Regulations assessed	Not Applicable	No comments
5.3	Compliance with any applicable laws or regulations	Yes	No comments
6.1	NHS Research Ethics Committee favourable opinion received for applicable studies	Yes	No comments

IRAS project ID	245799

Section	Assessment Criteria	Compliant with Standards	Comments
6.2	CTIMPS – Clinical Trials Authorisation (CTA) letter received	Not Applicable	No comments
6.3	Devices – MHRA notice of no objection received	Not Applicable	No comments
6.4	Other regulatory approvals and authorisations received	Not Applicable	No comments

Participating NHS Organisations in England and Wales

This provides detail on the types of participating NHS organisations in the study and a statement as to whether the activities at all organisations are the same or different.

This is a tissue study with one site type.

The Chief Investigator or sponsor should share relevant study documents with participating NHS organisations in England and Wales in order to put arrangements in place to deliver the study. The documents should be sent to both the local study team, where applicable, and the office providing the research management function at the participating organisation. Where applicable, the local LCRN contact should also be copied into this correspondence.

If chief investigators, sponsors or principal investigators are asked to complete site level forms for participating NHS organisations in England and Wales which are not provided in IRAS, the HRA or HCRW websites, the chief investigator, sponsor or principal investigator should notify the HRA immediately at hra.approval@nhs.net or HCRW at Research-permissions@wales.nhs.uk. We will work with these organisations to achieve a consistent approach to information provision.

Principal Investigator Suitability

This confirms whether the sponsor position on whether a PI, LC or neither should be in place is correct for each type of participating NHS organisation in England and Wales, and the minimum expectations for education, training and experience that PIs should meet (where applicable).

As per the Statement of Activities a Principal Investigator will be in place at the NHS organisation.

GCP training is not a generic training expectation, in line with the HRA/HCRW/MHRA statement on training expectations.

IRAS project ID	245799

HR Good Practice Resource Pack Expectations

This confirms the HR Good Practice Resource Pack expectations for the study and the pre-engagement checks that should and should not be undertaken
It is unlikely that letters of access or honorary research contracts will be applicable, except where local staff employed by another Trust (or University) are involved (and then it is likely that arrangements are already in place). Where arrangements are not already in place, such staff undertaking any of the research activities listed in the IRAS Form, would be expected to obtain an honorary research contract on the basis of a Research Passport (if university employed) or an NHS to NHS confirmation of pre-engagement checks letter (if NHS employed). These should confirm standard DBS checks and occupational health clearance.

Other Information to Aid Study Set-up

This details any other information that may be helpful to sponsors and participating NHS organisations in England and Wales to aid study set-up.
The applicant has indicated that they do not intend to apply for inclusion on the NIHR CRN Portfolio.

9.3 READ2 and CTV3 codes for patient record extraction

Demographics			
Definition	Term Name	CTV3	READ2
Ethnicity	Ethnic category - 2011 census England and Wales	XactE	9t0..
Age	DOB - date of birth	9155	
	No date of birth given	Xa1in	
Postcode	Patient postcode	9158	
LSOA			
Deprivation Score			
Deprivation decile			
NHS region			
Case Definitions			
Definition	Term Name	CTV3	READ2
HBV Screened	Hepatitis B screening	6828.	6828.
	Hepatitis B screening test	XaEXZ	
	SH-antigen (hepatitis B) test	XE254	
	Hepatitis B screening offered	XaLFK	9Op2
	Hepatitis B screening required	68280	68280
	Hepatitis B screening declined	XaLND	8I3u.
	Hepatitis B screening counselling	XaLTv	677R.
	Hepatitis B antigen screening	X77bi	
HBV Infected	History of Hepatitis B	XaLow	141E.
	Hepatitis B surface antigen level	XaFuS	43d9.
	[V]Hepatitis B carrier	XaG1R	ZV02B
	Hepatitis B carrier	X306n	
	Hepatitis B screening positive	XaPEy	9kZ..
	Hepatitis B infection	XE0TY	
	Chronic viral hepatitis B	X306i	A7073
	Chronic viral hepatitis B without delta-antigen	A7071	A7071
	Chronic viral hepatitis B with hepatitis D	X306i	A7070
Risk Group Definitions			
Risk Group Definitions	Term Name	CTV3	READ2
Born in high prevalence country	Country of birth	XaG2A	
Intravenous and injecting drug users	Drug user	Ub0mt	13c..
	Misuses anabolic steroids	XaZ3h	
	Uses drug paraphernalia	XaQ0k	
	Injecting drug user	Ub00U	13c0.
	Injecting drugs subcutaneously	Ub0n8	13c9.
	Injects drugs intramuscularly	ub0n9	
	Intravenous drug user	Ub0nA	13c1.
	Neck injector	XaMHY	
	Previously injecting drug user	XaKcY	13cJ.
MSM	Male Homosexual	E2200	1b21.
	Bisexual	X7766r	1b0..
	Homosexual relationship	Ub0oZ	
	Homosexual activity		1ABL.
	Sexual activity - anal sex	XaMlW	1ABA.
Pregnant	Pregnant	621..	
	Ovarian pregnancy		L032.
	Primigravida	X40Ac	
	Multigravida	X40Ad	
	Primiparous	X40Af	
	Multiparous	X40Ag	
	Pregnant - urine test confirms	6211.	6211.
	Preganat - blood test confirms	6212.	6212.
	Preganat - V.E. confirms	6213.	6213.
	Pregnant - on history	6214.	6214.
	Pregnant- planned		6216.
	Pregnant - unplanned - wanted		6217.
	Pregnant - unplanned - not wanted		6218.
	Concealed pregnancy		621D.
	Unwanted pregancy		13H7.
	Multiple pregnancy		L21..
	Urine pregnancy test positive		4654.

	unplanned pregnancy		621C.
	Normal pregnancy		ZV22.
	Pregnant - on abdom. Palpation	6215.	6215.
Individuals who live in house with kr	Hepatitis B contact	Xa1pO	65PL.
	Mother hepatitis B positive	XaYVx	12K5.
	At risk of hepatitis B infection	XagoH	
Inmates of previous inmates of corre	In prison	XE0pK	13HQ.
	Prison record	XE0pD	13H9.
	Prison sentence		13HQ.
	Imprisonment		ZV625
	Released from prison	Xa0re	
	Prison medical examination		6992.
	Prison inreach group therapy	Xac8w	
	Medically fit for prison transfer	XaQfN	
	Prison segregaton unit risk assessment	XaQji	
	Medically fit for activity outside prison	XaQfq	
	Prison sickness certificate issued	XaPij	
	Medically unfit for prison transfer	XaXNu	
	Prison record and criminal activity details	Xa8Ex	
	Prison first reception health assessment complete	XaYXV	
Hepatitis C Infected	Hepatitis C carrier	X306o and X306n	
	Hepatitis C	A70z0	
	Acute hepatitis C	X306e	
	Chronic hepatitis C	X306k	
	Hepatitis C resolved	XaXET	
	Hepatitis C GT1	XaZ5P	A70A.
	Hepatitis C GT2	XaZ5Q	A70B.
	Hepatitis C GT3	XaZ5S	A70C.
	Hepatitis C GT4	XaZ5T	A70D.
	Hepatitis C GT5	XaZ5U	A70E.
	Hepatitis C GT6	XaZ5V	A70F.
	Hepatitis C PCR positive	XaXBp	4JQD.
	Hepatitis C virus genotype	XalrZ	
	Unspecified viral hepatitis		A70z.
Individuals with HIV	HIV positive	43C3.	43C3.
	Human immunodeficieny virus viral load by log ra	XaFuL	4J3F.
	HIV infection wasting syndrome	X70O1	A789A
	HIV associated retinitis	X00cZ	
	HIV related sclerosing cholangitis	Xa1k1	
	HIV disease resulting in cadidiasis	A7892	A7892
	HIV-related gut diseases	Xa1k3	
	HIV disease resulting in kaposi syndrome	A7895	A7895
	HIV disease resulting in multiple infections	A7894	A7894
	HIV disease resulting in mycobacterial infection	A7890	A7890
	HIV disease resulting in cytomegaloviral disease	A7891	A7891
	HIV disease resulting in multiple malignant neopla	A7898	A7898
	HIV dis resulting oth types of non-Hodgkin's lymph	A7897	A7897
	HIV disease resulting in Pneumocystis carinii pneu	A7893	A7893
	HIV disease complicating pregnancy childbirth puerperium		L179.
	HIV dis reslt/ oth mal neopl/lymph,h'matopoetc+r	AyuC7	A789X
	HIV disease resulting in lymphoid interstitial pneu	A7899	A7899
	Acute human immunodeficiency virus infection	A7880	A7880
	Asymptomatic human immunodeficiency virus infe	A7881	A7881
	HIV infection with persistent generalised lymphadenopathy		A7882
	Human immunodeficiency virus infection with con	A7883	A7883
	Human immunodeficiency virus infection with neu	A7884	A7884
	Human immunodeficiency virus infection with sec	A7885	A7885
	Human immunodeficiency virus infection with sec	A7886	A7886
	Human immunodeficiency virus annual review	XaQOu	66j0.
	Human immunodeficiency virus type 1 subtype ide	Xabnk	4J3P.
Gonorrhoea Infection	Gonococcal urethritis	X30Oz	A9801
	Gonococcal cervicitis	X407O	A9851
	Acute gonococcal Bartholinitis		A9800

	Gonococcal vulvovaginitis	X407p	A9802
	Gonococcal pharyngitis	A986.	A986.
	Gonococcal proctitis	A987.	A987.
	Gonococcal cystitis	K1545	A9811
	Gonococcal seminal vesiculitis	Xa89S	A9814
	Gonococcal eye infeciton	A984.	A984.
	Gonorrhoea with local complication	X70Mm	
	Systemic gonococcal infection	X70N5	
	Gonococcal lymphangitis of penis	X501h	
	Gonorrhoea test positive	XaLos	4JQA.
	Gonorrhoea test equivocal	XaLor	4JQ9.
	Urine neisseria gonorrhoeae test positive - enhan serv admin		9ka..
Chlamydia Infection			
	Chlamydial infection	A78A.	
	Chlamydiosis	X70Hc	
	Chlamydial urethritis	X30P0	
	Chlamydial cervicitis	X407P	K4209
	Chlamydial peritonitis	J5504	J5504
	Chlamydial prostatis	X30Oi	
	Chlamydia PCR positive	XaJbE	43U4.
	Chlamydia test positive	XaLKB	43U8.
	Chalamydial vulvovaginitis	X407r	
	History of chlamydial infection	XaXJw	14150
	Chlamydial infection of the pharynx	X00mP	A78A1
	Chlamydia trachomatis infection	X70NF	
	Urine chlamydia trachomatis test positive	XaKID	46H6.
	Chlamydial infection of lower genitourinary tract		A78A0
	Chlamydial infection of anus and rectum		A78A2
	Chlamydial inf of pelviperitoneum oth genitourinary organs		A78A3
	Chlamydial infection of genital organs NEC		A78A5
	Chlamydial infection, unspecified		A78AW
	Chlamydial infection of genitourinary tract, unspecified		
Syphilis Infection	Syphilis	X70M7	A97..
	Primary syphilis	XE0Rk	
	Secondary syphilis	X70MJ	
	Acquired syphilis - early latent	XE0Rn	
	Tertiary syphilis	X70MV	
	Quaternary syphilis	Xa0kV	
	Acquired syphilis - late latent	XE0Rt	
	Oral syphilis	X20RM	
	Peritonitis - syphalic	J5501	
	Nasal syphilis	X00IS	
	Syphilitis oral leukoplakia	X20Qi	
	Syphilis of the breast	X40Fb	
	Cardiovascular syphilis		Gy0..
	Cardiovascular syphilis	A93..	Gy0..
	Late syphilis of the kidney	A954	K0y0.
	Prostatitis in syphilis	K2142	
	Keratitis due to syphilis	F4A54	
	Lung disease with syphilis	H57y5	A951.
	Hepatitis in late syphilis		J6321
	Hepatitis in secondary syphilis	J6322	J6322
	Meningitis due to secondary syphilis	F0075	F0075
	Syphilis and other veneral diseases	XE0Rh	A9...
	Syphilis screen 1 year post treatment	XaPE7	9kF6.
	Postinfective arthropathy in syphilis	N0381	N0381
	Syphilis titre test positive	4382.	4382.
	Treponema pallidum ELISA positive	XaIQI	438B.
	Primary genital syphilis	A910.	A910.
	Primary anal syphilis	A911.	A911.
	Other primary syphilis	A921.	A912
	Secondary syphilis of skin or mucus membrane	A913.	A913.
	Secondary syphilis relapse	A917.	A917.

	Latent early syphilis	A92..	A92..
	Other forms of late syhpilis with symptoms	A95..	A95..
Human Papilloma Virus Infection	Human papilloma virus infection	X70LN	A79B.
	HPV - Human papillomavirus test positive	XaIVA	4K3D.
	high risk human papillomavirus genotyping test nc	XaZmP	8IBD.
Trichomoniasis Infection	Interstitial trichomoniasis	A063.	A063.
	Cystitis in trichomoniasis	K1547	K1547
	Trichomoniasis - trichomonas		AD1..
	Unspecified urogenitial trichomonas		AD100
	Trichomonal urethritis	AD102	AD102
	Trichomonal prostatitis	K2146	AD103
	Trichomonal balanoposthitis	X4009	
	Trichomonal vulvitis	X4085	
	Trichomonal vulvovaginitis	XE0Sc	AD101
	Trichomonal vaginitis	Xa0Er	
	Asymptomatic trichomoniasis	X70Nm	
	Trichomonal cystitis	K1547	K1547
	Urogenitial trichomonas NOS		AD10z
	Other specified site trichomonas		AD1y.
	Trichomonas NOS		AD1z.
	Prostatitis in trichomoniasis		K2146
Scabies Infection	Scabies	XE0Se	AD30.
Herpes Infection	genital herpes simplex	A541.	A541.
	History of genital herpes	XaaEh	14153
	treatment of recurrent genital herpes	XaPNc	9kF8.
	Herpes simplex type 2 nucleic acid detection assay		43w5
	Genital herpes simplex type 2	XaPED	A5417
	Recurrent genital herpes simplex type 2 infection	XaPES	A5419
	herpetic vulvovaginitis	A5411	A5411
	herpetic ulceration of the vulva	A5412	A5412
	herpetic infection of the penis	A5413	A5413
	herpesviral infection of the perianal skin and rectum		A5414
	Anogenital herpesviral infection		A5415
	genital herpes simplex type 1	XaPEC	A5417
	Referrals		
Referral Service	Term Name	CTV3	READ2
Gastroenterology	Referral to gastroenterology	8H48.	8H48.
	Referral to gastroenterology service		
	Referral to gastroenterology clinical assessment service		8Hm1.
	Referral to hepatology service	XaLrh	8Hk5.
	Referral to gastroenterologist	XaBTW	
GUM	Referral to genitourinary medicine - service	XaAW5	
	Referral to genitourinary physician	XaAfz	
	Referral to venerologist		8H4A.
ID	Referral to infectious diseases service	XaAch	8HTq.
	Referral to infectious diseases physician	XaAg1	

9.4 Brief description of gates used to identify T-cell compartments in Chapter 6

Table 1. Gates used to distinguish cell populations stained by the Maxpar Direct Immune Profiling Assay (201325)*. All listed cell populations should also include the cleanup gates described in the cleanup strategy.

		Population	Gate #	Gates	Population	Gate #	Gates
	Granulocytes	Neutrophils	02	CD45loCD66b+	Eosinophils	02	CD45loCD66b+
			04	CD294-CD16+		03	CD294+CD16-
		Basophils	01	CD45+CD66b-			
			10	CD19-CD20-			
			11	CD3-CD56-			
			57	HLA-DR-CD11c-			
			58	CD123+CD294+			
Lymphocytes	CD8 T Cells	CD8 αβ T cells (Total; CD161-)	01	CD45+CD66b-	CD8 αβ T cells, Naïve	01	CD45+CD66b-
			10	CD19-CD20-		10	CD19-CD20-
			26	CD14-CD11c-		26	CD14-CD11c-
			27	CD45+CD3+		27	CD45+CD3+
			28	CD3+TCRγδ-		28	CD3+TCRγδ-
			29	CD4-CD8+		29	CD4-CD8+
			30	CD8+CD161-		30	CD8+CD161-
						31	CD8+CCR7hi
						32	CD45RA+CD45RO-
		CD8 αβ T cells, Central Memory	01	CD45+CD66b-	CD8 αβ T cells, Effector Memory	01	CD45+CD66b-
			10	CD19-CD20-		10	CD19-CD20-
			26	CD14-CD11c-		26	CD14-CD11c-
			27	CD45+CD3+		27	CD45+CD3+
			28	CD3+TCRγδ-		28	CD3+TCRγδ-
			29	CD4-CD8+		29	CD4-CD8+
			30	CD8+CD161-		30	CD8+CD161-
			31	CD8+CCR7hi		34	CD8+CCR7lo/-
			33	CD45RA-CD45RO+		35	CD8+CD27+
		CD8 αβ T cells, Terminal Effector	01	CD45+CD66b-			
			10	CD19-CD20-			
			26	CD14-CD11c-			
			27	CD45+CD3+			
			28	CD3+TCRγδ-			
			29	CD4-CD8+			
			30	CD8+CD161-			
			34	CD8+CCR7lo/-			
			36	CD8+CD27-			

* Maxpar Direct Immune Profiling Assay is available in a new configuration (201334).

		Population	Gate #	Gates	Population	Gate #	Gates
Lymphocytes	CD4 T Cells	CD4 αβ T cells (Total)	01	CD45+CD66b-	CD4 αβ T cells, Naïve	01	CD45+CD66b-
			10	CD19-CD20-		10	CD19-CD20-
			26	CD14-CD11c-		26	CD14-CD11c-
			27	CD45+CD3+		27	CD45+CD3+
			28	CD3+TCRγδ-		28	CD3+TCRγδ-
			37	CD4+CD8-		37	CD4+CD8-
						38	CD4+CCR7hi
						39	CD45RA+CD45RO-
		CD4 αβ T cells, Central Memory	01	CD45+CD66b-	CD4 αβ T cells, Effector Memory	01	CD45+CD66b-
			10	CD19-CD20-		10	CD19-CD20-
			26	CD14-CD11c-		26	CD14-CD11c-
			27	CD45+CD3+		27	CD45+CD3+
			28	CD3+TCRγδ-		28	CD3+TCRγδ-
			37	CD4+CD8-		37	CD4+CD8-
			38	CD4+CCR7hi		41	CD4+CCR7lo/-
			40	CD45RA-CD45RO+		40	CD45RA-CD45RO+
						43	CD45RO+CD27+
		CD4 αβ T cells, Terminal Effector	01	CD45+CD66b-	Treg	01	CD45+CD66b-
			10	CD19-CD20-		10	CD19-CD20-
			26	CD14-CD11c-		26	CD14-CD11c-
			27	CD45+CD3+		27	CD45+CD3+
			28	CD3+TCRγδ-		28	CD3+TCRγδ-
			37	CD4+CD8-		37	CD4+CD8-
			41	CD4+CCR7lo/-		45	CD4+CCR4+
			40	CD45RA-CD45RO+		46	CD45RA-CD45RO+
			44	CD45RO+CD27-		47	CD25hiCD127lo/-
		Th1-like	01	CD45+CD66b-	Th2-like	01	CD45+CD66b-
			10	CD19-CD20-		10	CD19-CD20-
			26	CD14-CD11c-		26	CD14-CD11c-
			27	CD45+CD3+		27	CD45+CD3+
			28	CD3+TCRγδ-		28	CD3+TCRγδ-
			37	CD4+CD8-		37	CD4+CD8-
			48	CD4+CXCR5-		45	CD4+CXCR5-
			49	CD4+CCR4-		52	CD45RA-CCR4+
			50	CD45RA-CD45RO+		53	CXCR3-CCR6-
			51	CXCR3+CCR6-			
		Th17-like	01	CD45+CD66b-			
			10	CD19-CD20-			
			26	CD14-CD11c-			
			27	CD45+CD3+			
			28	CD3+TCRγδ-			
			37	CD4+CD8-			
			45	CD4+CXCR5-			
			52	CD45RA-CCR4+			
			54	CXCR3-CCR6+			

		Population	Gate #	Gates	Population	Gate #	Gates
Lymphocytes	Other T cells	Gamma-delta T cells, CD4-CD8-	01	CD45+CD66b-	MAIT/NKT CD4- cells	01	CD45+CD66b-
			10	CD19-CD20-		10	CD19-CD20-
			26	CD14-CD11c-		26	CD14-CD11c-
			27	CD45+CD3+		27	CD45+CD3+
			59	CD4-CD8-		55	CD3+CD4-
			60	CD3+TCRγδ+		56	CD28+CD161hi
	B cells	Total B cells	01	CD45+CD66b-	Naive B cells	01	CD45+CD66b-
			05	CD56-CD14-		05	CD56-CD14-
			06	CD19+CD3-		06	CD19+CD3-
						07	CD19+CD27-
		Total Memory B cells	01	CD45+CD66b-	Plasmablasts	01	CD45+CD66b-
			05	CD56-CD14-		05	CD56-CD14-
			06	CD19+CD3-		06	CD19+CD3-
			08	CD19+CD27+		08	CD19+CD27+
						09	CD38+CD20-
	NK cells	Total NK cells	01	CD45+CD66b-	Early NK cells	01	CD45+CD66b-
			10	CD19-CD20-		10	CD19-CD20-
			17	CD3-CD14-		17	CD3-CD14-
			18	CD45RA+CD123-		18	CD45RA+CD123-
			19	CD45+CD56+		19	CD45+CD56+
						20	CD56+CD57-
		Late NK cells	01	CD45+CD66b-			
			10	CD19-CD20-			
			17	CD3-CD14-			
			18	CD45RA+CD123-			
			19	CD45+CD56+			
			21	CD56+CD57+			
	Monocytes	Total Monocytes	01	CD45+CD66b-	Classical Monocytes	01	CD45+CD66b-
			10	CD19-CD20-		10	CD19-CD20-
			11	CD3-CD56-		11	CD3-CD56-
			12	CD11c+HLA-DR+		12	CD11c+HLA-DR+
			13	CD14+/-CD11c+		13	CD14+/-CD11c+
						14	CD38+CD14hi
		Transitional Monocytes	01	CD45+CD66b-	Nonclassical Monocytes	01	CD45+CD66b-
			10	CD19-CD20-		10	CD19-CD20-
			11	CD3-CD56-		11	CD3-CD56-
			12	CD11c+HLA-DR+		12	CD11c+HLA-DR+
			13	CD14+/-CD11c+		13	CD14+/-CD11c+
			15	CD38lo/-CD14int		16	CD38-CD14-
	Dendritic cells	Plasmacytoid Dendritic cells	01	CD45+CD66b-	Myeloid Dendritic cells	01	CD45+CD66b-
			10	CD19-CD20-		10	CD19-CD20-
			17	CD3-CD14-		17	CD3-CD14-
			22	HLA-DR+		22	HLA-DR+
			23	CD123+CD11c-		24	CD123-CD11c+
						25	CD11c+CD38+

Table 2. Active cell populations identified in Cytobank for manual gating of the Maxpar Direct Immune Profiling Assay (201325)*. Active populations that contain parentheses are descriptors of intermediate populations for which those gates are used. Populations ending with a descriptor following a colon and starting with a checkbox sign (☑) are end populations.

01 CD45+CD66b- (Lymphocytes, DCs, Monocytes)	31 CD8+CCR7hi
02 CD45loCD66b+ (Granulocytes)	32 CD45RA+CD45RO-: ☑ CD8 Naive
03 CD294+CD16-: ☑ Eosinophils	33 CD45RA-CD45RO+: ☑ CD8 Central Memory
04 CD294-CD16+: ☑ Neutrophils	34 CD8+CCR7lo/-
05 CD56-CD14- (B cells)	35 CD8+CD27+: ☑ CD8 Effector Memory
06 CD19+CD3-: ☑ Total B cells	36 CD8+CD27-: ☑ CD8 Terminal Effector
07 CD19+CD27-: ☑ Naive B cells	37 CD4+CD8-: ☑ CD4 αβ T cells
08 CD19+CD27+: ☑ Total Memory B cells	38 CD4+CCR7hi
09 CD38+CD20-: ☑ Plasmablasts	39 CD45RA+CD45RO-: ☑ CD4 Naive
10 CD19-CD20- (non-B)	40 CD45RA-CD45RO+: ☑ CD4 Central Memory
11 CD3-CD56- (non-T, non-NK)	41 CD4+CCR7lo/-
12 CD11c+HLA-DR+ (Mono)	42 CD4+CCR7lo/-CD45RA-CD45RO+
13 CD14+/-CD11c+: ☑ Total Monocytes	43 CD45RO+CD27+: ☑ CD4 Effector Memory
14 CD14+CD38+: ☑ Classical Monocytes	44 CD45RO+CD27-: ☑ CD4 Terminal Effector
15 CD38lo/-CD14int: ☑ Transitional Monocytes	45 CD4+CCR4+
16 CD38-CD14-: ☑ Nonclassical Monocytes	46 CD4+CCR4+CD45RA-CD45RO+
17 CD3-CD14- (NK, DC)	47 CD25hiCD127lo/-: ☑ Treg
18 CD45RA+CD123- (NK)	48 CD4+CXCR5-
19 CD45+CD56+: ☑ Total NK	49 CD4+CCR4-
20 CD56+CD57-: ☑ Early NKs	50 CD4+CCR4-CD45RA-CD45RO+
21 CD56+CD57+: ☑ Late NKs	51 CXCR3+CCR6-: ☑ Th1-like
22 HLA-DR+ (DC)	52 CD45RA-CCR4+
23 CD123+CD11c-: ☑ pDC	53 CXCR3-CCR6-: ☑ Th2-like
24 CD123-CD11c+ (DC)	54 CXCR3-CCR6+: ☑ Th17-like
25 CD11c+CD38+: ☑ mDC	55 CD3+CD4-
26 CD14-CD11c- (non-Mono)	56 CD28+CD161hi: ☑ CD4- MAIT/NKT
27 CD45+CD3+ (T cells)	57 HLA-DR-CD11c-
28 CD3+TCRγδ- (αβ T cells)	58 CD123+CD294+: ☑ Basophils
29 CD4-CD8+ (CD8 αβ T cells)	59 CD4-CD8-
30 CD8+CD161-: ☑ CD8 αβ T cells	60 CD3+TCRγδ+: ☑ CD4-CD8- γδ T cells

* Maxpar Direct Immune Profiling Assay is available in a new configuration (201334).

9.5 sPD-L1 analysis excluding outliers

Figure 1a and 1b: Recombinant and patient derived sPD-L1 measured by Ella and SIMOA platforms

1a: Recombinant sPD-L1 measured by Ella and SIMOA

1b: Patient derived sPD-L1 measured by Ella and SIMOA

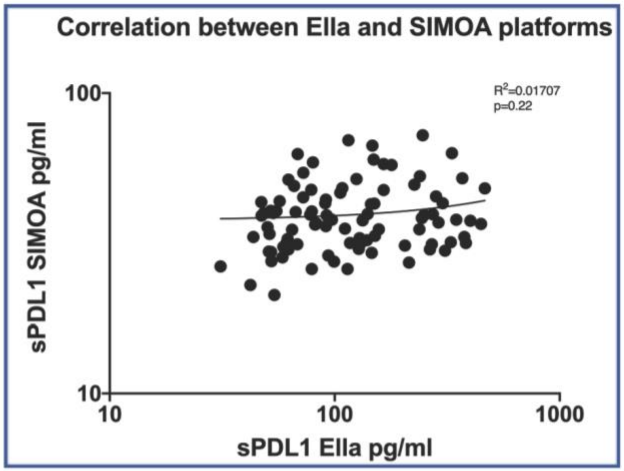

Table 1: Characteristics of patients by phase of CHB disease phase

Characteristic		**Total** N=93	**HBeAg+ Infection** N=5	**HBeAg+ Hepatitis** N=3	**HBeAg- Infection** N=24	**HBeAg- Hepatitis** N=4	**HBeAg+ Hepatitis on NUCs** N=15	**HBeAg- Hepatitis on NUCs** N=42
sPD-L1 pg/ml (Ella)		**111 (66-214)**	**146 (129-151)**	**125 (79-246)**	**95 (64-194)**	**107 (84-192)**	**244 (108-332)**	**81 (57-150)**
sPD-L1 pg/ml (SIMOA)*		**38 (32-45)**	**33 (29-33)**	**52 (48-72)**	**38 (31-41)**	**63 (27-70)**	**38 (31-48)**	**38 (32-44)**
Age, median (IQR)		40 (33-48)	33 (30-38)	28 (27-47)	43 (35-46)	36 (34-41)	36 (25-42)	42 (37-51)
Gender, (%)	Male	56 (60)	1 (20)	2 (67)	15 (63)	4 (100)	6 (40)	28 (67)
	Female	37 (40)	4 (80)	1 (33)	9 (37)	0 (0)	9 (60)	14 (33)
Ethnicity, n (%)	Asian	56 (60)	4 (80.0)	2 (67)	13 (54)	1 (25.0)	13 (87)	23 (55)
	Black	19 (21)	0 (0.0)	1 (33)	7 (30)	2 (50)	0 (0)	9 (21)
	White	18 (19)	1 (20)	0 (0)	4 (16)	1 (25)	2 (13)	10 (24)
HBsAg $\log_{10}$ IU/ml, median (IQR)π		3.2 (2.7-3.8)	4.7 (4.3-4.8)	4.2 (2.8-5.2)	3.3 (3.0-3.6)	4.3 (2.3-4.3)	3.2 (2.7-3.9)	3.0 (2.6-3.5)
HBV DNA $\log_{10}$ IU/ml, median (IQR)		0.5 (0.0-3.4)	8.9 (8.4-8.9)	8.1 (6.8-9.5)	3.3 (2.5-4.4)	3.8 (2-6.3)	2.0 (0.0-3.0)	0.0 (0.0-0.5)
HBV DNA, n (%)	Below LLOQ	48 (52)	0 (0)	0 (0)	1 (4)	1 (25)	6 (40)	40 (95)
	10-1,999	19 (20)	0 (0)	0 (0)	10 (42)	0 (0)	7 (47)	2 (5)
	2,000-19,999	10 (11)	0 (0)	0 (0)	6 (25)	2 (50)	2 (13)	0 (0)
	≥20,000	16 (17)	5 (100.0)	3 (100.0)	7 (30)	1 (25)	0 (0)	0 (0)
HBV RNA $\log_{10}$ copies/ml, median (IQR)		0.5 (0.0-3.5)	7.2 (7.0-7.4)	7.1 (6.2-8.6)	0.5 (0.0-2.9)	1.6 (0.5-4.7)	4.7 (1.9-6.9)	0.0 (0.0-1.7)
Duration of therapy overall in those on NUCs at sampling, median (IQR)		2.2 (1.1-8.9)	N/A	N/A	N/A	N/A	2.2 (1.1-2.8)	3.5 (1.3-9.9)
ALT, median (IQR)		24 (19-35)	21 (21-32)	63 (41-186)	23 (18-28)	44 (42-111)	29 (22-46)	23 (17-32)
Raised ALT	>40 IU/ml	17 (18)	0 (0)	3 (100)	0 (0)	4 (100)	4 (27)	6 (14)

Figure 2a and 2b: Distribution of sPD-L1 by CHB disease phase

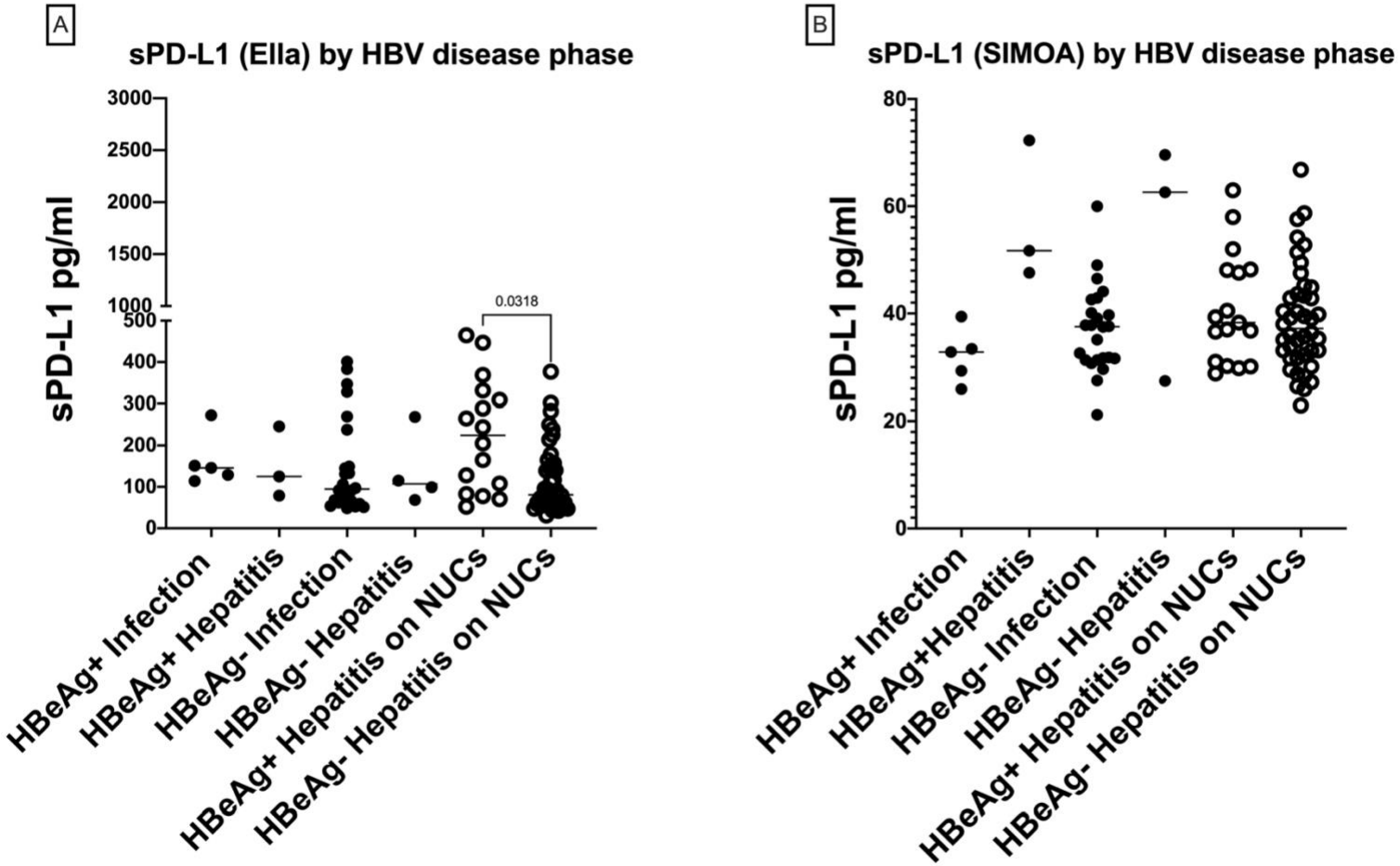

Table 2: Associations between cellular bound PD-1 and sPD-L1

	sPD-L1 (Ella)			sPD-L1 (SIMOA)		
Cell Type	Spearman's Rho	95% CI	p-value	Spearman's Rho	95% CI	p-value
$CD4^{+}PD\text{-}1^{+}$	+0.06	-0.18 to +0.30	0.65	+0.26	+0.06 to +0.45	0.01
$CD8^{+}PD\text{-}1^{+}$	+0.03	-0.18 to +0.22	0.83	+0.06	-0.15 to +0.28	0.57
$CD3^{-}\ CD56^{+}\ PD\text{-}1^{+}$	-0.10	-0.29 to +0.09	0.32	+0.05	-0.15 to +0.25	0.64
$CD19^{+}\ PD\text{-}1^{+}$	-0.87	-0.28 to +0.10	0.38	-0.12	-0.33 to +0.08	0.24

Table 3a:Univariate and multivariate factors associated with levels of sPD-L1 fold change (ELLA)

		Univariate			Multivariable 1			Multivariable 2		
Characteristic		FC	95% CI	p-value	FC	95% CI	p-value	FC	95%CI	p-value
Age	Per 5 year older	0.96	0.93-0.98	<0.01	0.96	0.94-0.99	<0.01	0.96	0.93-0.98	<0.01
Gender	Male vs Female	0.88	0.78-0.99	0.04	0.91	0.81-1.03	0.13	0.90	0.79-1.02	0.09
Ethnicity	Asian	0.98	0.84-1.15							
	Black	1.00	0.83-1.22							
	White	REF		0.95						
HBeAg	Positive vs Negative	1.26	1.11-1.44	<0.01	1.17	1.02-1.35	0.13			
HBsAg	Per $\log_{10}$ increase	1.05	0.99-1.12	0.11	0.99	0.94-1.06	0.94	0.99	0.92-1.06	0.82
HBV DNA	Per $\log_{10}$ increase	1.01	0.99-1.04	0.28						
HBV DNA	Below LLOQ	REF		0.50						
	10 – 1,999	1.00	0.85-1.17							
	2,000 – 19,999	1.16	0.94-1.42							
	≥20,000	1.06	0.89-1.26							
HBV RNA $\log_{10}$ cps/ml	Per log increase	1.03	1.00-1.05	0.02				1.02	0.99-1.04	0.25
On NUCs at sampling	Yes vs no	0.98	0.86-1.11	0.72						
Duration of therapy overall	Per year on NUCs	0.99	0.98-1.01	0.65						
ALT	Per 5 unit increase	1.00	0.99-1.02	0.47						
ALT >40	Yes vs no	1.07	0.92-1.25	0.38						

Table 3b: Univariate and multivariate factors associated with levels of sPD-L1 (SIMOA)

		Univariate			Multivariable 1		
Characteristic		FC	95% CI	p-value	FC	95%CI	p-value
Age	Per 5year increase	0.99	0.99-1.01	0.66			
Gender	Male vs Female	1.03	0.98-1.08	0.25			
Ethnicity	Asian	0.93	0.88-0.99		0.95	0.89-1.00	
	Black	0.95	0.89-1.02		0.98	0.91-1.05	
	White	REF		0.06	REF		0.17
HBeAg	Positive vs Negative	1.02	0.97-1.08	0.39			
HBsAg	Per log_{10} increase	1.03	1.00-1.05	0.05	1.01	0.98-1.04	0.63
HBV DNA	Per log_{10} increase	1.00	0.99-1.01	0.29			
HBV DNA	Below LLOQ	REF		0.65			
	10-1,999	0.99	0.93-1.05				
	2,000-19,999	1.03	0.95-1.11				
	$\geq$ 20,000	1.03	0.96-1.10				
HBV RNA log_{10} cps/ml	Per log increase	1.01	0.99-1.02	0.07	1.01	0.99-1.02	0.21
On NUCs at sampling	Yes vs no	1.01	0.96-1.06	0.76			
Duration of therapy overall	Per year on NUCs	1.00	0.99-1.01	0.64			
ALT	Per 5 unit increase	1.01	1.00-1.01	<0.01			
ALT >40	Yes vs no	1.11	1.05-1.18	<0.01	1.10	1.04-1.17	<0.01

9.6 UVA for CyTOF T-cell signature associations

Factors associated with T-cell signature phenotype n=30

		Univariate		
		FC	95% CI	p-value
Characteristic				
Age per 5 years older	Per 5 years older	1.14	0.96 – 1.36	0.13
Sex	Male vs Female	1.49	0.72 – 3.07	0.27
Ethnicity, n(%)	Asian	REF		0.66
	Black	0.64	0.23 – 1.77	
	White	0.99	0.39 – 2.59	
HBeAg	Positive vs Negative	0.58	0.26 – 1.30	0.18
HBeAg quantification	Per log increase	0.92	0.60 – 1.41	0.64
HBsAg quantification	Per log increase	0.93	0.74 – 1.17	0.52
HBV DNA	Per log increase	0.95	0.82 – 1.10	0.47
HBV DNA	<10	REF		0.90
	10-1999	0.84	0.39 – 1.85	
	≥2,000	0.85	0.18 – 3.98	
HBV RNA detected	Yes vs No	0.99	0.46 – 2.19	0.99
HBV RNA	Per log increase	0.93	0.80 – 1.07	0.29
On NUC therapy	Yes vs No	0.88	0.41 – 1.88	0.72
Duration of NUC therapy overall	Per year increase	1.10	1.01 – 1.19	0.04*
ALT	Per unit increase	0.99	0.98 – 1.01	0.66
ALT >40 IU/ml	Yes vs No	2.15	0.83 – 5.53	0.11
Platelets $x10^9$ cells/mm^3	Per $x10^9$ cell/mm^3 increase	1.00	0.99 – 1.01	0.67
sPD-L1	(Ella) per log increase	0.75	0.46 – 1.23	0.25
	(Ella) per log increase (<114pg/ml)	0.98	0.95 – 1.01	0.20
	(Ella) per log increase (≥114pg/ml)	0.99	0.99 – 1.00	0.47
	(Simoa) per log increase	1.76	0.43 – 7.13	0.42

Factors associated with PD-1+ T-cell signature cluster phenotype n=30

		Univariate		
		FC	95% CI	p-value
Characteristic				
Age per 5 years older	Per 5 years older	0.97	0.85 – 1.11	0.64
Sex	Male vs Female	0.69	0.40 – 1.19	0.17
Ethnicity, n(%)	Asian	REF		0.20
	Black	1.49	0.71 – 3.10	
	White	1.74	0.88 – 3.45	
HBeAg	Positive vs Negative	0.92	0.49 – 1.73	0.80
HBeAg quantification	Per log increase	0.90	0.69 – 1.18	0.36
HBsAg quantification	Per log increase	1.20	1.02 – 1.40	0.03*
HBV DNA	Per log increase	1.02	0.92 – 1.14	0.68
HBV DNA	<10	REF		0.63
	10-1999	1.32	0.74 – 2.36	
	≥2,000	1.14	0.36 – 3.58	
HBV RNA detected	Yes vs No	0.96	0.53 – 1.73	0.90
HBV RNA	Per log increase	1.03	0.92 – 1.15	0.63
On NUC therapy	Yes vs No	0.87	0.49 – 1.54	0.61
Duration of NUC therapy overall	Per year increase	0.99	0.92 – 1.06	0.67
ALT	Per unit increase	1.00	0.98 – 1.03	0.91
ALT >40 IU/ml	Yes vs No	1.17	0.56 – 2.46	0.67
Platelets $x10^9$ cells/mm^3	Per $x10^9$ cell/mm^3 increase	0.99	0.99 – 1.00	0.20
sPD-L1	(Ella) per log increase	1.05	0.72 – 1.53	0.80
	(Ella) per log increase (<114pg/ml)	0.98	0.96 – 1.00	0.10
	(Ella) per log increase (≥114pg/ml)	1.00	1.00 – 1.01	<0.01*
	(Simoa) per log increase	1.17	0.40 – 3.46	0.78

9.7 Extended Appendix Files

To ensure complete electronic data access and comply with thesis size requirements, the extended appendix files including full correlation analysis detailed in chapters 5 and 6 are available by following the link below to the dedicated FigShare portal for the data presented.

Austin, Harrison (2022): Chapter 5_Correlation_cell to characteristic_95CI.xlsx. figshare. Dataset. https://doi.org/10.6084/m9.figshare.20288601.v1

Austin, Harrison (2022): Chapter 5_PD1 graphs with outliers. figshare. Figure. https://doi.org/10.6084/m9.figshare.20291409.v1

Austin, Harrison (2022): Chapter 6- Deep Immunoprofiling HBV PD1/PD-L1. figshare. Dataset. https://doi.org/10.6084/m9.figshare.20327226.v1

Austin, Harrison (2022): Chapter 6- deep immunoprofiling HBV extended cell types. figshare. Figure. https://doi.org/10.6084/m9.figshare.20327244.v1